Advances in Remote Sensing and GIS applications in Forest Fire Management
From local to global assessments

Jesus San-Miguel Ayanz, Ioannis Gitas, Andrea Camia, Sandra Oliveira
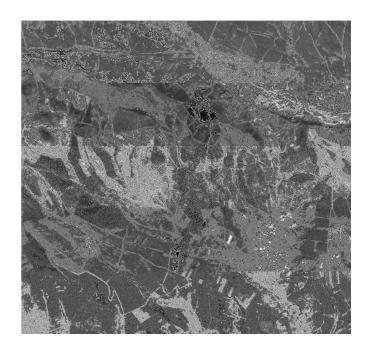**Editors**

JRC
EUROPEAN COMMISSION

ies
Institute for
Environment and
Sustainability

ARISTOTLE
UNIVERSITY
OF THESSALONIKI

Advances in Remote Sensing and GIS applications in Forest Fire Management

From local to global assessments

Edited by:

Jesus San-Miguel Ayanz
Andrea Camia
Sandra Santos de Oliveira
Institute for Environment and Sustainability
Joint Research Centre (Italy)

Ioannis Gitas
Laboratory of Forest Management and Remote Sensing
Aristotle University of Thessaloniki (Greece)

The mission of the JRC-IES is to provide scientific-technical support to the European Union's policies for the protection and sustainable development of the European and global environment.

Europe Direct is a service to help you find answers
to your questions about the European Union

Freephone number (*):

00 800 6 7 8 9 10 11

(*) Certain mobile telephone operators do not allow access to 00 800 numbers or these calls may be billed.

A great deal of additional information on the European Union is available on the Internet.
It can be accessed through the Europa server http://europa.eu/

SCIENTIFIC COMMITTEE

- Vincent Ambrosia - *NASA Ames Research Center (USA)*
- Pietro Alessandro Brivio - *Consiglio Nazionale delle Ricerche (Italy)*
- Andrea Camia - *Joint Research Centre (Italy)*
- Emilio Chuvieco - *University of Alcalá (Spain)*
- Juan de la Riva - *University of Zaragoza (Spain)*
- Angela De Santis - *INSA, Ingeniería y Servicios Aeroespaciales (Spain)*
- Mike Flannigan - *Canadian Forest Service (Canada)*
- Ioannis Gitas - *Aristotle University of Thessaloniki (Greece)*
- Nikolaos Koutsias - *University of Ioannina (Greece)*
- Rosa Lasaponara - CNR-IMAA 9Italy)
- Pilar Martin - *Consejo Superior de Investigaciones Cientificas (Spain)*
- George Mitri - *University of Balamand (Lebanon)*
- José Miguel Pereira - *Instituto Superior de Agronomia (Portugal)*
- David Riaño - *Consejo Superior de Investigaciones Cientificas (Spain)*
- Dar Roberts - *University of California - Santa Barbara (USA)*
- Jesus San-Miguel Ayanz - *Joint Research Centre (Italy)*
- Kevin Tansey - *University of Leicester (UK)*
- Sander Veraverbeke - *Jet Propulsion Laboratory, California Inst. Technology (USA)*
- Jan van Wagtendonk - *US Geological Survey (USA)*
- Martin Wooster - *University of London (UK)*

ORGANIZING COMMITTEE

- Jesus San-Miguel Ayanz - *Joint Research Centre (Italy)*
- Andrea Camia - *Joint Research Centre (Italy)*
- Ioannis Gitas - *Aristotle University of Thessaloniki (Greece)*
- Sandra Santos de Oliveira – *Joint Research Centre (Italy)*
- EARSeL secretariat

Table of Contents

Preface

The importance of wildfires as a natural or a human-induced phenomenon has gained importance at regional and global levels in the last years. Improved remote sensing and computational capabilities enable the fast processing of large image datasets in real time. As a result, remote sensing and geographic information systems are today, more than ever before, common tools for fire monitoring at local, regional and global levels.

However, the gap between research and operational use of remote sensing and GIS still exists. The complexity in automating pre-processing and posterior classification of remotely sensed imagery poses a great problem for wildfire and civil protection managers. It is thus the duty of the remote sensing community to develop systems and tools that facilitate the access to information of forest fires to these managers.

The EARSeL Special Interest Group (SIG) on Forest Fires actively promotes the integration of these advanced technologies in the day-to-day of forest managers at all scales, embracing researchers, local governments and global organizations.

In this context the EARSeL SIG on Forest Fire is happy to organize the VIII EARSeL Workshop on "Remote Sensing of Forest Fires: From Local to Global Assessments." This conference will thus bring together remote sensing communities that work at local level with those working at the global level. Although these communities have a common goal, the monitoring of forest fires, they approach the issue in very diverse ways.

The Stresa Workshop builds upon the success obtained in previous workshops held since the foundation of the EARSeL SIG on Forest Fires in 1995. These took place in Alcalá de Henares (1995), Luso (1998), Paris (2001), Ghent (2003), Zaragoza (2005), Thessaloniki (2007) and Matera (2009), and provided a great impulse for the progress in forest fire research.

The Proceedings book includes papers divided in 4 sections which focus on the following topics:

I- Local to regional applications of remote sensing in pre and during fire conditions
II- Local to regional applications of remote sensing in post-fire assessment
III- National to global applications of remote sensing in pre and during fire conditions
IV- National to global applications of remote sensing in post-fire assessment

Jesus San-Miguel Ayanz
Andrea Camia   **Ioannis Gitas**
Sandra S. Oliveira
Local Organizing Committee   *FF-SIG Chair*

I - Local to regional applications of remote sensing in pre and during fire conditions

ESTIMATION OF FUEL MOISTURE CONTENT FOR FIRE DANGER ASSESSMENT: TURNING POTENTIAL INTO REALITY?

Marta Yebra

CSIRO Land and Water, GPO Box 1666, Canberra 2601, Australia. Marta.Yebra@csiro.au

Abstract

Live Fuel Moisture Content (FMC) has been monitored for about 30 years to assess fire risk in different types of ecosystems. FMC data collected in the field following standard protocols have provided a direct indication of fire risk in a specific area and has been and it is still widely used by forest managers. However, these measurements are inadequate to develop response plans due to the difficulty in obtaining sufficient samples over a realistically wide spatial extent in a brief period of time. Remote sensing (RS) researchers have attempted to develop methods for spatial mapping of FMC from signals detected by sensor (temperature, reflectance, etc.). The initial hypothesis was that the impact of FMC variations on the detected signal was strong enough to be discriminated from other factors affecting spectral variation. Several studies have been published in the last decades to test this hypothesis and several vegetation indices (VIs), directly or indirectly related to water content have been developed. First FMC models were based on empirical fittings between field measured FMC and vegetation indices such as NDVI derived from NOAA/AVHRR. Since then a lot of effort has been put into improving these RS derived estimations. Seeking for more accuracy, robustness and operationality new launched sensors, more sophisticated methodologies and ancillary information have been used. Huge progress has been done, but are these models performing a lot better? Even more important, are FMC maps being operationally used by forest fire managers? After more than 20 years, we are still individually developing new models. A community joined effort should be established for a better fire risk prediction and a more operational use of FMC data and products. For example, field sampling is still an essential component for the validation and calibration of our models. Consequently, there are still a number of teams involved in field sampling but there is not a good network for data sharing. Additionally, there are several models published but very little effort in inter-comparing them to conclude which is the most suitable. This talk reviews the developments in estimating FMC in the context of fire risk assessment, highlights the main problems on the operational use of these FMC models including the conversion of FMC into a common fire risk scale, present some examples of operational fire risk models and concludes on research priorities toward operationalising the research models. There are signs that managers are not using our FMC models operationally due to their complexity, the shortage of knowledge about their uncertainties, the lack of integration with others variables affecting fire risk and the shortage of long term interactions between managers and the researchers. Fire managers have to take decision to save lives. We should understand how those decisions are taken so we can better integrate FMC with other risk variables. Additionally, research projects should go beyond scientist papers and should search for long term operationality of products. Finally, the need to measure FMC should be more recognized and a formal evaluation program for methods should be organized.

Keywords: Water content, Wildfire, pre-fire assessment, regional and local scale

NASA'S AIRBORNE AUTONOMOUS MODULAR SCANNER (AMS) – WILDFIRE SENSOR: INSTRUMENTATION SUPPORTING FIRE INTENSITY, RADIANT ENERGY MEASUREMENTS, AND DISASTER MANAGEMENT

V. G. Ambrosia[1], J. S. Myers[2], E. A. Hildum[2], C. Ichoku[3], W. Schroeder[4], B. Lobitz[1]

[1]*California State University – Monterey Bay, NASA-Ames Research Center, Moffett Field, California, 94035-0001, U.S.A., vincent.g.ambrosia@nasa.gov & bradley.m.lobitz@nasa.gov*
[2]*University Affiliated Research Center (UARC), NASA-Ames Research Center, Moffett Field, CA. 94035-1000, U.S.A., jeffrey.s.myers@nasa.gov and edward.a.hildum@nasa.gov;*
[3]*Climate & Radiation Branch, NASA-Goddard Space Flight Center, greenbelt, MD, U.S.A., charles.m.ichoku@nasa.gov*
[4]*Earth System Science Interdisciplinary Center, University of Maryland, College Park, MD, U.S.A., wilfrid.schroeder@noaa.gov*

Abstract

The NASA Autonomous Modular Scanner (AMS) – Wildfire sensor is an airborne, 16-channel line scanner with bands in the VIS-IR-MIR-TIR spectral region. Four AMS thermal channels replicate the spectral bandpass region of two of the proposed NPOESS VIIRS channels and allow improved discrimination of wildfire conditions over other airborne wildfire sensor systems. The AMS has operated on a range of manned and unmanned aircraft, including the NASA Ikhana UAS, and more recently the NASA Beechcraft B-200 King-Air manned aircraft. On-board processors allow near-real-time Level 2 products to be derived from the spectral data and sent through a satellite link to investigators on the ground. The AMS processing algorithms can be modified in flight to allow derivation of various fire property indices to be calculated. Real-time, on-board processing includes terrain / geo-rectification procedures that allow generation of standard Open Geospatial Consortium (OGC) – qualified data. The AMS-Wildfire instrument has been flown extensively in the western U.S. since 2006, supporting disaster managers with real-time fire products such as the CCRS hot spot / temperature threshold detection algorithm, a Normalized Burn Ratio (NBR) product for post-fire burn assessment and a Burn Area Emergency Response (BAER) data set to allow rapid post-fire burn area / fire intensity assessment. The data sets were routinely delivered to fire incident management teams to support operational mitigation efforts, as a demonstration of new sensor technologies, utility of UAS platforms, and autonomous processing capabilities. The AMS data processing is being further modified to provide additional fire-related products that support the wildfire science community and support calibration / validation of current and future earth observation satellite systems, such as MODIS and NPOESS - VIIRS. The AMS has supported satellite calibration and validation efforts with collections over wildfire events simultaneously with MODIS data collections during campaigns in 2007-2010. These measurements have led to improved understanding of the satellite observations and allowed a renewed focus on the AMS sensor as an instrument capable of deriving critical fire parameters to allow improved estimation of wildfire thermal properties. With high spatial, temporal and radiometric measurement capabilities of the AMS instrument, improved discrimination of fire properties are achieved. The "lingering" capabilities afforded by airborne platforms, allow temporal observations of fire properties, rather than the single observations provided by satellite systems. A new fire radiative power (FRP) algorithm is being added to the suite of on-board, autonomous-generated, real-time image processing capabilities, to allow cross-referencing with the MODIS-derived FRP product for coincident wildfire observations. Additionally, the airborne AMS FRP measurements will allow assessment of the future NPOESS VIIRS FRP product, and can also be used to support validation efforts of the GOESS-R ABI Active Fire Product parameters. The AMS operations, successful missions, and plans for future use to support both the fire science community and the disaster management community are described here.

Keywords: wildfire, AMS, Fire Radiative Power (FRP), TIR, MODIS, VIIRS, GOES-R ABI

Background

The National Aeronautics and Space Administration (NASA) Autonomous Modular Sensor (AMS) – Wildfire scanner, is a 16-channel airborne instrument imaging in the visible / near-infrared / mid-infrared / thermal-infrared (VIS-IR-MIR-TIR) electromagnetic regions. Between 2006 and 2011, the AMS was employed on manned / unmanned platforms, to support imaging science capabilities and provide near-real-time, on-board-processed, Level 2 data products to wildfire incident management teams. The products included near-real-time geo-rectified imagery, fire detection shapefiles, Normalized Burn Ratio (NBR), and Burn Area Emergency Response (BAER) imagery [*Ambrosia, et al. 2011a; Ambrosia, et al. 2011b*]. In 2011, an on-board processed, real-time FRP algorithm was added to the product delivery suite.

While the AMS-Wildfire sensor is useful for wildfire mapping at local scales, satellite data represent the primary source of information for mapping of biomass burning activity at regional to global scales [e.g., *Freitas et al*. 2005; *Davies et al*. 2009; *Ichoku et al*. 2008; *Kahn et al. 20*08*; Reid et al*. 2009; *van der Werf et al*. 2010]. The Moderate-resolution Imaging Spectro-radiometer (MODIS) aboard the NASA Terra and Aqua satellites was the first satellite-borne sensor capable of measuring fire radiative energy (FRE) release rate, or power (FRP), quantitatively on a global scale [e.g. *Kaufman et al*. 1998a; *Justice et al*. 2002; *Giglio et al*. 2003, *Ichoku et al. 20*08]. Subsequently, FRP is being derived from a few other satellite sensors [e.g., *Wooster et al*. 2003; *Xu et al*. 2010]. Planned satellite systems, including the polar orbiting Visible / Infrared Imager Radiometer Suite (VIIRS) and the geostationary GOES-R Advanced Baseline Imager (ABI) will provide enhanced spatial resolution and temporal observations of fire events and require validation of their fire products to ascertain their effectiveness for fire detection using airborne sensors such as the calibrated AMS [*Schroeder et al. 2010, Giglio et al. 2008; Schroeder et al. 2008*]. Deriving airborne AMS-Wildfire FRP measurements coincident with satellite-derived measurements (MODIS, VIIRS, etc.) will improve both regional and global estimates of fire radiative properties.

AMS Sensor Characteristics

The NASA AMS-Wildfire scanner has operated on-board both manned and UAV platforms and is a 16-channel (12 discrete VIS-IR-MIR-TIR bands) airborne multi-spectral imaging line scanner. Table 1 indicates the sensor specifications for the AMS.

Table 1. AMS-WILDFIRE 16-channel Scanner Specifications. Channels replicating the equivalent Landsat Thematic Mapper (TM) and VIIRS Moderate resolution (M) bands are identified.

Spectral Band	Wavelength μm
1	0.42- 0.45
2	0.45- 0.52 (TM1)
3	0.52- 0.60 (TM2)
4	0.60- 0.62
5	0.63- 0.69 (TM3)
6	0.69- 0.75
7	0.76- 0.90 (TM4)
8	0.91- 1.05
9	1.55- 1.75 (TM5) (high gain)
10	2.08- 2.35 (TM7) (high gain)
11	3.60- 3.79 (VIIRS M12) (high gain)
12	10.26-11.26 (VIIRS M15) (high gain)
13	1.55- 1.75 (TM5) (low gain)
14	2.08- 2.35 (TM7) (low gain)
15	3.60- 3.79 (VIIRS M12) (low gain)
16	10.26-11.26 (VIIRS M15) (low gain)
Total Field of View: 42.5 or 85.9 degrees (selectable)	
IFOV: 1.25 mrad or 2.5mrad (selectable)	
Spatial Resolution: 3 – 50 meters (variable based on alt)	

On-Board, Real-Time Sensor Data Processing

The AMS provides a series of Level 2 products directly from the aircraft, through a satellite communications link, to investigators on the ground. To derive the Level 2 products, the selected raw digital data counts are converted to at-sensor radiance for visible and near-infrared wavelength channels, and bright-

ness temperature for the thermal channels. Radiometric correction is performed using pre-flight (labor-atory) calibration coefficients. Two on-sensor black-body calibration reference source temperature readings provide a linear digital count-to-radiance conversion which is then used in an approximate inverse Planck's equation to produce a brightness temperature for each pixel in the thermal channels. This on-board pre-processing calibration step allows data to be spectrally and thermally consistent from mission to mission.

AMS-Derived Fire Hot-Spot Detection Algorithm

A fire hot-spot detection algorithm based on the satellite-derived hot spot detection algorithm developed by the Canadian Center for Remote Sensing (CCRS) [*Li, et al. 2000a, Li, et al. 2000b, Flasse and Ceccato 1996, and Cahoon, et al. 1992*], was implemented using the representative AMS thermal channels. The fire hot-spot detection algorithm uses the AMS-Wildfire 3.6μm channel to define a fire temperature threshold, and two or more additional channels to refine the classification and eliminate fire commission errors. The fire detection algorithm uses a difference-minimum between a temperature threshold from AMS channels 11 and 12, and a shortwave IR reflectance maximum in channel 7 (to screen high-reflectance commission errors), to derive a pixel-based fire hot-spot data set. The hot spot pixel data are then aggregated / produced as shapefiles (*.SHP), geo-rectified and provided as a near-real-time Level 2 product.
AMS –Derived Fire Radiative Power (FRP) Algorithm

In 2011, a FRP algorithm was added to the AMS on-board processing suite to derive finer spatial and temporal scale FRP estimates over wildfires [*Ichoku, et al. 2010*]. FRP is a measure of the radiant energy liberated per-unit-time from burning vegetation. The MODIS FRP is estimated as:

$$R_{fre} = a \ (T_4{}^8 - T_{4b}{}^8)$$

Where:
a is a constant used for MODIS (4.34 x 10^{-19});
R_{fre} (in MW or MJ/s for MODIS) is the pixel fire radiative power;
T_4 (in K) is the fire pixel brightness temperature at the 4-μm channel;
T_{4b} is the 4-μm brightness temperature of the background surrounding the fire pixel [*Kaufman, et al. 1998*].

The same FRP measurements are made from MODIS fire observation data daily for the US, and improvements can be made to those satellite measurements with coincident, higher spatial and temporal resolution AMS airborne measurements. The MODIS FRP algorithm is being adapted with AMS data by using the radiance to temperature calibration for the MIR region covered by the AMS channel 11 (3.60- 3.79 μm). The AMS FRP equation is then the same as the MODIS FRP equation above, but with units of W/m^2/pixel. This method was first tested on the Eagle Fire, collected in July 2011 during an AMS sensor operational check flight and provided as a post-processed data product of planned on-board-derived FRP measurements (Figure 1).
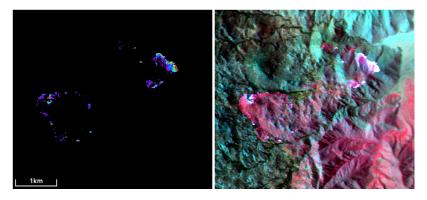
Figure 1. AMS FRP measurement for the Eagle Fire, California, 26 July 2011 (left). The colors range from purple (150W/m2) to red (3000+W/m2. Values below 150 are non-fire. The three-channel color composite of the Eagle Fire (right) (AMS channels 12, 9, 10) vividly show the hottest regions of the burning.

Discussion

The AMS-Wildfire airborne instrument, in operation since 2006 on both manned and unmanned aircraft, has been shown to be an effective sensor for deriving and delivering near-real-time Level 2 fire-related data products to fire incident management teams and scientists. Recent modifications to the sensor improve the quantification of wildfire indices, calibration and validation of current and planned satellite observation systems, and also improve active- and post-fire information for wildfire incident teams. In 2011, the AMS was flown to support both the wildfire management community and the fire science community with improved, higher spatial- and temporal-resolution data collection campaigns. Those missions included testing of a new AMS-derived FRP product to help validate / calibrate the MODIS FRP product. Additionally,

the sensor can /will serve as a test-bed for validating the NPOESS VIIRS satellite fire detection capabilities, and the NOAA GOES-R ABI sensor. The airborne AMS validation efforts will undoubtedly improve the satellite-based regional / global estimates of fire properties, thereby improving measurement of fire impacts on global climate change.

References

Ambrosia, V.G., Wegener, S., Zajkowski, T., Sullivan, D.V., Buechel, S., Enomoto, F., Hinkley, E., Lobitz, B., and Schoenung, S. 2011a. The Ikhana UAS western states fire imaging missions: from concept to reality (2006-2010). Geocarto International Journal, 26 (2): 85-101.

Ambrosia, V.G., Buechel, S., Wegener, S., Sullivan, D.V., Enomoto, F., Hinkley, E., Zajkowski, T. 2011b. Unmanned airborne systems supporting disaster observations: near-real-time-data needs. Proceedings of 34th International Symposium on Remote Sensing of Environment. CD Proceedings, paper reference # 144, TS-55-1, ISRSE, Sydney, Australia, April 2011, 1-4.

Cahoon, D. R., Jr., Stocks, B.J., Levine, J.S., Cofer, III, W.R., and Chung, C.C. 1992. Evaluation of a technique for satellite-derived area estimation of forest fires. Journal of Geophysical Research, 97, 3805-3814.

Davies, D.K., Ilavajhala, S. et al. 2009. Fire information for resource management system: archiving and distributing MODIS active fire data. IEEE Transactions on Geoscience and Remote Sensing, 47(1), 72-79.

Flasse, S. P., and Ceccato P. S. 1996. A contextual algorithm for AVHRR fire detection. International Journal of Remote Sensing, 17, 419-424.

Freitas, S., Longo, K.M., et al. (2005). Monitoring the transport of biomass burning emissions in South America. Environmental Fluid Mechanics, 5, 135-167.

Giglio, L., Csiszar, I., Restas, A., et al. 2008. Active fire detection and characterization with the Advanced Spaceborne Thermal Emission and Reflection Radiometer (ASTER). Remote Sensing of Environment, 112, 3055-3063.

Giglio, L., Descloitres, J., Justice, C., & Kaufman, Y. 2003. An enhanced contextual fire detection algorithm for MODIS. Remote Sensing of Environment, 87, 273– 282.

Ichoku, C., Ellison, L., and Ambrosia, V. G. 2010. Evaluation of satellite measurements of fire radiative power (FRP) using airborne measurements. Proceedings of IEEE International Geoscience and Remote Sensing Symposium (IGARSS), Session: WE4.L03.3 - Optical and Infrared Modeling, Honolulu, Hawaii, 28 July 2010.

Ichoku, C., L. Giglio, M. J. Wooster, and Remer, L. A. 2008. Global characterization of biomass-burning patterns using satellite measurements of Fire Radiative Energy. Remote Sens. Environ., 112, 2950-2962 2008a.

Justice, C., Giglio, L., Korontzi, S., Owens, J., Morisette, J., Roy, D., Descloitres, J., Alleaume, S., Petitcolin, F., & Kaufman, Y. 2002. The MODIS fire products. Remote Sensing of Environment, 83, 244–262.

Kahn, R.A., Y. Chen, D.L. Nelson, F-Y. Leung, Q. Li, D.J. Diner, and J.A. Logan 2008. Wildfire smoke injection heights – Two perspectives from space. Geophysical Research Letters 35, doi:10.1029/2007GL032165.

Kaufman, Y., Justice, C., Flynn, L., Kendall, J., Prins, E., Giglio, L., Ward, D., Menzel, W., and Setzer, A. 1998. Potential global fire monitoring from EOS-MODIS. Journal of Geophysical Research-Atmospheres, 103(D24), 32,215–32,238.

Li, Z., Nadon, S., Cihlar, J., Stocks, B. 2000a. Satellite mapping of Canadian boreal forest fires: evaluation and comparison of algorithms. International Journal of Remote Sensing, 21, 3071-3082.

Li, Z., Nadon, S., Cihlar, J. 2000b. Satellite detection of Canadian boreal forest fires: development and application of an algorithm. International Journal of Remote Sensing, 21, 3057-3069.

Reid, J.S., Hyer, E.J., et al. 2009. Global monitoring and forecasting of biomass-burning smoke: Description of and lessons from the fire locating and modeling of burning emissions (FLAMBE) Program. IEEE Journal of Selected Topics in Applied Earth Observations and Remote Sensing, 2(3): 144-162.

Schroeder, W., Csiszar, I., Giglio, L., et al. 2010. On the use of fire radiative power, area, and temperature estimates to characterize biomass burning via moderate to coarse spatial resolution remote sensing data in the Brazilian Amazon. Journal of Geophysical Research, 115(D21121), doi: 10.1029/2009JD013769.

Schroeder, W., Prins, E., Giglio, L., et al. 2008. Validation of GOES and MODIS active fire detection products using ASTER and ETM+ data. Remote Sensing of Environment, 112, 2711-2726.

van der Werf, G.R., Randerson, J.T., et al. 2010. Global fire emissions and the contribution of deforestation, savanna, forest, agricultural, and peat fires (1997-2009). Atmospheric Chemistry and Physics, 10, 11707-11735.

Wooster, M.J., Zhukov, B., and Oertel, D. 2003. Fire radiative energy for quantitative study of biomass burning: Derivation from the BIRD experimental satellite and comparison to MODIS fire products. Remote Sensing of Environment, 86, 83-107.

Xu, W., Wooster, M.J., Roberts, G., and Freeborn, P. 2010. New GOES imager algorithms for cloud and active fire detection and fire radiative power assessment across North, South and Central America. Remote Sensing of Environment, 114, 1876-1895.

DEVELOPMENT OF A FIRE-INDUCED FLASHOVER PROBABILITY INDEX (FIFPI) FOR ESKOM TRANSMISSION LINES

P. Frost[1], H. Vosloo[2], J. Meeuwis[3]

[1]CSIR Meraka Institute, Pretoria, South Africa - pfrost@csir.co.za

[2]ESKOM TSI, Rivonia, Johannesburg - Hein.Vosloo@eskom.co.za

[3]University of Johannesburg, Department of Geography, Environmental Management and Energy Studies - junem@uj.ac.za

Abstract

The need for a fire-induced flashover probability index (FIFPI) for Eskom's transmission lines (South Africa) became evident soon after the installation the Advanced Fire Information System (AFIS) in 2004. Thousands of wildfires were detected by satellites close to transmission lines, but only a small percentage (4%) of these fires caused a flashover. Historical flashover data was compared to satellite fire information as well as air temperature, relative humidity, wind speed and wind direction within a logistic regression analysis to develop a flashover prediction model. The FIFPI model was able to predict problem fires with a misclassification cost of only 3.87%. The aim of this study was to develop a prediction model with the ability to accurately predict fire-induced flashover occurrences on Eskom transmission lines in order to reduce the large amount of false alarms (SMS and E-mail messages) produced annually by AFIS.

Introduction

During the 2004 fire season, South Africa's largest power company Eskom, implemented satellite based fire information for the first time to help combat flashovers caused by wildfires underneath transmission lines. The quality of electricity supply through transmission lines are severely affected (in the form of line faults) by natural phenomena such as, bird streamers, lightning, fires and pollution. Flashovers cause very short interruptions in the supply of power and these in turn have major financial implication to customers with continuous process factories.

Eskom operates 28 000 km of high voltage transmission lines (132kV to 765kV) and is South Africa's national electricity utility. Electricity is generated predominantly by means of coal-fired power stations and one nuclear station with three hydro peaking stations. This constitutes 95% of the electricity of Africa (Anon 2004). The rights-of-way (ROW or servitudes) of these power lines cover large areas and traverse a number of biomes, ranging from arid vegetation through grasslands and savanna, to tropical vegetation.

The Council for Scientific and Industrial Research (CSIR) in collaboration with Eskom developed the Advanced Fire Information System (AFIS) with the main focus on the prediction, detection and assessment of wildfires in South Africa. The system combines fire detection information from the TERRA and AQUA MODIS (Moderate Resolution Imaging Spectro Radiometer) polar orbiting satellite sensors with the Meteosat Second Generation (MSG) geostationary satellite sensor from Eumetsat. As soon as a fire is detected within 3 km of a transmission line, a cell phone text message or E-mail alert is automatically generated and sent to the relevant line manager as well as Eskom control centre.

Because of its dielectric properties, air acts as an isolation medium between live conductors and the ground below it. During a fire, the properties of the air change as smoke particles fill the space between the ground and transmission line which could result in an electrical discharge or flashover to occur. The mechanism active during a fire-induced flashover of a power line is highly dynamic and complex and authors explain the phenomenon in different terms (Sukhnandan and Hoch 2002). In order to prevent the spread of fires underneath transmission lines early fire detection information is required to pinpoint the location and possibly provide additional info on the temperature and size. In the past Eskom line managers were dependant on information from local residents about fire occurrences and locations

The problem with fire-induced flashovers is not entirely unique to South Africa – countries such as the U.S.A., Australia and Mexico also struggle with flashovers caused by fires (Primen 2001). The AFIS system has become a useful tool for the early detection of fires close to Eskom transmission lines. The ability to send SMS and E-mail messages to the relevant person as soon as a fire is detected is one of the biggest advantages of the system (Frost *et al*. 2007). The problem, however, remains that thousands of fires are detected in the proximity of transmission lines annually, but only a small percentage of those fires cause a fire-induced flashover on the transmission lines (Vosloo 2005). Studies have indicated that an average of 2% to 4% of all fires close to Eskom transmission lines cause a flashover (Vosloo 2005).

The development of a fire-induced flashover prediction model required the adoption of various image processing and data analysis techniques to deal with the variety of data sources that ranged from satellite imagery and GIS map layers to numerical weather forecasts. A variety of data sets were acquired for both the training of the prediction model as well as the validation of the results. With the MODIS active fire product as base layer, weather forecast variables served as input to the predictor data set of the model, while flashover statistics for 2007 provided the target data set within the logistic regression analysis.

1.1 *Target variable*

The main inputs for the development of the target variable were the MODIS active fire data, a shape file of the Eskom transmission grid and historical fire-induced flashover point records for 2007. In order to develop the target variable for the prediction model, two GIS functions were applied to extract MODIS active fire pixels close to Eskom transmission lines. The "buffer" function in ArcMap was used to create a 3 km buffer around all transmission lines in the study area. MODIS active fire pixels that fell within these buffer zones were extracted with the "clip" function and a new data set was created containing only the selected MODIS active fire pixels close to the transmission lines.

1.2 *Predictor variable*

The main inputs for the development of the predictor variables were the MODIS active fire data, a shape file of the Eskom transmission grid and four primary input data sets (air temperature, relative humidity, wind speed and wind direction). In order to develop the predictor variables for the prediction model, two GIS functions were applied to extract MODIS active fire pixels close to Eskom transmission lines. The "buffer" function in ArcMap was used to create a 3 km buffer around all transmission lines in the study area. MODIS active fire pixels

that fell within these buffer zones were extracted with the "clip" function and a new data set was created containing only the selected MODIS active fires pixels close to the transmission lines.

1.3 *MODIS fire detection*

MODIS active fire satellite products are produced daily by the MODIS Direct Broadcast (DB) reception and processing systems located at the Satellite Application Centre (SAC) at Hartbeesthoek as well as the CSIR Meraka Institute in Pretoria. The collection 5 version of the MODIS fire detection algorithm (Giglio et al. 2003) produce daily active fire locations that feeds in to the Advanced Fire Information System (AFIS). An ASCII file is created after each satellite overpass from the Terra and Aqua satellites, including the following parameters, latitude and longitude of each fire, the time and the date of each fire location, the brightness temperature in Kelvin, the satellite ID and a confidence factor.

1.4 *Numerical weather forecasting*

Numerical meteorological forecast models (Marchuk 1974) of the atmosphere are run daily and form the basis for routine weather forecasts provided by National Weather Services around the globe. In 2006 the South African Weather Service (SAWS) implemented the Unified model (SAWS 2006) from the UK Met office. The model makes use of a horizontal resolution of 12 km and consists of 38 vertical layers (Ndabambi and Poolman 2007).

The MODIS active fire data set was used as reference data source during the extraction of the numerical weather forecast data for every fire point. The following numerical weather forecast parameters were extracted for each of the MODIS fire pixel locations from the SAWS database:

- Air Temperature (2 m above land surface).
- Relative Humidity (2 m above land surface).
- Wind Vectors (The geostrophic wind approximations are broken into its two horizontal components.

The parameters were 14:00 pm (SAST) forecasts, predicted at 08:00 am (SAST) daily. The time difference between the 14:00 pm (SAST) forecast data and the MODIS active fire data were never more than an hour and thirty minutes. The U and V wind vectors were converted to wind speed and direction.

1.5 *Logistic Regression analysis*

Logistic regression (LR) is part of a category of statistical models called *generalised linear models* and allows one to predict a discrete outcome from a set of variables that may be continuous, discrete, dichotomous, or a mix of any of these. LR does not involve decision trees and is especially effective as a predictive analysis tool on non-linear data sets (Perlich et al. 2003).

Results and Discussion

Model prediction accuracies of each of the predictor variable combinations in Table 1 were calculated based on three statistical tests. These included the cross validated relative cost,

misclassification cost and the Receiver Operating Characteristics (ROC) value for the learning and validation data sets (Perlich et al. 2003).

Table 1. Model predictions for different variable combinations

Variable	Cross Val Cost	Misclass (%) (Learning data)	ROC	Misclass (%) (Validation data)
T,RH,WS,WD	0.07	1.01	0.98	3.87
WS, RH,WD	0.10	2.50	0.98	5.70
WS, RH, T	0.07	1.01	0.98	4.45
WS, RH	0.13	3.50	0.98	7.50

T = Temperature, RH = Relative humidity, WS = Wind speed, WD = Wind direction

The results were focused on the target class, "True" flashovers. The misclassification error on the validation data set (Table 1) illustrated the true capability of each of the predictor variable combinations to predict a fire-induced flashover. Of the 2248 MODIS fire pixels tested in the logistic regression, 10% (224) of the pixels were left out of the model for validation purposes. The 10% validation data was thus a fully independent data set on which the misclassification error (validation data) in the last column was calculated. By comparing the results in Table 1 for the different variable combinations, the combination of air temperature, relative humidity, wind speed and wind direction provided the lowest misclassification error on the validation data set of 3.87%, while recording a low cross validation error of only 0.07%. The second best combination was the wind speed, relative humidity and air temperature variables which scored a misclassification error on the validation data set of 4.45% while also recording a cross validation error of 0.07%. The third best combination was the wind speed, relative humidity and wind direction group that showed a misclassification error on the validation data of 5.87% and a cross validation error of 0.10%. Lastly the wind speed and relative humidity combination showed a misclassification cost of 7.5% and the highest cross validation error of 0.13%. The Receiver Operator Characteristics (ROC) analysis for all the variable combinations showed a very high model accuracy of 0.98%, indicating a strong ability of predicting "True" flashover events for all the variable combinations

The results confirm that the variable combination of air temperature, relative humidity, wind speed and wind direction provides the most accurate fire-induced flashover predictions and implies that each of them contribute something unique to the models prediction capabilities

The relative importance test provided an analysis of the sensitivity of each of the variables in the logistic regression and assigned a relative importance (%) to each. Figure 2 illustrates the results from the relative importance test with the predictor variables on the Y axis and the relative importance (%) on the X axis. Wind direction was assigned the highest relative importance (primary splitter) by the LR analysis, followed by wind speed with an 80% importance. Relative humidity scored a 50% importance while air temperature was the lowest of the four variables, with a 20% relative importance.

The results from the logistic regression importance test indicate that wind direction is strongly correlated to the "True" flashover target category. Together with wind speed the two variables seem to outweigh the importance of air temperature and relative humidity. Wind direction is a

much more complex variable compared to the other three variables. A 0 degree angle does not simply relate to a low flashover probability or a 360 degree angle to a high flashover probability. The non-linear nature of the LR might be better for describing the relationship between wind direction and fire-induced flashovers.
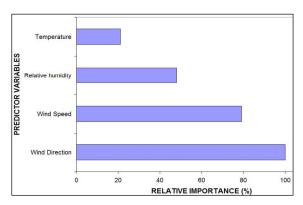
Figure 1. Relative Importance test on predictor variables

Development of the Fire-induced Flashover Probability Index (FIFPI)

Based on the results obtained from the evaluation of the different models the LR was used to calculate the fire-induced flashover prediction model with air temperature, relative humidity, wind speed and wind direction as the main predictor variables. The logistic model formula computed the probability *P* of a "True" flashover based on the predictor variables.

A maximum likelihood analysis was performed which provided the probability coefficients (parameters) for each of the predictor variables, which enabled the calculation of the FIFPI according to the logistic model formulae:

$$FIFPI = \frac{1}{(1+\exp(-(196+6.24*RH+0.0505*T+0.557*WD-0.909*WS)))}$$

Where RH describes the relative humidity in %, T the air temperature in degree Celsius, WD the wind direction in degrees from North and WS the wind speed in m s^{-1}.

Validation of the FIFPI model against existing Fire Danger Indices

The FIFPI model prediction capability was tested against the derived fire danger index variables. This data set included three variations of the Lowveld Fire Danger Index (LFDI) currently being used by Eskom, and the McArthur Grassland Fire Danger Index (MK 4) from Australia. A LR model was used to validate the FIFPI model against the LFDI and MK 4 models by calculating the variable importance as well as a confusion matrix. These tests indicated the significance and contribution of each of the models to the prediction of a "True" flashover.

Table 2 illustrates the relative importance of the different models to predicting a fire-induced flashover. The FIFPI achieved a 100% relative importance, followed by the Australian MK 4 model with 85% importance. The LFDI 2 and LFDI 3 models scored lower importance values of 56% and 54%, while the LFDI 1 model scored a very low 12%.

Table 2. Relative Importance between FIFPI and Fire Danger Indices

Prediction models	Relative importance (%)
FIFPI	100
MK 4	85
FDI 3	56
FDI 2	54
FDI 1	12

A multiple regression analysis was performed to determine the correlation between the different models as well as the relationship with the flashover (target) data. Correlation is a measure of the association between two variables (FIFPI and FDI's), indicating if the value of one variable changes reliably in response to changes in the value of the other variable. The correlation coefficient can range from 0 to 1.0, where 0 indicates a low correlation and 1 a very strong correlation.

Conclusion

This study has shown that modeled weather forecast data and satellite based fire products can be used to provide predictions of fire-induced flashovers underneath Eskom transmission lines. The FIFPI was able to correctly predict 98.9% of the flashovers in the validation data set using the LR model. During the assessment each of the variables contributed uniquely to the predictive capabilities of the model as was evident in the rise of the misclassification cost with the removal of any of the four variables.

Wind direction and wind speed was found to be the most important variables causing sharp increases in flashover probabilities, as soon as north westerly winds with wind speeds above $4 \, \text{m s}^{-1}$ were reached. While wind direction was previously seen as only an indicator of other meteorological factors, the study has shown it to also be a unique predictor of fire related flashovers. By including wind direction in the predictive model, the misclassification cost of the flashover prediction model decreased from 4.45% (wind speed, relative humidity and temperature) to 3.87% (wind direction, wind speed, relative humidity and temperature).

The validation study comparing the flashover prediction capabilities of the FIFPI with a number of existing fire danger indices demonstrated the effectiveness and the model to provide improved prediction of dangerous fire weather conditions. The three Lowveld models (LFDI) were unable to provide consistent accurate predictions. The MK 4 model provided the second best prediction capability which could be attributed to the fact that the model is also a LOG function similar to the FIFPI. Linear models such as the Lowveld FDI's seem to have limited capabilities for flashover prediction as demonstrated in this study

References

Aicher, L. 1949. Variations in the Dielectric Strength of Air. *Allis-Chalmers Electrical Review,* Third Quarter.

Anon,. Eskom Annual Report 2003. http://www.eskom.co.za

Cheney, P. & Sullivan, A. 2008. *Grassfires: Fuel, Weather and Fire Behaviour,* (7th ed). Collingwood, Australia: CSIRO Publishing

Frost, P. E., Vosloo, H. & Annegarn, H. 2007. Providing satellite-based early warnings of fires to reduce fire flashovers on south Africa's transmission lines. *Geoscience and Remote Sensing Symposium 2007. IGARSS 2007. IEEE,* Barcelona

Giglio, L. 2003. An enhanced contextual fire detection algorithm for MODIS. Remote Sensing of Environment, 87, pp273-282

Marchuk, G. I. 1974. *Numerical methods in weather prediction,* New York, New York: Academic

Ndabambi, M. & Poolman, E. 2007. Severe Weather Forecasting Demonstration project 9SWFDP). South-Eastern Africa. *RSMC-Pretoria First Progress Report.* Maputo, Mozambique, South African Weather Service

Perlich, C., Provost, F. & Simonoff, J. 2003. Tree Induction vs Logistic Regression: A Learning -Curve Analysis. *Journal of Machine Learning,* 4

Primen 2001. The Cost of Power Disturbances to Industrial and Digital Economy Companies. Madison, Retrieved February 8 2009, from http://www.epriintelligrid.com/intelligrid/docs/Cost_of_Power_Disturbances_to_Industrial_and_Digital_Techn ology_Companies.pdf

SAWS 2006. Summary of data processing facilities and available products at regional specialised meteorological centre Pretoria (South African Weather Service). *Meeting of severe weather forecasting demonstration project - regional subproject RA I.* Pretoria, South Africa.

Sherrod, P. 2003. NLREG Nonlinear Regression Analysis Program. Retrieved on April 6 2009, www.nlreg.com

Sukhnandan A. and D. Hoch.. Fire induced Flashovers of Transmission Lines: Theoretical Models. 6th Africon Conference in Africa, George, 2 October 2002.

Vosloo, H. 2005. The need for and contents of a Life Cycle Management Plan for Eskom Transmission Line Servitudes. Masters Thesis, Department of Geography

INTEGRATION OF IMAGE PROCESSING METHODS FOR FUEL MAPPING

E. Maillé, L. Borgniet, C. Lampin-Maillet, M. Jappiot, C. Bouillon, M. Long-Fournel, D. Morge,
M. A. El Gacemi, D. Sorin

Cemagref, Centre of Aix-en-Provence, Mediterranean Ecosystems and Risks Reasarch Unit, Le Tholonet, 13612 Aix-en-Provence, France. Eric.maille@cemagref.fr; Marlene.long@cemagref.fr

Abstract

Fuel mapping is a key activity for forest fire risk management. It is based on remote sensing images processing methods.

Spatial patches of fuel types are complex and highly heterogeneous spatial entities. Complexity of fuel types, in relation to their remote sensing-based mapping problem, is classified in four sorts (Borgniet 2009): purely spectral complexity, i.e., complexity of the relationship between fuel types and spectral signatures, spatial heterogeneity of fuel types spectral signatures, spatial horizontal structures of fuel types, and fuel types vertical structure heterogeneity. Some methods are developed to solve each kinds of complexity: pixel based spectral methods, texture analysis based methods, object based methods and 3D analysis methods. On an operational point of view, most of the methods are mixed. But it is not possible to propose one unique method able to produce a fuel map valid in any context with the same parameters. Proposed methods are context dependent and might be complementary in order to solve the global problem of fuel mapping in a given geographical and ecological context. They are usually implemented in one specific software environment.

This lead us we choose an open knowledge based system, opposed to a closed processing solution. The system is aimed at helping the user to build a global successive processing approach that we call a "demarche", in order to better respond to his needs.

Conceptual specification of the system is based on the model integration paradigm, in which methods are represented by models. In a first stage, the coupled DEV'S formal system (Ziegler 1999) to conceptually specify coherent demarches. In a second stage, semantic integration is aimed at solving semantic heterogeneity between models to be integrated at a conceptual level. It specifies the semantic relationships between concepts handled by the models to be integrated. If semantics (i.e. list of concepts) handled by the models are different, integration will require the specification of models for models integration (Maillé 2008): such models specify the relationship between concepts of the initial models. Finally, syntax integration is aimed at solving heterogeneity of representation terms of information handled by the models to be integrated. It permits models interoperability which allows proper functioning of the resulting model, without referring to its semantic consistence (Müller 2008). Syntax integration might be specified at different abstraction levels: organisational level (architecture), logical level (data models, communication protocols, etc.), physical levels (networks), etc. The specified tool architecture includes a knowledge database of methods and resources, and an expert system for methods selection in relation to the user needs and constraints specification. It is a distributed system, where the different resources, either data or processing systems, are distributed on a network of "nodes". Although the data-base is unique, it is also distributed on the nodes. Selected methods can then be organized into demarches by the user. An executive engine is designed to execute the different methods of the demarche in their respective computer environment, through mediating wrappers.

A research prototype called "Fuel Mapping Methods Integration Platform" (FMMIP) was developed.

Keywords: fuel mapping, remote sensing image processing, image processing integration, decision support systems, forest fire risk

Introduction

Forest fire risk management is one of the major stakes of Mediterranean local territories land planning (Moulignier 2007). Land management decision makers require risk maps and risk models, based on fuels maps. Fuels are vegetal covers, classified in different types in relation to their combustibility (Jounet 2008).

In order to produce risk maps, fuel types have to be mapped using remote sensing images. At the European scale, both fuel typologies and image processing methods used to map them are very different, depending on the context, in particular the ecosystem type, but also the available data and available computer resources to process the images.

In the context of the FIREPARADOX European research project, aimed at proposing a generic forest fire risk mapping method valid all over Europe, different fuel mapping methods were proposed by the different partners, adapted to particular contexts and using specific images available on their zone of interest. Moreover, most of the methods don't lead to a final fuel type map, but to some spatial variables useful to assess the combustibility of the vegetal cover: cover ratio, vegetal height, biomass, etc. As a result, it was not possible to propose only one unique method valid all over Europe to map the whole diversity of fuels.

That is why we proposed an integration solution (Maillé 2008) that aims to articulate different fuel mapping methods in a global processing *demarche*, as well adapted as possible to the user working context (Borgniet 2009). It is a distributed solution, where methods are assessed in relation to the user specified context, and then can be associated and sequentially executed in their respective computer environment. The solution was developed as a research prototype called "Fuel Mapping Methods Integration Platform" (FMMIP).

In the first section of this paper, we quickly describe different images processing methods problematic for fuel mapping. The second part describes a general architecture for a fuel mapping method integration framework and its different components. Finally, we present the implementation of the FMMIP, and an example of use of the tool.

Images processing methods for fuel mapping

Complexity of fuel mapping by using remote sensing image is related to the complexity of objects to be detected. So image processing methods are designed to try to solve the different levels of complexity. Four types of complexity of fuel types are specified, in relation to their remote sensing based mapping problematic (Borgniet 2009):

- *"purely spectral complexity"*: two different fuel types might have very close spectral signature.
- *"The spatial heterogeneity"* of the spectral signal, for one given fuel type (texture).
- *The spatial complexity of fuel types themselves*: fuel types have spatial horizontal structures that determine their fuel characteristics.
- *The vertical complexity of the fuel types:* fuel characteristics of a fuel type are highly determined by the vegetation stand "structure", i.e. the description of the grass, bushy and trees strata. Simple remote sensing methods can only "view" the vegetal cover, i.e. highest stratum. Advanced remote sensing methods and tools have to be used in order to map stands vegetation structure.

The different methods studied by the different partners of the project permits to solve or to bring elements in order to contribute to solve one or more components of the complexity of fuel mapping.

1.1 Notion of "methods"

Methods are defined as **series of several image *atomic processing***. Methods were developed by partners using particular input data, generally satellite images, and are so often both *data dependent* and *Software dependent (if implemented)*. Moreover, methods are often applied to particular land cover fuel (for example, continuous forest land, bushlands, etc.): so several methods might be required to map the whole area fuel. Finally fuel mapping methods always depend on the geographical context.

We distinguish four groups of methods:

- spectral methods *(or "pixel based methods"), aimed at solving spectral complexity, usually* based on multi-spectral classification processing and/or on spectral indexes calculation (NDVI, RVI, SAVI, …).

- textural methods are convenient to solve textural complexity of fuel types. This is a key element of *continuous* or *dense discontinuous* fuel type mapping that have a regular (not structured) heterogeneity (forest, scrubland, etc.)

- Objects oriented methods are convenient to solve horizontal spatial structure complexity. They aim to detect *geographical* objects in relation to some of their spectral, textural, or geometrical attributes (shape, size, etc.). These methods are more particularly dedicated to *discontinuous horizontally structured* fuel type detection.

- 3D methods are convenient to solve to solve vegetal vertical complexity. At least three kinds of 3D methods were developed: phtogrammetric, LIDAR based and particular spectral methods (correlation between some vegetal indexes values (RVI) and some vertical structure characters).

Finally, most of the methods studied by the different partners of the project are mixed. But it appears that it is not possible to propose one unique method able to produce a fuel map valid in any context with the same parameters. Proposed methods are context dependent and might be complementary in order to solve the global problem of fuel mapping in a given geographical and ecological context.

This lead us we choose not to provide a closed processing solution, but an open knowledge based system, which aim to help the user to build a global demarche of successive processing, in order to better respond to his needs. We present the architecture of the integration framework in the next section.

The Fuel Mapping Method Integration Platform (FMMIP)

The fuel mapping methods integration platform is an open knowledge based system, aimed at helping the user to build and operate a global demarche by articulating different *methods* in order produce a fuel map adapted to his context and responding to his needs. Context parameters might concern geographical variable related to the user's working zone (location, geology, climate, etc.) but also user's available data and available computer resources, in particular commercial image processing or spatial analysis software. Needs concerns the targeted produced (targeted fuel typology, scale of the fuel map) and the previewed usage: (global risk calculation, operational planning, etc.).

The demarche is to organise different methods into a processing framework, allowing the user to take into account his different constraints and specificities. Then, the global demarche is not unique, because it has to be adapted to the use of the fuel map. A global demarche articulates different methods with other standard geo-data processing in relation to the different available resource (Figure 1).
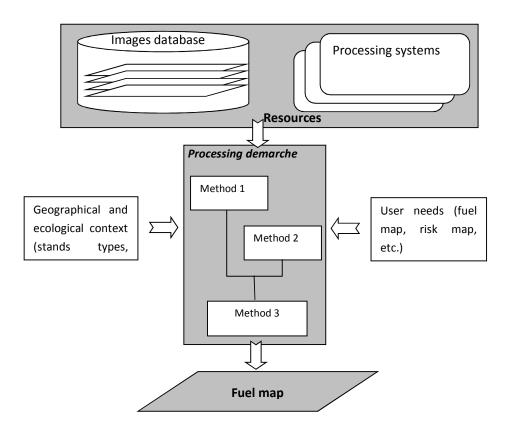
Figure 1. Processing demarche combining several processing methods

In this purpose, the fuel mapping method integration platform manages and operates *resources*. Resources are either geo-data or geo-data processing systems. For example, implemented methods are considered as geo-data processing resources. Resources might be open access or limited access. Most of the geo-data used, in particular satellite images, are limited access resources because the user must have license rights to process them. Commercial software dependent implemented methods are also limited access resource, because of the required license to use the commercial software.

In order to access to limited access resources, particular agreements will have to be passed between the platform user and the owner of the resource.

1.2   *The FMMIP "nodes"*

The fuel mapping methods integration framework is composed of a network of FMMIP "nodes". Nodes architecture is structured by a kernel surrounded by peripheral software modules, and linked to a knowledge database (Figure 2). Software modules are image processing or GIS software, and associated *methods* implemented in the macro-language of the given software.

The nodes kernel is composed of three main components: a driving Graphical User Interface, an *expert system* engine, that help the user to choose the best resources to use in relation to his needs, and an *executive engine* that can *operate* the resource, if possible. In particular, it can execute *methods* by operating their implementing software. To do so, the executive engine accesses the software modules through wrappers (Figure 2).
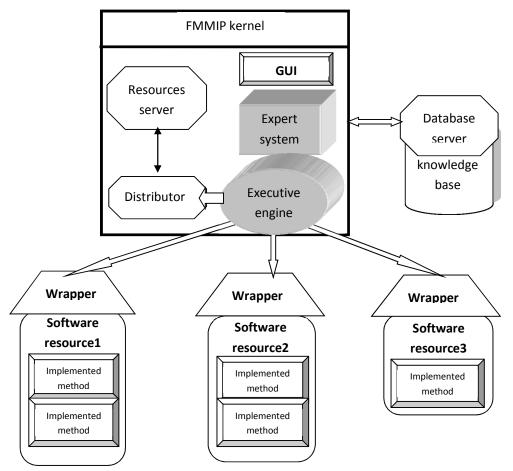
Figure 2. A FMMIP node architecture

The *knowledge database* gathers information about available resources. It contains all information about the resources (location, accessibility, operability, etc.), but does not contain any resource i.e. data or data processing software. Most of the kernel components might get information from the database server.

Moreover, each node kernel might be endowed with three components dedicated to the system distribution: a database server, a process server and a distributor. We develop the role of these different components in the next part 3.3 of this section.

1.3   *Functioning scheme of a FMMIP node*

Figure 3 presents the components used in a standard use case of the FMMIP.

Nodes of the mapping methods integration framework might communicate through a wide area network (WAN) like the Internet network, in a distributed service oriented architecture. Node can be addressed by their URL. Any node can be client, server or both. Moreover, a FMMIP node might be a *resource* server, so that it offers processing services or data providing services, or/and a *knowledge server* so it can offers read access to its node database. Distribution is ensured by the "Distributor" component of each node, that takes in charge the "*client*" role, and the "Resources server" that plays the role of the *server*.

When the executive engine of *node 1* has to execute a particular process on some given data, it invokes the "Distributor". This one queries the local knowledge data base to check if all data and processing resources are available locally. If no, it finds the URL of a FMMIP *node 2* where data or processing resource might be found. So the "Distributor" can invoke the remote "Resource server" of *node 2*. The "Resource server" checks into its own node database if the resource is available on *node 2*. If yes and the required resources are data, the resources server temporarily uploads the data back to *node 1*. If the required resources are processing resources, the Resources server temporarily downloads data from *node 1* to *node 2*. Then it asks the Executive engine to process these data through the convenient wrapper. Finally, it uploads back the result data to node 1.

The required resource might also not be locally available on *node 2*. In that case, the *node 2*'s Resource server should find in its node database the URL of a remote *node 3.* It will the invoke *node 2* Distributor, so that the process can be repeated recursively.

The prototype implementation and validation

A prototype of the FMMIP platform was developed in the context of the Fireparadox project. It permits to build and share multi-environment processing demarches based on specific methods developed by different partners of the project.

The platform is developed around a kernel and wrappers in the JAVA language, by using the respective software macro-languages (Gacemi 2009). For example, in order to communicate with the image processing software ITT ENVI©, used to operate some "object oriented" methods, the IDL language is used. Many image processing software also use script-like macro-language (ESRI ArcInfo© AML, ERDAS Imagine© batch, etc.). The GIS software ESRI ArcGIS language is VBA© (Visual Basic for Application) or Python©. A specialised image processing tool kit, called the "fuel mapping resources tool kit" was also developed in C++ language, for open access standard image processing (Sorin 2009). This software uses standard system script macro-language.

The node databases are managed by the shareware database server POSTGRES. So they might not be "*local*", but can also be remote. The node can use, for example, a centralised shared knowledge database. However, the database related to a node is unique for each node, during a FMMIP session.
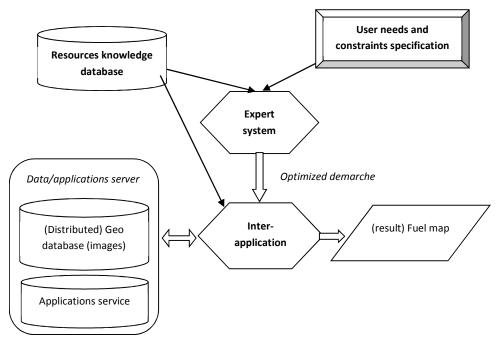
Figure 3. Functioning scheme of a FMMIP Node
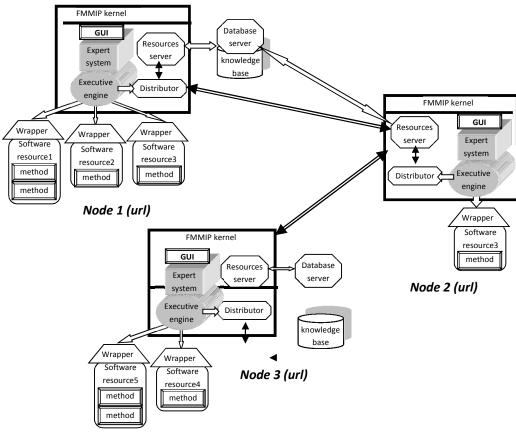
Figure 4. The FMMIP framework distribution

Conclusion

We propose a fuel mapping system that aims to take into account the complexity of the fuel geographical object definition and typology on one hand, the wide diversity of geographical and ecological contexts in which fuel might be mapped , and finally the diversity of resources potential users can have access to. To do so, the system is organised around the concept of method and demarches that is processing sequence, based on specific data type, adapted to a particular context, and aiming to detect a specific fuel typology (or a particular sub-set of fuel types of a universal fuel typology).

The prototype being implemented is composed of several components: a system kernel, that includes a knowledge database and an expert system to choose the best adapted methods in relation to requirements, an open access resource toolkit that provide common processing algorithms, and different methods implemented on their particular software environment. All these elements have to be able to communicate, through an adapted distributed architecture. Potential distribution of this architecture makes possible a physically distributed system, based on a shared method knowledge database, but also shared images database.

References

Borgniet, L., Maillé, E., Long, M., Capel, A-C., Bouillon, C., Morge, D., Ganteaume, A., Lampin-Maillet, C., Jappiot, M., Curt, T., Machrouh, A., Sesbou, A., Mantzavelas, A., Apostolopoulou,I., Partozis, T., Gitas, I., Marell A., Cassagne N., Pimont F., Rigolot E., Morsdorf F.,Koetz B., Allgower B. 2009. Development of an easy to use tool to recognize and mapfuel models: Deliverable 5.1-6 of the Integrated project "Fire Paradox", Project no. FP6-018505, European Commission, 107 p.

Capel A.C. 2008. Gray Level Coocurence Matrix Tool (GLCMTool), Manuel d'utilisateur, *Cemagref*, UR Ecosystèmes Méditerranéens et Risques, Aix-en-Provence, F

Gacemi M. A. 2009. "Spécification et développement d'une plateforme d'intégration de méthodes de traitement d'image pour la cartographie du combustible", rapport de stage, Ecole Nationale des Sciences Geographiques, *Cemagref*, UR Ecosystèmes Méditerranéens et Risques, Aix-en-Provence.

Journet S. 2008. Caractérisation et cartographie du combustible dans les interfaces habitat/forêt., Mémoire de Master II EGEPM Évaluation et Gestion de l'Environnement et des paysages de montagne, *Cemagref* Aix-en-Provence, 120p.

Lampin-Maillet C. 2009. Caractérisation de la relation spatiale entre organisation spatiale d'un territoire et risque d'incendie : Le cas des interfaces habitat-forêts du sud de la France Thèse de doctorat en Géographie Analyse spatiale de l'université de Provence, 321p.

Maillé E. 2008. "Intégration conceptuelle et opérationnelle de modèles spatio-dynamiques, Application à la dynamique du risqué d'incendie de forêt", Thèse de doctorat, Laboratoire des Sciences de l'Information et des Systèmes, UMR CNRS 6168, Université Paul Cézanne Aix-Marseille III, F., *Cemagref*, UR Ecosystèmes Méditerranéens et Risques, Aix-en-Provence, F

Moulignier A. (Dir) 2007. "Prévention des incendies de forêt", Dossier de presse, Direction Générale de la Forêt et des Affaires Rurales, Ministère de l'Agriculture et de la Pêche, Paris, F.

Sorin D. 2009. "Spécification et développement.d'une solution de traitements d'images satellites pour la cartographie du combustible, dans le cadre du projet FIREPARADOX", rapport de stage, Institut Universitaire de Technologie d'Arles, *Cemagref*, UR Ecosystèmes Méditerranéens et Risques, Aix-en-Provence.

FUEL TYPE MAPPING IN THE MEDITERRANEAN REGION OF NORTH LEBANON USING OBJECT-BASED IMAGE ANALYSIS OF ASTER IMAGERY

G. H. Mitri*, M. Nader, L. Salloum

*Institute of the Environment, University of Balamand, Lebanon; Faculty of Science, University of Balamand - P.O.Box: 100, Tripoli - Lebanon. *Corresponding author: george.mitri@balamand.edu.lb*

Abstract

Forests and Other Wooded Land in Lebanon are a unique feature in the semi-arid environment of the Eastern Mediterranean. Until 2006, they covered approximately 24% of the overall area of Lebanon. The forests are di-vided into three main classes, namely mixed forest, broadleaves, and coniferous. The Other Wooded Land is di-vided into the following classes: coniferous shrubs, broadleaved shrub, mixed shrublands and grassland with trees. Like other Euro-Mediterranean countries, forest fires have been especially damaging in Lebanon in recent years, representing one of the most important elements that contributes to the destruction of Lebanon's natural resources. Most recently, a National Strategy for forest fire management was officially endorsed by the Govern-ment of Lebanon. One of the main activities of the National Strategy is to develop a fuel management plan aim-ing at reducing the highly flammable biomass. Most commonly, fuel maps in the Mediterranean are generated from remote sensing data, mainly, medium resolution sensors such as Landsat data and Very High Resolution sensors such as IKONOS data. The aim of this work was to present a classification approach to generate fuel type maps in the Eastern Mediterranean using ASTER imagery. The Prometheus fuel type classification system which is adapted to the ecological characteristics of the European Mediterranean basin was adopted. Field visits for the recognition of different fuel types were conducted. The field data were used as ground-truth dataset to train the classification model and to assess the classification results obtained for the study area. The Object-Based Image Analysis (OBIA) approach was used for fuel type mapping. This involved three steps, namely, image segmentation, object training and object classification. The process resulted in the separation of six fuel type classes. Varying degree of accuracy levels among the different fuel type classes was preliminary achieved. The results showed that the use of spectral and spatial information of ASTER imagery in OBIA allowed obtaining satisfactory results in extremely heterogeneous vegetated areas (70% of overall accuracy). Future work will involve 1) improving the accuracy of the classification results, 2) testing the transferability of the developed approach to map fuel types in different areas in the country, and 3) comparing the results with those derived from studies conducted in other Mediterranean countries.

Keywords: Fuel type mapping, the Mediterranean, Object-Based Image Analysis, ASTER

Introduction

Forests in Lebanon are a unique feature in the semi-arid environment of the Eastern Mediterranean. Until June 2006, they covered along with Other Wooded Land approximately 24% of the overall area of Lebanon (Mitri and Elhajj 2008). Increasingly, Lebanon's forests, which include remnants of valuable broad-leaved trees, conifer forests and evergreen trees that cover the Lebanese mountains in patches are exposed to degradation due to fires. Forest fires have been especially damaging in Lebanon in recent years, representing one of the most important elements that destroy Lebanon's forest cover. This has given rise to concern at the national and international levels. In response to the increasing number of fires in the country, a National Strategy for forest fire management was officially endorsed by the Government of Lebanon in 2009 (Mitri 2009). The provision of valuable information in relation to fuel type classes is a process that was essentially highlighted in Lebanon's National strategy for forest fire

management. The development of a fuel management includes the adoption of an operational mapping of fuel type.

Fuel type is considered to be an important factor in pre-fire planning. In addition, fuel maps are essential for computing fire risk assessment and simulating fire behaviors and intensity across a landscape (Riano et al. 2002). Fuel maps are essential to fire management at many spatial and temporal scales. Fire managers have tried to summarize the physical parameters and spatial distribution of fuel in different classes also known as "fuel models" (Burgan and Rothermel 1984). The spatial distribution of the fuel characteristics can be displayed as fuel type maps. The Prometheus classification system is considered to be better adapted to the Mediterranean ecosystem (Riano et al. 2002, Lasaponara et al. 2006).

Extensive field efforts are required to update fuel type maps due to the temporal dynamism of fuel conditions. Remote sensing multispectral data proved to be an effective source of information for use in fuel type mapping at different levels, namely, regional and local (Chuvieco 2009).

Several satellite sensors have been used in the last decades for fuel type mapping. Satellite images such as NOAA- AVHRR (McKinley et al. 1985), Landsat-TM (Cohen 1989, Riaño et al. 2002, van Wagtendonk and Root 2003), Ikonos (Giakoumakis et al. 2002) and QuickBird (Arroyo et al. 2006) were employed. Most of the techniques that were employed in fuel type mapping have been based on differences within spectral information. The use of spatial information was mainly adopted in the case of Very High Spatial resolution imagery. Object-Based Image Analysis (OBIA), which is based on a fuzzy concept, is an approach that uses not only spectral information but also spatial information (Mitri and Gitas 2010). Segmentation, the first step in OBIA, involves merging the pixels in the image into image object primitives called objects or segments with a certain heterogeneous and homogeneous criterion. This step is critical because segmentation generates the objects that will be treated as a whole in the classification.

The aim of this study was to develop an OBIA model for fuel type mapping in the Eastern Mediterranean using ASTER imagery. The specific objectives were:

1. To adopt and adapt the Prometheus system in the classification process of the ASTER image; and

2. To assess the accuracy of the results using field data.

Study area and dataset description

The study area is the central forested land of North Lebanon (Fig. 1). Its surface area is 145 km2 extending from 35º51'42'' to 36 º 0'27'' East and 34 º 17'27''to 34 º 22'56'' North. Elevation ranges from 300 m to 1700 m (300 - 1000 m in the main area of interest). The major forest species, namely Pinus brutia and Quercus calliprinos often form dense stands with a canopy cover ranging from 10 to 80%. In addition to the forests, other types of Mediterranean vegetation, such as maquis and garrigue, are also present. An ASTER image captured on 6 September 2010 was obtained. The first three bands, namely Band 1 (0.52–0.60 μm), Band 2 (0.63–0.69 μm), and Band 3 (0.78–0.86 μm) were employed. In addition to the satellite image, fuel type field measurements were recorded involving plots of 30x30m. Measurements such as

the height of trees and shrubs, the height of grass and the thickness of litter and the percentage coverage of each were recorded. In addition, GPS coordinates were recorded for each plot.

Figure 1. Location of Lebanon in the Mediterranean (left), and location of the study area in Lebanon (right)

Methodology

1.1 *Image segmentation*

The strategy before classification of the ASTER image was to create a segmented image (Mitri and Gitas 2010). The segmentation of the ASTER image was generated by adjusting the parameters of scale and by using equal band weights. The composition of homogeneity criteria in the employed algorithm for segmentation was set to high values for colour criterion (90%) and low values for the shape criterion (10 %). The reason for this is that for most cases the colour criterion is the most important one to create meaningful objects; it defines to which percentage the spectral values of the image layers contribute to the entire homogeneity criterion, as opposed to the percentage of the shape homogeneity. A scale of 10 was selected for the segmentation of the image. The scale parameter here is an abstract term which determines the maximum allowed heterogeneity for the resulting image objects.

1.2 *Classification*

First, a classification scheme was developed. The creation of classes in the scheme was determined by the "Prometheus" fuel type classification system (Lasaponara et al. 2006). The main problem lies in the detection of the understory that may exist in a forest area. As such, the last 2 classes can be condensed into 1, as satellite imagery such as ASTER are not expected provide enough information for such a detailed classification. Eventually, a classification scheme resulted in two parent classes, namely, "no vegetation" and "vegetation". Six subclasses were attributed to "vegetation" as follows: "fuel type 1", "fuel type 2", "fuel type 3", "fuel type 4", "fuel type 5", and "fuel type 6". Fuel type 6 (tree stands >4m with medium surface fuels and shrub cover > 30%) and fuel type 7 (tree stands > 4m with heavy surface fuels and shrub cover >30%) in the Prometheus classification system were merged together to form "fuel type 6" in the adapted classification scheme. Second, the segmented image was classified taking into account the devel-oped classification scheme. The parent classes were classified using the normalized-difference vegetation index (NDVI). The Nearest Neighbour Classifier (NNC) was employed for classification of the subclasses, taking into account training objects based on field data. In comparison with pixel-based training, the object-based approach of the nearest neighbour which is adopted in this work requires fewer training samples for each class: one to

two sample objects already cover many typical pixel samples and their variations. Therefore, object samples were selected for each class (two object samples per class) by taking the field survey information into account.

Classification results and discussion

A thematic fuel type map from the ASTER classification model was obtained (Fig. 2). All classes as determined by the "Prometheus" fuel type classification system were represented except for the last two classes which were merged together. After the classification, an accuracy measure, derived on the basis of a comparison of the classification in question with field reference data, was applied. Field-collected data from 92 plots were employed in order to assess the accuracy of the results. The overall classification accuracy was found to be 70%, while the overall Kappa Index of Agreement was 0.583 (Table 1). A closer examination of the accuracy assessment revealed that the classes "fuel type 4" and "fuel type 5" had the lowest accuracies. This confusion could be attributed to the difficulty of depicting small differences between the classes. Overall, the observed confusions could be explained by the spectral overlap among the different classes especially in area affected by topographic effects, canopy shadows, and the illumination conditions. Still, the accuracy assessment of the classification showed very promising results when mapping fuel types in Lebanon using OBIA of ASER imagery, an application that was not tested before in this region.

Table 1. Accuracy assessment

	Fuel type 1	Fuel type 2	Fuel type 3	Fuel type 4	Fuel type 5	Fuel type 6
Producer	0.7	0.75	0.8	0.5	0.625	0.744
User	1	0.6	0.4	0.1	0.789	0.875
KIA/class	0.675	0.735	0.775	0.439	0.527	0.548
Overall Accuracy	**0.706**					
KIA	**0.583**					
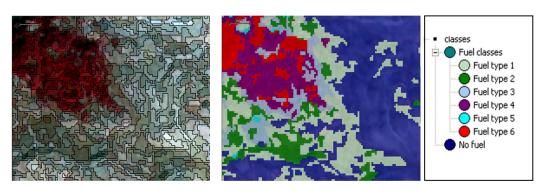
Figure 2. Subset of the segmented image (left) and corresponding subset of the classified image (right)

Conclusion

The result of this work comes in line with the Lebanon's National strategy for forest fire management.
The use of OBIA and ASTER imagery could present an affordable and operational approach for fuel type mapping at the national level. However, further investigations are needed in case of aiming at higher overall classification accuracy (above 70%). In this work, not enough

information is obtained about the forest understory. Conversely, the combination of ASTER imagery with Very High Spatial resolution imagery such as SPOT, IKONOS, and QuickBird would provide the users with the information necessary to recognize each of the seven fuel type classes of the Prometheus classification system. The availability of height information from an active sensor (e.g. LIDAR) of the same area might provide much more detailed information for more accurate classification results at the local level.

Acknowledgements

References

Arroyo, L., Healy, S., Cohen, W. and Manzanera, J. 2006. Using object-oriented classification and high-resolution imagery to map fuel types in a Mediterranean region. Journal of Geophysical Research 11: 1-10.

Burgan, R. and Rothermal, R. 1984. BEHAVE: Fire behavior prediction and fuel modeling system-FUEL subsys-tem. General Tech. U. F. S. Rep. INT-167: 126.

Chuvieco, E., (Ed.) 2009. Earth Observation of Wildland Fires in Mediterranean ecosystems, Springer Heidelberg Dor-drecht London New York.

Cohen, W. 1989. Potential utility of the TM tasseled cap multispectral data transformation for crown fire hazard assessment. ASPRS/ACSM Annual Convention: Agenda for the 90's, Baltimore, MD.

Giakoumakis, M., Gitas, I. and San-Miguel, J. 2002. Object-oriented classification modelling for fuel type mapping in the Mediterranean, using LANDSAT TM and IKONOS imagerv: Preliminary results. Foresf Fire Research and Wildland Fire Safety, Portugal, Millpress.

Lasaponara, R., Lanorte, A. and Pignatti, S. 2006. Characterization and Mapping of Fuel Types for the Mediterra-nean Ecosystems of Pollino National Park in Southern Italy by Using Hyperspectral MIVIS Data. Earth Interac-tions 10(13): 1-11.

McKinley, R., Chine, E. and Werth, L. 1985. Operational fire fuels mapping with NOAA-AVHRR data. Tenth Pec-ora Memorial Remote Sensing Symp.: Remote Sensing in Forest and Range Resource Management.

Mitri, G. (Ed.) 2009. Lebanon's National Strategy for Forest Fire Management. Beirut, Ministry of Environment and AFDC.

Mitri, G. and Elhajj, R. 2008. State of Lebanon's Forests. Beirut, AFDC.

Mitri, G. and Gitas, I. 2010. Mapping post-fire vegetation regeneration using EO-1 Hyperion. IEEE Transactions on Geoscience and Remote Sensing 48(3): 1613-1618

Riaño, D., Chuvieco, E., Salas, J., Palacios-Orueta, A. and Bastarrika, A. 2002. Generation of fuel type maps from Landsat-TM images and auxiliary data in Mediterranean ecosystem. Can. J. For. Res. 32: 1301–1315.

Van Wagtendonk, J. and Root, R. 2003. The Use of multitemporal Landsat Normalized Difference Vegetation Index (NDVI) data for mapping fuels models in Yosemite national Park, USA. International Journal of Remote Sensing 24: 1639–1651.

MAPPING CANOPY FUEL LOAD IN ALEPPO PINE (PINUS HALEPENSIS MILL.) FORESTS IN GREECE USING HIGH SPATIAL RESOLUTION SATELLITE IMAGERY

I. D. Mitsopoulos[1], G. Mallinis[1], P. Stournara[2], A. P. Dimitrakopoulos[1], I. Z. Gitas[1], P. Patias[2]

[1]*School of Forestry and Natural Environment, Aristotle University of Thessaloniki, P.O.Box , 54124, Thessaloniki, Greece*
[2]*Department of Cadastre, Photogrammetry and Cartography, Faculty of Rural and Surveying Engineering, Aristotle University of Thessaloniki, GR-54124, Thessaloniki, Greece*

Abstract

Wildland fires are the most destructive disturbance of the natural lands in the Mediterranean Basin. The abandonment of management practices of Aleppo pine forests in Greece has increased fuel loads and fuel continuity in these ecosystems, resulting in forest stands that are vulnerable to catastrophic crown fires. This study presents an approach to canopy fuel load prediction in Aleppo pine stands at spatial level. Allometric equations for the estimation of crown fuel weight of Aleppo pine (Pinus halepensis Mill.) trees in the Mediterranean Basin were developed based on crown diameter. An IKONOS multispectral image was used originally for LCLU mapping and identification of Aleppo pine stands. Following that, two different approaches were evaluated for individual tree crown recognition and crown diameter measurement using IKONOS imagery. The first one was based on object based extraction of tree crowns using the commercial Cognition software while the second one relied on the use of in-house developed MATLAB routines and a fused IKONOS imagery.

Crown recognition and diameter estimation results were evaluated based on field measurements over a randomly selected sample of Aleppo pine trees. The application of the allometric equations allowed us to extent the remote sensing based information about tree crown diameters, in order to accurately map the canopy fuel load spatial distribution.

Mapping canopy fuel load across landscape provide quantitative fuel attributes for use in crown fire behavior models and fire management in Aleppo pine stands

Keywords: canopy fuel load, crown fire, IKONOS, GEOBIA, fire hazard, crown diameter, Aleppo pine forests

TOWARDS A DYNAMIC BURNING EFFICIENCY FACTOR

P. Oliva[1], E. Chuvieco[2]

[1]Departament of Geography, University of Alcalá. Alcalá de Henares 28801, Spain. patricia.oliva@uah.es
[2]University of Alcala, Alcala de Henares, Spain. emilio.chuvieco@uah.es

Abstract

The proportion of biomass consumed by the fire is commonly named Burning efficiency (BE) or combustion completeness (CC). Traditionally, this parameter is assumed constant for each vegetation or fuel type, which im-plies that the fire has consumed equally each fuel complex. However, it is well known that inside a burned area there are different levels of burn severity, depending on fire behaviour. Consequently, the same fuel type may be consumed in very different proportions, and BE should be considered as a spatially dynamic variable related to burn severity levels.

The Fire Effects Modeling and Mapping (FEMM) project is carried out in the frame of the Changing Earth Sci-ence Network initiative (http://due.esrin.esa.int/stse/index.php) of the European Space Agency (ESA). This pro-ject aims to test and validate methods to estimate spatial distribution of burning efficiency from burn severity mapping, using several study sites in Europe. This estimation will be based on images acquired by the ENVISAT-MERIS sensor, which has a spatial resolution of 300 meter (approx.). This sensor compensates the lack of SWIR bands with narrow and frequent spectral bands in the visible and near infrared spectral regions.

The study area is located in Teruel (Spain) where a large fire occurred in 2009. The fire severity map of the area was computed and validated obtaining a R2 of 0.95. To estimate BE, the classification of burn severity values was reduced to three classes: low, medium and high. The minimum and maximum values of burning efficiency by vegetation type found in the literature were used to define the low and high severity classes. The medium burning efficiency value was computed by interpolation. The results were compared with the biomass loss estimated by means of decrement of LAI in the burned area.

The results of this study highlighted the need of a spatially variable burning efficiency, since this simple approach revealed how variable the BE can be inside a single fire.

Keywords: Fire severity, Burning Efficiency, ESA

Introduction

Biomass burning due to forest fires is a major source of greenhouse gases emissions and a significant factor in the carbon cycle. In order to quantify the amount of greenhouse gasses (GHG) released to the atmosphere the equation proposed by the IPCC (2006) (Intergovernmental Panel on Climate Change) is normally used,

$$L_{FIRE} = A \times M_B \times C_f \times G_{ef} \times 10^3$$

Where L_{FIRE} is the volume of GHG released in a fire (ton), A is the area burned (m^2), M_B is the biomass available for combustion (Mg/m^2), C_f is the burning efficiency or proportion of that biomass that is actually consumed (dimensionless), and G_{ef} is the emission factor of each GHG (g/kg of dry matter burned).

Burning efficiency (BE) is defined as the proportion of biomass consume by the fire. Most of studies used a constant BE value by vegetation type assuming that the cover has been completely consumed by the fire (French *et al*. 2004). However some authors pointed out that BE factors should be considered a dynamic variable instead (Sá *et al.* 2005).

The project Fire Effects Monitoring and Mapping (FEMM) aims to estimate a dynamic burning efficiency factor based on the burn severity maps previously obtained (Oliva and De Santis 2010). Here we present the first approach to the estimation of a dynamic BE factor.

Study area and input data

Several large fires occurred in Mediterranean Europe during 2009 fire season. One of them was selected due to the large surface affected by the fire and the potentiality to find a wide range of severity levels within it. The forest fire occurred in Teruel (northwest of Spain) burned almost 6315 ha of pine forests, mixed forests, shrublands and croplands. This fire started the 22nd of July by lightning and was completely extinguish after four days.

MERIS FR level 1b data were used in this study. This sensor measures the solar radiation reflected by the Earth at a spatial resolution of 300 meters in 15 spectral bands between 390 nm and 1040 nm (Bézy *et al.* 2000). The image selected was dated on the 25th of September 2009. The software SCAPE-M (Guanter *et al.* 2008) was applied to obtain atmospherically corrected reflectance.

In this study we used the GlobCover vegetation map to identify the vegetation covers in the study area. This map was produced from MERIS data, so it has a spatial resolution of 300 metres. Therefore, it facilitated the overlapping with our MERIS data.

Methodology

1.1 *Burn severity estimation*

Burn severity was estimated by means of the simulation model developed by De Santis *et al.* (2009). These authors proposed the inversion of two linked Radiative Transfer Models (RTMs), PROSPECT and GeoSail (De Santis and Chuvieco 2009). The model was composed by a *Look-up-table* of 30 spectra corresponding to GeoCBI values ranging from 0 to 3. These spectra were organized as a spectral library which provided reference spectra to run a *spectral angle mapper* supervised classification (Debba *et al.* 2005; Krusse *et al. 19*93) of a single post-fire image. The result was a burn severity map, in which a corresponding GeoCBI value was assigned to each pixel. This model was applied in Landsat-TM and MERIS data. Landsat-TM data were validated with field measures and were used then to validate the MERIS data (Oliva and De Santis 2010).

The validation results of the MERIS burn severity estimation showed values of the coefficient of determination higher than 0.92 with a slope of the regression line higher than 0.9 (Oliva and De Santis 2010). Those results proved the potential ability of MERIS data to estimate burn severity levels.

1.2 *Burning efficiency estimation*

After a detailed bibliographic search of burning efficiency values, we found just a few of them able to be adapted to the Mediterranean ecosystem (i.e., Deeming *et al.* 1997; IPCC 2006; Wiedinmyer *et al.* 2006).

In this first approach to burning efficiency estimation we decided to follow Kasischke *et al.* (1995) methodology. Therefore, the burn severity levels were grouped into three categories defining the level of damage produced by the fire: low, medium and high. The BE values were adapted to the levels of damage taking into account the following premises:

Low damage: burn severity values lower than 2.5 means low damage to the tree cover, the shrubland is scorched and the ground is consumed.

Medium damage: burn severity values between 2.5 and 2.8 are produced when ground and Shrubland strata are completely consumed by the fire, and the lower braches of the trees are burned but the higher branches remain unaffected.

High damage: burn severity values higher than 2.8 means leaves and branches of the tree cover are severely affected by the fire. Shrubland and ground are completely consumed.

Minimum and maximum values found in the previous studies were assigned to the low and high damage classes, respectively. The BE value for the medium damage class was computed by interpolation from the previous values. This approach marked the start point of burning efficiency estimation by vegetation type and burn severity level.

Table 1. Burning efficiency values adjusted to damage level

Vegetation type	BE adjusted to damage level		
	Bajo	Medio	Severo
Grassland	0.85	0.9	0.98
Shrubland	0.7	0.85	0.95
Conifer forest	0.25	0.42	0.57
Deciduous forest	0.25	0.4	0.56

Results

Figure 1 shows on the left the vegetation map used as input data and the burning efficiency values attached to the vegetation classes. On the right of figure 1 is displayed the burning efficiency map with the adjusted values to the level of damage presented in table 1. The adjusted BE map shows a higher variability of values inside the burned area.
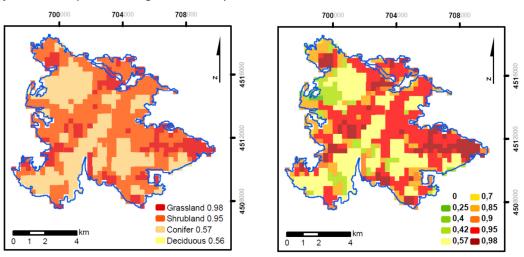
Figure 1. The map on the left shows the vegetation map with their respective burning efficiency values, whereas the map on the right displays the burning efficiency values adjusted to the level of damage.

Conclusions

Traditionally, the emissions estimates assume an average value of BE for each vegetation or fuel type, considering the vegetation affected as completely burnt. However, the different burn severity levels within a fire make evident that the BE should be a dynamic factor instead. We

used the burn severity values as an estimation of the remaining biomass, since the Composite Burnt Index (CBI) takes into account several parameters to estimate the post-fire damage level which describes how the fire affected the vegetation cover (Key and Benson 2005). Then we showed a first estimation of BE that varies spatially according to burn severity values.

The results obtained in this study support those authors who estimated that the use of an average BE value may lead to uncertainties ranging from 23% to 46% (Sá et al. 2005; Ward et al. 1996). From the maps displayed is clear the variation in the BE values and then the implications of this parameter in GHG emissions estimation.

Acknowledgments

References

Bézy, J.L., Delwart, S., Rast, M. 2000. MERIS - A new generation of ocean-color sensor onboard Envisat. ESA Bulletin. 103: 48-56.

Debba, P., van Ruitenbeek, F.J.A., van der Meer, F.D., Carranza, J.M., Stein, A. 2005. Optimal field sampling for targeting minerals using hyperspectral data. Remote Sensing of Environment. 99: 373-386.

Deeming, J., Burgan, R., Cohen, J. 1977. The National fire-danger rating system. U.S. Department of Agriculture, Forest Service.

De Santis, A., Chuvieco, E., Vaughan, P.J. 2009. Short-term assessment of burn severity using the inversion of PROSPECT and GeoSail models. Remote Sensing of Environment. 113: 126-136.

De Santis, A., Chuvieco, E. 2009. GeoCBI: A modified version of the Composite Burn Index for the initial assessment of the short-term burn severity sensed data. Remote Sensing of Environment. 113: 554-562

French, N. H. F., Kasischke E. S., Hall R. J., Murphy K. A., Verbyla D. L., Hoy E. E., Allen J. L. 2008. Using Landsat data to assess fire and burn severity in the North American boreal forest region: an overview and summary results. International Journal of Wildland Fire 17: 443-462.

Guanter, L., Gómez-Chova, L., Moreno, J. 2008. Coupled retrieval of aerosol optical thickness, columnar water vapor and surface reflectance maps from ENVISAT/MERIS data over land. Remote Sensing of Environment. 112: 2898-2913.

IPCC 2006. Agriculture, forestry and other land use. In 2006 IPCC Guidelines for National Greenhouse Gas Inventories. S. Eggleston, L. Buendia, M. Miwa, T. Ngara y K. Tanabe (Eds). Hayama, Japan, Institute for Global Environmental Strategies (IGES). Vol. 4.

Kasischke, E. S., French N. H. F., Bourgeau-Chavez L. L., Christensen N. L. J. 1995. Estimating release of carbon from 1990 and 1991 forest fires in Alaska. Journal of Geophysical Research 100(D2): 2941-2951.

Key, C.H., Benson, N. 2005. Landscape assessment: Ground measure of severity, the composite burn index; and remote sensing of severity, the normalized burn ratio. In Lutes D.C., Keane R.E., Caratti J.F., Key C.H., Benson N.C., Gangi L.J. (Eds.), FIREMON: Fire Effects Monitoring and Inventory System (pp. CD:LA1-LA51). Ogden, UT: USDA Forest Service, Rocky Mountain Research Station, Gen. Tech. Rep. RMRS-GTR-164

Kruse, F. A., Lefkoff A. B., Dietz J. B. 1993. Expert system-based mineral mapping in northern Death Valley, California/Nevada, using the Airborne Visible/Infrared Imaging Spectrometer (AVIRIS). Remote Sensing of Environment 44: 309-336.

Oliva, P., De Santis, A. 2010. Burn severity estimation using MERIS Full Resolution imagery. In Proceedings of ESA Living Planet Symposium. Bergen (Norway). ESA Communications.

Sá, A.C.L., Pereira, J.M.C. Silva, J.M.N. 2005. Estimation of combustion completeness based on fire-indiced spectral changes in a dambo grassland (Western province Zambia). International Journal of Remote Sensing, 26, 4185-4195

Ward, D.E., Hao, W.M., Susott, R.A., Babbitt, R.E., Shea, R.W., Kauffmann, J.B., Justice, C.O. 1996. Effect of fuel composition on the combustion efficiency and emission factors for African savanna ecosystems. Journal of Geophysical Research, 101, 23569-23576

Wiedinmyer, C., Quayle, B., Geron, C., Belote, A., McKenzie, D., Zhang, X. 2006. Estimating emissions from fires in North America for air quality modelling. Atmospheric Environment, 40, 3419-3432

DETERMINATION OF THE FOREST FIRE POTENTIAL BY USING REMOTE SENSING AND GEOGRAPHICAL INFORMATION SYSTEM, CASE STUDY-BODRUM/TURKEY

E. Özelkan, C. Örmeci, M. Karaman

Istanbul Technical University, Center for Satellite Communications and Remote Sensing, Ayazaga Campus, Maslak, Istanbul. emre@cscrs.itu.edu.tr; cankut@itu.edu.tr; muhittin@cscrs.itu.edu.tr

Abstract

Bodrum town, which is located in the southwest Turkey, is in the Mediterranean region and has many unique natural and historical beauties. The construction, the urbanization and the social activities increase and spread very fast in Bodrum. Bodrum has high fire risk potential because of its climatologic, topographic and social features. There have been 10 major forest fires in the last five years in the region. In this research, Bodrum forest areas were studied by using Remote Sensing (RS) and Geographical Information Systems (GIS) techniques. Landsat and Spot satellite images were used to examine past and current status of Bodrum forest areas. The land use classification of the images was made to show the land use temporal change. For creation of risk map and determination of vegetation pattern situation normalized difference vegetation index (NDVI) image was produced. Also land surface temperature (LST) is derived from a thermal band as an alternative meteorological station's data to show the temperature distribution of the study area. To examine the structure of the region's land Aster GDEM digital elevation model was used and slope, aspect and elevation maps were created. The Bodrum fire risk map was produced by using all data in GIS platform. The results clearly show the fire risk potential and the importance of the fire risk map for Bodrum.

Keywords: GIS, remote sensing, LST, forest fire, risk map

Introduction

A Mediterranean touristic county, Bodrum that is famous for the countless beauties, is in trouble with forest fires. Although complete prevention is not possible, it is possible to know the forest fire potential of the region by creating a forest risk map that gives important information for disaster management. The NDVI that is extracted from the infrared visible regional band arithmetic can exhibit the health and moisture contents of the vegetation (Ozelkan et al. 2011). Slope, aspect and the altitude are important topographic parameters that can help identify potential areas for forest fire (Ozelkan et al. 2008) and the distributions of the settlement and roads are key factors at determining fire risk. The meteorological temperature data distribution shows the sensitivity to fire. Using and integrating these data in GIS platform, the fire potential can be shown by a fire risk map. Hernandez et al studied the 1995 fire that occurred in Island in Canary Islands (Spain) (Hernandez et al. 2006). They used the NDVI, Advanced Very High Resolution Radiometer and GIS to create a Fire Risk Dynamic Index (FRDI) over the study area. They exhibited that the relationship between NDVI and FRDI was inversely proportional during the summer of 1995 and this relationship was considered for their existing model. Erten et al. (2004) used Landsat satellite data and topographic maps to create a forest fire risk map for the Gallipoli Peninsula. They showed that integrating parameter such as topography, vegetation type, distance to roads and settlements satellite data in GIS are suitable to create forest fire risk map. Ozelkan et al. (2008) used Landsat satellite data and digital terrain model (DTM) to generate forest fire risk map for Kibriz Stream Canyon where is very hard to interfere during the fire. In this research, Landsat and Spot satellite images were used to

examine past and current status of Bodrum forest areas. For creation of risk map and to see the actual vegetation pattern NDVI image were produced. To examine the structure of the region's topography Aster GDEM was used and slope, aspect and elevation maps were created. The settlement and road maps were produced by using satellite images. Also the temperature distribution was analyzed to associate with the forest fires by using the thermal band of the Landsat image. The Bodrum fire risk map was produced by using all data in the GIS platform.

Study area

Bodrum, which is between 36° 95' and 37° 17' northern parallels, 27° 20' and 27° 80' eastern meridians, is a city in the south-western Turkey. In Bodrum, summers are hot and dry; the winters are mild and rainy. Temperature stands between +43.7°C-12.6°C and annual total precipitation can vary between 1180-414 mm. (Ikiel 2000). Nearly 61.3% of Bodrum was covered with forests but in recent years the forest fires reduced vegetation pattern significantly (URL-1).

Materials and methods

1.1   *Materials*

In this study, multispectral Landsat 5-TM data acquired on 05.08.1986, 10.08.2011 and 08.08.2011 dated Spot5 data were used. Thermal infrared band of 10.08.2011 dated Landsat image was used to obtain actual LST values. Near infrared and visible red bands of Spot image were used to obtain actual NDVI values. Spot 5 image was used to create road and settlement maps. Also Aster GDEM digital elevation model was used to create slope, aspect and elevation maps.

1.2   *Methods*

In this study, unsupervised and supervised classification algorithms were used to classify 05.08.1986 Landsat 5-TM and 08.08.2011 Spot 5 satellite images. The images were grouped as 100 clusters using unsupervised classification method with having number of iterations as 50 and using ISODATA algorithm. After unsupervised classification the supervised classification was applied for both images. The vegetation type was classified using the NDVI. The high NDVI values indicate healthy vegetation, while the low values indicate the unhealthy and non-vegetation areas. (Ozelkan et al. 2008) The NDVI values vary between -1 and 1. The NDVI formula is NDVI= (NIR-RED)/(NIR+RED). To compose NDVI for Spot 5-NDVI=(Band1-Band2)/(Band1+Band2) formula is used. Spot 5 NDVI image was extracted to use as an actual risk parameter. To obtain temperature distribution of Bodrum Landsat 5-TM thermal band was used. The Landsat TM sensors acquire temperature data that is in the form of digital number (DN) with a range between 0-255. The first step is converting the DNs to radiance values using the bias and gain values, specific to the individual scene. $CV_R=G(CV_{DN})+B$ is the formula used to convert DN to radiance where, CV_R is the cell value as radiance, CV_{DN} is the cell value digital number, G is the gain, B is the bias values. The conversion formula radiance to temperature for Landsat 5-TM was $T=K_2/ln((K_1*ε)/CV_R+1)$ where T is Kelvin degrees, CV_R is the cell value as radiance, ε is emissivity (typically 0.95). Also K_1 is 607.76 and K_2 is 1260.56 for Landsat 5-TM

(URL-2). To convert Kelvin values to Celsius=Kelvin-273.15 unit transformation is used. (Ozelkan et al 2011). The settlement and road maps were produced by using Spot 5 images to show the human effect to forest fire as a parameter. AsterGDEM was used and slope, aspect and elevation maps were created in the GIS platform. Forest risk map of the study area was created by performing a multi-criteria analysis by using these data. The parameters taken into account, weights, class and the factor values used for the risk mapping are given in Table1. Risk was calculated according to the formula: RISK: 0.15 * "settlement" + 0.17 * "roads" + 0.10 * "slope" + 0.13 * "aspect" + 0.09 * "altitude" + 0.19 * "NDVI" + 0.17 * "LST"

Results

05.08.1986 Landsat and 08.08.2011 Spot 5 images classification can be seen in Figure1a&b. Dark green represents the wooded, green represents treeless vegetation, black represents non-vegetated and blue represents the water area. In 1986 the wooded area is 39426, the treeless vegetation is 26543, non-vegetated is 1928 and the water area is 2 hectares. In 2011 the wooded is 32758, the treeless vegetation is 28879, non-vegetated is 6407 and the water area is 117 hectares. 6668 hectares decrease of wooded, 2336 hectares increase of treeless vegetation, 4479 hectares increase of non-vegetated and 115 hectares increase of water areas were calculated. When the total area of 2011 was decreased from 1986, the result is 272 hectares that is the products of the coastal and the marine construction. The overall classification accuracy for Spot 5 product is 90% and for Landsat product is %85. The NDVI values that are mostly low can be seen in Figure 2 reflect the vegetation situation clearly. The LST shows that the temperature values totally vary between 30-50 Co (Figure 3). In the study area the slope values are generally not high (Figure 4). The aspect values are generally south and south west (Figure 5). The risk order of the aspect is South > South West > South East > Flat > West > East > North West > North East > North. With increasing altitude, the humidity values decrease which causes quick spread of the fire. The altitude values with a maximum of 860 meters are generally not high (Figure 6). In the study areas the settlement and the road areas are very dense which create very high risk (Figure 7).

Table 1: Risk parameters, weights, classes and factor values.

Parameter	Weight	Class	Factor	Parameter	Weight	Class	Factor	Parameter	Weight	Class	Factor	Parameter	Weight	Class	Factor
NDVI	0,19	No vegetation	2	Aspect	0,13	South	10	Slope	0,1	60-65	10	LST	0,17	0-20	4
		Few vegetation	1			South West	9			70-80	9			20-30	6
		Very dry	10			South East	8			65-70	8			30-40	8
		Dry	9			Flat	7			50-60	7			40-50	10
		Less dry	8			West	6			60-50	6				
		Moist	7			East	5			52-62	5				
		Less Moist	6			North east	3			20-50	4				
		Fresh	5			North west	3			10-20	3				
		Very Fresh	4			North	2			0-10	2				
Distance to Roads	0,17	0-100	10	Distance to settlement	0,15	0-100	10	Altitudes	0,09	0-100	1				
		100-200	9			100-200	9			100-200	2				
		200-300	8			200-300	8			200-300	3				
		300-400	7			300-400	7			300-400	4				
		400-500	6			400-500	6			400-500	5				
		500-600	5			500-600	5			500-600	6				
		600-700	4			600-700	4			600-700	7				
		700-800	3			700-800	3			700-800	8				
		800-900	2			800-900	2			800-900	9				
		900-1000	1			900-1000	1			900-1000	10				

Considering all fire risk parameters (distance to roads, distance to settlement, slope, aspect, altitude, NDVI and LST) a fire risk map is established using the risk formula given in section

"Methods" (Figure 8). The fire risk values are between 1-10, the risk values, spatial and percentage distribution values of the fire risk potential can be seen at Table 2. As a result 54% of the study area is over 5, which means that 36604 hectares area is in fire danger.

Figure1a: Classified Landsat image, Figure1b: Classified Spot image

Figure 2: 2011 Spot 5 NDVI image, Figure 3: 2011 Landsat 5-TM LST image

Figure 4: Slope Map, Figure 5: Aspect Map

Figure 6: Altitude Map, Figure 7: Settlement and road map

Risk Value	Area	Percentage
10	2290,282	3,4%
9	4648,903	6,9%
8	6861,789	10,2%
7	11167,65	16,5%
6	11635,63	17,2%
5	11748,13	17,4%
4	8471,945	12,6%
3	6322,043	9,4%
2	3397,052	5,0%
1	951,489	1,4%
	67494,92	100%

Figure 8: Fire Risk Map, Table 2: Fire risk value, spatial and percentage distribution

Conclusion

Forests are often damaged from fires, disaster management activities have to be focused by using actual risk maps that make disaster management fast and sustainable. RS and GIS are very effective tools to observe the vegetation and in this study, the main problem of the region forest fire risk potential was analyzed using RS and GIS technology by the way of creating fire

risk map. As a result it can be said that, while it is impossible to prevent forest fires, a well-made forest fire map can ensure successful preparedness and rapid intervention.

References

Erten, E., Kurgun, V., Musaoglu, N. 2004. Forest Fire Risk Zone Mapping From Satellite Imagery and GIS a Case Study, International Society for Photogrammetry and Remote Sensing, pp.2-5.

Hernandez, P.A., Arbelo, M., Gonzales Calvo, A. 2006. Fire Risk Assessment Using Satellite Data. Advances in Space Research 37, pp. 741–746. doi:10.1016/j.asr.2004.12.053

Ozelkan,E., Ormeci, C. 2008. Risk Assessment Of Forest Fires By Using Satellite Data With Remote Sensing Techniques, Istanbul, Turkey, EARSEL Volume 0.

Ozelkan,E., Papila, I., Uca Avci, D.Z., Karaman, M. 2011. Drought Determination By Using Land Surface Temperature And Normalized Difference Vegetation Index, 34th International Symposium on Remote Sensing of Environment, Sydney

URL-1, Wikipedia Free Encyclopaedia, 04.07.2011 http://en.wikipedia.org/wiki/Bodrum

URL-2, Landsat DN_to_Klevin, The Yale Center for Earth Observation, 04.07.2011, http://www.yale.edu/ceo

BURNING PROBABILITY ASSESSMENT FOR NORTH-WESTERN SPAIN

M. L. Pettinari[1], M. Finney[2], E. Chuvieco[1]

[1]*Departamento de Geografía, Universidad de Alcalá. C/ Colegios, 2. 28801 Alcalá de Henares (Madrid), Spain.* mlucrecia.pettinari@uah.es

[2]*USDA Forest Service, Rocky Mountain Research Station, Missoula, USA.* mfinney@fs.fed.us

Abstract

Forest fires are a major factor of environmental transformation, playing an important role in land cover change, soil degradation and air quality. Recently, with the growing development of the wildland-urban interface, they also pose an increasing risk to the safety of people and property. Hence, a thorough fire risk assessment is needed to prevent fire occurrence or reduce its negative impacts. In Spain, the largest number of fires occurs in the northwest, specifically in the Autonomous Communities of Galicia and Asturias. One way to address the fire risk is to compute the burning probability of the territory (defined as the number of times each pixel is estimated to burn divided by the total number of years), which would represent its potential to burn.

This paper estimates the burning probability for those regions using the large-fire simulation system (FSim). The system uses historical weather observations, historical fire records and spatial data on fuel structure and topography in order to simulate the occurrence and growth of fires for thousands of "virtual" years.

The simulation was performed at a 250m spatial resolution. Five simulations were run, one for each province within the study area. The Energy Release Component (ERC) was used as a proxy for fuel moisture content. Fire occurrence was stochastically modelled based on the historical fire relationship to ERC. Fire growth was simulated taking into account the fuel model for each pixel, the canopy structure, the topography, and the weather generated from a time-series analysis of ERC to represent daily and seasonal variability and the distribution of wind speed and direction from weather records. The simulation was run for 20,000 years.

The resulting burned probabilities ranged between 0 and 0.1448 for the entire study area. The simulated average burn probabilities for each province were compared to the ones derived from historical records, obtaining mean errors between 6.26% and 94.66%. Some causes of error were detected, related to sharp transitions between provinces and longer than real fire periods, which will be improved in future simulations.

Keywords: Forest fires, Burn Probability, Spain, FSim

Introduction

The importance of forest fires as a source of land cover transformation and greenhouse emissions, amongst other disturbances, has been widely studied (Eva et al. 2000; Langner et al. 2007; Mouillot et al. 2006; van der Werf et al. 2003). In the past decades, the increase of the wildland-urban interface has also increased both the human-caused fires, and the risk those fires pose to the safety of people and property (Syphard et al. 2007; Theobald et al. 2007; Venevsky et al. 2002). These facts show the importance of thoroughly assessing the fire risk potential, in order to alleviate the negative impacts of fires whenever possible, to better allocate fire-fighting resources for protecting people and structures and to reduce burned area. Within Europe, Spain is one of the countries most affected by fires, with more than 450,000 fires in the period 1980-2009, and more than 5 million hectares burned in that period (Schmuck, et al. 2010). And within Spain, the Autonomous Community of Galicia has the highest incidence of fire, with 53,56% of total fires for the period 1996-2005, followed by "Castilla y León" (9,89%) and Asturias (7,76%) (ADIF 2007).

In this project, we selected the Spanish geographical area with the highest density of fires, i.e. the Autonomous Communities of Galicia and Asturias, which are comprised of a total of 5 Provinces. As a method to estimate the fire risk, we calculated the susceptibility of the territory to burn, using the Large-fire Simulation system, also known as FSim (Finney et al. 2011). We selected this methodology because it allows us to integrate the probability of fire ignition with the expected fire behavior, based on real data taken from historical fire and weather records. Furthermore, it calculates the fire risk probability throughout the whole territory, instead of just doing it for one or a few fires, as is the case of other systems like FARSITE (Finney 1998) or FSPro (Calkin et al. 2011).

Methods

FSim calculates the burn probability for each pixel (defined as the number of times each pixel is estimated to burn divided by the total number of years), simulating fire ignitions and fire growth based on historical fire records and weather information, as well as spatial data on fuel structure and topography. The structure of the methodology is shown in Figure 1. Since the probability of a particular pixel to ignite in a particular year is extremely low, we run the simulation for 20,000 years in order to produce moderately stable burn probabilities.
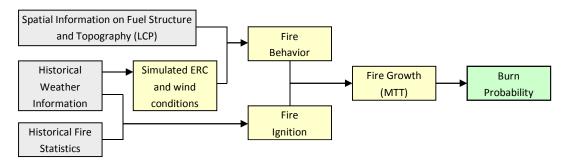
Figure 1. Methodology

For our study, we extracted the fire records from the Forest Fires General Statistic Database (EGIF - Estadística General de Incendios Forestales), which includes the statistical information for all the fires in Spain for the period 1988-2009. The weather records for that period were provided by the Spanish Meteorological State Agency (AEMET, Agencia Estatal de Meteorología, Ministerio de Medio Ambiente y Medio Rural y Marino). One weather station was selected for each of the five provinces in the study area as representative of the weather of that province.

We performed the simulation separately for each province in the study area, using a 250 m resolution grid. To account for fuel structure and topography, we used a Landscape file (LCP) (Stratton 2006) developed in Flammap (Finney 2006), using the following inputs: the elevation, slope and aspect of the terrain where computed from the MDT25 digital elevation model of the Spanish National Geographic Institute (IGN, Instituto Geográfico Nacional, http://www.ign.es/ign/layoutIn/modeloDigitalTerreno.do, last accessed August 2011); the fuel models corresponded to the 13 NFFL models (Rothermel 1983) and were extracted from the Spanish Fuel Model Map (MMC, Mapa de Modelos de Combustibles) developed by the Spanish Forest Fire Defence Area; the stand height, crown bulk density and crown base height were

assigned based on expert knowledge to the predominant tree species extracted from the Spanish Forestry Map (MFE200, http://www.marm.es/es/biodiversidad/temas/montes-y-politica-forestal/mapa-forestal/digital_mfe200.aspx, last accessed August 2011); and the tree canopy cover for each pixel was computed from the Vegetation Continuous Fields, Collection 4, Version 3 product (VCF, http://glcf.umiacs.umd.edu/data/vcf/, last accessed August 2011), which contains proportional estimates for tree cover for each pixel.

The weather data were input into the FireFamilyPlus v4.1 software (http://www.firemodels.org, last accessed August 2011), in order to obtain the Energy Release Component (ERC) fire danger rating index for each day (Cohen, et al. 1985). This ERC was used as a proxy for the influence of fuel moisture on fire behavior. The "virtual" daily ERC for each simulated year were modelled using time-series analysis, which accounted for both daily and seasonal variations in fuel moisture (see Finney, et al. 2011). Wind speed and direction were assigned according to their historical probability for each month of the year. With this weather information and the LCP, fire behavior (rate of spread and intensity of surface fire, crown fire and spotting distance from torching trees) was pre-processed for every province using Flammap, in order to make the fire growth simulation more efficient.

FireFamilyPlus also computed a probabilistic relationship between the daily historical values of ERC and fire occurrence - from the historical record for each province - using a logistic regression equation. Since FSim was intended to simulate only large fires, we set the minimum fire size for each province at the 97th percentile of fire size, with a minimum threshold of 30 ha. The probability of multiple number of simultaneous large fire ignitions in a particular day was also extracted from the historical fire records. The simulated locations of the fire ignitions were determined randomly within each province. Fire growth for each fire was simulated by FSim using the Minimum Travel Time (MTT) algorithm (Finney 2002).

Results

Figure 2 shows the map of the simulated burn probabilities for each pixel, which was computed by FSim as the number of times the pixel burned divided by the number of years of the simulation. The void areas correspond to not forested areas (urban areas or crops).

The highest burn probabilities were found in the province of Pontevedra, with a value of 0.1448, followed by La Coruña (0.1021), Orense (0.1013), Lugo (0.0483) and Asturias (0.0376). The fact that we used a single weather station for each province resulted in the sharp transition of burn probabilities between some of the provinces, as is most evident between Lugo and its western provinces. This error is expected to be solved in the future, with a new version of FSim that will allow for gridded weather information.
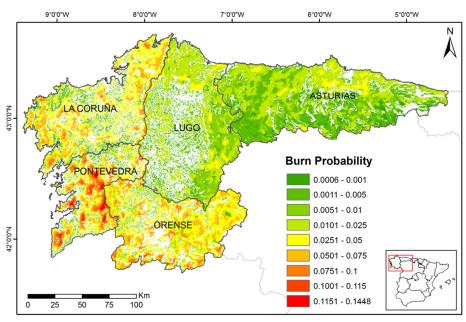
Figure 2. Map of the Simulated Burn Probabilities

Historical burn probability for each province was estimated as the total area burned divided by the total area and number of years. The simulated average burn probability was calculated as the average burn probability of all the pixels within each province. Table 1 shows the values of the probabilities of each province, as well as the mean error of the simulation, which was calculated as:

$$\text{Mean Error}(\%) = \frac{|\text{Historical Burn Probability} - \text{Simulated Average Burn Probability}|}{\text{Historical Burn Probability}} * 100$$

Table 1. Simulated Average Burn Probabilities and Mean Errors for each Province.

Province	Historic Burn Probability	Simulated Average Burn Probability	Mean Error (%)
Asturias	0.010425	0.007777	25.40
La Coruña	0.011054	0.020520	94.66
Lugo	0.006894	0.007326	6.26
Orense	0.021280	0.028762	35.16
Pontevedra	0.020372	0.032845	44.79

In most of the cases, excepting Asturias, the simulated burn probabilities are higher than the historical ones, with the province of La Coruña showing the biggest mean error. This could be partially due to the fact that the simulation is running the fires for much longer periods of time than the historical observations, deriving in much larger fires, and hence increasing the burn probability for the pixels involved. At this point, there is no option to limit the fire period in a way that would represent the Spanish conditions, but this capability will be added to future versions of FSim. Other sources of error could be due to the selection of a particular weather

station for the provinces. Future simulations will include the use of other weather stations, to test their influence in the results, until the gridded option is available.

Since within each province the simulated weather conditions remained constant throughout the territory, the results highlight the importance of fuels and topography on fire behavior and burning probability.

This study is a first approach towards a static fire risk assessment for Spain, based on a probabilistic analysis and fire simulation models. Future work should focus on solving the detected problems, and analyzing the fire size distributions of the modeled fires compared to the historical ones.

Acknowledgements

References

ADIF 2007. Los incendios forestales en España. Decenio 1996-2005. Área de Defensa contra los Incendios Forestales, 106 pages. http://www.marm.es/es/biodiversidad/temas/defensa-contra-incendios-forestales/decenio_1996_2005_tcm7-19437.pdf, last accessed August 2011

Calkin, D. E., Thompson, M. P., Finney, M. A., Hyde, K. D. 2011. A real-time risk assessment tool supporting wildland fire decision making. Journal of Forestry 109 (5): 274-280.

Cohen, J. D., Deeming, J. E. 1985. The National Fire-Danger Rating System: basic equations. General Technical Report PSW-82, 23 pages. last accessed

Eva, H., Lambin, E. F. 2000. Fires and land-cover change in the tropics: a remote sensing analysis at the landscape scale. Journal of Biogeography 27 (3): 765-776. DOI: 10.1046/j.1365-2699.2000.00441.x

Finney, M. A. 1998. FARSITE: Fire Area Simulator - model development and evaluation. Forest Service Department of Agriculture, Rocky Mountain Research Station., Res. Pap. RMRS-RP-4, 47 pages. last accessed

Finney, M. A. 2002. Fire growth using minimum travel time methods. Canadian Journal of Forest Research 32: 1420-1424. DOI: 10.1139/X02-068

Finney, M. A. 2006. An Overview of FlamMap Fire Modeling Capabilities. Fuels management - how to measure success. Portland, Oregon: 213-220

Finney, M. A., McHugh, C. W., Grenfell, I. C., Riley, K. L., Short, K. C. 2011. A simulation of probabilistic wildfire risk components for the continental United States. Stoch Environ Res Risk Assess: doi:10.1007/s00477-011-0462-z

Langner, A., Miettinen, J., Siegert, F. 2007. Land cover change 2002-2005 in Borneo and the role of fire derived from MODIS imagery. Global Change Biology 13: 2329-2340. doi: 10.1111/j.1365-2486.2007.01442.x

Mouillot, F., Narasimha, A., Balbanski, Y., Lamarque, J.-F., Field, C. B. 2006. Global carbon emissions from biomass burning in the 20th century. Geophysical Research Letters 33 (L01801): doi:10.1029/2005GL024707

Rothermel, R. C. 1983. How to predict the spread and intensity of forest and range fires. INT-143, 166 pages. last accessed

Schmuck, G., San-Miguel-Ayanz, J., Camia, A., Durrant, T., Santos de Oliveira, S., Boca, R., Whitmore, C., Giovando, C., Libertá, G. 2010. Forest Fires in Europe 2009. JRC Scientific and Technical Reports, 88 pages. http://effis.jrc.ec.europa.eu/effis-news/89-forest-fires-in-europe-2009, last accessed August 2011

Stratton, R. D. 2006. Guidance on spatial wildland fire analysis: models, tools, and techniques. RMRS-GTR-183, 15 pages. last accessed

Syphard, A. D., Radeloff, V. C., Keeley, J. E., Hawbaker, T. J., Clayton, M. K., Stewart, S. I., Hammer, R. B. 2007. Human influence on California fire regimes. Ecological Applications 17 (5): 1388-1402.

Theobald, D. M., Romme, W. H. 2007. Expansion of the US wildland-urban interfase. Landscape and Urban Planning 83: 340-354. doi:10.1016/j.landurbplan.2007.06.002

van der Werf, G. R., Randerson, J. T., Collatz, G. J., Giglio, L. 2003. Carbon emissions from fires in tropical and subtropical ecosystems. Global Change Biology 9: 547-562.

Venevsky, S., Thonicke, K., Sitch, S., Cramer, W. 2002. Simulating fire regimes in human-dominated ecosystems: Iberian Peninsula case study. Global Change Biology 8: 984-998.

FIELD ESTIMATION OF ASH AND CHAR COLOUR-LIGHTNESS USING A STANDARD GREY SCALE

D. P. Roy[1], L. Boschetti[2], S. W. Maier[3], A. M. S. Smith[4]

[1]South Dakota State University, USA; [2]University of Maryland, USA; [3]Charles Darwin University, Australia; [4]University of Idaho, USA. David.Roy@sdstate.edu

Abstract

Vegetation fires produce biomass combustion residues, with colour varying from dark black char to white mineral ash. The colour-lightness of char and ash combustion residues is a qualitative parameter describing the post-fire condition of burned areas, and has been correlated with the completeness of combustion, fire intensity, and fire duration. Researchers have suggested that visual comparison of combustion residue samples with a standard grey scale would enable reliable combustion residue colour-lightness estimation. This paper illustrates an experiment aimed at assessing if colour-lightness can be estimated using a standard grey scale. Fifteen combustion residue samples with colour-lightness ranging from black char to white mineral ash were collected in the Northern Territory, Australia, and visually evaluated by three individuals using a grey scale. The grey scale scores (0–19) were compared with the mean visible (390 to 830 nm) wavelength combustion residue reflectance (0–1) measured with a portable spectroradiometer. A significant linear relationship between the grey scale scores and the mean visible combustion residue reflectance was found (R^2 = 0.816 with a linear fit, R^2 = 0.936 with a logarithmic-transformed fit). This finding suggests that combustion residue colour-lightness can be assessed in the field using inexpensive grey scales, and that this technique is a suit-able avenue for future research on the field assessment of fire characteristics and effects.

FOREST FIRE RISK MAPS IN A GIS OPEN SOURCE ENVIRONMENT FOR NORWEST OF PORTUGAL

A.C. Teodoro[1], L. Duarte[2]

[1]Geo-Space Sciences Research Centre, Faculty of Sciences, University of Porto, Rua Campo Alegre, 687 4169-007 Porto, Portugal. amteodor@fc.up.pt

[2]Dep. Geosciences, Environment and Land Planning, Faculty of Sciences, University of Porto, Rua Campo Alegre, 687 4169-007 Porto, Portugal. up060306005@alunos.fc.up.pt

Abstract

Forest fires threaten natural resources and even human lives in many areas of the world. Portugal suffers from forest fires. The forecast of forest fire risks can be achieved with the use of fire risk zone maps. The management of these disasters is of importance to both government authorities and the public. Forest fire risk zoning requires integration of natural (topography) and anthropogenic factors (such as roads and settlements). This article presents the results of a research project aimed to producing fire risk maps in a GIS open source environment. The requirements of open source is better quality, higher reliability, more flexibility, lower cost, and an end to predatory vendor lock-in. This project was developed in QuantumGIS (http://www.qgis.org/) platform and the interface is in Python (http://www.python.org/). The thematic and individual maps generated were merged into an integrated risk map. The application, developed through QuantumGIS plugins, incorporates seven procedures under a single toolbar. The production of the forest fire risk map comprises several steps and the production of several maps: probability, susceptibility, hazard, vulnerability, economic value, potential damage and fire risk map. The probability map incorporates the information of the number of fires that occurs in the last 15 years, for each pixel. After, an annual average is calculated (in %), for each pixel. The susceptibility map contains the slope map and the land cover information (Corine Land Cover). The mathematical product of these two maps (probability and susceptibility) is the hazard map. The vulnerability map represents the degree of loss of each element, and varies between 0 to 1.The economic value map contains the price (in euros) of the land (for each pixel) and considers the distance from roads and the distance from settlements. This information is given by the local authorities and is public. The mathematical product of the vulnerability map and economic value map gives the potential damage map. Finally, the forest fire risk map is created multiplying the hazard map by the potential damage map. The forest fire risk map comprises six classes: no risk (black), very low risk (dark-green), low risk (green), medium risk (yellow), high risk (orange) and very high risk (red). This application was tested in three different municipal governments of the Norwest zone of Portugal. The results obtained were similar to the results obtained in a commercial GIS. This application has the advantages of grouping in a unique toolbar all the procedures needed to produce forest fire risk maps and are free for the institution/user. This work presents several contributions for the area of the GIS open source applications to forest fire management.

Keywords: forest fire; risk map; GIS open source; Portugal

Introduction

Forest fire risk zones are locations where a fire is likely to start, and from where it can easily spread to other areas. A precise evaluation of forest fire problems and decision on solutions can only be satisfactory when a fire risk zone mapping is available (Erten et al. 2002). Forest fires are one of the major natural risks in Portugal. Fires occur frequently in Portugal and there is a need for supranational approaches that analyse wide scenarios of factors involved and global fire effects. It is impossible to control nature, but it is possible to map forest fire risk zone and thereby minimise the frequency of fire (Erten et al. 2002).

Geographical Information Systems (GIS) are an important and efficient tool that can be used by local administrations to minimize natural disasters, as forest fires. Thus, GIS technologies have

been used in several fire analyses (e.g., Chuvieco and Congalton 1989; Chuvieco and Sales,1996, Erten et al. 2002). However, these fire analyses were mainly conducted in GIS commercial software.

This paper presents the results of a research project aimed to producing fire risk maps in a GIS open source environment. The promise of open source is better quality, higher reliability, more flexibility, lower cost, and an end to predatory vendor lock-in. This project was developed in Quantum GIS (http://www.qgis.org/) platform and the interface is in Python (http://www.python.org/).

Methodology

The production of the forest fire risk map comprises several steps and the elaboration of several maps (Figure 1). All the maps were produced according to the rules of the Portuguese Forestry Authority (PMDFCI 2008).

The probability map incorporates the information of the number of fires that occurs in the last 15 years, for each pixel. After, an annual average is calculated (in %) for each pixel.

The susceptibility map contains the slope map and the land cover information (Corine Land Cover). The mathematical product of these two maps (probability and susceptibility) is the hazard map.

The vulnerability map represents the degree of loss of an element and varies between 0 to 1 (this value is tabulated and available for each pixel). In other words the vulnerability value represents the ability of each element to recover from a fire event.The economic value map contains the price (in euros) of the land (for each pixel) and considers the distance from roads and the distance from settlements. This information is given by the local authorities and is public. The mathematical product of the vulnerability map and economic value map gives the potential damage map. Finally, the forest fire risk map is created multiplying the hazard map by the potential damage map.
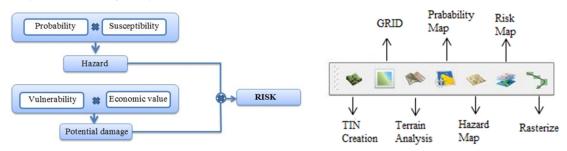
Figure 1. Forest fire risk map procedure steps   Figure 2. Toolbar created

This project was developed in QuantumGIS (http://www.qgis.org/) platform and the interface is in Python (http://www.python.org/). The application, developed through QuantumGIS plugins, incorporate seven procedures under a single toolbar (Figure 2).

The first icon (TIN Creation) allows for a TIN generation based on Delaunay triangulation. The second icon (GRID) allows for a grid generation considered as input a vector file. The pixel size was defined as 25 m (according to the Portuguese Forestry Authority rules). The next icon

(Terrain Analysis) produces the slope and the aspect maps. Topography is an important physiographic factor, which is related to wind behavior, and hence affects the fire proneness of the area. Fire travels most rapidly up slopes and the least rapidly down slopes. The Probability Map feature gives the probability map, considering the information of the number of fires that occurs in the last 15 years, for each pixel. The next icons (Hazard Map and Risk Map) allow for the generation of the hazard and risk map, respectively. In this generation the application automatically uploads all the information needed and already created. The last icon (Rasterize) is transversal to the project and converts a vector file (shapefile) into a raster.

All the procedures/icons of this project were created using commands available in GDAL (Geospatial Data Abstraction Library) and OGR (Simple Features Library) libraries, and have also been based on plugins already implemented, demonstrating the concept of open source. GDAL is a translator library for raster geospatial data formats that is released under an X/MIT style Open Source license by the Open Source Geospatial Foundation. As a library, it presents a single abstract data model to the calling application for all supported formats. It also comes with a variety of useful command line utilities for data translation and processing. The GDAL raster support formats such as GeoTIFF, Erdas Imagine, SDTS, ECW, MrSID, JPEG2000, DTED, NITF, among others. The OGRis a C++ open source library (and command line tools) providing read (and sometimes write) access to a variety of vector file formats including ESRI Shapefiles, S-57, SDTS, PostGIS, Oracle Spatial, and Mapinfo mid/mif and TAB formats. GDAL/OGR is considered a major free software project with "extensive capabilities of data exchange" and also in the commercial GIS community due to its widespread use and comprehensive set of functionalities (Neteler and Raghavan 2006).

Results

In figure 3 are presented some of the maps produced for the Santa Maria da Feira municipality (located in the Norwest part of Portugal). The final product, the forest fire risk map comprises six classes: no risk (black), very low risk (dark-green), low risk (green), medium risk (yellow), high risk (orange) and very high risk (red). The developed application was tested in three different areas, and compared with the risk maps already produced in a GIS commercial software (Figure 4).
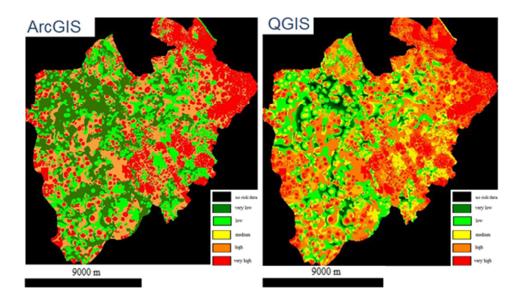
Figure 3. Example of the maps generated for Santa Maria da Feira using the open source
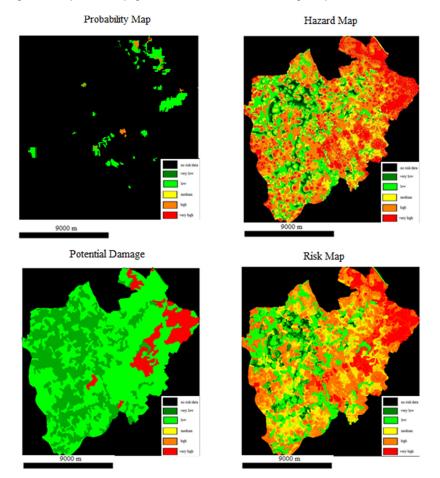
Figure 4. Risk map generated through a commercial GIS software (left) and through an open source GIS software (right)

The two risk maps given in the Figure 4 are quite similar. However, some differences were detected related to the classification method. Although the two (ArcGIS and QuantumGIS) software use the same method (quantiles method), the ArcGIS quantiles code is not available. Therefore, the quantiles method employed in our application differs somewhat from the ArcGIS quantiles method. However, the differences are minimal and the final results were similar.

Discussion and conclusion

The application described in this paper is an open source GIS application to produce forest fire risk maps. Besides being an open source application, it can be freely utilized by any user, and may be customized and improved by the authors or users. This application also presents the advantages of grouping in a unique toolbar all the procedures needed to produce forest fire risk maps. In the future the authors intend to improve some aspects of the application and publish the codes and plugins developed, as a mandatory of the open source software.

This work presents several contributions for the area of the GIS open source applications to forest fire management.

References

Chuvieco, E., Congalton. R.G. 1989. Application of remote sensing and geographic information systems to forest fire hazard mapping. Remote Sensing of the Environment 29, 147-159.

Chuvieco, E., Sales, J. 1996. Mapping the spatial distribution of forest fire danger using GIS. International Journal of Geographical Information Systems 10, 333–345.

Erten, E., Kurgun, V., and Musaoglu, N. 2002. Forest fire risk zone mapping from satellite imagery and GIS case study. International Journal of Applied Earth Observation and Geoinformation, 4, 1-10.

Neteler, M., Raghavan, V. 2006. Advances in Free Software Geographic Information Systems. Journal of Informatics [Online], 3(2).

PMDFCI 2008. Plano Municipal da Defesa da Floresta Contra Incêndios. Technical report.

II - Local to regional applications of remote sensing in post-fire assessment

ASSESSING FIRE SEVERITY IN THE TROPICAL SAVANNA OF NORTHERN AUSTRALIA

Stefan W. Maier

Research Institute for the Environment and Livelihoods, Charles Darwin University, Darwin, Northern Territory 0909, Australia. Stefan.Maier@cdu.edu.au

Abstract

Knowledge of fire severity is important to assess ecological impacts of fires. In recent years it has also gained importance in estimation greenhouse gases emitted by fires. To develop a remote sensing algorithm for estimating fire severity in the tropical savanna of northern Australia reflectance spectra have been collected within two days after fires of varying severity using a full range (400-2500 nm) spectroradiometer in a helicopter. Corresponding field data has been collected along 50m transects. Field variables collected were amount of photosynthetic/non-photosynthetic vegetation and scorched/charred material in four strata (ground, lower, mid and upper canopy). For the ground layer amount of ash, dry grass and bare soil has been assessed as well. Additionally scorch height and ground patchiness have been estimated.

Analysis of field variables showed fire severity can be summarised by a combination of scorch height and ground patchiness. Using the spectra collected in the helicopter it could be shown that ΔNBR and ΔNDVI were able to separate severe from non-severe fires. Further discrimination of non-severe fires into low and moderate severity fires was possible using the reflectance in the near-infrared portion of the spectrum. To further discriminate low severity fires an algorithm based on linear unmixing has been developed to estimate sub-pixel patchiness. The algorithms are currently being implemented for the generation of an operational fire severity/sub-pixel patchiness product for northern Australia utilising data from MODIS. To validate this product over large areas a methodology has been developed utilising a combination of observations from a low flying helicopter and within the field. An extensive field program is underway this dry season to collect large amounts of validation data.

LANDSCAPE, FIRE DISTRIBUTION AND VEGETATION RECOVERY IN PORTUGAL: 2003 AND 2005 FIRE SEASONS

A. Bastos[1], C. Gouveia[1,2], C. DaCamara[1], R. Trigo[1]

[1]Centro de Geofísica da Universidade de Lisboa, Campo Grande, Ed. C8-3º Piso, 1749-016 Lisboa, Portugal. afbastos@fc.ul.pt; [2]Escola Superior de Tecnologia, Instituto Politécnico de Setúbal, Campus do IPS, Estefanilha, 2910-761 Setúbal, Portugal.

Abstract

Fires respond differently to landscape composition and structure patterns, burning preferentially certain topographic features and different land-cover types. In turn, post-fire vegetation recovery is determined by several factors, such as fire characteristics, vegetation cover, climate, topography, and land-use history. Landscape patterns are also shaped by fire, inducing feedbacks that affect fire regime characteristics, such as recurrence and severity. Wildfires are, thus, better understood in the context of the interactions between landscape, fire regimes, and ecosystem response to disturbances.

The dependence of wildfire regimes on landscape factors, such as ecosystem composition, topography and human occupation, in Portugal is well known. In 2003 and 2005 Portugal registered two outstanding fire seasons, with burnt areas of 450 000ha and 338 000ha, respectively, considerably higher than the previous maximum for burnt area since 1980, circa 182000 ha in 1991. The authors have previously studied post-fire vegetation recovery following these two fire seasons (Gouveia et al. 2010; Bastos et al. 2011). Despite the fact that these extraordinary fire seasons were mainly driven by climatic factors, namely the strong heat wave in 2003 and the severe drought in 2005, it is important to evaluate the contribution of landscape characteristics to the larger fire events registered in those fire seasons, as well as to the response of post-fire vegetation recovery.

This work focuses on burnt scars from 2003 and 2005 and relies on monthly NDVI datasets from the sensor VEGETATION, at 1km spatial resolution, over an 11-year period (September 1998 to August 2009) to evaluate vegetation dynamics. Land-cover was assessed using Corine Land-Cover 2000 and 2006 datasets, which were degraded to 1km spatial resolution. A Digital Elevation Model for Continental Portugal, at 1km spatial resolution, was extracted from the GLOBE project dataset in order to analyse landscape structure. In order to identify fire-prone land-cover types, vegetation composition over the burnt scars was compared to the overall land-cover composition of the territory before and following the fire events. Coniferous, broad-leaved and transitional woodland-shrub were selectively more affected by fire, with some differences between the two fire seasons. Transitional woodland-shrub markedly dominated the burnt scars from 2003 fire season in the post-fire period. Finally, the influence of topography in vegetation recovery was assessed by relating the spatial distribution of estimated recovery times for some scars to altitude, slope and aspect. Distinct behaviours observed indicate that these factors may have some influence on vegetation recovery, motivating further work on this subject.

Keywords: Wildfire, vegetation recovery, landscape, remote sensing

Introduction

Fire is an ecological phenomenon characterized by the interaction of a large variety of factors such as landscape composition and structure, climate conditions as well as the differentiated post-disturbance ecosystem dynamics (Costa et al 2010). Fires respond differently to landscape composition and structure patterns, burning preferentially certain topographic features and different land-cover types (Viedma 2008). In turn, post-fire vegetation recovery is determined by several factors, such as fire characteristics, vegetation cover, climate, topography, and land-use history (Pérez et al. 2003; Pausas and Vallejo 2004). Within the Mediterranean basin, landscape patterns are also shaped by fire, inducing feedbacks that affect fire regime characteristics, such as recurrence and severity (Loepfe et al. 2010). Wildfires are, thus, better

75

understood in the context of the interactions between landscape, fire regimes, and ecosystem response to disturbances (Viedma et al. 2006). This interactive context is particularly relevant in Portugal, the area that presents currently the largest amount of average burned area per year in within the entire Mediterranean basin (Pereira et al. 2011).

Moreira et al. (2001) have shown that, for north-western Portugal, in the period from 1958 to 1995 agricultural land decreased by 29%, being replaced mainly by shrublands and forests, which increased fuel accumulation and fire proneness of the landscape. These changes, combined with the increasing trend in temperatures, have increased markedly fire risk and both the number and extent of fires in Portugal has been increasing since 1980 (DGRF 2008). It should be nevertheless mentioned that the observed increase in number of fires also reflects the report of much smaller areas (e.g. smaller than 1 ha) that used to be underrepresented during the 1980s and early 1900s (Pereira et al. 2011). In 2003 and 2005 Portugal registered two outstanding fire seasons, with burnt areas of 450 000ha and 338 000ha, respectively. These amounts are considerably higher than the previous maximum for burnt area since 1980 that reached circa 182.000 ha in 1991 (DGRF 2008). These extraordinary fire seasons were mainly driven by climatic factors, particularly the outstanding heat wave in early August 2003 (Trigo et al. 2005) and the severe drought that stroke Iberia between 2004 and 2005 (Garcia-Herrera et al. 2007).

Nunes et al. (2005) and Carmo et al. (2011) studied fire selectivity for large fires occurred in 1990 and 1991, concluding that very large wildfires have a propensity to burn preferentially shrublands and coniferous, broad-leaved or mixed forests. Furthermore, Carmo et al. (2011) analysed the influence of topography in fire occurrence in northern Portugal, concluding that fires tend to occur selectively in northern and eastern aspects and in moderate to steep slopes. However, due to the extraordinary magnitude of both 2003 and 2005 fire seasons, it is important to evaluate the contribution of landscape characteristics to the larger fire events registered in those fire seasons, as well as to the response of post-fire vegetation recovery. Vegetation recovery rates are affected by fire regime and depend largely on water availability, which is higher in topographic features with higher water retention capacity or lower losses by evapotranspiration.

The main goals of this work are: (i) to evaluate the influence of landscape composition on fire occurrence during the two extraordinary fire seasons of 2003 and 2005; ii) to assess fire driven changes in land-cover following the fire season of 2003; (iii) to analyse the dependence of post-fire vegetation recovery on altitude, slope and aspect.

Data and Methods

The study relies on monthly NDVI datasets as derived from the sensor VEGETATION on board SPOTs 4 and 5 satellites, at 1km spatial resolution, selected from September 1998 to August 2009 over a region extending from 37º to 42ºN and from 10º to 6ºW. Land-cover was assessed using Corine Land-Cover 2000 and 2006 datasets, which were degraded to 1km spatial resolution. A Digital Elevation Model for Continental Portugal, also at 1km spatial resolution, was extracted from the GLOBE project dataset (http://www.ngdc.noaa.gov/mgg/topo/globe.html) in order to analyse landscape structure (Figure 1 right panel). This work focuses on large burnt

scars from 2003 and 2005 fire seasons in Portugal (Fig. 1, left panel), which were identified using the procedure proposed by Gouveia et al. (2010).

For the assessment of post-fire vegetation dynamics, eleven regions were selected enclosing some of the largest scars, four corresponding to 2003 fires and another seven from 2005 fires (Figure 1, left panel). Selected areas for the present work and respective organization are identified by the rectangular frames labelled from 1 to 11.

In order to identify fire-prone land-cover types the relative frequency of each of the CLC2000 sub-classes corresponding either to agricultural land or forest (sub-classes 12 to 33) was evaluated for burnt pixels of 2003 and 2005 and compared to the corresponding overall abundance. With the aim of evaluating the impacts of fire on landscape composition, the post-fire composition of burnt scars from 2003 was evaluated using CLC2006.

The authors have previously studied post-fire vegetation recovery following these two fire seasons (Gouveia et al 2010; Bastos et al 2011), using a mono-parametric model which has shown to be adequate to analyse spatial patterns of recovery.

Results

As shown in Figure 2, the comparison of relative abundance of certain land-cover types over the territory and on burnt areas reveals a marked difference in land-cover composition between burnt scars and the overall territory. Results suggest that coniferous forests, followed by shrubland and broadleaved/mixed forests correspond to the most fire-prone vegetation types, being burned preferentially over other land-cover types, especially in very large wildfires. On the contrary, all types of agricultural land are clearly avoided by fire, since they present much lower fractions of burnt areas than their overall abundance. The slightly higher fraction of area classified as burnt in CLC2000 that is registered in the fire season of 2003 is also worth noting since it indicates the existence of pixels which were re-burnt in a short period of time.
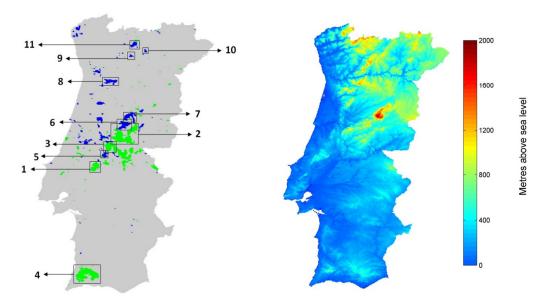
Figure 1. Burnt areas over Continental Portugal (left panel), as identified by the cluster analysis of NDVI anomalies following the fires seasons of 2003 (green pixels) and 2005 (blue pixels). Selected areas for the present work and respective nomenclature are identified by the rectangular frames labelled from 1 to 11. DEM for Portugal, as provided by GLOBE (right panel).

Nevertheless, it must be stressed that the results shown in Figure 2 correspond to an analysis performed at a very large scale and may be partially influenced by regional differences. In fact, while broad-leaved forests are clearly preferred by fire in southern Portugal, both coniferous forests and shrublands present very high fire-proneness over all regions in both years, particularly in Northern and Central Portugal.

Moreover, an evaluation of land-cover composition in 2006 (based on data from CLC2006) indicates that the scars from 2003 wild fires suffered major changes in their composition, being mostly replaced by shrublands. All forests present steeper decreases in burnt scars than the respective observed trends over Portugal, being coniferous the land-cover type most severely reduced by fire. These results indicate a dramatic fire-driven replacement of forests, especially coniferous, for shrublands over the country. Despite the existence of regional patterns, the broad extent of this analysis enlightens the crucial role that wildfires, especially very large ones, have in landscape composition.

In order to evaluate post-fire vegetation recovery, the mono-parametric model proposed by Gouveia et al. (2010) was applied to individual pixels of the fire scars on selected Regions 1 to 11, to estimate vegetation recovery time fields. These scars are located in distinct regions of Portugal, with different topography (Fig. 1) and pre-fire land-cover composition, which were previously evaluated. The distribution of recovery times over the north and southern hillsides was assessed only for forests (Fig. 3). Since there is high diversity of land-cover types each region, recovery times would present larger dispersion if all vegetation types were considered. It should be noted that there are very few pixels corresponding to forests in Region 9, and all of them are located in south facing slopes.
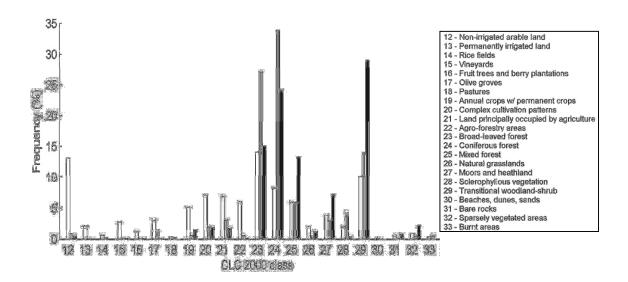
Figure 2. Relative frequency of agricultural and forest land-cover classes according to CLC 2000 nomenclature (legend) for Portugal (white bars), for burnt areas from 2003 (grey bars) and for 2005 (black bars) fire seasons.
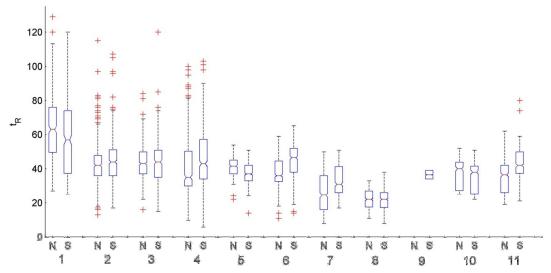
Figure 3. Recovery time (in months) distribution over each slope aspect (North and South) for Regions 1 to 11. Red lines indicate median values; blue boxes indicate the 25% and 75% interquartile ranges and black whiskers encompass the 1.5% and 98.5% interquartile ranges. Notches identify the 95% confidence limits for the median values. Red crosses represent outliers.

For most of the regions, recovery times were not significantly related to terrain aspect. However, Regions 5, 6, 7 and 11, present marked differences between the respective distributions over the two hillsides. Over all regions, with exception for R5 that presents the opposite behaviour, pixels on northern aspects tended to present lower recovery times than pixels located in south facing slopes.

Final remarks

Fire occurrence over Portugal in 2003 and 2005 burned selectively certain topographic features and land-cover types, and in turn, led to dramatic changes in landscape composition. Shrublands and coniferous forests were the vegetation types generally preferred by fires, although some regional differences were observed. The dramatic expansion of shrublands at the expense of all types of forests in burnt areas from 2003 is consistent with other studies in Portugal (Moreira et al. 2001; Silva et al. 2011) and in the Mediterranean region (Viedma et al. 2006).

In some central and northern areas of Portugal, vegetation recovery was influenced by aspect, being faster at north facing slopes than at southern ones. The faster recovery rates at northern aspects are related to the higher soil moisture content that characterizes north facing slopes, since they have less radiation exposure. Distinct behaviours observed such as the one of R5 indicate that other factors have to be taken into account, motivating further work on this subject that is certainly useful for land and territory management.

References

Bastos,A., Gouveia, C. , DaCamara, C. C., Trigo, R. M. 2011. Modelling post-fire vegetation recovery in Portugal. Biogeosciences Discuss., 8, 4559-4601 (under discussion).

Carmo, M., Moreira, F., Casimiro, P., Vaz, P. 2011. Land use and topography influences on wildfire occurrence in northern Portugal. Landscape and Urban Planning, 100, 169-176.

Costa, L., Thonicke, K., Poulter, B., Badeck, F.W. 2010. Sensitivity of Portuguese forest fires to climatic, human, and landscape variables: subnational differences between fire drivers in extreme fire years and decadal averages. Reg Environ Change, doi:10.1007/s10113-010-0169-6.

DGRF 2008. Incêndios Florestais – Portugal. Ministério da Agricultura, Pescas e Florestas (in Portuguese).

Garcia-Herrera, R., Paredes, D., Trigo, R. M., Trigo, I. F., Hernández, E., Barriopedro, D., Mendes, M. A. 2007. The Outstanding 2004/05 Drought in the Iberian Peninsula: Associated Atmospheric Circulation. Journal of Hydrometeorology, 8, 483-498.

Gouveia C., DaCamara C.C, Trigo R.M. 2010. Post fire vegetation recovery in Portugal based on SPOT-VEGETATION data. Natural Hazards and Earth System Sciences, 10, 673-684.

Loepfe, L., Martinez-Vilalta, J., Oliveres, J., Piñol, J., Lloret, F. 2010. Feedbacks between fuel reduction and landscape homogenisation determine fire regimes in three Mediterranean areas. Forest Ecology and Management, 259, 2366-2374.

Nunes, M. C. S., Vasconcelos, M. J., Pereira, J. M. C., Dasgupta, N., Alldredge, R. J., Rego, F. C. 2005. Land Cover type and fire in Portugal: Do fires burn land cover selectively? Landscape Ecol. 20, 661–673.

Pausas, J.G.,Ribeiro, E., Vallejo, V. R,. 2004. Post-fire regeneration variability of Pinus halepensis in the eastern Iberian Peninsula. Forest Ecology and Management 203, 251-259.

Pereira M.G., Malamude B.D., Trigo R.M., Alves P.I. 2011. The History and Characteristics of the 1980–2005 Portuguese Rural Fire Database.   (in press)

Pérez, B., Cruz A., Fernández-González, F., Moreno, J.M. 2003. Effects of the recent land-use history on the postfirevegetation of uplands in Central Spain. Forest Ecology and Management, 182, 273–283.

Silva, J. S., Vaz, P., Moreira, F., Catry, F., Rego, F.C. 2011. Wildfires as a major driver of landscape dynamics in three fire-prone areas of Portugal. . Landscape and Urban Planning, 101, 349-358.

Trigo, R.M., García-Herrera, R., Díaz, J., Trigo, I.F., Valente, M.A. 2005. How exceptional was the early August 2003 heatwave in France? Geophysical Research Letters, 32, l10701.

Viedma, O., Moreno, J. M.,Rieiro, I. 2006. Interactions between land use/land cover change, forest fires and landscape structure in Sierra de Gredos (central Spain). Environmental Conservation, 33, 212-222.

Viedma, O. 2008. The influence of topography and fire in controlling landscape composition and structure in Sierra de Gredos (Central Spain). Landscape Ecol, 23, 657–672.

ASSESSMENT OF AFFECTED AREAS BY FOREST FIRES IN MEXICO

M.I. Cruz-Lopez[1], G. Lopez-Saldaña[2]

[1]*Sub direction of Remote Sensing, National Commission for Knowledge and Use of Biodiversity, Liga Periferico – Insurgentes Sur 4903, Col. Parques del Pedredal C.P 14010 Tlalpan, Mexico D.F., icruz@conabio.gob.mx*
[2]*University College London, Holmbury St. Mary, Dorking, Surrey, RH5 6NT, U.K.s, lsg@mssl.ucl.ac.uk*

Abstract

During March and April 2011 the state of Coahuila in Mexico suffered the worst wildfire season ever. The fires burned more than 291,000 ha and some of them stayed active for about a month in mountainous regions. The surface affected represents 54 % of all affected areas in the whole country.

These events triggered a state of emergency. A rapid assessment was necessary, which was performed in three main stages: i) active fire detection; ii) fire monitoring; and iii) post-wildfire vegetation recovery assessment. Information used was obtained from the Forest Fire Early Warning System of the National Commission for Knowledge and Use of Biodiversity (CONABIO 2011) and the first results of the burnt area operational algorithm for Mexico, also developed in CONABIO.

In order to evaluate the affected areas, different spatial and temporal resolution imagery were used, ranging from very high spatial resolution, RapidEye (4m); high resolution, SPOT (10m); to moderate resolution, MODIS (250 m). The pre- and post– fire vegetation characterization was conducted extracting multi-temporal spectral information from the available datasets, and this information was used, in turn, to validate and refine the burnt area operational algorithm.

The steps described below are aimed at establishing a methodology to assess the impact of wildfires in biodiversity and fire-affected vegetation long-term monitoring using multi-sensor remote sensing techniques.

Keywords: Forest fire, early warning system, burnt area assessment, biodiversity

Introduction

Each year fire events are common in Mexican territory; however 2011 has been one of the most difficult years in the last decade, due to the presence of mega-fires that caused alterations in biodiversity. This is because fires can disturb and interfere in the succession of forest ecosystems and affect both, diversity species and their functional processes (Flores-Garnica, J.G 2009).

The mega-fires that occurred in the state of Coahuila are a clear example. They were active for over a month, mainly in difficult to access mountainous areas. In order to establish a method to monitor and assess the recovery of fire-affected vegetation, two of them are discussed in this paper: "El Bonito" and "El Sabinal". Some progress has been made in this project; but further work is necessary to establish the corresponding method and make it operational.

CONABIO has worked in wildfire identification since 1999, providing information to institutions responsible for fire management (Cruz-López MI 2008, Ressl *et al*. 2009). Information generated from the wildfire early warning system is the main input for fire monitoring and is used here to assess impact and recovery in the area of study.

Methods

Our area of study includes El Bonito and El Sabinal areas affected by wildfires, located in the Serranias del Burro mountain range, state of Coahuila, Mexico. The fire in El Bonito affected oak

forest, oak-pine forest, chaparral and piedmont shrubland. The fire in El Sabinal mainly affected oak-pine forest, desertic rosetophyllous shrubland and natural grassland.

1.1 *Active fire detection and monitoring with MODIS images*

Hotspots identified with MODIS imagery received at CONABIO's receiving station by applying the contextual fire detection algorithm for MODIS developed by Giglio *et al.* (2003) were used to monitor fires in the affected area during the time wildfires were active in the zone of interest.

1.2 *Burnt area identification with RapidEye imagery*

Hotspots information allowed a preliminary determination of the area of study. Four RapidEye images were obtained, from 8th April 20011, to identify the burnt area in El Bonito, up to the date of such image.

These are four-band images covering 400nm to 850nm at a spatial resolution of 5m, with two bands in the red region, Red and Red-Edge sensitive to chlorophyll and nitrogen changes. However, the short-wave infrared (SWIR) band is necessary to analyze burnt areas. Therefore, the Normalized Difference Vegetation Index (NDVI) was calculated, and visual interpretation applied. The presence of smoke in all images made identification of the burnt area difficult.

1.3 *Vegetation Anomaly Index (INV)*

Fires continued for more than one month, so the vegetation anomaly index was used to make a preliminary identification of affected areas. The vegetation anomaly index is generated every 10 days and published in the early warning system. It is computed by comparing the actual NDVI with an estimated NDVI for the same date, based on NDVI historical behavior (1000 m resolution) according to the Harmonic Analysis Time Series (HANTS) technique (De Badts, *et al. 20*05), considering 9 years of satellite information, from June 2002.

Such comparison is used to determine if vegetation greenness and vigor are similar to, above or below historical figures. If current NDVI is below historical figures, the vegetation is deemed to have less greenness and vigor than usual; therefore, there is a danger of propagation if fire is present.

1.4 *Burnt area identification with MODIS images*

Finally, an algorithm for burnt areas adjusted for Mexico was applied. Such algorithm is based on Normalized Burned Ratio differencing (dNBR) and Normalized Difference Vegetation Index differencing (dNDVI), computed using daily MODIS imagery after downscaling to 250m using the surface reflectance product (MOD09 and MYD09). To identify the burnt area, three factors were considered (Chuvieco *et al.* 2008): presence of fuel (vegetation), sudden index change and permanence throughout time.

Index thresholds were established according to ecoregions identified for Mexico, because such geographical units have characteristic flora, fauna and ecosystems (CONABIO 2011). Those characteristic allow to extract NDVI temporal profiles which can be related to vegetation behavior and identify dramatic changes in that behavior.

The area of interest is located between two ecoregions: Texas-Louisiana coastal plains and warm deserts; in the latter, wildfires occur at the highest elevations, where temperate forests are generally present, such as oak or pine forests.

Due to the duration of the fires and the extent of the area affected by them, mainly two images were used: one for March 3, before the wildfires, and another for May 25, after them, with the purpose of characterizing vegetation before and after the fires. Intermediate imagery was also used to meet the three principles for the identification of burnt areas. Efforts were made to use images from the same satellite and around the same times.

In order to validate the burnt area identified with MODIS imagery, the following adjustments were made to the burnt area identified with RapidEye imagery: projection changed from UTM to Lambert Conformal Conic and minimum mapping area was established (1ha).

We wanted to know if the burnt area identified using RapidEye imagery would be identified as well using MODIS imagery, because high resolution images were not available for the entire area of study.

Results

2,638 hotspots were identified in the area, 64% of which were in El Bonito and 36% in El Sabinal. The first hotspots identified in such areas appeared on 10th March, and the last hotspot was identified on 9th May.

The burnt area identified using RapidEye imagery covered 53,150 ha for El Bonito until 8th April. Figure 1 shows NDVI behavior for 5 observation sites, they were randomly chosen within burnt areas. The dotted lines show NDVI estimated values from the analysis of the time line, and the solid lines represent the actual NDVI value. As shown in this figure, values are similar until those months where an anomaly occurs, such as wildfires.

NDVI values for 2011 were expected to be below historical values, because during the last months of 2010 and the first months of 2011, less precipitation occurred than the historical record for the same months (CONAFOR 2011). Figure 1 shows this trend; however, there is a point in time where the estimated and actual NDVI values are significantly apart, during February, March, April and May.
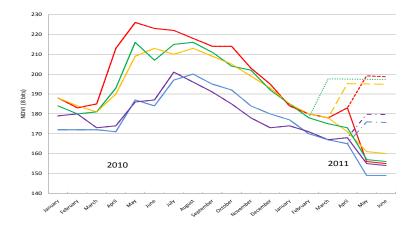
Figure 1. NDVI behavior for five sites in burnt areas; only the last and the current year are shown, to identify changes.

The burnt area computed from MODIS images was 191,255 ha for El Bonito, and 164,200 ha for El Sabinal, making a total of 355,425 ha. Based on the Key & Benson proposal (2006) to establish severity levels, the dNBR was used to characterize the burnt area; results are shown in Figure 2. The two fires together showed: 0.05-0.134 low severity in 164,012.5 ha; 0.135-0.21 moderate-low severity in 179,031.25 ha; and 0.22-0.32 moderate-high severity in 12,381.25 ha. High severity did not occur. The most affected areas have steeper slopes, mainly located in El Sabinal.

80% of the area identified using RapidEye imagery was identified also using MODIS satellite images. The remaining 20% was identified mainly along the limits of the burnt area and in places where the inside area was not likely to be burned; possibly, the understory was burned, but not tree canopies.
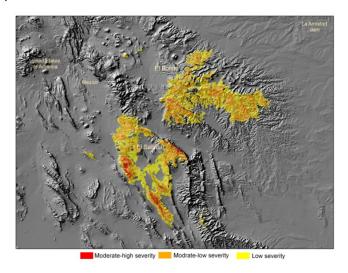
Figure 2. Burnt severity

Final remarks

So far, the burnt area has been identified using three products of the wildfire early warning system, hotspots, anomaly index and burnt area.

The vegetation anomaly index allowed us to identify the areas to be analyzed, because the presence of fire caused a severe difference between estimated and actual NDVI values. The index result is expected to change once the vegetation recovers.

Monthly monitoring is possible because the vegetation anomaly index is operational in the early warning system. However, it is important to verify any such anomaly with hotspots and burnt areas, as vegetation anomalies may be the result of various causes, not only fire.

Threshold values used in the burnt areas algorithm were conservative. Our results show that a more accurate assessment is necessary for areas that were not burned according to the MODIS imagery algorithm, but fire may have affected the areas below tree canopies.

The next step is to use SPOT imagery dated before and after the fires to conduct a detailed analysis of affected areas and verify recovery in that zone. Such images have the short-wave infrared band (SWIR), so it is possible to apply the similar method of MODIS images.

References

CONABIO. 2011. ¿Qué es una ecorregión? Sitio oficial de la Comisión Nacional para el Conocimiento y Uso de la Biodiversidad. http://www.biodiversidad.gob.mx/region/quees.html

CONABIO. 2011. Sistema de alerta temprana de incendios forestales en México y Centroamérica. Sitio oficial de la Comisión Nacional para el Conocimiento y Uso de la Biodiversidad http://www.conabio.gob.mx/incendios/

CONAFOR. 2011 Presentación de los resultados del Programa de Protección Contra Incendios Forestales 2010 y Programa 2011. México. Comisión Nacional Forestal.

Cruz-López M.I. 2008. Implementación de las técnicas de percepción remota para el conocimiento de la biodiversidad en México. Informe para obtener el grado de Maestría en Geografía. México. Universidad Nacional Autónoma de México.

Chuvieco, E., Englefild, P., Trishchenko, A.P., Luo, Yi., 2008. Generation of long time series of burn area maps of the boreal forest from NOAA-AVHRR composite data. Remote Sensing of Environment. 112: 2381-2396

De Badts, E. López, G., Wickel, B., Cruz, I., Jiménez, R. 2005. A fire risk propagation map base on NDVI anomalies. In De la Riva, J., Pérez-Cabello, F., Chuvieco, E. (Eds) Proceedings of the 5th inter-national workshop on remote sensing and GIS application to forest fire management: fire effects as-sessment. EARSel-GOFC-GOLD, JRC-Zaragoza University: 113-117.

Flores-Garnica, J.G. 2009. El papel del fuego en la dinámica de los ecosistemas forestales. En Flores-Garnica, J.G. (Coord.) Impa,cto ambiental de incendios forestales. México. Mundi Prensa.

Giglio, L., Descloitres, J., Justice, C., Kaufman,Y. 2003. An enhanced contextual fire detección algorithm for MODIS. Remote sensing of Environment. 87: 273-282.

Key, C.H., Benson, N.C. 2006. Landscape Assessment Sampling and analysis methods. In Lutes, D.C. (ed.) FIREMON: Fire effects monitoring and Inventory System. Gen. Tech. Rep. RMRS-GTR-164-CD. Fort Collins, CO:U.S. Department of Agriculture, Forest Services, Rocky Mountain Research Station.

Ressl, R., Lopez, G., Cruz, I., Colditz, R.R., Schmitdt, M., Ressl, S., Jimenez, R. 2009. Operational active fire mapping and burnt area identification applicable to Mexican nature protection areas using MODIS and NOAA-AVHRR direct readout data. Remote Sensing of Environment. 113:113-1126.

A PERFORMANCE EVALUATION OF SUPPORT VECTOR MACHINES AND THE NEAREST NEIGHBOR CLASSIFIER IN CLASSIFYING IMAGE OBJECTS FOR BURNED AREA MAPPING

E. Dragozi[1], I. Z. Gitas[1], D.G. Stavrakoudis[2], J.B. Theocharis[2]

[1]Laboratory of Forest Management and Remote Sensing, Aristotle University of Thessaloniki, P.O. Box 248, University Campus, Greece. edragozi@for.auth.gr
[2]Department of Electrical and Computer Engineering, Aristotle University of Thessaloniki Thessaloniki, 54124, Greece

Abstract

The present study addresses the problem of burned area mapping using a single post-fire Very High Resolution (VHR) satellite image. The aim of this work was to examine the efficiency of two classifiers, Support Vector Machine (SVM) and Nearest Neighbor (NN), in classifying image objects for accurate mapping of recently burned areas. In this work the image objects were classified into two classes, namely, burned and unburned. The object-oriented classifications were applied on an IKONOS image which was acquired immediately after the 2007 fire in Parnitha, Attiki, Greece. The results obtained from the two classifications, were compared with the burned area resulted from visual interpretation of the same IKONOS image. The overall accuracies achieved by each classifier were 98.12 % for SVM and 96.97 % for NN. Analysis of the results per class revealed that the two classifiers perform differently in each class. More specifically SVM achieved an overall accuracy of 95.17% in the burned class and 99.16% in the unburned while NN achieves an overall accuracy of 96.47% in the burned class and 97.14% in the unburned. A closer examination of the results revealed that the SVM classifier demonstrated higher ability in discriminating the different classes comparatively to the NN. However, the implementation of SVM on objects is still difficult and the methodology at its current form could not be used as an operational tool for burned area mapping.

Keywords: Burned area mapping, Object-based Image Analysis, Support Vector Machines, Nearest Neighbor classifier.

Introduction

Remotely sensed data are used in many environmental applications. Although a number of parametric and non-parametric classifiers has been developed and employed, so far, in order to convert image data into meaningful information, image classification still remains an open task (Mountrakis et al. 2011). Many researchers are trying to develop new classification schemes by combining different classifiers, approaches and sensors in order to improve classification accuracy. Despite the existence of several classification approaches such as per-pixel, subpixel, per-field, contextual-based, knowledge-based, and a combination of multiple classifiers; the pixel-based classification and the object-based classification remain the most widespread ones (Lu and Weng 2007). Pixel-based classification techniques are reported to have some limitations and difficulties when dealing with Very High Resolution (VHR) satellite images (Li et al. 2010). To overcome these limitations in analyzing VHR images, emphasis has been recently given on the use of object-oriented classification methods (Blascke et al. 2006). Object-based image analysis has demonstrated significant advantages for analyzing VHR imagery (Benz et al. 2004). The aforementioned classification approach does not operate directly on individual pixels, but on objects consisting of many pixels that have been grouped together in a meaningful way by image segmentation (Dang et al. 2008). However, beyond the selection of the classification approach, great consideration should be given in the choice of the classification algorithm as

well. This study focused on two classifiers, namely, Nearest Neighbor (NN) and Support Vector Machine (SVM), which were applied on objects created from segmentation of an IKONOS satellite image. NN is a non-parametric classifier (i.e., a classifier that makes no assumptions about the underlined statistical distribution of the data), which labels an unclassified object according to its nearest neighboring training object(s) in the feature space (Yu et al. 2006). The algorithm is widely used in the field of pattern recognition (Zammit et al. 2006). Support Vector Machine (SVM) is another more recent non-parametric classifier which is well known in the fields of machine learning and pattern recognition (Waske and Benediktsson 2007). SVM which is based on the statistical learning theory has the aim of determining the location of the decision boundaries that produce the optimal separation of classes (Vapnik 1995). Both, NN and SVM are reported to be successfully employed in a number of environmental applications in remote sensing. More specifically, NN has been successfully used in vegetation mapping (Yu et al. 2006), burned area mapping (Zammit et al. 2006) among many other applications while a recent review of different SVM applications can be found in Mountrakis et al. (2011). Independently of the application, the two aforementioned algorithms are usually employed to classify pixels as opposed to objects.

This study addresses the problem of accurate burned area mapping, which is very important in the Mediterranean region since forest fires are considered as one of the major factors of degradation of the Mediterranean ecosystems (De Luís et al. 2001). After a disastrous event, accurate and detailed assessment of the damaged areas is required, in order to plan the appropriate restoration and rehabilitation measures (Gitas et al. 2004). Up until now several studies have shown the great potential of remote sensing classification in burned area mapping (Chuvieco et al. 2002).

The aim of the present study was to examine the efficiency of the two classifiers, namely, SVM and Nearest Neighbor, in classifying image objects for accurate mapping of recently burned areas.

The specific objectives were:

- to employ the Nearest Neighbor classifier in order to classify objects derived from IKONOS imagery for mapping a recently burned area;
- to employ SVM in order to classify the objects derived from the IKONOS image for mapping the same burned area;
- to evaluate the ability of SVM to map a recently burned area accurately, by comparing it with the map which resulted from the use of the Nearest Neighbor classifier, as well as with the burned area resulted from visual interpretation of the IKONOS image.

Study area and dataset

The study area was Mount Parnitha, Attiki, Greece (Figure 1) that was affected by a large fire in 2007. Mount Parnitha is the highest (1,413 m) and most extended mountain of Attica, in central Greece, being a National Park since 1961.The main dataset used in the analysis was a pan-sharpened (1m) IKONOS image. The satellite imagery was captured on the 8th of July 2007, ten days after the fire. The pan- sharpened IKONOS image was acquired geometrically corrected.
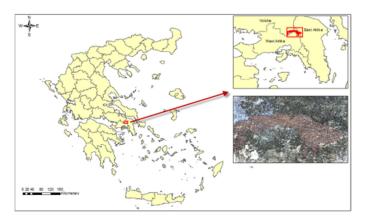
Figure 1. Location of the study area

Methodology

This section presents the procedures of two different object-oriented classification schemes. The first one utilizes the NN algorithm and the second one the SVM. A general sample-based classification scheme was followed in both cases in order to classify the IKONOS image. Initially, for the IKONOS image, the first four Principal Components (PC) were computed. The second PC (which exhibited the highest discrimination capabilities between the burned area and the other land uses) was selected and stacked in the primary image. Subsequently, the whole process was fulfilled in three main phases.

In the first phase, multi-resolution segmentation was applied to the image with the extra band. Throughout the segmentation procedure, the whole image was segmented and image objects were generated based on several adjustable criteria of scale, band weights, and homogeneity in color and shape. After segmentation, the image was subdivided into a number of objects. These objects were exported in vector format and a column with a unique identity field for every object was added. This step was essential because the segmentation algorithm creates objects which may share the same id (identity number). The unique id per sample is an essential requirement for extracting the samples from eCognition software, at a following phase.

In the second phase the image was segmented again using the information from the thematic layer. At this stage the objects created, had the same boundaries as the objects from the first segmentation and an extra field id derived from the thematic layer ensuring their uniqueness. In the case of the NN classification, samples that are typical representatives for each class ('burned' and 'unburned') were selected. The number of samples per class was proportional to the percentage of the area occupied by each category in the image. Additionally, the most appropriate features for the discrimination of the two classes arose from the Feature Space Optimization algorithm. The Feature Space Optimization is a feature selection algorithm which determines the most suitable combination of features for separating the classes, in conjunction with a nearest neighbor classifier (eCognition 2009). Furthermore, different sets of samples were created, in order to be tested for their effectiveness in the classification. The NN was trained on the different sets of samples and then applied on image objects using the eCognition commercial software. Finally, a set of 160 samples and 16 features for both classes was selected to be used in the final classification.

In the last phase a sample-based classification was also conducted with the implementation of the SVM classifier. SVM was trained on the same samples and applied on the same image objects as in the case of the NN. The implementation of SVM was carried out using the objects and the labeled samples exported in vector format. Generally the SVM classifier is constructed using a kernel function (Vapnik 1995). In this study the radial basis kernel function (RBF) was used and the parameters C and γ were selected through a cross-validation procedure, considering a grid of possible values. C is a penalty value for misclassification errors and γ is a parameter controlling the width of the Gaussian kernel (Vapnik 1995). Specifically for this application, the highest overall classification accuracy was succeeded for C=1 and γ=1. Since SVM is not available on the most widely used commercial object image analysis software, a Graphical User Interface (GUI) which uses the LIBSVM software (Chang and Lin 2011) to implement the algorithm, was developed in MATLAB. All the essential steps for the classification by SVM were conducted using the GUI interface; data scaling, cross validation, training and testing of the classifier and finally classification.

The final step in the methodology was to examine the classification accuracy of the two classifications. Therefore, the resulting maps were compared with a reference map. The reference map was constituted by two classes, namely, 'burned' and 'unburned', same as the two classifications. In order to obtain the reference classes, the burned area was delineated by visual interpretation of the IKONOS image, whereas the remaining part of the image was labeled as 'unburned'.

Results and Discussion

The burned area resulted from visual interpretation was estimated to be 4991, 33 ha (Figure 2a) while the area derived from NN and SVM were 5221, 1 ha and 4869.14 ha respectively (Figure 2b & 2c).

Initially, the performance of each classifier for the entire image was computed. Results showed an overall accuracy of 96.97% for the NN classification and 98.12% for the SVM. Additionally, the accuracy for each class (burned, unburned) was computed.

The percentage of spatial agreement between the burned area derived from NN classification (Figure 2(b)) and the reference fire perimeter was 96.47 % (4815.48 ha). Similarly the class 'unburned' from the aforementioned classification showed a spatial agreement of 97.14% (13810.09 ha) with the corresponding class in the reference map.

Likewise, the spatial comparison between the classified image by SVM (Figure 2(c)) and the reference areas, showed a spatial agreement of 95.17 % (4750.63 ha) in the classified burned area and 99.16% (14097.30 ha) in the unburned. The analysis of the results reveals that both classifiers performed very well. However, both classifications included errors but in different classes.

In order to understand better the performance of the two classifiers, the differences between the classification maps and the reference map were also computed. In the case of the NN classifier, the difference between the classification and the reference map revealed that the classified burned area exceeds the reference burned area for about 229.77 ha (4.6% of the

delineated burned area). This fact indicates that the NN classifier had a tendency to overestimate the class 'burned' against the 'unburned' class.

Similarly, in the case of the SVM classifier, a difference of 122.2 ha (2.44% of the delineated burned area) in the area classified as burned was observed between the two maps. In this case, the classifier exhibits the tendency to underestimate the class 'burned' against 'unburned' class, albeit to a smaller degree than the NN classifier.

The statistics per class showed that the NN classifier performed slightly better inside the delineated burned area comparatively to SVM. However, as Figure 2(b) clearly demonstrates, the NN classifier overestimated the 'burned' class in the whole image to a large extent. Hence, many objects outside the delineated burned area were erroneously classified as burned. The SVM classifier yielded higher accuracy in the overall classification and demonstrated higher ability in discriminating the different classes inside and outside the fire perimeter.

In order to explain the differences in the thematic maps, a visual examination of the classification maps was also conducted. The main differences were observed in objects with shadows, bare soil, roads, surface fire, slightly burned vegetation, objects with old dry vegetation (especially coniferous) and recently ploughed fields. Furthermore, misclassifications were observed in mixed objects, that is, objects containing both classes. In these cases, the segmentation process failed to partition the image in homogeneous regions, leading to the creation of objects with two classes. This problem existed mainly in dense forested areas which suffered from surface fires and in bare lands with sparsely distributed shrubs. Considering this fact, it seems that the segmentation process is of great importance for the accuracy of the classification and should be further investigated. Finally, it should be noted that the selection of training samples affected the classification; the selection of the ideal training set remains an open issue (Foody and Mathur 2006), especially when dealing with objects instead of pixels.

Although both classification models provided a very accurate identification of the burned areas, it is important to evaluate the two classification methods considering other criteria besides the classification accuracy. The NN method is implemented inside the eCognition software. Hence, the whole process of object extraction and subsequent classification is conveniently conducted inside a single software interface. On the other hand, the SVM classifier requires additional preprocessing steps, which consist of extracting the object information from eCognition and subsequently import it in Matlab, in order to train the SVM and perform the final classification. Furthermore, specialized knowledge is required for manipulating the data and running the SVM classifier in Matlab. As a result, the application of SVM on objects is still difficult and the methodology at its current form could not be used as an operational tool for burned area mapping.
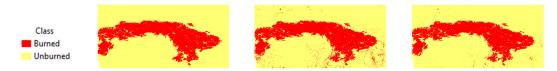
Figure 2. Burned area derived from IKONOS visual interpretation and classification results using NN and SVM. (a). Burned Area from visual interpretation   (b). NN Classification results   (c). SVM Classification results

Conclusions

In this research the efficiency of the two classifiers, namely, SVM and Nearest Neighbor, in classifying image objects for accurate mapping of recently burned areas was examined. The general conclusion drawn from this study was that both classification models produced very accurate burned area maps. However, the results reveal that the SVM classifier yielded higher accuracy in the overall classification comparatively to the NN, despite the fact that the statistical differences are very small. Also it should be noted that SVM exhibited better ability in discriminating the different classes. In conclusion, presently the main drawback of this object-oriented SVM method is that it is difficult to be used as an operational tool for burned area mapping, as-in most cases-the present SVM based method can not be implemented in a single software interface.

References

Benz, U., Hofmann, P., Willhauck, G., Lingenfelder, I., Heynen, M. 2004. Multi-resolution, object-oriented fuzzy analysis of remote sensing data for GIS-ready information. ISPRS Journal of Photogrammetry and Remote Sensing 58: 239-258.

Blaschke, T., Burnett, C., Pekkarinen, A. 2006. Image segmentation methods for object-based analysis and classification. Remote sensing image analysis: Including the spatial domain. Springer.

Chang, C.C., Lin, C.J. 2011. LIBSVM: A library for support vector machines. ACM Transactions on Intelligent Systems and Technology 2: (27:1-27:27).

Chuvieco, E., Martin, M., Palacios, A. 2002. Assessment of different spectral indices in the red-near-infrared spectral domain for burned land discrimination. International Journal of Remote Sensing 23:5103-5110.

Dang Huu, N., Luong Chi, M. & others,,2008. An object-oriented classification techniques for high resolution satellite imagery.

De Luis, M., Francisca, G. & others 2001.Climatic trends, disturbances and short-term vegetation dynamics in a Mediterranean shrubland.Forest Ecology and Management 147:25-37.

ECognition. 2009. User Guide,Version 8. Definiens AG.

Foody, G., Mathur, A. 2006 . The use of small training sets containing mixed pixels for accurate hard image classification: Training on mixed spectral responses for classification by a SVM. Remote Sensing of Environment 103:179-189

Gitas, I.Z., Mitri, G.H., Ventura, G. 2004 Object-based image classification for burned area mapping of Creus Cape, Spain, using NOAA-AVHRR imagery Remote Sensing of Environment

Li, H.,Gu, H., Han, Y., Yang, J. 2010. Object-oriented classification of high-resolution remote sensing imagery based on an improved color structure code and a support vector machine. International Journal of Remote Sensing 31:1453-1470.

Lu, D., Weng, Q. 2007. A survey of image classification methods and techniques for improving classification performance. International Journal of Remote Sensing 28:823-870.

Mountrakis, G., Im, J., Ogole, C. 2011. Support vector machines in remote sensing: A review. ISPRS Journal of Photogrammetry and Remote Sensing.

Vapnik, V. 1995. The nature of statistical learning theory.New York, Springer-Verlage.

Waske, B.,Benediktsson, J. 2007. Fusion of support vector machines for classification of multisensor data. Geoscience and Remote Sensing, IEEE Transactions 45(12):3858-3866.

Yu, Q., Gong, P., Clinton, N., Biging, G., Kelly, M., Schirokauer, D. 2006. Object-based detailed vegetation classification with airborne high spatial resolution remote sensing imagery. Photogrammetric Engineering and Remote Sensing 72: 799.

Zammit, O., Descombes, X., Zerubia, J. 2006. Burnt area mapping using support vector machines. Forest Ecology and Management 234(1 S 240):15.

POST-FIRE VEGETATION RESPONSE AS A PROXY TO QUANTIFY THE MAGNITUDE OF BURN SEVERITY IN TROPICAL PEAT SWAMP FOREST, CENTRAL KALIMANTAN, INDONESIA

A. Hoscilo[1,2], K. Tansey[2], S.E. Page[2]

[1]Institute of Geodesy and Cartography, 02-679 Warsaw, Poland. agata.hoscilo@igik.edu.pl

[2]Department of Geography, University of Leicester, Leicester, LE1 7RH, UK.   ah165@le.ac.uk, kjt7@le.ac.uk, sep5@le.ac.uk

Abstract

In recent years, fires in tropical forests in Southeast Asia have become more frequent and widespread, resulting in an increased need to evaluate fire impacts at a landscape scale. Burn severity is an important indicator of fire impact on the ecosystem and can be defined as the magnitude of ecological changes between pre- and post-fire conditions. Several studies of fires in the extra-tropics have used single and multi-temporal change detection techniques to map the magnitude of burn severity but to date these have not been extended to the tropical forest environment. We examined if post-fire vegetation regrowth could be used as a proxy to evaluate burn severity in tropical peatland in Central Kalimantan, Indonesian Borneo that has been subject to multiple fires. Several single and bi-temporal indices as well as spectral fraction endmembers derived from either a post-fire image or a combination of pre- and post-fire images obtained by the Landsat sensor were studied. Spectral data were correlated with several vegetation variables obtained from in situ measurements collected four years after the last fire. Of the tested spectral data, the bi-temporal and single normalised burn ratio (dNBR and NBR) showed the strongest correlations with the sets of vegetation variables, i.e. total woody aboveground biomass, tree density and number of trees less than 10 cm in DBH, followed by the normalised difference water index (NDWI). Further results as reported in Hoscilo et al. (2011, in press) show that the results of an ANOVA test indicated that these three indices together with green vegetation fraction provided the best differentiation of vegetation regrowth classes defined in the field, whilst a Tukey Multiple Comparison of Means Test confirmed that NBR, dNBR and NDWI could clearly delineate four regrowth classes, thus confirming their utility in separating areas subject to a single fire from those affected by multiple fires as well as for discrimination between fires of differing severity. This study clearly demonstrates that even four years after the last fire, variation in vegetation structure in locations subject to multiple fires is strongly related to the magnitude of burn severity of the last fire. In addition, the results provide evidence of the long-lasting impact that multiple fires have on forest recovery in this ecosystem. Locations experiencing second fires of high severity enter a critical phase of vegetation regeneration, where even four years after the last fire, the landscape is largely dominated by non-woody vegetation, particularly ferns.

Keywords: burn severity, peatland, tropical forest, burned area, regrowth

Introduction

Fire plays an important role in deforestation and degradation of tropical peatlands in Southeast Asia. Large-scale forest degradation and drainage of tropical peatlands also increase the risk of widespread and intensive fires (Wosten et al. 2008). In recent years, fires in tropical forests in Southeast Asia have become more frequent and widespread (Langner and Siegert 2009), resulting in an increased need to evaluate fire impacts at a landscape scale. Burn severity is an important indicator of fire impact on the ecosystem and can be defined as the magnitude of ecological changes between pre- and post-fire conditions. Typically burn severity is assessed using ground based co-called the Composite Burn Index (CBI) that was originally developed for coniferous forests in Montana, USA (Key and Benson 2006). The CBI approach is relatively quick

and relies mostly on accurate estimation and judgment of post-fire condition assessed directly after a fire event. The CBI estimates are typically coupled with remote sensed data in order to determine the burn severity over a larger area. Several studies performed in boreal and temperate mixed-coniferous forests and Mediterranean ecosystems have confirmed a strong correlation between bi-temporal normalized burn ratio (dNBR) and ground-based CBI (Allen and Sorbel, 2008; Cocke et al. 2005; De Santis and Chuvieco 2006 , Epting et al. 2005; Hall et al. 2008; Key and Benson 2006; Kokaly et al. 2007; Miller and Thode 2007; Soverel et al. 2010; van Wagtendonk et al. 2004; Veraverbeke et al. 2010; Wimberly and Reilly 2007; Zhu et al. 2006). It seems that burn severity is relatively well studied in boreal and temperate ecosystems, whereas tropical ecosystems, where fire becomes more frequent, are still under-investigated. In the tropics, however, the assessment of fire affect shortly after burning can be a difficult, if not impossible task. This is owing to the weather condition, since the end of burning season always coincides with the start of the wet season which can make field assessment difficult due to accessibility issues. Therefore we examined if post-fire vegetation regrowth could be used as a proxy to evaluate burn severity in tropical peatland in Central Kalimantan, Indonesian Borneo.

Data and methods

1.1   *Study area*

The study was carried out in the degraded part of tropical peatlands, south from Palangka Raya - the provincial capital of Central Kalimantan, Borneo, Indonesia. The study area was affected by fires in 1997 and 2002. Before 1997 the entire area was covered by tropical mixed peat swamp forest (Hoscilo et al. 2011). We used a time-series of satellite images to separate the areas affected by a single fire (SF) (1997) from those affected by multiple fires (MF) (1997 and 2002) (Hoscilo et al. 2011).

1.2   *Ground data collection*

The inventory of post-fire vegetation cover was conducted during the dry season in 2006; four years after the last 2002 fire. In areas affected by multiple fires we identified three classes of vegetation regrowth in the field taking into account vertical and horizontal vegetation structure and presence of woody canopies. These three classes are: MF1–more advanced (five plots), MF2–intermediate (five plots) and MF3–least advanced (six plots). In the area burnt in 1997, we established four plots. Each plot was 20 by 20m. In each plot we calculated number of trees, saplings and seedlings, measured DBH, height, canopy coverage, ground coverage and fern fraction. The DBH and height were used to calculate above ground biomass of woody stratum. We also sample and calculate biomass of fern.

1.3   *Satellite data*

We used the pre-fire Landsat image acquired in July 2000 and post fire Landsat image obtained in January 2003 to calculate several single and bi-temporal indices, namely normalized difference vegetation index (NDVI), normalized difference water index (NDWI) and normalized burn ratio (NBR). In addition, a three endmember model representing green vegetation (GV),

non-photosynthetic vegetation (NPV) and Shade was selected from the post-fire 2003 image. The GV endmembers were extracted from green vegetation (grass and dense fern), NPV from heavily senesced vegetation (along canal banks) and Shade from deep, dark water (rivers). All images were atmospherically corrected using the ATCOR model.

1.4   *Methods*

The mean value of a 3 by 3 pixel window for each vegetation plot was extracted from a series of single and bi-temporal spectral indices and from the three types of endmembers. The Spearman's rank correlation was then used to analyze if the spectral indices and endmembers are correlated with vegetation variables. The ANOVA and Tukey Multiple Comparison of Means Tests were used to examine if our hypothesis that the variation in post-fire vegetation regrowth observed in the field can be explained by differences in the magnitude of burn severity.

Results and discussion

This study has established a strong correlation between spectral data derived from pre- or/and post-fire images and sets of vegetation variables collected four years after the last fire. The results of a non-linear Spearman's rank correlation show that nearly all the analyzed spectral variables are strongly correlated with a number of vegetation variables. These include tree density, total woody AGB, tree AGB, fern biomass, tree basal area and number of trees less or greater than 10 cm in DBH (Figure 1). It also confirms that these vegetation variables, derived from in situ measurements collected four years after a fire event, can be proposed as indicators characterizing the magnitude of burn severity in tropical peatlands subjected to multiple fires. Amongst the vegetation variables, total woody AGB, tree density and number of trees < 10 cm have the strongest correlation with spectral variables, in particular with single and bi-temporal NBR and NDWI. Both NBR and dNBR followed by dNDWI and NDWI also show the strongest correlation with density of trees and number of trees < 10 cm (r above +/-0.87). Several studies conducted in non-tropical countries had previously recommended the use of dNBR for the assessment of burn severity in non-tropical ecosystems. This study has also shown that NDWI and dNDWI correlate well with the vegetation variables. The NDWI is known as being particularly sensitive to water content and thus it performed very well in areas subjected to two intensive fires, where there was a large reduction in canopy cover. In addition, the good performance of the NDWI can be associated with the post-fire data acquisition (wet season). The number of tree species and density of saplings demonstrate the weakest correlations with all the spectral variables, while the Shade fraction demonstrates the weakest relationship with each of the vegetation variables. Figure 1 reveals the character of the relationship between vegetation and spectral variables.

The high correlation demonstrates the long-lasting effect of multiple fires on vegetation structure and recovery, which supports the hypothesis that the variation in the characteristics of post-fire vegetation regrowth observed in the field could be explained by differences in burn severity. Second fires of moderate or high severity had more profound effects on the ecosystem, with very slow or no recovery of woody-biomass and invasion by non-woody plant communities dominated by two species of fern.

Matrix Plot of vegetation vs. spectral variables
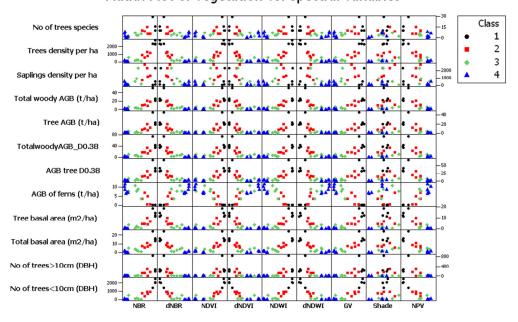
Figure 1. Dependence of the vegetation variables against spectral variables; class: 1–SF, 2–MF1, 3–MF2 and 4–MF3 (from Hoscilo et al., in press).

The ANOVA test indicated that both NBR and dNBR followed by NDWI and GV fraction provide the best differentiation among any of the regrowth classes. The Tukey multiple comparisons test confirmed that NBR, dNBR and NDWI can delineated between all classes at a 95% confidence level ($p < 0.02$). The results of this study demonstrate that the variation in the structure and species composition of post-fire vegetation regrowth observed in the field (i.e. MF1, MF2 and MF3 plots) could be explained by differences in the magnitude of burn severity for the 2002 fire.

References

Allen, J.L., Sorbel, B. 2008. Assessing the differenced Normalized Burn Ratio's ability to map burn severity in the boreal forest and tundra ecosystems of Alaska's national parks. International Journal of Wildland Fire 17: 463-475.

Cocke, A.E., Fulé, P.Z., Crouse, J.E. 2005. Comparison of burn severity assessments using Differenced Normalized Burn Ratio and ground data. International Journal of Wildland Fire 14, 189-198.

De Santis, A., Chuvieco, E. 2006. Burn severity estimation from remotely sensed data: Performance of simulation versus empirical models. Remote Sensing of Environment 108: 422–435.

Epting, J., Verbyla, D., Sorbel, B. 2005. Evaluation of remotely sensed indices for assessing burn severity in interior Alaska using Landsat TM and ETM+. Remote Sensing of Environment 96: 328-339.

Hall, R.J., Freeburn, J.T., de Groot, W.J., Pritchard, J.M., Lynham, T.J., Landry, R. 2008. Remote sensing of burn severity: experience from western Canada boreal fires. International Journal of Wildland Fire 17: 476–489.

Hoscilo, A., Page, S.E., Tansey, K.J., Rieley, J.O. 2011. Effect of repeated fires on land-cover change on peatland in southern Central Kalimantan, Indonesia, from 1973 to 2005. International Journal of Wildland Fire 20: 578-588.

Hoscilo, A., Tansey, K.J. and Page, S.E., in press. Post-fire vegetation response as a proxy to quantify the magnitude of burn severity in tropical peatland. International Journal of Remote Sensing.

Key, C.H., Benson, N.C. 2006. Landscape Assessment: Sampling and Analysis Methods: Ground measure of severity, the Composite Burn Index; and Remote sensing of severity, the Normalized Burn Ratio. In FIREMON: Fire Effects Monitoring and Inventory System, Lutes, D.C, Keane, R.E., Caratti, J.F., Key, C.H. Benson, C., Sutherland,

S., Gangi, L.J. 2006. USDA Forest Service, Rocky Mountain Research Station, Ogden, UT. Gen. Tech. Rep. RMRS-GTR-164-CD.

Kokaly, R.F., Rockwella, B.W., Haireb, S.L., Kinga, T.V.V. 2007. Characterization of post-fire surface cover, soils, and burn severity at the Cerro Grande Fire, New Mexico, using hyperspectral and multispectral remote sensing. Remote Sensing for Environment 106: 305-325.

Langner, A., Siegert, F. 2009. Spatiotemporal fire occurrence in Borneo over a period of 10 years. Global Change Biology 15: 48-62.

Miller, J.D., Thode, A.E. 2007. Quantifying burn severity in a heterogeneous landscape with a relative version of the delta Normalized Burn Ratio (dNBR). Remote Sensing of Environment 109: 66-80.

Soverel, N.O., Perrakis, D.D.B., Coops, N.C. 2010. Estimating burn severity from Landsat dNBR and RdNBR indices across western Canada. Remote Sensing of Environment 114, 1896-1909.

van Wagtendonk, J.W., Rootb, R.R., Key, C.H., 2004. Comparison of AVIRIS and Landsat ETM+ detection capabilities for burn severity. Remote Sensing of Environment 92: 397-408.

Veraverbeke, S., Lhermitte, S., Verstraeten, W.W., Goossens, R. 2010. The temporal dimension of differenced Normalized Burn Ratio (dNBR) fire/burn severity studies: The case of the large 2007 Peloponnese wildfires in Greece. Remote Sensing of Environment 114: 2548-2563.

Wimberly, M., Reilly, M. 2007. Assessment of fire severity and species diversity in the southern Appalachians using Landsat TM and ETM plus imagery. Remote Sensing of Environment 108: 189-197.

Wösten, J.H.M., Clymans, E., Page, S.E., J.O., R., Limin, S.H. 2008. Peat–water interrelationships in a tropical peatland ecosystem in Southeast Asia. Catena 73: 212-224.

Zhu, Z., Key, C., Ohlen, D., Benson, N.C. 2006. Evaluate Sensitivities of Burn-Severity Mapping Algorithms for Different Ecosystems and Fire Histories in the United States. Final Report to the Joint Fire Science Program. Project JFSP 01-1-4-12, October 12: 35.

RESAC FOREST COVER MONITORING AND FOREST DAMAGE ASSESSMENT IN THE FRAME OF GMES PROJECTS – CASE STUDY FROM BULGARIA

I. Ivanov, R. Chausheva, V. Vassilev

Remote Sensing Application Center, Sofia, 1463, Bulgaria.
ivan.ivanov@resac-bg.org, radostina.chausheva@resac-bg.org, vassil.vassilev@resac-bg.org

Abstract

In the frame of 7FP of the EC the preoperational services of the Global Monitoring of Environment and Security Programme (GMES) of the EU were developed. The Remote Sensing Application Center – ReSAC, Bulgaria is partner in two of the GMES projects, namely: SAFER (Emergency Response Core Service) and Geoland2 (Land Monitoring Core Service). In parallel with the Core Services of GMES several downstream services projects were financed by the FP7. In January 2011 the EUFODOS Project began (in which ReSAC is partner), which goals are to develop specific downstream forest services related to forest monitoring and forest damage assessment.

In the frame of SAFER ReSAC developed forest fire damage assessment maps for the fire on 9th of April 2011 where more than 230 ha forest and grassland areas were burned in Gostun region, Bulgaria.

The processing approach includes automatic classification of VHR satellite images, with later manual editing and change detection techniques. The software used is ERDAS Imagine. In order to estimate the real forest damage differentiation between the surface and crown cover fire was made. The resultant information was combined with data from the updated Forest management Plan (update based on the manual editing using VHR image) in order to deliver detailed information on: type of three species burned; age of forest burned; area of forest burned with different density.

For the analyses the following reference and post event EO data were used: WorldView-2, Formosat-2, RapidEye.

The final results we delivered in digital and paper maps, as well as GIS database in which the forest polygons from the Forest Management Plan we updated with information on type of forest fire they were subject to.

Keywords: GMES, forest monitoring, forest fire damage assessment, earth observation, GIS databases

Fire Event

In Saturday – 09/04/2011, in the vicinity of the forest area fund in the Blata area above Gostun village, Bansko municipality, Bulgaria fire event initiate. Immediately fire brigades are sent to fight the disaster. The fire is spread over forest massif in difficult to reach area. The strong wind and the rugged terrain make the fire extinguishing activities more difficult. As a result around 230 ha forest is burned (according to data from Executive Forest Agency) mainly coniferous species: *Pinus nigra, Pinus sylvestris, Picea abies* and *Abies alba.* In the late 10/04/2011 the fire is localized and the spread of the fire in new territories is stopped. The fire is extinguished completely on 11/04/2011.

Main goal of the research

To prepare maps and thematic products which gives information for:
- Type of the forest fire (crown or surface)
- The real area of burned forest and non-forest areas
- Type of the damages forest
- Age of the forest

Figure 1. Location of the forest fire in Gostun village, Bansko municipality, Bulgaria

Data used

For the purposes of the above mentioned tasks three types of satellite images are used: WorldView-2 (reference image acquired on 11th of March 2011, spatial resolution 2m); RapidEye (post event image, acquired on 11th of April 2011, spatial resolution 5m); Formosat-2 (post event image acquired on 12th of April 2011, spatial resolution 2m). The satellite data supplied are from project SAFER, after the GMES SAFER mechanism was activated through the National Focal Point for Bulgaria. In order to extract information on forest species and forest density Forest Management Plans supplied from Executive Forest Agency were used.

Field Work

On 18th of May 2011 team from Remote Sensing Application Center - ReSAC together with representative from the local forestry made a field trip to the burned area. The main goal was to collect ground truth data for the extent of the fire, as well as the type of the fire (crown or surface). The trace was selected with the support of the experts from the Mesta forestry. During the field trip key locations were chosen with good visibility to the burned areas, they were tracked with GPS and photographed. These activities supported later the satellite image interpretation and especially distinguishing crown from surface fire.

Figure 2. Photos on the forest fire in Gostun village 18th of May 2011 a) crown fire in young pine forest – 10 years of age, b) overview of the forest fire, c) border between the burned and healthy forest, d) example of the activities performed by the fire brigades to stop the spreading of the fire.

Stages of the work done

The main activities done to reach the goals established are related with the processing of the satellite images. On one hand they are related with the software classification of the images and on the other the Forest Management Plans were subject to manual editing on the base of the recent satellite acquisitions.

1.1 *Satellite image processing*

The processing of the satellite images requires preprocessing related with orthorectification and image enhancement in order to assist the later analyses. In order to analyse the forest area burned classification between forest and non-forest land cover is needed. Unsupervised approach using ERDAS Imagine was used resulting in good differentiation of the boundaries of the forest area. In addition the resulting data were processed in order to smooth the boundaries between forest - non-forest areas as well as to correct some wrongly classified pixels.

The satellite images from RapidEye and WorldView-2 were used in order to classify the burned area. Supervised classification was used with the ground truth collected during the field trip. Later on the resulting data were manually corrected. Based on this analyses the area of crown and surface fire was derived..

The resulting thematic data for the forest territories, as well as the information for the extent of the forest fire were spatially analysed and give information for the concrete forest structures damaged. The results derived were processed in forms of maps and tables.

Figure 3. Main stages of work related with processing and analyses of the satellite images: a) classification of the fire extent, b)land cover classification from the reference image, c)determination of crown and surface fire and types of forest subject to it

1.2 *Processing of the Forest Management Plans*

The processing of the Forest Management Plans (FMP) is related with analyses of their state of update, accuracy etc. which should be taken into account in the estimation of the characteristics of the forest area damaged. The graphical part of the FMPs was related with the attributive data in order to obtain information of the forest type, age and density for each polygon.

With the support of the reference satellite image from March 2001 visual correction was made on the boundaries of the forested area included in each polygon of the FMPs. In order to speed up the correction the work was focused only on polygons where according to classification

burned area was detected. Together with the boundaries of the forested area correction was made also on degree of density and presence of change.

After the correction of the FMPs, spatial analyses were performed in order to estimate the forest area types, forest age and density damaged by the fire. The results obtained were delivered as maps and tables.
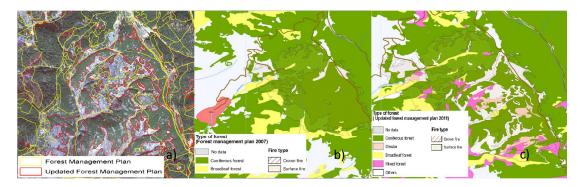
Figure 4. Main stages in the processing of the FMPs and related analyses: a) update of the FMPs, b) map of the main forest types subject to crown and surface fire (not-corrected FMP), c) map of the main forest types subject to crown and surface fire (corrected FMP)

Results

As a final result from the analyses performed information for the area and types of the forest cover was delivered, based on three types of source information – satellite images, FMPs and updated FMPs. The results are presented in Table 1. The results from the updated FMP and satellite images are very close. The difference of 4.29 ha could be explained by the forested areas classified from the image, but not included in the FMP. The big discrepancy between the classification results and not-updated FMP are explained by some inaccuracies in the FMP – meadows, roads, etc. area included in the forested polygons, which are cleared after the update. This fact shows the advantage of the use of recent satellite images for more accurate detection of the area subject to forest fires. On the other hand only the satellite images and especially high and medium resolution data could not give accurate enough information on forest species and forest density – values which are of high importance for the foresters when calculating the forest damages after disasters. Using the combined approach we overcome the limitations of the datasets and provided more accurate results to decision-makers.

Table 1. Area in hectares affected by fire (by different source data). * in this figure 14.3 ha of non-forest area is included.

Areas in hectares affected by fire (Satellite images 2011)			
Fire type	**Forest vegetation**	**Area**	**Total area**
Surface fire	Coniferous and deciduous forest	75.96	**170.56**
Crown fire	Coniferous and deciduous forest	94.6	
Areas in hectares affected by fire (forest management plan 2007)			
Fire type	**Forest vegetation**	**Area**	**Total area**
Surface fire	Coniferous and deciduous forest	83.81	**205.8**
Crown fire	Coniferous and deciduous forest	121.99	
Areas in hectares affected by fire (updated forest management plan 2011)			
Fire type	**Forest vegetation**	**Area**	**Total area**
Surface fire	Coniferous and deciduous forest	77.65	**166.27**
Crown fire	Coniferous and deciduous forest	88.62	
Areas in hectares declared to Executive Forest Agency			
Fire type	**Forest vegetation**	**Area***	**Total forest area**
Surface fire	Coniferous and deciduous forest	101.4	**216.3**
Crown fire	Coniferous and deciduous forest	129.2	

References

Cocke, A., Fule, P., Crouse, J., 2005. Comparison of burn severity assessement using Differenced Normalized Burn Ratio and ground data. Ratio and ground data, International Journal of Wildland Fire, 14: 189-198

Milenova, L., Vassilev, V. - Remote Sensing Application Center Bulgaria; Spirodonov, V., Kolev, S. - National Institute of Meteorology and Hydrology; Konstantinov, V. - Ministry of Agriculture and Forestry National Forestry Board. 2003. Integrated System for Information and Management of Forest Fire in Bulgaria – National Concept. United Nations/Romania Regionl Workshop on the Use of Space Technology for Disaster Management for Europe, Poiana-Brasov, Romania, 19-23May 2003

Mitri G.H. and Gitas I.Z. (2004). A semi-automated object-oriented model for burned area mapping in the Mediterranean region using Landsat-TM imagery. International Journal of Wildland Fire, Volume 13, Number 3, 367-376.

TREND ANALYSIS OF TIME SERIES IMAGE DATA FOR BURNED AREA MAPPING AND POST-FIRE MONITORING

T. Katagis, I. Z. Gitas, P. Toukiloglou

Laboratory of Forest Management and Remote Sensing, School of Forestry and Natural Environment, Aristotle University of Thessaloniki, P.O. Box 248, Greece. thkatag@for.auth.gr

Abstract

In this study, a newly developed trend analysis technique of satellite time series imagery was em-ployed for the mapping of recently burned areas and post-fire monitoring of Mediterranean ecosystems. The Breaks For Additive Seasonal and Trend (BFAST) method enables the decomposition of time series into trend, seasonal and noise components, resulting in the detection of gradual and abrupt changes in ecosystems. MODIS 8-day composites covering a period from 2004 to 2010 were utilized in this study. Analysis was based on MODIS derived vegetation indices (VIs), namely NDVI, SAVI, GEMI and BAI, focusing on an area burned during the 2007 fires in Peloponnese, Greece. The BFAST method was applied to each VI dataset leading to the detection of fire affected areas (sudden changes) with a high performance for every index. In addition, gradual changes were also detected in the trend component for all indices, except the BAI which is specifically developed for burned area discrimination, indicating post-fire vegetation recovery.

Keywords: burned area mapping, post-fire monitoring, time series, remote sensing, trend analysis

Introduction

Detection of changes in natural ecosystems after a fire event is of primary importance in terms of not only estimating the size of the burned area, but also in monitoring the post-fire vegetation condition over time. Especially in the Mediterranean region, fires cause significant changes in vegetation composition and dynamics and can potentially increase degradation processes (Vila et al. 2001). Satellite remote sensing data have been widely used in burned area mapping and post-fire assessment studies providing valuable and accurate information (Pereira et al. 1997, Chuvieco et al. 2005, Mitri and Gitas 2010).

Time series of satellite imagery contribute to the generation of burned area maps over long time periods (Chuvieco et al. 2007), offering at the same time the advantage of monitoring current conditions (van Leeuwen et al. 2004), and predicting future hazards. Multitemporal medium/coarse satellite imagery from sensors such as MODIS, SPOT-VGT and NOAA-AVHRR, is also used for assessing fire severity (Veraverbeke et al. 2011) and monitoring vegetation phenology and regrowth in fire affected areas (Goetz et al. 2006; Casady et al. 2010). Most of these post-fire monitoring studies are based on time-series change detection analysis of vegetation indices (VIs) and mainly of the NDVI.

However, it should be mentioned that when change detection techniques are based on short time series, there is a high risk that seasonal variation can be interpreted as change (de Beurs and Henebry 2005). Moreover, when specific thresholds or change trajectories are involved in change detection methods, misleading results may be produced due to different spectral and phenological characteristics of land cover types (Lu et al. 2004; Verbesselt et al. 2009). A newly introduced method of detecting changes has been successfully applied to time series data, without having to define specific thresholds or change trajectories and that is not influenced by seasonal variation. The Breaks For Additive Seasonal and Trend (BFAST) approach enables the

iterative decomposition of time series into trend, seasonal and noise components, resulting in the detection of gradual and abrupt changes in ecosystems (Verbesselt et al. 2009).

The BFAST method has been successfully applied to MODIS NDVI series in forest plantations in southeastern Australia (Verbesselt et al. 2009). The aim of this work was to apply BFAST to several MODIS VIs time series for mapping burned areas and assessing post-fire vegetation regrowth in Mediterranean ecosystems. More specifically, the specific objectives were:

- to investigate the potential of BFAST method to detect burned areas in a Mediterranean ecosystem,
- to investigate the potential of BFAST method to detect post-fire vegetation recovery, if any, and
- to validate the derived results.

Study area

The area of interest is located in the Peloponnese, in southern Greece (36°30'-38°30' N, 21°-23° E). Elevations range between 0 and 2404m above sea level and the climate is characterized as typically Mediterranean with hot, dry summers and mild, wet winters. The main vegetation types in the area are coniferous and broadleaved forests, shrublands (*maquis* and *phrygana* communities), and olive groves. Black pine (Pinus nigra) and Aleppo pine (*Pinus halepensis*) are the dominant conifer species while oaks are the dominant broadleaved species (Veraverbeke et al. 2010). In August 2007 after a severe drought, large fires broke out in the Peloponnese resulting in human losses and the destruction of infrastructures and more than 150000 ha of natural and managed land. The 2007 fires are considered to be one of the worst natural disasters recorded during the past decades in Greece (Gitas et al. 2008).

Datasets and Methods

1.1 *Datasets*

MODIS surface reflectance 8-day composites at 250m were used for the analysis in this work. The dataset was acquired from the National Aeronautics and Space Administration (NASA) warehouse inventory search tool (WIST) (http://wist.echo.nasa.gov) for the period from 01/01/2004 to 31/12/2010, covering the area of interest. The MOD09Q1 (Surface Reflectance (SR) 8-Day L3 Global 250m) products provide 2 spectral bands, red and near-infrared, at 250-meter resolution in an 8-day gridded level-3 product in the Sinusoidal projection. Additionally, a Quality Assurance (QA) layer is included in this product that provides quality information for the product. For validation purposes, a Disaster Monitoring Constellation (DMC) image with 32m resolution captured after the 2007 fire, as well as a Landsat-5 TM scene of summer 2010 were also employed.

1.2 *Methods*

Time-series pre-processing

The MODIS data initial pre-processing activities included importing of the raw imagery and reprojection to WGS-84 Lat/Lon projection system, geographical subsetting to the Peloponnese boundaries and masking of the sea. The QA information was used to further exclude from

analysis low quality, as well as cloud affected and not atmospherically corrected pixels in the red and NIR bands. The processed MODIS bands were used for the generation of the Vegetation Indices (VIs):

$$NDVI = (\rho_{NIP} - \rho_{RED})/(\rho_{NIP} + \rho_{RED}) \tag{1}$$

$$GEMI = (\gamma(1-0.25\gamma) - (\rho_{RED} - 0.125))/(1 - \rho_{RED}) \tag{2}$$

where $\gamma = (2(\rho^2_{NIR} - \rho^2_{RED}) + 1.5\,\rho_{NIR} + 0.5\,\rho_{RED})/(\rho_{NIR} + \rho_{RED} + 0.5)$,

$$SAVI = ((1+L) * (\rho_{NIP} - \rho_{RED}))/(\rho_{NIR} + \rho_{RED} + L) \tag{3}$$

where the term L can vary from 0 to 1 depending on the amount of visible soil. L=1 is generally used when the amount of soil is unknown, and

$$BAI = 1/((\rho c RED - \rho RED)^2 + (\rho c NIP - \rho NIP)^2) \tag{4}$$

where ρcRED and ρcNIR are the red and near-infared reference reflectances, which are defined as 0.1 and 0.06 according to Martin (1998).

The Normalized Difference Vegetation Index (NDVI), see Eq. (1), is one of the most widely used indices in burned area mapping and monitoring applications and provides a good estimate of vegetation photosynthetic activity. The Global Environmental Monitoring Index (GEMI) is less affected by soil and atmospheric variations than NDVI (Pinty and Verstraete 1992), see Eq. (2), and has proven to be more sensitive in burned land discrimination (Chuvieco et al. 2002). The soil background variation is considered by the Soil Adjusted Vegetation Index (SAVI) (Huete 1988), which has shown to be sensitive in discriminating vegetation in sparsely vegetated areas, see Eq. (3). Finally, the Burned Area Index (BAI), see Eq. (4), has been specifically developed for burned area discrimination (Martin 1998).

Prior to the VIs series analysis, continuous time series were generated by smoothing any noisy data with the use of TIMESAT software (Jonsson & Eklundh 2004). For the generation of the continuous time series, a local second-order polynomial function, also known as an adaptive Savitzky–Golay filter, was applied to replace affected and noisy observations.

BFAST implementation

BFAST was applied to every MODIS VI time-series in order to detect the sudden (burned areas) and gradual (vegetation regrowth) changes within the trend component. BFAST is an additive decomposition model that iteratively fits a piecewise linear trend and seasonal model, given by the equation: $Y_t = T_t + S_t + e_t$, t=1,…, n, where Y_t is the observed data at time t, T_t is the trend component, S_t is the seasonal component, and e_t is the remainder component (Verbesselt et al. 2009). The implementation of the method identified breakpoints for all major changes and indicated the number and time of these in the trend component. The selected time series covered the period from 2004 to 2010 (46 images per year), in order to facilitate the discrimination between the seasonal variations and the trend changes. Input settings and parameters of the BFAST package had first to be tested and evaluated before processing the VI datasets as single time series. A subset of the area was selected due to existing validation data, therefore the implementation focused on that area and spatial comparison of the results was finally performed.

Results and discussion

The implementation of BFAST to MODIS VIs time series resulted in the detection of the time and direction of the sudden and gradual changes in the study area. The fire caused abrupt decrease in the values of all VIs that were analyzed. Therefore, the breakpoints identified in the trend component presented the time and range of these changes caused by the fire event in August of 2007, leading to the detection and mapping of all fire affected pixels (Figure 1). In Figure 2, the decomposition of the GEMI time series into trend, seasonal and remainder components is indicative of the BFAST fitting operations. The produced fire perimeters per VI were spatially compared with a validated perimeter derived by the resampled DMC image. The percentage of the common area for every pair compared was found to be quite high (over 90%) and only minor differences existed among the estimated perimeters. More specifically, comparison revealed a common area of 95.2%, 94.7%, 93.8% and 91.5% for GEMI, BAI, SAVI and NDVI perimeters, respectively. However, it should be mentioned that unburned patches within the estimated perimeters were not detected, unlike the validated perimeter, probably due to the coarse resolution of the MODIS pixel.
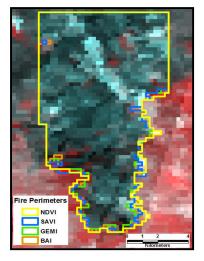
Figure 1. Fire perimeters of the study area as derived by the BFAST implementation to every MODIS VI time series.
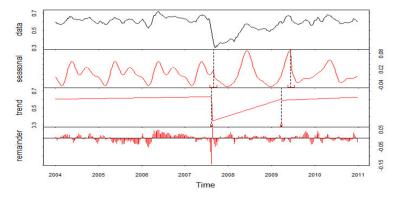
Figure 2. Seasonal, trend and remainder fitted components of the GEMI time series as derived from a single pixel in a conifer forest of the study area. Dash lines (- - -) indicate the time of observed changes (breakpoints) in the trend component. A sudden major change (fire) is detected in 2007.

Regarding the post-fire vegetation condition, the observed gradual changes within the trend component reveal a positive increase of the VIs values over time. This increase is shown by the slope of the gradual change (Figure 3). The inclination and intercept of the slope varies for every vegetation index and according to different vegetation types, however in any case post-fire recovery is evident. Analysis revealed that values tend to increase right after the fire and despite the fact that the post-fire period is relatively short, recovery rates appear to be satisfactory. This can be attributed to the immediate vegetation succession, mainly shrub communities, which is common after fires in Mediterranean landscapes. Validation of these trend results is not a straightforward procedure, especially when single date validated data exist. However, some preliminary validation tests performed with the assistance of the 2010 LANDSAT validated dataset showed an overall satisfactory performance of the VIs. Future work aims at providing complete and more precise estimations of the performance of each vegetation index. It should be mentioned that the BAI index is not considered in these estimations, since it is specifically developed for burned area discrimination.
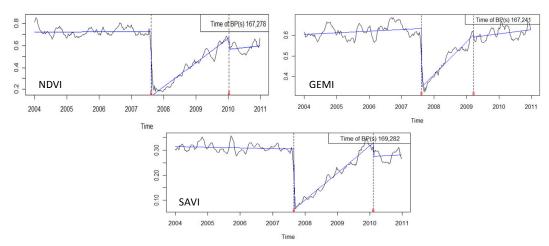
Figure 3. Changes detected in the trend component for the MODIS NDVI, GEMI and SAVI time series in a conifer forest. Sudden changes are observed in 2007 (fire) and the slope of the gradual change indicates vegetation recovery.

Conclusions

In this work, the potential of a new trend analysis technique of satellite time series to map burned areas and monitor post-fire vegetation recovery was investigated. The BFAST (Breaks For Additive Seasonal and Trend) method decomposes time series into seasonal, trend and noise components, enabling the detection of sudden and gradual changes. The BFAST application to derived vegetation indices resulted in the detection of the time and direction of the sudden changes, that occurred due to the fire event. Spatial comparison of the produced fire perimeters with validated data was found to be quite high, with the GEMI index performing slightly better than the other indices. Moreover, the slope of the gradual change observed in the trend component revealed post-fire vegetation recovery in every VI time series that was analyzed. However, more work is needed in order to provide more complete and precise estimations of the vegetation recovery. It should be mentioned, that although BFAST provides the time, number and range of changes, one should combine this information in order to characterize the type of change, otherwise misleading results could be yielded. Finally, BFAST

succeeded in estimating changes in the trend component, without being influenced by seasonal variations or noise.

Acknowledgements

References

Casady, G., van Leeuwen, W., Marsh, S. 2010. Evaluating Post-wildfire Vegetation Regeneration as a Response to Multiple Environmental Determinants. Environmental Modeling and Assessment 15(5): 295-307.

Chuvieco, E., Martin, M.P., Palacios, A. 2002. Assessment of different spectral indices in the red-near-infrared spectral domain for burned land discrimination. International Journal of Remote Sensing 23, 5103–5110.

Chuvieco, E., Ventura, G., Martín, M.P. 2005. AVHRR multitemporal compositing techniques for burned land mapping. International Journal of Remote Sensing 26(5): 1013–1018.

Chuvieco, E., Englefield, P., Trishchenko, A.P., Luo, Y. 2007. Generation of long time series of burn area maps of the boreal forest from NOAA-AVHRR composite data. Remote Sensing of Environment, Volume 112, Issue 5, Earth Observations for Terrestrial Biodiversity and Ecosystems Special Issue, 15 May 2008, Pages 2381-2396.

de Beurs, K. M., Henebry, G.M. 2005. A statistical framework for the analysis of long image time series. International Journal of Remote Sensing 26(8), 1551–1573.

Gitas, I.Z., Polychronaki, A., Katagis, T., Mallinis, G. 2008. Contribution of remote sensing to disaster management activities: A case study of the large fires in the Peloponnese, Greece. International Journal of Remote Sensing 29(6): 1847-1853.

Goetz, S., Fiske, G., Bunn, A. 2006. Using satellite time-series data sets to analyze fire disturbance and forest recovery across Canada. Remote Sensing of Environment, 92, 411–423.

Huete, A.R. 1988. A soil-adjusted vegetation index (SAVI). Remote Sensing of Environment. 25, 295–309.

Jonnson, P., Eklundh, L. 2004. TIMESAT - a program for analysing time-series of satellite sensor data, Computers and Geosciences 30, 833-845.

Lu, D., Mausel, P., Brondizio, E., Moran, E. 2004. Change detection techniques. International Journal of Remote Sensing 25(12), 2365–2407.

Martín, M.P. 1998. Cartografía e inventario de incendios forestales en la Península Ibérica a partir de imágenes NOAA–AVHRR, Doctoral thesis, Departamento de Geografía. Alcalá de Henares: Universidad de Alcalá.

Mitri, G., Gitas, I.Z. 2010. Mapping Postfire Vegetation Recovery Using EO-1 Hyperion Imagery. IEEE Transactions on Geoscience and Remote Sensing 48(3), 1613-1618.

Pereira, M., Chuvieco, E., Beudoin, A. Desbois, N. 1997. Remote sensing of burned areas: a review. In: A review of remote sensing methods for the study of large fires, (Ed. E Chuvieco): pp.127-184.

Pinty, B., Verstraete, M.M. 1992. GEMI: a non linear index to monitor global vegetation from satellites. Plant ecology 101, 15–20.

van Leeuwen, W.J.D., Orr, B., Marsh, S.E., Casady, G., Tuttle, D., Baker, L. 2004. The use of MODIS products in a geospatial decision support tool for rangeland monitoring. In J. D. Greer (Ed.), Remote Sensing for Field Users Proceedings of the Tenth Forest Service Remote Sensing Applications Conference, Salt Lake City, Utah, April 5–9. American Society for Photogrammetry and Remote Sensing.

Veraverbeke, S., Lhermitte, S., Verstraeten, W.W., Goossens, R. 2011. A time-integrated MODIS burn severity assessment using the multi-temporal differenced normalized burn ratio (dNBRMT). International Journal of Applied Earth Observation and Geoinformation 13(1): 52-58.

Veraverbeke, S., Lhermitte, S., Verstraeten, W.W., Goossens, R. 2010. The temporal dimension of differenced Normalized Burn Ratio (dNBR) fire/burn severity studies: The case of the large 2007 Peloponnese wildfires in Greece. Remote Sensing of Environment, 114(11): 2548-2563, ISSN 0034-4257.

Verbesselt, J., Hyndman, R., Newnham, G., Culvenor, D. 2009. Detecting trend and seasonal changes in satellite image time series. Remote Sensing of Environment 114(1): 106-115.

Vila, M., Lloret, F., Ogheri, E., Terradas, J. 2001. Positive fire-grass feedback in Mediterranean basin shrub land. Forest Ecology and Management. 147: 3–14.

FIRE RADIATIVE ENERGY AND BIOMASS BURNED ESTIMATION UNDER SPARSE SATELLITE SAMPLING CONDITIONS: USING POWER LAW PROBABILITY DISTRIBUTION PROPERTIES OF MODIS FIRE RADIATIVE POWER RETRIEVALS

S. Kumar [1], D. P. Roy [1], L. Boschetti [2]

[1]*Geographic Information Science Center of Excellence, South Dakota State University, USA.*

sanath.kumar@sdstate.edu; [2]*Department of Geography, University of Maryland, USA*

Abstract

Spatially and temporally explicit mapping of the amount of biomass burned by fire is needed to estimate atmospheric emissions of green house gases and aerosols. The instantaneous Fire Radiative Power (FRP) [units: W] is retrieved at active fire detections from mid-infrared wavelength remotely sensed data and can be used to estimate the rate of biomass consumed. Temporal integration of FRP measurements over the duration of the fire provides the Fire Radiative Energy (FRE) [units: J] that has been shown to be linearly related to the total biomass burned [units: g]. However, FRE and thus biomass burned retrieval, is sensitive to the satellite spatial and temporal sampling of FRP that can be sparse due to infrequent satellite overpasses, cloud and smoke obscuration, and failure to detect cool and/or small fires under cloudy conditions. In this paper the FRE is derived in a new way as the product of the fire duration and the expected FRP value derived from the FRP power law probability distribution function. MODIS FRP data retrieved over savanna fires in Australia and deforestation fires in Brazil are shown to have power law distributions with different scaling parameters that are related to the fire energy in these two contrasting systems. The FRE derived burned biomass estimates computed using this new method is compared to estimates using the conventional temporal FRP integration method and with literature values. The results of the comparison suggest that the new method may provide more reliable burned biomass estimates under sparse satellite sampling conditions if the fire duration and the power law distribution parameters are characterized a priori.

Keywords: Fire Radiative Power, Fire Radiative Energy, Burned Biomass, Power law probability

EVALUATING POST FIRE VEGETATION RECOVERY USING SATELLITE MODIS DATA

R. Lasaponara, T. Montesano, F. Desantis, A. Lanorte

CNR-IMAA, Contrada S. Loya, 85050, Italy. lasaponara@imaa.cnr.it

Abstract

The ability of NDVI (Normalized Difference Index) time series to capture the different fire induced dynamics on covers has been widely investigated by Telesca and Lasaponara (2007 2008) using the detrended fluctuation analysis (DFA), which permits the detection of persistent properties in nonstationary signals. Nevertheless, up to now no comparative evaluation has been performed with other methods or   indexes, such as Normalized Burn Ratio (NBR) considered quite effective in the identification and mapping of burned areas and fire severity level. In this study, we compared the evolution of dynamical trend of time series of NDVI and NBRd obtained from MODIS data. Satellite time series from 2000 to 2009 has been analyzed for two, test sites, located in Southern Italy, using DFA in order to study the persistence in the time series. For both the fire, the time series was split into two parts, a first subset consists of the data before the fire and a second consists of the data after the fire occurrence. Our results point out that the persistence of dynamics is significantly increased by the occurrence of fires in the NDVI compared to NBR

Keywords: Fire recovery, time correlation, Detrended Fluctuation Analysis, NDVI, NBR

Introduction

Post fire trends have been analyzed in a wide range of habitats in the Mediterranean-type communities, but these investigations have been generally performed at stand level. Fire-induced dynamic processes are very difficult to study since they affect the complex soil-surface-atmosphere system, due to the existence of feedback mechanisms involving human activity, ecological patterns and different subsystems of climate. Therefore, the patterns constrain fires and at the same time are constrained by the fire processes that influence them.

Remote sensing technologies can provide useful data for fire management from risk estimation (Lasaponara 2005), fuel mapping (Lasaponara and Lanorte 2007a,b); Lasaponara and Lanorte 2007), fire detection (Lasaponara et al. 2003), to post fire monitoring (Lasaponara 2006). The identification, mapping and recovery after fire using remote sensing is based on the recognition of the spectral response of burned, which is typically different from that of unburned surfaces.

Effective sources of information for this purpose are the indices derived from satellite imagery and in particular here we will analyze the time series of these indices.

In particular, satellite Normalized Difference Index (NDVI) time series may allow the assessment of post fire dynamics from local up to a global scale. This can be performed thanks to the availability of satellite data time series, acquired systematically for the whole globe and freely available from the national and international space agencies, such as NASA, ESA; etc.

The NDVI is the most widely used index for investigating cover and monitoring recovery after fire (see, for example Telesca and Lasaponara 2007 2008, Escuin et al. 2008). In particular, the ability of NDVI time series to capture the different fire induced dynamic on covers has been investigated by Telesca and Lasaponara using the detrended fluctuation analysis (DFA) in natural area (i. e. not managed). Up to now, no comparative evaluation has been performed using different indices. In this study, we compared the evolution of dynamical trend of time series of NDVI and NBR obtained from MODIS data. Satellite time series from 2000 to 2009 has

been analyzed for two, test sites, located in Southern Italy, using DFA in order to study the persistences in the time series.

Method: The temporal autocorrelation basic concepts

The method used in this work is the DFA, which is suited for the study of long-range correlations. Traditional approaches, such as power spectrum or Hurst analysis useful to quantify the correlations, are applicable only to stationary signals. A time series is stationary if its mean, standard deviation, higher moments and correlation functions are invariant under time translation, otherwise signals are nonstationary.

The DFA method has emerged as an important tool for the detection of long-range correlations in non-stationary time series and it works well for certain types of no stationary behaviour especially slowly varying trends, as in the case of behaviour.

The DFA provides a quantitative parameter, the scaling exponent, which describes the properties of autocorrelation in long-range signals.

The main advantages of DFA compared to traditional methods are the following:

(i) it is capable to capture correlations in seemingly non-stationary time series and also prevent false detections (i.e. 'artifact of non-stationarity);

(ii) it can systematically eliminate spurious trends due to different no physical meaningful external effects;

(ii) it reduces noise caused by imperfect measures.

The DFA method investigates the temporal evolution of the variance of integrated time series by analyzing the scaling of a fluctuation function. It consists of the following steps:

1) The considered interval time series (of total length N) is integrated using formula 1

$$y(k) = \sum_{i=1}^{k} (x(i) - < x >)$$

(1)

where <x> is the mean value of x

2) The integrated signal y(k) is divided into boxes of equal length n.

3) For each n-size box, we fit y(k), using a linear function, which represents the trend in that box. The y coordinate of the fitting line in each box is indicated by yn(k).

4) The integrated signal y(k) is detrended by subtracting the local trend yn(k) in each box of length n.

5) For given n-size box, the root-mean-square fluctuation, F(n), for this integrated and detrended signal is given by

$$F(n) = \sqrt{\frac{1}{N} \sum_{k=1}^{N} [y(k) - y_n(k)]^2}$$

(2)

6) The above procedure is repeated for all the available scales (n-size box) to furnish a relationship between F(n) and the box size n, which for long-range power-law correlated signals is a power-law

$$F(n) \propto n^{\alpha}$$

(3)

The scaling exponent α quantifies the strength of the long-range power-law correlations of the signal: if $\alpha=0.5$, the signal is random; if $\alpha>0.5$ the correlations of the signal are persistent, which means that a large (small) value (compared to the average) is more likely to be followed by a large (small) value; if $\alpha<0.5$ the correlations of the signal are anti-persistent, in other words a large (small) value (compared to the average) is more likely to be followed by a small (large) value.

Applications to SATELLITE data

In this study, we investigated two sites both of them situated in southern Italy, the first is close to the Crotone municipality (Calabria) and the second (Andriace) close to Scanzano (Basilicata). A wildfire occurred in Crotone on September 10 2004 and affected an area of approximately 210 ha of which only around 10 ha was covered by forest. In Andriace, the fire took place on July 19 2003 and affected an area of approximately 234 ha, of which around 154 ha covered by forest.

For each pixel the type of vegetation cover was obtained from the Corine (Coordination of Information on the Environment) Land Cover 2006 which is the most recent updated land cover map for Italy**.**

To analyze the behavioral trends induced by fire events in our test sites, time series of MODIS images from 2001 to 2009 were used. The time series was split into two subset before and after fire occurrences.

 So that, for Crotone we obtained two subsets made up of 170 and 243 data samples related to pre and post fire occurrence, respectively.

Similarly, for Andriace we obtained two subsets made up of 156 and 296 data samples related to pre and post fire occurrence, respectively.

In this study, we used the NDVI (from formula 4) which is the most widely used vegetation index for vegetation studies**.**

$$NDVI = \frac{\rho_{NIR} - \rho_R}{\rho_{NIR} + \rho_R}$$

(4)

The index relates to vegetation vigor and moisture by combining near infrared (NIR) and mid infrared (MIR) reflectance. These two bands provide the best contrast between photosynthetically healthy and burned vegetation (Howard et al. 2002). NBR is defined as:

$$NBR = \frac{\rho_{NIR} - \rho_{MIR}}{\rho_{NIR} + \rho_{MIR}}$$

(5)

For both the investigated sites, 4 pixels were considered in the areas affected by fire (around 100 ha).

A threshold value equal to 0.10 in NDVI difference observed before and after fire was considered as significant variation for discriminating fire affected from fire-unaffected pixels.

In order to eliminate the phenological fluctuations, for each NDVI composition of each pixel, we focused on the departure NDVId = [NDVI - <NDVI>] from the decadal mean <NDVI>. The decadal mean <NDVI> is calculated for each decade, e.g. 1st decade of January, by averaging over all years in the record. Investigations were conducted on the NDVId and NBRd departure series computed using formula 5.

Table 1 and 2 show the results obtained from DFA for both Crotone and Andriace test sites.

The averages of scaling factors relating to NDVI and NBR for the site of Crotone and Andriace are greater in the pre-fire phase than in the post-fire. Moreover, it can be seen that NDVI enable us to better discriminate than NBR index pre-fire and post-fire vegetation behavior.

The estimated scaling exponents for all the investigated pixels suggest a persistent character of vegetational dynamics. However, for both of two investigated sites the pre-fire subset exhibited scaling exponents much larger than those calculated for the post-fire subset. It can be noted that the pixels for which the scaling is greater than 1 for both sites (all the pixels relating to Crotone pre-fire phase - and pixel 2 to the Andriace pre-fire phase) correspond to naturally vegetated areas (pine forests, shrubs and high bush) and not to agricultural lands.

Results from this investigation clearly pointed out the diverse vegetation behavior observed for natural and managed areas before and after fire occurrence, compared to those obtained from several investigations conducted by the same authors group using the same method applied to VEGETATION/ NDVI time series recorded before and after fire for natural (i.e. unmanaged) vegetation covers. This suggests the possibility to adopt the DFA for discriminating illegal post-fire management activities such as changes in the land use and land cover, namely natural vegetated areas used for intensive farming which not allowed by the Italian Law

Table 1. Results of DFA for Crotone test site

a coefficients	Pixel_1 shrubbery and / or herbaceous	Pixel_2 shrubbery and / or herbaceous	Pixel_3 high bush	Pixel_4 high bush
NDVId_pre fire	1,0814	1,1152	1,1236	1,0947
NDVId_post fire	0,8275	0,7716	0,8168	0,8652
NBRd_ pre fire	1,0588	1,0557	1,0660	1,1246
NBRd_ post fire	0,9111	0,9261	0,9491	0,8923

Table 2. Results of DFA for Andriace test site

a coefficients	Pixel 1 intensive farming	Pixel 2 forests dominated by pine trees and cypresses	Pixel 3 cultural systems and particle complex	Pixel 4 intensive farming
NDVId_pre fire	0,9529	1,0591	0,9538	0,9387
NDVId_post fire	0,8241	0,8731	0,9959	0,6323
NBRd_ pre fire	0,9574	1,1023	0,9939	0,8486
NBRd_ post fire	0,9032	0,9615	0,9511	0,9257

References

Escuin, S., Navarro, R., Fernàndez, P. 2008. Fire severity assessment by using NBR (Normalized Burn Ratio) and NDVI (Normalized Difference Vegetation Index) derived from LANDSAT TM/ETM images. International Journal of Remote Sensing, 29, Issue 4 1053-1073.

Kun, H., Plamen, Ch. I., Chen, Z., Carpena, P., Stanley, H.E. 2001. Effect of trends on detrended fluctuation analysis. Physical Review E, 64.

Lasaponara, R. 2005. Inter-comparison of AVHRR-based fire danger estimation methods. International Journal of Remote Sensing. Vol. 26, no 5, pp. 853-870.

Lasaponara, R. and Lanorte, A. 2007a. VHR QuickBird data for fuel type characterization in fragmented landscape. Ecological Modelling in press (ECOMOD845R1) 204, 79-84

Lasaponara, R. and. Lanorte, A. 2007b. Remotely sensed characterization of forest fuel types by using satellite ASTER data. International Journal of Applied Earth Observations and Geoinformation vol. 9 - 225

Lasaponara R. and Lanorte, A. 2006. Multispectral fuel type characterization based on remote sensing data and Prometheus model. Forest Ecology and Management vol. 234, S226

Lasaponara, R., Cuomo, V., Macchiato, M. F. and Simoniello, T. 2003. A self-adaptive algorithm based on AVHRR multitemporal data analysis for small active fire detection. International Journal of Remote Sensing, vol. 24, No 8, 1723-1749.

Lasaponara, R. 2006. Estimating Spectral separability of satellite derived parameters for burned areas mapping   in the Calabria Region by using SPOT-Vegetation data. Ecological Modelling vol. 196, pp. 265-270.

Telesca, L., Lasaponara, R. 2008. Investigating fire-induced behavioural trends in vegetation covers. Communications in Nonlinear Science and Numerical Simulation, 13, 2018-2023.

Telesca, L., Lasaponara, R. 2007. Long-range persistent correlations in decade-long SPOT-VGT NDVI records of fire affected and fire unaffected Sites. African Journal of Agricultural Research 2(2), 36-40.

ESTIMATING BURN AREA SEVERITY USING SPATIAL AUTOCORRELATION ANALYSIS

R. Lasaponara [1], A. Lanorte [1], G. Nolè [1], B. Murgante [2]

[1]CNR-IMAA, Contrada S. Loya 85050, Italy. lasaponara@imaa.cnr.it

[2]UNIBAS Potenza 85100, Italy. beniamino.murgante@unibas.it

Abstract

Traditional methods of recording fire burned areas and fire severity involve expensive and time - consuming field surveys. The available remote sensing technologies may allow us to develop standardized burn-severity maps for evaluating fire effects and addressing post fire management activities. This paper is fo-cused on the characterization of burn severity using ASTER (Advanced Spaceborne Thermal Emission and Re-flection Radiometer). satellite pictures have been processed using geo-statistic analyses to capture pattern features of burned areas. Even if in last decades different authors tried to integrate geo-statistics and remote sensing image processing methods used since now are only variograms, semivariograms and kriging. In this paper, we propose an approach based on the use of spatial indicators of global and local autocorrelation. Spatial autocorrelation statistics, such as Moran's I, Geary's C, and Getis-Ord Local Gi index (see Anselin 1995; Getis and Ord 1992), were used to measure and analyze the degree of dependency among spectral features of burned areas. This approach enables the characterization of the pattern features of burned area and improves the estimation of burn severity.

Keywords: Fire severity, geospatial analysis, classification,

Introduction

In the Mediterranean Basin, composition and structure of vegetation have been and are generally strongly shaped by fires, which tend to operate as a selective force, increasing species diversity, as well as a filter favouring the dominance of some species rather than of other ones. Effects of fires on soil, plants, landscape and ecosystems depend on many factors (among them fire frequency and plant resistance). Burn severity is a qualitative indicator of the effects of fire on ecosystems, since it affects forest floor, canopy, etc. Assessing and mapping burn severity is important to monitor fire effects, to model and evaluate post-fire dynamics and to estimate the ability of vegetation to recover after fire (generally indicated as fire-resilience). In an operational context, burn severity estimation is critical for short-term mitigation and rehabilitation treatments. Traditional methods of recording fire severity involve expensive and time-consuming field surveys. The use of satellite remote sensing can help in overcoming such drawbacks.

Remote sensing technologies can provide useful data for fire management, from risk estimation (Rauste et al. 1997, Lasaponara 2005), fuel mapping (Lasaponara and Lanorte 2006, Lasaponara and Lanorte 2007a, Lasaponara and Lanorte 2007b), fire detection (Lasaponara et al. 2003), to post fire monitoring (Lasaponara 2006), including burn area and severity estimation (Gitas and Desantis 2009). Methods generally used to estimate fire severity from satellite are based on spectral indexes, obtained as a combination of bands which emphasize changes induced by fire in vegetation spectral behaviour. Such evaluations are generally performed on fire perimeter maps (a priori known), mainly using fixed threshold values to classify and map the different levels of burn severity. Nevertheless, as suggested by many authors, such fixed threshold values are generally not suitable for fragmented landscapes and inadequate for vegetation types and geographic regions different from those for which they were devised.

In order to overcome such limitations, a new approach, based on geo-statistical analyses applied to satellite data, is herein proposed both to estimate burn area perimeter and to evaluate the different degree of burn severity.

Method: The spatial autocorrelation basic concepts

Spatial autocorrelations take into account the spatial attributes of geographical objects under investigation, evaluate and describe their relationship and spatial patterns also including the possibility to infer such patterns at different times for the study area. The spatial patterns are defined by the arrangement of individual entities in space and the spatial relationships among them. Spatial autocorrelations in the field of archaeological investigations measure the extent to which the occurrence of one object/feature/site is influenced by similar objects/features/sites in the adjacent areas. As such, statistics of spatial autocorrelation provides: (i) indicators of spatial patterns and (ii) key information for understanding the spatial processes underlying the distribution of object/feature/site and/or a given phenomenon under observation.

Geographical observations should be arranged in spatial and temporal order, by latitude and longitude, and historical periods. In this context time series data, such aerial and satellite images can provide useful traces of past human activities and, therefore, can enable us: (i) to some extent predict the amount and types of interaction, (ii) to investigate spatial predictions between objects/features/sites and also to infer potential relations considering different "historical" time windows being that Everything is related to everything else, but nearest things are more related than distant things"(Tobler 1990) ".

In absence of spatial autocorrelation the complete spatial randomness hypothesis is valid: the probability to have an event in one point with defined (x, y) coordinates is independent of the probability to have another event belonging to the same variable. The presence of spatial autocorrelation modifies that probability; fixed a neighbourhood for each event, it is possible to understand how much it is modified from the presence of other elements inside that neighbourhood.

A distribution can show three types of spatial autocorrelation: i) the variable exhibits positive spatial autocorrelation, when events are near and similar (clustered distribution); ii) the variable exhibits negative spatial autocorrelation, when, even if events are near, they are not similar (uniform distribution); the variable exhibits null autocorrelation when there are no spatial effects, neither about the position of events, or their properties (random distribution)

The presence of autocorrelation in a spatial distribution is caused by two effects that could be clearly defined (Gatrell et al. 1996), but not separately studied in the practice: i) first order; and ii) second order effect.

    i) First order effects depend on the region of study properties and measure how the expected value (mean of the quantitative value associated to each spatial event) varies in the space with the following expression:

$$\hat{\lambda}_{\tau}(s) = \lim_{ds \to 0} \left\{ \frac{E(Y(ds))}{ds} \right\}$$

[1]

where ds is the neighbourhood around s, E is the expected mean and Y(ds) is the events number in the neighbourhood.

ii) Second order effects express local interactions between events in a fixed neighbourhood, that tends to the distance between events i and j. These effects are measured with covariance variations expressed by the limit:

$$- \quad \gamma(s_i s_j) = \lim_{ds_i ds_j \to 0} \left\{ \frac{E(Y(ds_i)Y(ds_j))}{ds_i ds_j} \right\}$$

[2]

where symbols are similar to those used in equation 1.

The characterization of spatial autocorrelation requires detailed knowledge on: i) the quantitative nature; ii) the geometric nature.

i) the quantitative nature of dataset is also called intensity of the spatial process that is how strong a variable occurs in the space (Murgante et al. 2008), with the aim to understand if events are similar or dissimilar.

ii) the geometric nature needs the conceptualization of geometric relationships, usually done with the use of matrixes:

(a) a distance matrix is defined to consider at which distance the events influence each other (distance band);

(b) a contiguity matrix is useful to know if events influence each other;

(c) a matrix of spatial weights expresses how strong this influence is.

Concerning the distance matrix, a method should be established to calculate distances in module and direction. For this concern the module, namely Euclidean distance (3), is the most used.

$$d_E(s_i, s_j) = \sqrt{(x_i - x_j)^2 + (y_i - y_j)^2}$$

[3]

As for any type of dataset also in the case of digital image analysis there are many indicators of spatial autocorrelation that can be distinguished into the following: Global indicators, Local indicators and the variogram approach to spatial association in the geostatistical perspective.

Global statistics summarizes the magnitude of spatial autocorrelation for the entire region by a single value. The Global indicators of autocorrelation utilize distance to define the neighbourhood of a region and measure if and how much the dataset is autocorrelated in the entire study region.

One of the principal global indicator of autocorrelation is the Moran's index I (Moran 1948), defined in formula (4)

$$I = \frac{N \sum_i\sum_j w_{ij}(X_i - \bar{X})(X_j - \bar{X})}{(\sum_i\sum_j w_{ij})\sum_i(X_i - \bar{X})^2}$$

[4]

where, N is the total pixel number, Xi and Xj are intensity in points i and j (with i≠j), $\bar{X}$ is the average value, wij is an element of the weight matrix.

I∈ [-1; 1]; if I∈ [-1; 0) there's negative autocorrelation; if I∈ (0; 1] there's positive autocorrelation. Theoretically, if I converges to 0 there's null autocorrelation, in most of the cases, instead of 0 the value used to affirm the presence of null autocorrelation is given in equation 5:

$$E(I) = -\frac{1}{N-1}$$

[5]

where N is the number of events in the whole distribution.

The second global indicator of spatial autocorrelation is the Geary's C (Geary 1954), expressed by:

$$C = \frac{(N-1)\sum_i\sum_j w_{ij}(X_i - X_j)^2}{2w_{ij}(\sum_i(X_i - \bar{X})^2}$$

[6]

Where symbols have the same meaning than expression 4.

C∈ [0; 2]; if C∈ [0; 1) there's positive autocorrelation; if C∈ (0; 2] there's negative autocorrelation; if C converges to 1 there's null autocorrelation.

The local versions of the spatial autocorrelation statistics is used to measure the magnitude of spatial autocorrelation within the immediate neighborhood. Values indicating the magnitude of spatial association can be derived for each areal unit and they are mappable. The local version of the statistic utilizes distance information to identify local clusters and relies on the distance information captured in Distance matrix.

Global measures of spatial autocorrelation provide a single value that indicates the level of spatial autocorrelation within the variable distribution, namely the homogeneity of a given values within the image under investigation.

Local measures of spatial autocorrelation provide a value for each location within the variable distribution and, therefore, they are able to identify discrete spatial patterns that may not otherwise be apparent. The statistics output is an image for each calculated index, which contains a measure of autocorrelation around that pixel.

Applications to ASTER data

ASTER data were used to compute NBR based indexes using ASTER 3 (760-860 nm) and 7
29 (2235-2285 nm) spectral channels, with a spatial resolution of 30 m, using the formula:

NBR_ASTER = (ASTER 2 – ASTER 7)/ (ASTER 2+ ASTER 7)

[7]

Using these two bands we obtained a NBR map which is particularly sensitive to changes occurring in vegetation cover affected by fire, such as amount of live green vegetation, moisture content, etc. NBR values generally range between 1 and −1 as well as NDVI. Strongly negative NBR values would indicate a larger reflectance in SWIR than NIR band, and this only occurs over not vegetated areas where fire cannot occur. Text areas have been investigated, in different area of North and South Italy. For all the investigated test sites geospatial data analysis enabled us to discriminate burned from unburned and the different degree of fire severity evaluated also using independent data set and field survey.

Conclusion

In this paper we present our preliminary results obtained from ongoing research based on the evaluation of spatial variability of fire effects using satellite ASTER (Advanced Spaceborne Thermal Emission and Reflection Radiometer) data.

In this study, both single (post-fire) and multi-date (pre and post fire) ASTER images were processed for some test areas selected from within Italian peninsula.

ASTER derived indices were processed using spatial autocorrelation statistics, such as Moran's I, Geary's C, and Getis-Ord Local Gi index (see Anselin 1995; Getis and Ord 1992). Such spatial statistics enable us to map the areas affected by fire and to estimate the degree of fire severity.

The new approach is independent on sensors used for the evaluation as well as on vegetation cover types affected by fire. The model could be incorporated directly into the mapping process from local up to global scale.

References

Lasaponara, R. 2005. Inter-comparison of AVHRR-based fire danger estimation methods. International Journal of Remote Sensing. Vol. 26, no 5, pp. 853-870.

Lasaponara, R. and Lanorte, A. 2007a. VHR QuickBird data for fuel type characterization in fragmented landscape. Ecological Modelling in press (ECOMOD845R1) 204, 79-84

Lasaponara, R. and. Lanorte, A. 2007b. Remotely sensed characterization of forest fuel types by using satellite ASTER data. International Journal of Applied Earth Observations and Geoinformation vol. 9 - 225

Lasaponara R. and Lanorte, A. 2006. Multispectral fuel type characterization based on remote sensing data and Prometheus model. Forest Ecology and Management vol. 234, S226

Lasaponara, R., Cuomo, V., Macchiato, M. F., Simoniello, T. 2003. A self-adaptive algorithm based on AVHRR multitemporal data analysis for small active fire detection. International Journal of Remote Sensing, vol. 24, No 8, 1723-1749.

Lasaponara, R. 2006. Estimating Spectral separability of satellite derived parameters for burned areas mapping in the Calabria Region by using SPOT-Vegetation data. Ecological Modelling vol. 196, pp. 265--270.

CONTRIBUTION OF REMOTE SENSING APPROACHES TO ASSESS POST-FIRE DAMAGE IN WILDLAND URBAN INTERFACES

M. Long-Fournel, A. Tribotte, C. Lampin, M. Jappiot, D. Morge

Mediterranean Ecosystems and Risks Research Team, Cemagref, Aix en Provence, 13182, France.
marlene.long@cemagref.fr, antoine.tribotte@cemagref.fr, corinne.lampin@cemagref.fr,
marielle.jappiot@cemagref.fr, denis.morge@cemagref.fr

Abstract

The wildland urban interfaces (WUI) defined as the area where structures and other human development meet or intermingle with undeveloped wildland (Vince et al.,2005), which create an environment in which fire can move easily between housing and vegetation fuels and where fire frequently occurs due to human activity. Assessing the impact of fire on the vegetation especially in WUI is so considered as a key issue to evaluate the consequences of past fires, and to improve the prevention and the protection of Mediterranean human population against the fire risk.

The study considers the fires of July 17 and 28 in 2003, which burned 12,390 hectares of vegetation in the Massif of the Maures in the south of France and destroyed more than 50 buildings. The aim is to propose an effective method based on field and remote sensing data sets to map post-fire damage within WUI according to intensity levels. An Intensity Scale developed by Lampin et al. (2002) has to assess the severity of a wildfire after the event. It takes into account physical variables related to the fire and is based on the qualitative assessment of damage to specific assets observed on the ground. The scale has six qualitative intensity levels: very low, low, moderate, high, very high and exceptional. Very high resolution images are used: Ikonos image acquired before the fires in August 2001 and Quickbird image acquired after the fire in September 2003.

The remote sensing methodology considered two main approaches: a mono-temporal analysis based on one unique post-fire image, and a multi-temporal approach including the image acquired before fire and based on the difference image dNDVI calculated as the subtraction between 2003 NDVI and 2001 NDVI. For each approach, unsupervised and supervised classifications were performed considering multispectral bands, NDVI and EVI indices. On the post-fire images, these classifications allowed (i) the mapping of "burned vegetation" and "unburned vegetation" in order to define the WUI that are supposed to be affected by the fire, (ii) a damage mapping inside the WUI. The image acquired before fire allowed us to perform a land-cover mapping into five classes (mineral, grassland, shrubland, broad-leaved tree, resinous tree) designed to improve the validation of damage mapping and also make relationships between damage and existing land cover before the fire.

According to the results obtained in this study, the mono-temporal approach leads the distinction of five damage levels in WUI with 80% of global accuracy. These levels correspond to five levels of the intensity scale elaborated by Cemagref (from very low damage to very high level of damage). The multi-temporal approach improves slightly the results with 82% of global accuracy. The land cover map generated from before-fire image participates to better understanding the impact of fire for each type of vegetation: shrubland is the most impacted by fire (more than 80% is concerned by moderate, and especially high and very high levels of damage); broad-leaved trees are a bit less impacted by the fire than resinous trees (60% and 70% respectively).

Keywords: wildfire risk, post fire damage assessment, damage mapping, remote sensing, wildland urban interfaces

Introduction

Context of the study

Every year, forest fires destroyed thousands of hectares of vegetation in the European Mediterranean region. According to the scenarios of climate change (GIEC 2007) and the expansion of piecemeal construction of dwellings in rural areas and urban sprawl, the fire risk is

supposed to increase in the next years. The impact of fire on the vegetation can be assessed by a spatial analysis of post-fire damage. Assessing the impact of fire on the vegetation especially in the wildland urban interfaces is so considered as a key issue to evaluate the consequences of past fires, and to improve the prevention and the protection of Mediterranean human population against the fire risk.

Definition

The study focuses on the wildland urban interfaces (WUI), defined as the area where structures and other human development meet or intermingle with undeveloped wildland (Vince et al.,2005), which create an environment in which fire can move easily between housing and vegetation fuels and where fire frequently occurs due to human activity.

The wildland urban interfaces were identified according to the method described by C. Lampin *et al.* (2010). This method considers houses used as dwellings – i.e. where people live permanently, temporarily or seasonally (agricultural, industrial, commercial and public buildings were not included) – located at less than 200 meters from forests or shrublands and their environment defined by a 100 meters radius. This definition is based on the French Forest Orientation Law of July 9 2002, which makes brush clearing obligatory within a maximum radius of 100 meters around each house located at a distance of less than 200 meters from forests or scrublands.

Research problem

The aim of this study is to propose an effective method based on field and remote sensing data sets to map post-fire damage according to the intensity scale developed by Lampin *et al.* (2002). This method implies treatments that could be processed by landscape managers.

Material

Study area

The study area is located in the south of the Var department, on siliceous soil in Provence. Before the fire, the main vegetation types in the Maures area were cork oak stands and high shrublands. The effects of fires of Vidauban I and II are studied: the first fire happened on July 17 2003 and affected an area of 6,744 ha, and the second one burned 5,646 ha on July 28 2003. These fires destroyed more than 50 buildings.
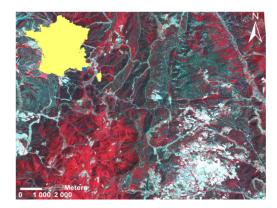
Datasets

The objective of the study is the evaluation of post fire damages within the wildland urban interfaces from the intensity scale developed by Lampin et al. (2002) and very high spatial satellite images.

The wildfire intensity scale was developed by Cemagref in 2001, on behalf of the French Ministry for the Environment and in partnership with GSC Consultant and Météo France. This scale can be used to assess the severity of a wildfire after the event on the basis of physical variables related to the fire and on the qualitative estimation of damage to specific assets

observed on the ground. It is independent of the location and its vulnerability. In this scale, the physical variables used are the speed at which the fire spreads, the colour of the smoke produced, the occurrence of spotting and the surface area threatened. In addition to these variables, damage to specific assets such as vegetation and buildings is estimated by several qualitative variables. The scale has five qualitative intensity levels (very low, low, moderate, high and very high). For each level, it matches ranges of values of physical variables to corresponding ranges of specific damage. Each level of intensity corresponds to a maximum level of specific damage that the physical conditions can be considered as liable to produce (Lampin et al. 2002).

The remote sensing datasets consist of 2 very high spatial resolution images: Ikonos image acquired before the fires on August 7 2001 (1 meter resolution in panchromatic, 4 meters in multispectral bands) and Quickbird image acquired after the fire on September 16 2003 (0.6 meter in panchromatic, 2.4 meter in multispectral bands). The Ikonos image acquired before the fire constitutes a reference to characterize the "original" landcover. The Quickbird image taken few days after the fire will be used to identify damage on the burned vegetation. These images cover a common area of 154.87 sqkm on the west part of the fire, and concern the towns Les Arcs, La Garde-Freinet, Le Muy, Plan-de-la-Tour, Roquebrune-sur-Argens, Sainte-Maxime and Vidauban.
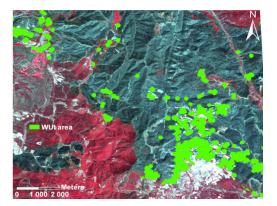
Figure 1. Images acquired before (Ikonos image on the left from August 7 2001) and after (Quickbird image on the right from September 16 2003) the Vidauban fires of July 2003.

Method

Before working on the post fire damage extraction, the images are ortho-rectified and geo-referenced to obtain maximal superimposition and minimize geographical deviation. Radiometric corrections were also performed on multi-temporal remote sensing data set to reduce any of the above influences and increase sensitivity to landscape change (Chen et al. 2005; Coppin et al. 2004; Song et al. 2001).

Burned area mapping

The first step of this damage mapping method consisted to realize a global distinction between the burned and the unburned vegetation on the whole fire area according the Quickbird image acquired after the fire. The aim was to define the wildland urban interfaces that are supposed to be affected by the fire.

127

Unsupervised classification was performed on the multispectral bands of the Quickbird image using the Isodata algorithm of the Erdas Imagine software. 12 classes were extracted then photo-interpreted and recoded into 2 classes "burned vegetation" and "unburned vegetation".

Landcover mapping

The landcover mapping was realized on the Ikonos image acquired before the fire in order to improve the validation of damage mapping and then to help understanding the effects of the fire on the vegetation. The landcover was performed in the wildland urban interfaces included in the burned area as defined previously. The landcover typology is composed with 5 classes, of which 1 mineral class and 4 classes of vegetation. The mineral class is composed with everything that is no vegetation, as water, roads, roofs of houses, bare soils, and uncultivated croplands. The vegetation was separated into 3 strata of vegetation (grasslands, shrublands, trees). In the last class, broad-leaved and coniferous trees are distinguished. These 4 vegetation classes are supposed to have different response to the fire, and should be separated by their spectral response.

A supervised classification based on the Maximum Likelihood algorithm was realized on the best combination of spectral bands and indexes: MS bands and NDVI index.

Damage mapping

Damage mapping was performed in the wildland urban interfaces included in the burned area as defined previously. The realization of the damage map was not dependant of the landcover map previously produced. The typology is composed with 10 classes, of which 5 classes corresponding to unburned types previously used in the landcover mapping (class 1 corresponds to mineral, class 2 to grasslands, class 3 to shrublands, class 4 to broad-leaved trees and class 5 to resinous trees) and 5 classes of fire damage. The number of fire damage classes corresponds to the 5 levels of the Cemagref intensity scale presented in part 2.2. Classes 5 and 6 can be interpreted as low damage classes, and are represented by scorched crowns. Classes 7, 8 and 9 can be considered as higher damage classes, where no crown is identifiable. It is now difficult to organize into a hierarchy these 3 classes of damage because of the lack of precise field data.
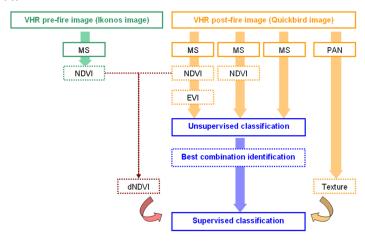
Figure 2. Methodology used for post fire damage mapping

According to figure 2, several treatments are processed in order to compare the relevance of the spectral bands and indices implied in classifications, the unsupervised and supervised classifications, and finally the mono-temporal and multi-temporal approaches to map these 5 classes of fire damage. First, unsupervised classifications were performed on the Quickbird image using the Isodata algorithm considering (i) the multispectral bands, (ii) the layer stacking of MS bands and NDVI index, (iii) the combination of MS bands, NDVI and EVI indexes. Then, supervised classifications are based on the Maximum Likelihood algorithm were realized on the best combination of spectral bands and indexes previously defined by the unsupervised classifications. A textural analysis, defined as the calculation of the variance of the panchromatic band with a 3 x 3 window size, was also be performed to be integrated to the supervised classification. The multi-temporal approach was made integrating to the supervised classification a new band derived from the subtraction of the post-fire NDVI from the pre-fire NDVI (Navarro et al. 2007).

Results

Burned area mapping

The burned area map is validated on the basis of 131 photo-interpreted points and the calculation of the global accuracy and the Kappa index. The unsupervised classification gives a global accuracy of 87.02% and a Kappa index of 76.42%.

Landcover mapping

Landcover classification previously performed was evaluated through statistical analyses, based on the generation of confusion matrix, the calculation of the global accuracy and the Kappa index, using the validation data set composed with 150 photo-interpreted points located in the wildland urban interfaces.
The supervised classification on the combination of MS bands and NDVI index presents a global accuracy of 87.33% in the wildland urban interfaces, the kappa index reaches 84.06%.

Damage mapping

Damage classifications previously performed were evaluated through statistical analyses, based on the generation of confusion matrix, the calculation of the global accuracy and the Kappa index, using the validation data set composed with 374 photo-interpreted points randomly generated according to the 10-classes damage typology.
For the VHR 2003 QuickBird image, the unsupervised classifications present global accuracies between 61.56% and 65.12%.The best results are obtained with the combination of MS bands and NDVI index. The supervised classification performed on this combination produces better damage maps with a global accuracy of 78.08%. The addition of the textural band significantly increases the quality of the classification: the global accuracy so exceeds 80%, with a Kappa index of 79.03%.

Damage mapping - Monodate and multidate approaches
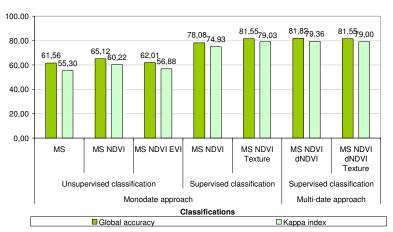
Figure 3. Damage mapping in the WUI using monodate and multidate approaches

The supervised classifications on VHR image improve the results to identify 5 levels of damage in the wildland urban interfaces. The main confusions affect the classes 8, 9 and 10 that correspond to 3 classes of a high level of damage, and particularly between classes 9 and 10 that are characterized by User and Producer's accuracies below 50%. The supervised classifications performed merging 9 and 10 classes reach a global accuracy of 86.63% in interfaces. Merging 8, 9 and 10 classes, the global accuracy is above 88 %. Recoded into 9 or 8 classes, the quality of classifications performed in the wildland urban interfaces present relative similar results, better than the classifications into 10 classes.

The multi-temporal approach, implying the Ikonos image before fire, was tested for supervised classifications, in order to look for 5 levels of damage corresponding to the levels of the intensity scale. The dNDVI band has a positive effect on the combination [MS + NDVI], from 78.08% to 81.82%. The global accuracies are similar when the textural band is included in treatments.

So, the multi-temporal approach can be considered as a relevant improvement of the supervised classifications performed on VHR images to produce good quality map with 5 levels of damage in wildland urban interfaces. When a before-fire VHR image is available, the textural analysis can be avoided.

Relations between damages and landcover types

The damage map previously generated could be related with the landcover map produced using the before-fire Ikonos image. The landcover could participate to understand the impact of the fire on the different types of vegetation.

The figure 4 presents, in the wildland-urban interfaces, the relation between the landcover supervised classification performed on the combination [MS NDVI] of VHR 2001Ikonos image and the damage supervised classification performed on the combination [MS NDVI dNDVI] of VHR 2003 QuickBird image.
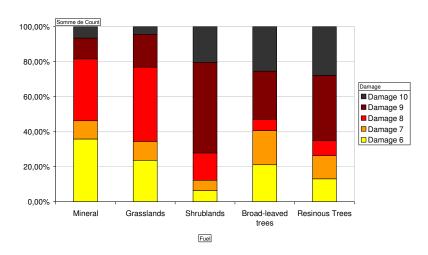
Figure 4. Damage representation within landcover type in the WUI

The graph shows the proportions of damage levels for each landcover type. The mineral and grasslands classes are mainly affected by damage 6 and 8, with only 18.28% of damage classes 9 and 10 for the mineral class, and 23.14% for grasslands. Shrublands are mainly affected by damage 9 (51.71%) when low damage classes 6 and 7 represent only 12.29%. Broad-leaved trees are affected by damage classes 6, 7, 9 and 10 in relatively similar proportions. The classes 6 and 7 represent 40.77%, and 52.85% for the classes 9 and 10. Resinous trees are more affected by high damage classes 9 and 10 (65.04%), and less affected by classes 6 and 7 (26.33%) in comparison with broad-leaved trees. Shrublands are the most impacted by fire: more than 80% is concerned by classes 8, 9 and 10 and more than 70% by high damages (classes 9 and 10).

References

Chen, X., Vierling L., Deering D. 2005. A simple and effective radiometric correction method to improve landscape change detection across sensors and across time. Remote Sensing of Environment 98: 63-79.

Collins, T.W.,2005. Households, forests, and fire hazard vulnerability in the American West: A case study of a California community. Environmental Hazards, 6, 23–37.

GIEC 2007. Bilan 2007 des changements climatiques. Contribution des Groupes de travail I, II et III au quatrième Rapport d'évaluation du Groupe d'experts intergouvernemental sur l'évolution du climat [Équipe de rédaction principale, Pachauri, R.K. et Reisinger, A.]. GIEC, Genève, Suisse, pp103.

Lampin C., Jappiot M., Alibert N., Manlay R., Guillande R. 2002. Prototype d'une échelle d'intensité pour le phénomène « incendie de forêts ». Ingénieries, 31, 49-56.

Lampin-Maillet, C., Jappiot, M., Long, M., Bouillon C., Morge, D., & Ferrier, J.P. 2010. Mapping wildland-urban interfaces at large scales integrating housing density and vegetation aggregation for fire prevention in the South of France. Journal of Environmental Management, 91, 732-741.

Navarro Cerrillo R. Mª , Hernández Clemente R., Escuin Royo S., Crespo Calvo R., Fernández Rebollo P., Lanjeri S. 2007. Forest fire effects assesment in Andalusía: a review of strategies and methodologies for severity mapping and vegetation recovery monitoring at the long-term. Wildfire 2007.

Vince, S. W., Duryea, M. L., Macie, E. A., & Hermansen, L. A. 2005. Forests at the wildland–urban interface: Conservation and management. Boca Raton: CRC Press.

AN INTEGRATED INDEX FOR THE MULTITEMPORAL VALIDATION OF BURNED AREA PRODUCTS

M. Padilla, S. Hantson, R. Cardozo, D. Corti, E. Chuvieco

Departamento de Geografía, Universidad de Alcalá. C/ Colegios, 2. 28801 Alcalá de Henares (Spain).
marc.padilla@uah.es, Hantson.stijn@gmail.com, carlos.cardozo@uah.es, dante.corti@uah.es,
emilio.chuvieco@uah.es

Abstract

In the last decade multiple effort have been undertaken to map Burned Area (BA) at a global scale, as input data for different earth system models. The validation of BA products, as any other cartography, is a critical step for its acceptance by final users, which needs standard procedures to select the most accurate one. The validation efforts of the most common BA products use different methods and results are not directly comparable. Most commonly, they try to estimate accuracy, but other components of validation, such as precision and temporal consistency have not been previously covered.

In this study we present a synthetic index that summarizes all the error components of burned area (BA) products raised from its validation against independent reference data. The validation analysis comprises: the detection ratio of burned patches, information from linear regression for course grid cells, errors from confusion matrices and temporal stability of the errors.

Our validation scheme has been applied to a three different global multi-annual BA products (GlobCarbon, MCD45 and L3JRC) in three study areas situated in Brazil, Canada and Portugal from 2000 to 2006. For these study areas, annual reference data were produced based on pre and post-fire analysis of Landsat imagery. Acquisition dates of images define the temporal periods with reference data available in each year. A semi-automatic algorithm for BA mapping was used for the generation of these reference data. Results show that the MODIS product produces better results than L3JRC and Globcarbon, with higher precision and accuracy, but it has a lower temporal stability.

Keywords: Burned Area, Validation, Error, Reference Data, Temporal Consistency

Introduction

Validation is a critical step of any remote sensing based product, since it provides a quantitative assessment on its reliability and provides a sound framework for product use. For this reason, international programs, such as Global Climate Observing Systems, have established specific requirements in terms of validation and error thresholds (GCOS 2010).

The Committee on Earth Observing Satellites Working Group on Calibration and Validation (CEOS-WGCV) defines validation as: "The process of assessing, by independent means, the quality of the data products derived from the system outputs" (http://lpvs.gsfc.nasa.gov/). This implies to compare those results with a reference source, which is assumed to be the ground truth. Validation should quantify the random and the systematic error components, which define the precision and the accuracy of the measurements, respectively. Validation should also explore the stability, the error variability through time, and the spatial consistency, the error variability across space or controlling factors.

During last years, several global and regional burned area (BA) products have been made available to the international community. The release of those products included a first stage validation, the GlobCarbon (2007), the L3JRC: Tansey et al. (2008), the MODIS MCD45A1: Roy et al. (2008), the GFED3: Giglio et al. (2010) or the Latin American AQL: Chuvieco et al. (2008). Results from those validation studies are not directly comparable as they use different validation methods. Little work has done to compare products using common validation

methods and reference data. Roy and Boschetti (2009) and Chang and Song (2009) presented the first attempts on the inter-comparison of global products, the former study compared GlobCarbon, MCD45 and L3JRC products in Southern Africa, and the later compared MCD45 and L3JRC in Canada, USA, Russia and China.

International bodies, such GOFC-GOLD Fire Implementation Team, try to coordinate efforts for generating standard validation methods for operational products. This paper follows this aim, as it presents a synthetic index that summarizes all the validation components, i.e. precision, accuracy and consistency of burned area (BA) products raised from its comparison against the same independent reference data. This study also present an application of the validation scheme with real data, using GlobCarbon, MCD45 and L3JRC global BA products for 3 study areas situated in Brazil, Canada and Portugal. The time series ranges from 2000 to 2006. This validation exercise is part of the fire_cci project, funded within the ESA initiative for improving the use of satellite products in climate change studies.

Methods

1.1 *Global products and reference data*

The validation scheme presented here has been applied to the MCD45, L3JRC and GlobCarbon global multi-annual BA products in 3 study areas situated in Brazil, Canada and Portugal from 2000 to 2006. MCD45 is produced by the NASA, has daily temporal resolution and 500 m pixel size, and it is derived from MODIS data on board the Terra and Aqua satellites (Roy et al. 2005). L3JRC is produced by the Joint Research Center, has daily temporal and 1km spatial resolution, and is derived from SPOT Vegetation (Tansey et al. 2008). GlobCarbon is produced by the European Space Agency, and it has daily temporal resolution at 1km2 pixel size. It is derived from ERS2-ATSR2 and ENVISAT AATSR (Plummer et al. 2007). GlobCarbon consist in results from three separated algorithms, in the present study we refer to a merge of the three algorithms: BA is defined as where at least two of the three algorithms detect a pixel as burned and unburned elsewhere.

The spatial distribution of the validation sites should include the complete range of environmental factors that affect burned area mapping accuracy. In this exercise, three validation sites were selected, as to be representatives of boreal forest (Central West of Canada), Mediterranean ecosystems (Portugal) and tropical biomes (central Brazil). All have a significant fire activity. Even though it is a small sample of fire conditions, they serve as an example to test the use of an integrated validation index for Burned Area products. In the three study areas, annual reference data were produced based on pre and post-fire analysis of Landsat imagery. Acquisition dates of images define the temporal periods with reference data available in each year. For each validation site, 7 years of BA reference data was produced, using 21 Landsat scenes in total. A semi-automatic algorithm for BA mapping, published in Bastarrika et al. (2011), was used for the generation of these reference data. These steps follow the standard procedure established in the fire_cci project (Chuvieco et al., 2011), available online at http://www.esa-fire-cci.org/webfm_send/241).

1.2   *Validation analysis and their metrics*

Three spatial comparisons between BA and reference fire perimeters were performed to derive error measures: (i) cross-tabulation, (ii) linear regression and (iii) patches detection.

From the cross-tabulation analysis, the burned/unburned confusion matrix was generated, which made it possible to compute commission and omission errors and the Kappa coefficient (based on the difference between observed and expected agreement by chance; Congalton and Green 1999). Since cross-tabulation is a pixel by pixel comparison, this analysis can be notably affected by differences in spatial resolution and co-registration errors between reference and target BA products. To avoid those problems, some authors alternatively recommend using a linear regression analysis, built upon the proportion of burned area in the two BA products using a grid coarser than the pixel resolution of the target product (Boschetti et al. 2004). In this study, a 10x10 km grid was used. Correlation coefficient, slope and intercept of the best fitted line between target and reference data was computed from a nonparametric linear regression based on Kendall's rank correlation (Roy et al. 2008; Sen 1968; Theil 1950). A strong linear relationship (high value of Kendall) indicates that the target and reference product include a similar estimation of BA extent for 10x10 km cells. Ideally, the fitted line would have slope 1 and intercept 0. The proximity of the fitted line to the ideal one (Prox) is assessed measuring the area between the two products in the scatter plot:

$$\mathrm{P}rox = 0.5 - \int_0^1 \left| fitted\ line\,(x) - identiy\ line\,(x) \right| dx \qquad (1)$$

The third criterion of accuracy was the patches detection index, defined as the ratio between the number of patches detected by the BA product and all BA reference patches . A patch was accounted as detected when at least 10% of its area was included in the BA product. This approach made it possible to identify the patch size below which the detection rate of the target product was unreliable.

1.3   *Components of validation*

The validation can be divided in three major components: precision, accuracy and stability.

Precision is the ability to produce repeatedly similar measurements over the same measurand, with a small random error (GOFC-GOLD 2010). For this study, we measured it by the Kendall correlation coefficient derived from the linear regression analysis, providing information at regional scale (Roy and Boschetti 2009).

Accuracy is the ability to produce measurements with a distribution centered to the true value, with a small systematic error (GOFC-GOLD 2010) and may be evaluated at local and/or regional scales (Roy and Boschetti 2009). The accuracy at local scale can be effectively characterized through the accuracy indices derived from the cross-tabulation, while accuracy and precision at regional scale through the linear regression analysis (Roy and Boschetti 2009). Local accuracy was computed as the mean of the kappa index and the complementary of omission and commission errors, and regional accuracy was computed as the mean of the detection index and the Prox.

Scores of precision and accuracy varied from 0 to 1, and resulted from the aggregation of their metrics in each of the three study areas. Precision and accuracy were computed for each study area, with data for all years, and, for the final integration index, the average values were used. Stability, *S*, was defined by the errors variability measured through time. According to the characteristics and sampling of the validation datasets, errors were measured once for each of the 7-years of the study period. A non-parametric measure of dispersion, the inter-quartile range, was used to estimate this parameter, for each metric *x*, and for each study site *ss*, through years *i*.

$$S_{ss,x} = 1 - IQR(x_{ss,i}) \qquad (2)$$

S will vary from 0 to 1 and will be the result of the average of stability indexes seen in each of the three study areas. Local stability is computed as the mean of stability indexes of kappa index and omission and commission errors, and regional stability is equal to the patches detection ratio.[1]

1.4   *Integration of validation components*

The final integrated index varied from 0 to 1, with high values indicating high reliability. The integrated index was computed as the mean between the three validation components (precision, accuracy and stability).Precision was equal to the Kendall coefficient (*k*) and accuracy index was the average between local and regional accuracy. Consistency index ideally should cover both spatial and temporal variation, but in this paper only the latter was considered, It was computed as the mean of local and regional S.

Results

The final integrated index and scores for the three validation components are shown in Table . MCD45 was the product with the highest precision and accuracy, although it showed lower stability values than L3JRC and GlobCarbon.

Table 1. Scores of the three validation components and the final integrated index

	Precision	Accuracy	Stability	Integrated Index
GlobCarbon	0.40	0.19	0.92	0.51
L3JRC	0.36	0.21	0.92	0.50
MCD45	0.59	0.44	0.83	0.62

Figure 1 shows local accuracy for each target product in the three validation sites through the 7-years of the study period. Accuracy and stability performances of the three global products agree, as expected, with scores of accuracy and stability components shown in Table 1. MCD45 was found slightly more accurate in Brazil and Portugal than L3JRC and GlobCarbon, which

---

[1] Similarly to the temporal stability, a spatial consistency (SC) index may be considered. It may related to how errors vary throughout space. SC could be assessed by errors variability found through ranges of different controlling factors. SC was not computed in this paper, since only three sites were available, but will be within the fire_cci project at a later stage.

showed similar results. Differences in performances were more important in Canada, where MCD45 was clearly the most accurate product, although with low stability, while L3JRC and GlobCarbon presented lower accuracy, but high statibility. Differences in product performances through validation sites suggested that they are affected by land cover or fire regimes of each study site. On the other hand, some degree of correlation was found on the temporal trends of local accuracy values within each study site, particularly in Portugal. Relative minimums coincide with low fire activity years (Figure 2), when fires patches are smaller and more difficult to detect by coarse spatial resolution sensors.
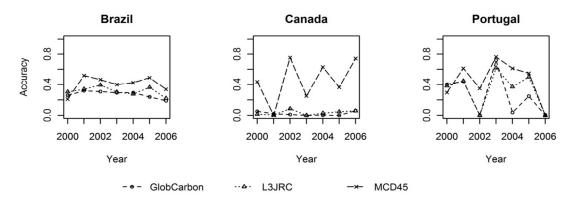
Figure 1. Local accuracy values for each global product in the three validation sites through the 7-years of the study period.
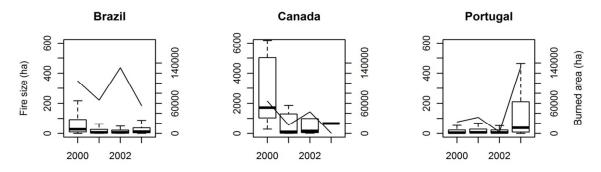
Figure 2. Fire size distribution (boxplots) and total annual burned area (lines, plotted on the secondary axis) in the three validation sites from 2000 to 2003, when fire sizes are available (years with Landsat images without the SLC-off problem)

Conclusions

A framework for validation is presented through a synthetic index that summarizes all the error components of burned area (BA) products, i.e. precision, accuracy and consistency, raised from its validation against independent reference data. Metrics derived from most common validation methods have been selected to be part of the three error components, according to their meanings.

The use of this validation scheme allowed to easily compare performances of three operational products, providing scores for precision, accuracy, temporal stability and for the integrated index. MCD45 showed highest precision and accuracy, however lower stability values. MCD45 is slightly more accurate than the two others in Brazil and Portugal, but much more in Canada, although with low stability, where L3JRC and GlobCarbon present low accuracy values, in a

consistent way. Burned patches size and land cover may be two important factors in product performances and further research could be done to investigate their effects. The validation framework here presented will now be implemented for the validation of the BA products at a more extensive spatial scale around the globe.

References

Bastarrika, A., Chuvieco, E., & Martin, M.P. 2011. Mapping burned areas from Landsat TM/ETM+ data with a two-phase algorithm: balancing omission and commission errors. Remote Sensing of Environment, 115, 1003-1012

Boschetti, L., Flasse, S.p.P., & Brivio, P.A. 2004. Analysis of the conflict between omission and commission in low spatial resolution dichotomic thematic products: The Pareto Boundary. Remote Sensing of Environment, 91, 280-292

Chang, D., & Song, Y. 2009. Comparison of L3JRC and MODIS global burned area products from 2000 to 2007. Journal of Geophysical Research D: Atmospheres, 114

Chuvieco, E., Opazo, S., Sione, W., Del Valle, H., Anaya, J., Di Bella, C., Cruz, I., Manzo, L., López, G., Mari, N., González-Alonso, F., Morelli, F., Setzer, A., Csiszar, I., Kanpandegi, J.A., Bastarrika, A., & Libonati, R. 2008. Global Burned Land Estimation in Latin America using MODIS Composite Data. Ecological Applications, 18, 64-79

Chuvieco, E., Padilla, M., Hantson, S., Theis, R., & Snadow, C. 2011. ESA CCI ECV Fire Disturbance - Product Validation Plan (v3.1). In: ESA Fire-CCI project (http://www.esa-fire-cci.org/)

Congalton, R.G., & Green, K. 1999. Assessing the Accuracy of Remotely Sensed Data: Principles and Applications. Boca Raton: Lewis Publishers

GCOS 2010. GCOS-143 - Guideline for the Generation of Datasets and Products Meeting GCOS Requirements. In: Global Climate Observing System

Giglio, L., Randerson, J., T., van der Werf, G.R., Kasibhatla, P., Collatz, G.J., Morton, D.C., & Defries, R. 2010. Assessing variability and long-term trends in burned area by merging multiple satellite fire products. Biogeosciences Discuss, 7, 1171

GlobCarbon 2007. Demonstration Products and Qualification Report. In (pp. 1-69): ESA

GOFC-GOLD 2010. A sourcebook of methods and rocedures for monitoring and reporting anthropogenic greenhouse gas emissions and removals caused by deforestation, gains and losses of carbon stocks in forests remaining forests, and forestation. In. Alberta, Canada: GOFC-GOLD Project Office, Natural Resources Canada

Plummer, S., Arino, O., Ranera, F., Tansey, K., Chen, J., Dedieu, G., Eva, H., Piccolini, I., Leigh, R., Borstlap, G., Beusen, B., Fierens, F., Heyns, W., Benedetti, R., Lacaze, R., Garrigues, S., Quaife, T., De Kauwe, M., Quegan, S., Raupach, M., Briggs, P., Poulter, B., Bondeau, A., Rayner, P., Schultz, M., & McCallum, I. 2007. An update on the GlobCarbon initiative: multi-sensor estimation of global biophysical products for global terrestrial carbon studies. In, Envisat Symposium 2007. Montreux, Switzerland

Roy, D., Jin, Y., Lewis, P., & Justice, C. 2005. Prototyping a global algorithm for systematic fire-affected area mapping using MODIS time series data. Remote Sensing of Environment, 97, 137-162

Roy, D.P., & Boschetti, L. 2009. Southern Africa validation of the MODIS, L3JRC, and GlobCarbon burned-area products. IEEE Transactions on Geoscience and Remote Sensing, 47, 1032-1044

Roy, D.P., Boschetti, L., Justice, C.O., & Ju, J. 2008. The collection 5 MODIS burned area product - Global evaluation by comparison with the MODIS active fire product. Remote Sensing of Environment, 112, 3690-3707

Sen, P.K. 1968. Estimates of the regression coefficient based on Kendall's tau. Journal of the American Statistical Association, 63, 1379-1389

Tansey, K., Grégoire, J.-M., Defourny, P., Leigh, R., Pekel, J.-F., Bogaert, E., & Bartholome, E. 2008. A new, global, multi-annual (2000-2007) burnt area product at 1 km resolution. Geophysical Research Letters, 35, L01401, doi:10.1029/2007GL03156

Theil, H. 1950. A rank-invariant method of linear and polynomial regression analysis. Nederlandse Akademie Wetenchappen Series A., 53, 386-392

DELINEATING UNBURNED ISLANDS WITHIN FIRE SCAR PERIMETER. THE ROLE OF SPECTRAL AND SPATIAL RESOLUTION OF SATELLITE DATA

M. Pleniou, P. Dimopoulos, N. Koutsias

Department of Environmental and Natural Resources Management, University of Ioannina, G. Seferi 2, Agrinio GR-30100, Greece. mpleniou@cc.uoi.gr, pdimopul@cc.uoi.gr, nkoutsia@cc.uoi.gr

Abstract

Forest fires govern ecosystem dynamics in a way that is defined by their particular characteristics such as intensity, type, periodicity, etc. Unburned patches within fire scar perimeter are very important especially for the succession and the restoration of the affected ecosystems. The ecological importance of unburned islands within fire scar perimeter is high in the succession process, especially for vegetation types whose regeneration pattern depends on the existence of unburned inlands. Satellite remote sensing offers practical benefits and is an ideal tool for mapping and monitoring, while it has been extensively applied to map burned surfaces at various scales. The aim of our study is to explore the role of spectral and spatial resolution of satellite data for delineating unburned inlands within fire scar perimeter. For that purpose, a study case was established in one very destructive wildfire occurred in Parnitha, Greece on July 2007. Satellite data at multiple spectral and spatial resolution, were acquired shortly after the fires from LANDSAT, ASTER, and IKONOS satellite sensors. Additionally from the basic data set we created satellite data at coarser spatial resolution (up to 512 meters). The spectral resolution of the sensors covers the visible, near and mid-infrared part of the electromagnetic spectrum. Classical image processing algorithms were applied to correct geometrically, radiometrically and atmospherically the satellite images used. Additionally, classical image processing techniques were applied to classify the satellite data with the maximum possible accuracy. Totally 412 classifications have been implemented considering different combinations of spectral and spatial resolutions. Unburned inlands were delineated by the different satellite sensor data used in the study, and compared with reference data acquired by field survey and aerial photographs taken shortly after the fire. The spatial and the spectral resolution of the satellite data is further explored and discussed on how they influence the acquired total accuracy. It seems that the spatial resolution is very critical while it is associated to the scale under which the mapping of the burned area is implemented. The spectral resolution of the satellite sensor data is also critical since the spectral differentiation between different land cover types is very important to discriminate burned and unburned patches. Linear regressions models were fitted to characterize the relationships between the accuracy and several others parameters. The main findings of our research are (a) at combinations of high separability values, the great factor which influences the mapping accuracy is the spatial resolution of the satellite data, and (b) the spectral resolution seems to play a more significant role as the separability values of the considered satellite images become widen.

Keywords: burned land mapping, maximum likelihood, IKONOS, ASTER, LANDSAT, separability

Introduction

Forest fires govern ecosystem dynamics in a way that is defined by their particular characteristics such as intensity, type, periodicity, etc. Unburned patches within fire scar perimeter are very important especially for the succession and the restoration of the affected ecosystems. The ecological importance of these unburned islands is the reason to determine which resolution (spatial-spectral) affects them more, so we can delineating them better with further aim a proper forest management. Satellite remote sensing offers practical benefits and is an ideal tool for mapping and monitoring, while it has been extensively applied to map burned surfaces at various scales (Koutsias and Karteris 1998). According to Roman-Cuesta et al. (2009) the post-fire mosaic, consisting of burned patches and islands of unburned vegetation, depends on the same variables as those influencing fire behavior: topography, meteorology and

fuels (Alexander et al. 2006). The key factors that determine fire characteristics (e.g. fire-line intensity and rate of spread), together with fire residence times determine the unburned patches within the fire scar perimeter (Turner et al. 1997). Roman-Cuesta et al. (2009) also stated that the role of unburned islands is important in various ecological processes, e.g. vegetation re-establishment patterns (Turner et al. 1994), forest succession and forest structure (Retana et al. 2002), fauna establishment (Gasaway and Dubois 1985), in erosion control and watershed dynamics (Lathrop 1994). Moreira et al. (2011) report that the effects of fire on landscape may vary from region to region as a result of local fire history, regeneration patterns and topographic constraints (Viedma 2008), while there is a scale-dependent relationship between fire and landscape heterogeneity.

Materials and Methods

1.1 *Study Area*

Mt Parnitha, situated in central Greece, distinguish three vegetation zones. The first one, extended from 400 to 1000 m, is dominated by Pinus halepensis Mill. forests, Quercus coccifera L., Pistacia lentiscus L., Arbutus unedo L. and A. andrachne L. formations, and phryganic ecosystems. The second zone extends from c.1000 m on the southern slopes of the mountain (and from 600–700 m on the northern ones) to 1400 m and is dominated by Abies cephalonica forest. Juniperus oxycedrus L. subsp. oxycedrus stands also occur and on the plateaus some grassland species grow. The third vegetation zone is observed on the highest mountain summits. This zone is vestigial and consists of spiny, caespitose and cushion-like bushes, together with several endemic and rare species of the high mountains (Aplada et al. 2007). Bioclimatically, Parnitha belongs to the subhumid zone with cold winters and the climate is characterized as Meso-Mediterranean for altitudes of 700–1100 m, and Sub-Mediterranean for the highest peaks of the mountain. The main substrates are limestones and marbles, followed by schists (which appear in the valleys), and some flysch.

1.2 *Satellite Data*

The satellite data used in our study come from Ikonos, Landsat and Aster sensors. Ikonos satellite: one satellite image acquired after the fire on 08/07/2007, with spatial resolution 4 meters multispectral and 1 meter pan-sharpened. The spectral resolution, which consists of four bands, covers the visible and the near infrared part of the electromagnetic spectrum. Landsat 5 satellite: one satellite images which acquired after the fire on 05/09/2007. Landsat images have a panchromatic band with 15 meters and other seven channels with spatial resolution of 30 meters, which one of them is thermal with 60 meters resolution. The spectral resolution ranges from 0.45 to 12.5 micrometers. Aster satellite: one satellite image acquired after the fire on 20/07/2007. Aster images have three bands in the visible and near infrared part of the electromagnetic spectrum with a 15 meters resolution, six more bands in the short wave with a spatial resolution of 30 meters and five thermal bands with a 90 meters resolution.
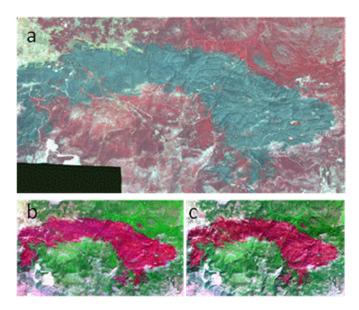
Figure 1. Satellite data in the study a. Ikonos, b. Aster, c. Landsat

1.3 *Methods*

Classical image processing algorithms were applied to correct geometrically, radiometrically and atmospherically the satellite images used. Additionally to the basic data set, we created satellite data at coarser spatial resolution (up to 512 meters) using resampling techniques. The spectral resolution of the sensors covers the visible, near and mid-infrared part of the electromagnetic spectrum. The maximum likelihood classifier was applied to classify the satellite data with the maximum possible accuracy. Totally 412 classifications have been implemented considering different combinations of spectral and spatial resolutions.

Unburned inlands were delineated by the different satellite sensor data used in the study and compared with reference data acquired by field survey and aerial photographs taken shortly after the fire. Linear regressions models were fitted to model the relationships between the accuracy and several others parameters.

Results and Discussion

Table 1 and Table 2 summarize the results of the regression analysis made. Standardized coefficients or beta coefficients show the expected change in the dependent variable for a standard deviation increase in the predictor variable. Therefore they show which of the independent variables have a greater effect on the dependent variable in a multiple regression analysis. When the analysis is made with all separability values then the spectral resolution is the most important since the beta coefficient is 5.80 as compared to the spatial resolution which is -1.29. When the analysis is made with the separability values higher 1280 then the spectral resolution is less important than the spatial resolution since the beta coefficient is 5.31 as compared to the beta coefficient of the spatial resolution which is -7.36. The estimation of these coefficients shows sensitivity to the considered range of the values of the spectral and the spatial resolution. Therefore the coefficients of the models should be evaluated considering the range of the spectral and the spatial resolution of the cases used. Apart from the spectral and

the spatial resolution we evaluated also the behavior of other independent variables like the type of the satellite sensor (Ikonos, Aster, Landsat) and weather the data are the original or the resampled (simulation).

Table 1. Standardized Coefficients (Beta) of the linear regression model between producer's accuracy of vegetation with the independent variables considering all separability values
R=.624 R2=0.389

Model	Standardized Coefficients (Beta)
Spatial resolution	-1.29
Spectral resolution	5.80
Ikonos	1.74
Aster (resampled to 15m)	0.31
Landsat	0.86
Simulation	0.12

Table 2. Standardized Coefficients (Beta) of the linear regression model between producer's accuracy of vegetation with the independent variables considering only those cases exceed the separability value of 1280
R=.81, R2=0.658

Independent variables	Standardized Coefficients (Beta)
Spatial resolution	-7.36
Spectral resolution	5.31
Ikonos	1.25
Aster (resampled to 30m)	0.45
Landsat	1.82
Simulation	-0.94

a. all separability values   b. separability values > 1280
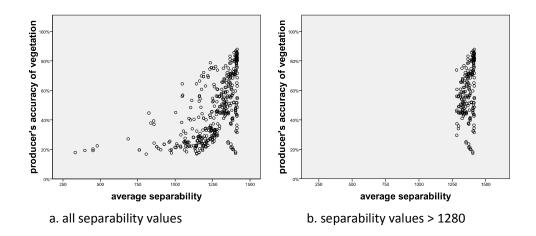
Figure 2. Scatter plot between producer's accuracy of vegetation with the average separability considering a. all cases, b. only those cases exceed the separability value of 1280

The main findings of our research are (a) the spectral resolution seems to play a more significant role as the separability values of the considered satellite images become widen (Table 1) and (b) at combinations of high separability values, the great factor which influences the mapping accuracy is the spatial resolution of the satellite data (Table 2). The spatial

resolution is very critical while it is associated to the scale under which the mapping of the burned area is implemented. The spectral resolution of the satellite sensor data is also critical since the spectral differentiation between different land cover types is very important to discriminate burned and unburned patches.

Acknowledgements

References

Alexander, J.D., Seavy, N.E., Ralph, C.J., Hogoboom, B. 2006. Vegetation and topographical correlates of fire se-verity from two fires in the Klamath-Siskiyou region of Oregon and California. International Journal of Wild-land Fire 15: 237-245

Aplada, E., Georgiadis, T., Tiniakou, A., Theocharopoulos, M. 2007. Phytogeography and ecological evaluation of the flora and vegetation of Mt Parnitha (Attica, Greece). Edinburgh Journal of Botany 64: 185-207

Gasaway, W.C., Dubois, S.D. 1985. Initial response of moose, Alces alces, to wildfire in interior Alaska. Canadian Field-Naturalist 99: 135-140

Koutsias, N., Karteris, M. 1998. Logistic regression modelling of multitemporal Thematic Mapper data for burned area mapping. International Journal of Remote Sensing 19: 3499-3514

Lathrop, J.R.G. 1994. Impacts of the 1998 wildfires on the water quality of Yellowstones and Lewis lakes,Wyoming. International Journal of Wildland Fire 4: 169-175

Moreira, F., Viedma, D., Arianoutsou, M., Curt, T., Koutsias, N., Mouillot, F., Vaz, P., Barbati, A., Corona, P., Ri-golot, E., Xanthopoulos, G., Bilgili, E. 2011. Landscape - wildfire interactions in Southern Europe: implications for landscape management. Journal of Environmental Management 92: 2389-2402

Retana, J., Espelta, J.M., Habrouk, A., Ordoñez, J.L., de Sola-Moràles, F. 2002. Regeneration patterns of three mediterranean pines and forest changes after a large wildfire in northeastern Spain. Ecoscience 9: 89-97

Roman-Cuesta, R.M., Gracia, M., Retana, J. 2009. Factors influencing the formation of unburned forest islands within the perimeter of a large forest fire. Forest Ecology and Management 258: 71-80

Turner, M.G., Hargrove, W.W., Gardner, R.H., Romme, W.H. 1994. Effects of fire on landscape heterogeneity in Yellowstone National Park, Wyoming. Journal of Vegetation Science 5: 731-742

Turner, M.G., Romme, W.H., Gardner, R.H., Hargrove, W.W. 1997. Effects of fire size and pattern on early succes-sion in Yellowstone National Park. Ecological Monographs 67: 411-433

Viedma, O. 2008. The influence of topography and fire in controlling landscape composition and structure in Sierra de Gredos (Central Spain). Landscape Ecology 23: 657-672

MONITORING POST-FIRE VEGETATION RECOVERY USING OPTICAL AND SAR DATA

A. I. Polychronaki[1], I. Z. Gitas[1], A. Minchella[2]

[1]*Laboratory of Forest Management and Remote Sensing, Aristotle University of Thessaloniki, P.O. Box 248, University Campus, Greece. anpolych@for.auth.gr, igitas@for.auth.gr*
[2]*RSAC c/o ESA-Esrin, Via G. Galilei 64, 00044 Frascati, Italy. andrea.minchella@esa.int*

Abstract

This paper presents the development of a classification scheme in order to assess the post-fire impact on the Mediterranean island of Thasos by using optical and SAR imagery and by employing object-based classification. For this purpose, 26 SPOT and 46 ERS1&2 images acquired during the period 1987-2010 were appropriately pre-processed. Subsequently, the multitemporal backscatter signatures of ERS images were investigated for monitoring vegetation regrowth. The next steps of the methodology involved: 1) the development of an object-based classification scheme in order to map the basic land-cover classes in Thasos using SPOT imagery, and 2) the investigation whether the synergy of optical and SAR imagery could overcome the limitations of optical data in mapping a Mediterranean landscape.
Results of the developed post-fire monitoring scheme indicated that the forest regeneration rate is rather slow even 20 years after the fire events. It can also be concluded that, the object-based classification procedure produced slightly more accurate results (87.89% overall accuracy) when SAR images were included in the analysis.

Keywords: post-fire monitoring, Mediterranean landscape, optical data, SAR data, object-based classification.

Introduction

Several satellite image analysis techniques are employed in the mapping and monitoring of post-fire recovery.

The most important traditional methods are image classification, Vegetation Indices (VIs) and Spectral Mixture Analysis (SMA). On the other hand, object-based classification, which includes both spectral and contextual information (Wicks et al. 2002), has been recently employed by Mitri and Gitas (2010) for mapping post-fire vegetation recovery using EO-1 Hyperion imagery with high accuracy.

Methodologies developed for mapping land-cover types in Mediterranean regions have shown limitations in their applicability over wide areas mainly due to the heterogeneity of the landscape. This heterogeneity cannot be regarded as a simple mixing of life-forms over large areas but, rather, the formation of transitional zones of varying mixtures resulting from disturbance and recovery cycles (Shoshany 2000).

Synthetic-aperture radar (SAR) data has been extensively used for various ecological processes (Kasischke et al. 1997). However, the application of SAR data in monitoring vegetation regrowth is rather limited (Minchella et al. 2009). Chust et al (2004) reported that a relatively good discrimination between dwarf shrubs and open shrublands was achieved by using a series of ERS images in combination with SPOT XS optical data.

The aim of this study was to map post-fire forest regeneration and vegetation recovery on the Mediterranean island of Thasos by using optical and SAR imagery and by employing object-based classification.

The specific objectives were: 1) to investigate the potential of ERS images for the monitoring the vegetation regrowth in the burned areas, 2) to develop an object-based classification

scheme for mapping the basic land-cover classes in Thasos using SPOT imagery, and 3) to investigate whether the synergy of optical and SAR imagery could overcome the limitations of optical data in mapping a mountainous Mediterranean landscape.

Study area and dataset description

The study area is the island of Thasos, Greece's most northerly island. Elevation ranges from sea level to 1217 m. Pinus brutia is the dominant tree species at lower elevations (0 to 800 m), whereas Pinus nigra is found at higher altitudes. In addition, other types of Mediterranean vegetation, such as maquis and garrigue (a shrubland vegetation of the Mediterranean region composed primarily of leathery broad-leaved

evergreen shrubs or small trees), are also present. The fires that occurred on Thasos Island in 1985 and 1989 resulted in the destruction of approximately 118.7 km2 and 95 km2, respectively, of different vegetation land cover types. Before 1984, forests and forested lands covered 47.5% of the island.

The data that were used in this study consisted of the following: 1) 26 SPOT images (20m spatial resolution) covering the period 1986 – 2008 (summer months) acquired in different incidence angles (ranging from 0.7º to 29º), 2) 46 ERS 1 and 2 PRIs (Precision Image) in descending and ascending passes, 3) a digital elevation model with 10 m pixel size generated from a 1: 5000 contour maps of Thasos, 4) colored orthophotos acquired between 2007 and 2009 available from Ktimatologio S.A. (Greek Cadastre), 5) black and white orthophotos acquired in 1996, 6) orthophoto land-cover maps produced in 1976 and 1977, 7) a forest service fire perimeter map of the two fires on Thasos.

Methodology

The methodology comprised three basic steps, namely, data preprocessing, the analysis of the multitemporal backscattering signatures, and the development of an object-based classification scheme for mapping the basic land-cover types on the island of Thasos.

1.1 *Data preprocessing*

This step included the preprocessing of both the optical (SPOT) and SAR (ERS) data. The 26 SPOT images were firstly orthorectified using the 10-meter DEM of the study area. Fifteen out of the 26 images were finally not used in the analysis due to large RMS errors. Following, the remaining 11 SPOT or thorectified images (acquisition dates: 1992/02/08, 1993/07/07, 1993/17/08, 1995/04/07, 1996/05/07, 1998/14/07, 2003/03/08, 2003/29/06, 2004/23/07, 2006/20/08, 2007/20/07), were atmospherically corrected (Chavez, 1996) and radiometrically normalized (Hall et al 1991, Jensen et al 1995). The 46 ERS PRIs were orthorectified and radiometrically normalized using the 10m DEM by employing the SAR simulation terrain correction operator of NEST software (Next ESA SAR Toolbox). The s0 images were created with a 12.5m pixel size, while layover-shadow masks were also generated. Layover and shadowed areas were excluded from further analysis.

1.2   *Analysis of the multitemporal backscattering signatures*

In order to investigate the potential of multitemporal s0 ERS images for monitoring vegetation regrowth in burned areas, samples were carefully chosen based on the land-cover map of the Island before the fires and the orthophotos of 1996 and 2007. Sample regions were chosen from the 2007 images and represented different land-cover types (e.g. low vegetation, regeneration) in the burned areas.

1.3   *Object-based classification*

The classification scheme consisted of five basic land-cover categories, namely, forested areas (pine trees), shrubs (this category included maquis and shrublands with scattered trees), areas covered with low vegetation (this category included garrigue, areas with scattered vegetation where soil is exposed in high degree and agricultural areas), artificial areas and bareland (this category included urban areas and land without vegetation cover) and broadleaves (this category included broadleaved trees and some agricultural areas mainly olive trees). These classes were chosen in order to cover the major land-cover types of the study area, without having to compromise the classification results by including detailed classes (Dimitrakopoulos et al. 2010).

The object-based classification started with the segmentation procedure which resulted in the creation of image objects and was followed by the classification into the aforementioned basic land-cover categories using the appropriate attributes (intrinsic, topological, semantic features) of the resulting image objects (Benz et al. 2004). The developed object-based classification scheme comprised of 3 levels. In level one the land-cover categories were mapped using only the SPOT images. Features such as the mean (mean intensity of all pixels forming an object) and NDVI values were used to achieve optimum separation of the classes. Five classes were created at this level: 'forest', 'broadleaves', 'low vegetation', 'shrubs' and 'artificial areas/bareland'. At level two the s0 ERS images were employed in order to enhance the classification of the class 'forest', which was created at level one since a confusion between forested areas and areas covered with dense shrubs was observed. Class 'not forest' was finally created at level two. The last level of the classification served as to combine the two results from level one and two. The final classes that were created were: 'forest a' (class 'forest' excluding the areas which were classified as 'not forest' at level two), 'broadleaves', 'low vegetation', 'shrubs' and 'artificial areas/bareland'. The development of the classification scheme was based on 5 SPOT images and ERS s0 images and which was subsequently transferred to the remaining images in order to classify the land-cover categories.

Results and discussion

From the multitemporal analysis of the backscatter signatures, not clear conclusions could be drawn, given that similar land-cover types showed different mutlitemporal behaviour. However, it has to be noted that the signal from low vegetated areas showed high dynamics which could be attributed to weather conditions, while the signal from undisturbed forested areas showed an increasing trend, a behaviour that could be attributed to increasing forest biomass (Figure 1).

The main difficulty during the development of the classification scheme was the confusion between forested areas and areas occupied by shrubs with dense vegetation cover. This confusion could be explained by the spectral overlap among the two vegetation types due to the topographic effect, the canopy shadows, and the illumination conditions. The use of ERS imagery in the process helped in slightly overcoming this problem, given that even after the inclusion of the s0 information the confusion between the two land cover types could not be solved in some areas.

In addition, both SPOT and ERS images showed limitations over the mountainous region of Thasos Island. Almost half of the available SPOT images could not be used due to the high incidence angle by which the images were acquired, while a large part of the ERS images could not be analyzed due to the layover-shadow effect. In order to assess the classification accuracy the appropriate descriptive statistics were generated. The stratified sampling method was employed and reference points were identified using the colored orthophotos. Overall classification accuracy was estimated to be 87.89% while overall kappa was equal to 0.8318.
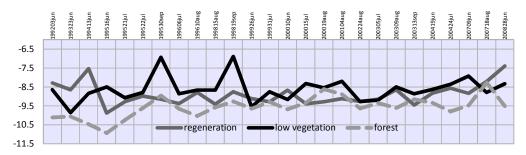
Figure 1. Behaviour of backscatter through time corresponding to three different land-cover categories. Y-axis is showing the backscatter coefficient (db).

11 classification maps of the five basic land-cover classes were finally created. In order to assess the post-fire forest regeneration and vegetation recovery the classification maps of 1996/05/07 and 2007/20/07, were used. The analysis was performed in a GIS environment using the fire perimeters of the 1985 and 1989 fires and the land-cover map of the Island which were generated from the digitization of the ortho photo land-cover maps that were produced before the fires. Statistics were extracted for each of the land-cover class existed before the fires. Results showed that only a small area of the burned forests has been regenerated (Figure 2) indicating a very slow regeneration rate even almost 20 years after the fire events. In addition, it can be observed that in fire affected areas, low vegetation is been replaced gradually by shrubs (Figure 2).
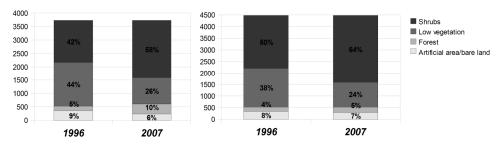
Figure 2. Statistics extracted for forested areas that have been burned in 1989 (left) and 1985 (right). Figures show which land-cover categories dominate the burned areas based on the classifications using images acquired in 1996 and 2007.

Conclusions

Based on the aim and objectives of this work the following conclusions can be drawn: 1) from the multi temporal analysis of the backscattering coefficient for monitoring vegetation regrowth, not clear conclusions could be extracted. However, the signal of undisturbed forested areas showed an increasing trend which could be attributed to increasing forest biomass, 2) the use of object-based classification for mapping basic land-cover categories when employing SPOT images resulted in a very accurate (87.89% over all accuracy) and transferable classification scheme, 3) the synergy of optical and SAR imagery overcame slightly the limitations of optical data in mapping a Mediterranean landscape, especially the confusion between forested areas and areas covered with dense shrubs.

Acknowledgments

References

Benz, U. P., Hofmann, P., Willhauck, G., Lingenfelder, I., Heynen, M. 2004. Multi-resolution, object-oriented fuzzy analysis of remote sensing data for GIS-ready information. ISPRS Journal of Photogrammetry & Remote Sensing 58, 239– 258.

Chust, G., Ducrot, D., Pretus, J. L.L. 2004. Land cover discrimination potential of radar multitemporal series and optical multispectral images in a Mediterranean cultural landscape, International Journal of Remote Sensing, Vol. 25, No. 17, 3513–3528.

Dimitrakopoulos, K., Gitas, I. Z., Polychronaki, A., Katagis, T., Minakou, C. 2010. Land Cover/Use Mapping Using Object Based Classification of SPOT Imagery Proceedings of the 30th EARSeL Symposium, 31 May-3 June 2010, Paris, France.

Hall, F. G., Strebel, D. E., Nickeson, J. E., Goetz, S. J. 1991. Radiometric rectification: toward a common radiomet ric response among multidate, multisensor images. Remote Sensing of Environment, 35, 11–27.

Jensen, J. R., Rutchey, K., Koch, M. S., Narumalani, S. 1995. Inland wetland change detection in the Everglades Water Conservation Area 2A using a time series of normalised remotely sensed data. Photogrammetri c Engineering and Remote Sensing, 61, 199–209.

Kasischke, E. S., Melack, J. M. and Dobson, M. C. 1997. The use of imaging radars for ecological applications-A review. Remote Sensing Environment 59: 141-156.

Minchella, A., Del Frate, F., Capogna, F., Anselmi, S., Manes, F., 2009. Use of multitemporal SAR data for monitoring vegetation recovery of Mediterranean burned areas. Remote Sensing of Environment 113: 588-597.

Mitri, G., Gitas, I. Z. 2010. Mapping postfire vegetation recovery using EO-1 Hyperion imagery. IEEE Transactions on Geoscience and Remote Sensing 48: 1613-1618.

Shoshany, M. 2000. Satellite remote sensing of natural Mediterranean vegetation: a review within an ecological context, Progress in Physical Geography 24,2 pp. 153–178.

Wicks, T., Smith, G., Curran, P. 2002. Polygon-based aggregation of remotely sensed data for regional ecological analysis. International Journal of Applied Earth Observation and Geoinformation 4: 161-173.

IDENTIFICATION OF BURNED AREAS IN THE LIGURIA REGION USING LANDSAT AND QUICKBIRD IMAGES. THE CASE STUDY OF MONTE FASCE.

M. Sirtori[1], G. Barberis[1], P. Gamba[2], M. Mariotti[1]

[1]Dipartimento per lo Studio del Territorio e delle sue Risorse, Università degli Studi di Genova, Genova, 16136, Italy.
mariaelena.sirtori@unige.it, giuseppina.barberis@unige.it, m.mariotti@unige.it
[2]Dipartimento di elettronica, Università di Pavia, Pavia, 27100, Italy. paolo.gamba@unipv.it

Abstract

The aim of this study is to test and compare different remote sensing techniques to define burned areas in Liguria. The test area is the Monte Fasce site, affected by a huge fire in September 2009. The work is based on the Landsat TM and the QuickBird images acquired before and after the event. We considered bands, PCA, texture analysis and several spectral indices reported in literature. The indices were compared empirically and using two algorithms (ROI separability and the software SEATH) to find the most suited ones to detect the burned zones. Once the base data have been characterised, the burned area was extracted using different methods: thresholds, decision trees, the Maximum Likelihood classification, the ENVI and RHSEG segmentation and the Change Detection technique. The maps' accuracy of the areas covered by fire was estimated by comparing the satellite data with those taken on the ground by the Forest Service and the ones provided by a visual analysis of the post-event QuickBird image. The best results were obtained with the multitemporal technique computing the pre- and post-image difference: the Landsat data give an overall error of 22.75% applying a multithreshold technique with the indices NDVI, NBR and NBRT; the QuickBird data show an error of 22.8% using the NDVI index. Future improvements should envisage a methodology to reduce the error and a thorough analysis on a range of burned areas in the Liguria region.

Keywords: burned areas, Liguria region, remote sensing, Landsat, QuickBird

Introduction

Fires are a major cause of depletion and degradation of the Liguria region. According to the Italian law 353/2000, municipalities are expected to create a register showing the events occurred, their location and their perimeter, with the aim of applying the fifteen-year constraint to no-change of land use and the ten-year constraint to not-suitability for building, grazing and hunting (LQMIB 2000). It is within this context that our project develops an experimental activity on burned areas detection through remote sensing. To date, there is not a standard procedure to identify and map burned areas. We aim at identifying the most appropriate approach to achieve a fast and semi-automated delineation of burned areas in the Liguria region.

Materials and methods

Monte Fasce (44°24'34'' N, 9°02'04'' E) is located just behind the town of Genoa. From 6 to 13 of September 2009 (CFS 2009) this area was affected by a huge fire that destroyed around 1200 ha of vegetation. The prevailing injured land covers are: grassland (49%), shrubs (16%), mixed conifer and broadleaf high forest (11%), simple mixed coppice (9.5%), simple coppice of *Quercus ilex* L. (3.5%), high forest of tall pines (3%) and cultivated land (2.3%).
The analysis is based on remote sensing data that include pre- and post-fire images acquired by medium and high geometric resolution sensors, in particular: two Landsat-5 TM images from 31

August 2009 and 23 September 2009; two QuickBird images from 11 May 2009 and 27 September 2009.

Additional data used in this work are a forestry map, the forest fire archives based on ground fire observations done by the Italian National Forestry Service and a validation perimeter provided by Consorzio LAMMA-Toscana through a visual analysis over a cutting of the post-event QuickBird image.

The main phases of processing are summarized in the diagram of Figure 1. All the satellite images (already orthorectified) were radiometrically corrected to convert Landsat TM digital numbers and QuickBird relative radiance to exoatmospheric reflectance, as described in V.V.A.A. (2008) and (DISAT 2011). Besides a scene-to-scene atmospheric normalization using pseudoinvariant features was applied between the pre- and post-event images (Krause 2005).
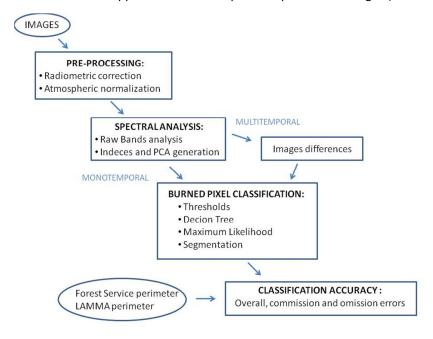
Figure 1. Scheme of the main phases of the work.

Based on previous burned area studies, some spectral indices were selected and calculated. Then they were compared through visual analysis and using two algorithms, the ENVI ROI separability function (V.V.A.A. 2008) and the SEATH software (V.V.A.A. 2010), in order to evaluate their capability to discriminate between burned areas and other land covers. The indexes finally chosen are reported in the following table:

Table 1. Indices considered in the study.

NDVI	$\dfrac{NIR - R}{NIR + R}$	[7]
NDII	$\dfrac{SWIR - NIR}{SWIR + NIR}$	[8]
NBR	$\dfrac{NIR - MIR}{NIR + MIR}$	[9]
NBRT	$\dfrac{NIR - (MIR * SB_T)}{NIR - (MIR * SB_T)}$	[10]
SAVI	$\dfrac{(1 + L) * (NIR - RED)}{NIR + RED + L}$	[11]
BI	$G * 0.098 + R * (-0.352) + NIR * 0.957$	[12]

In addition we considered the raw bands and we applied the Principal Component Analysis.

Starting from these base data, the detection of burned areas was carried out using different techniques: simple thresholds (Chuvieco et al. 2002), Decision Trees (V.V.A.A. 2008), the Maximum Likelihood classification (V.V.A.A. 2008) and the ENVI and RHSEG segmentation (V.V.A.A. 2008; RHSEG). These methods were applied to both post-fire images and temporal differences.

In the final phase the classifications accuracy was evaluated comparing the burned area maps with the ground data and the fire perimeter derived from visual interpretation of the post-fire QuickBird image. The parameter considered is the overall error, calculated using the following function:

$$\text{OVERALL ERROR} = ((\text{COM} + \text{OMI}) / \text{VAL}) * 100$$

where COM and OMI are respectively the commission and the omission errors and VAL is the validation area.

Results

Table 2 provides the overall errors obtained comparing the Landsat and the QuickBird images elaborations with the Forest Service's ground data. The multitemporal analysis shows the smallest errors. In particular the best combinations are the Decision Tree function applied to NDVI, NBR, NBRT (25.2%) for Landsat and the Threshold technique applied to NDVI (34.8%) for QuickBird.

Table 2. Overall, commission and omission errors obtained for different parameters and methods using as validation data the Forest Service's profile (dtr: Decision Tree; ml: Maximum Likelihood; segm: segmentation)

	LANDSAT MONOTEMPORAL											
	NDII+BI	NDII+BI+B6	NDVI+NDII+NBRT		NDII+NBRT	NDVI+NBR+NBRT			PCA(noB6)	PCA	BANDS	NDII+NBR
	dtr	dtr	dtr	ml	dtr	dtr	ml	segm	ml_PC2,4,5	ml_PC3,6	segm	segm
OVERALL ERROR (%)	41.014	42.881	38.203	41.135	38.014	37.780	41.339	37.228	47.997	49.638	51.580	42.201
COMMISSION ERROR (%)	8.910	4.708	4.912	3.537	4.958	5.215	2.864	4.512	2.494	2.676	12.636	3.129
OMISSION ERROR (%)	32.104	38.173	33.291	37.598	33.056	32.565	38.475	32.716	45.503	46.962	38.943	39.072

	LANDSAT MULTITEMPORAL							QB MONOTEMPORAL			QB MULTITEMPORAL
	NDII+NBR		NDVI+NDII+NBRT		NDVI+NBR+NBRT			NDVI	NDVI-SAVI	BANDS+NDVI	NDVI-DIFF
	dt	ml	dt	ml	dt	ml	segm	envi_segm	dt	segm	thres
OVERALL ERROR (%)	29.943	30.313	25.884	26.232	25.265	25.695	28.121	39.100	78.532	Image too large	34.843
COMMISSION ERROR (%)	15.410	4.179	6.628	5.086	6.696	5.608	5.003	12.152	19.461		6.993
OMISSION ERROR (%)	14.533	26.134	19.256	21.146	18.569	20.088	23.118	26.948	59.071		27.851

In order to understand the reason of the errors pointed out, Consorzio Lamma was asked to make a new delimitation of the burned area through a visual analysis over a cutting of the QuickBird image. Comparing this new perimeter with the Forest Service's profile (Figure 2a), the difference is relevant. The Forest Service's shape turns out to be less detailed, showing the difficulties of ground delimitation. The new fire perimeter was then used as validation data (Figure 2b-c) and the new resulting error values for the two best combination seen above are 22.7% for Landsat and 22.8% for QuickBird. The error trend remains however unchanged so that the ground data are still valid for a comparison between the different techniques.

LAMMA
Forest Service

7.402 %
15.355 %

1.874 %
20.934 %
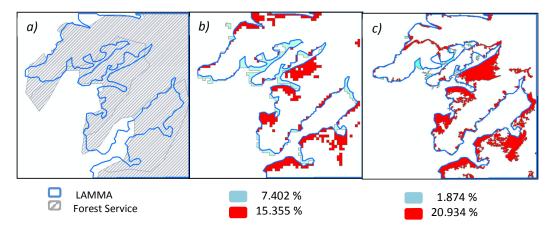
Figure 2. a) Overlay of LAMMA's and Forest Service's profiles. b- c) Commission (blue) and omission (red) errors obtained comparing Landsat (b) and QuickBird (c) best results with LAMMA's profile.

On the other side, a more detailed profile is necessary to establish the origin of the real error, with the aim of reducing it. The overall error can be split in the two components, omission and

commission. In all the test (i.e. Figure 2b-c), the leading factor is the first one, reflecting what was seen using the Forest Service's perimeter as validation data (Table 2). Then, we also checked the areas of confusion, verifying that the largest part of the omission areas is located on the shady side of the mountains. The remaining part of error instead overlaps with the boundary lines.

The fact that the geometric high-resolution images provide worse results (using the Forest Service's profile) or equivalent ones (using the LAMMA's profile) with respect to the medium-resolution images may be due to different reasons. First of all, the QuickBird images used in this study are Standard 2A products (normalized for topographic relief with respect to the reference ellipsoid using a coarse DEM), creating co-registration problems when employing a multitemporal approach. Moreover, QuickBird data lack medium and thermal infrared bands, preventing the computation of some important indices. Finally, we have to consider that the ground data contain errors due to the difficulties of field campaigns in a territory such complex from the topography point of view and that these errors become even worse with the improvement of the image resolution.

Conclusion

In this study, we observed that the Decision Tree function applied to NDVI, NBR and NBRT for Landsat image and the Threshold technique applied to NDVI for QuickBird image provide the greatest results for mapping the Monte Fasce burned area in Liguria. Further work will be focused on the topography influence on the mapping errors and testing the methods over other burned areas in Liguria.

Acknowledgements

References

Chuvieco, E., Congalton, R.G. 1988. Mapping and inventory of forest fires from digital processing of TM data. Geocarto International, 4, pp. 41–53.

Chuvieco, E., Martin M. P., Palacios A. 2002. Assessment of different spectral indices in the red–near-infrared spectral domain for burned land discrimination. Int. J. Rem. Sens. 23, 5103-5110.

Corpo Forestale dello Stato, 2009. Incendi boschivi 2009.

http://www3.corpoforestale.it/flex/cm/pages/ServeBLOB.php/L/IT/IDPagina/1665

DISAT 2011. Corso di telerilevamento e geofisica ambientale. http://www.disat.unimib.it/Telerilevamento

Hardisky, M. A., Klemas, V., and Smart, R. M. 1983. The influence of soil salinity, growth form, and leaf moisture on the spectral reflectance of Spartina alterniflora canopies. *Photogrammetric Engineering and Remote Sensing* , vol. 49, pp. 77-83.

Holden, Z.A., Smith, A.M.S., Morgan, P., Rollins, M.G., Gessler, P.E. 2005. Evaluation of novel thermally enhanced spectral indices for mapping fire perimeters and comparisons with fire atlas data. Int. J. Rem. Sens.21, 4801-4808

Huete, A.R. 1988. A soil-adjusted vegetation index (SAVI). Rem. Sens. Environ. 25, 295–309

Krause, K. 2005. Radiometric Use of QuickBird Imagery.

http://www.digitalglobe.com/downloads/products/QuickBird_technote_raduse_v1.pdf

LQMIB 2000. Legge quadro in materia di incendi boschivi (353/2000). Gazzetta Ufficiale n. 280, 30 novembre 2000.

RHSEG User's Manual http://opensource.gsfc.nasa.gov/projects/HSEG/RHSEG%20User's%20Manual%20V1.47.pdf

Rouse, J.W., Haas, H.R., Schell, J.A., Deering, D.W. 1974. Monitoring vegetation systems in the great plains with ERTS. Proceeding of the Third Earth Resources Technology Satellite-1 Symposium, Greenbelt: NASA SP-351, pp. 301-317.

San Miguel-Ayanz, J., Annoni, A., Schmuck, G. 1998. The use of satellite imagery for retrieval of information on wildfire damage in Mediterranean landscapes. Proceedings of ERIM'98, 27th International Symposium on Remote Sensing of Environment: Information for Sustainability, held on 8-12 June, in Tromsø, Norway, pp.758-762.

V.V.A.A. 2008. ENVI Help.

V.V.A.A. 2010. Processing Chain Optimization Report HYPER-I-NET Project pp.16-17 http://hyperinet.multimediacampus.it/images/HYPERINET_D4.3.pdf

EFFECTS OF ENVIRONMENTAL PROPERTIES, BURNING CONDITIONS AND HUMAN-RELATED VARIABLES ON FIRE SEVERITY DERIVED FROM LANDSAT TM IMAGES FOR A LARGE FIRE IN CENTRAL SPAIN

O. Viedma[1], L. A. Arroyo[2], R. Mateo[3], A. De Santis[4], J.M. Moreno[3]

[1]*Department of Environmental Sciences, Universidad de Castilla-La Mancha, Avda. Carlos III, s/n, Toledo 45071, Spain. olga.viedma@uclm.es;* [2]*Centro de Investigación del Fuego, Toledo, Spain;* [3]*Universidad de Castilla-La Mancha, Toledo, Spain;* [4]*Ingeniería y Servicios Aeroespaciales, S.A., Madrid, Spain*

Abstract

Large fires (LFs) are becoming more frequent in some areas of the Mediterranean Basin. LFs tend to occur under extreme weather conditions and their occurrence is predicted to increase due to the changes in weather and climate caused by global warming. LFs are not homogeneous. They are usually characterized by heterogeneous patches of fire severities, which can have long-lasting effects on the post-fire communities and on the landscape. Hence, understanding the role of the main factors driving fire severity is of upmost importance in LF–prone areas. In this study we assessed the role of 28 predictive variables on fire severity in a very large fire that occurred in the summer of 2005 in Guadalajara (Central Spain). The predictive variables were divided into four main groups (vegetation-related; topography-related, human-derived and burning condition), so the effects of each group of variables could be independently assessed. Fire severity was estimated from the Relative difference of the Normalized Burn Ratio (RdNBR) obtained from two Landsat TM images of the area (pre- and post-fire). The RdNBR was then related to the predictive variables by using complementary boosted regression tree (BRT) and regression tree analysis (RTA). First, each group of variables was independently used to model fire severity; later, the significant variables from each group were combined in a fifth fire severity model. Our results suggest that, when considered independently, the topography-related variables explain the greatest variability of RdNBR (50%), followed by vegetation (24%), human-derived (20%) and burning condition variables (17%). However, when all variables were considered together, the variance explained by the model increased considerably (76%). Topographic wetness (soil humidity), topographic complexity (elevation and slope), vegetation structure (basal area of Pinus pinaster and number of trunks of Quercus pyrenaica), distance to roads, distance to villages and burning conditions (mainly, position in relation to the fire advance) interacted in a hierarchical and non-linear way to explain fire severity variability. Higher severities were found in areas with high solar radiation and medium to high soil humidity conditions, where conifer forests of Pinus pinaster were dominant, and in areas with lower solar radiation and at high elevation, where number of trunks of Quercus pyrenaica was higher; whereas lower fire severity values were found in the lowest illuminated areas and steep slopes with high density of deciduous species. Also, higher severities occurred near to roads and at intermediate distance to villages, where there was greater fuel accumulation and high basal area of Pinus pinaster; whereas lower fire severities were found in areas very distant to roads and near to villages very close to villages, with greater presence of shrublands of Cistus sp. Finally, higher severity values were found in the front fire and the windward flank under high speed winds; and fire severity was lower in the leeward fire flank and in areas that burned at night, under cooler conditions. These results support the idea that fire severity is the result of complex and non-linear relationships between biophysical conditions, land management and specific burning conditions.

Keywords: fire severity; decision trees; land uses; fire weather conditions; large fires

Introduction

Wildfires are a recurring phenomenon in many regions of the world, and they can cause major modifications in the landscape. The intensity of wild fires, and therefore the severity of the damage, is affected by several factors, including the properties and quantity of available fuel, the topography of the affected area, or the nature and intensity (if any) of suppression

activities. Several studies have investigated the relation between environmental variables and fire severity (Alexander et al., 2006, Hammill and Bradstock, 2006, Odion et al., 2004). However, the degree to which fire severity varies as a result of fuel condition, topography and/or weather conditions remains poorly understood (Schoennagel et al., 2004, Thompson and Spies, 2009). Moreover, very little is known about the effects of human-related variables or the burning conditions on fire severity. The aims of the present study were: (1) to determine how much (if any) fire severity can also be explained by human-derived and burning condition variables and (2) to assess the relative importance of environmental variables over human-related and burning conditions variables for predicting patterns of fire severity. In this study, the term "fire severity" will be used to account for the amount of change in a burned area with respect to the pre-fire conditions (as suggested by Keeley, 2009).

Methods

Study area

In summer 2005, the Guadalajara fire (in central Spain) swept through 12,697 ha (Fig. 1). The area affected by the fire was mountainous, with elevations ranging between 1000 and 1400 m, and considerable slope variability (from 0 to more than 30 degrees). The burned area was mainly composed of sandstones (77%), with some areas of limestone and dolomite (14%) and slate and quartzite (9%). The area affected by the fire was dominated by mixed forests of *Pinus pinaster Aiton* with scattered oaks (*Quercus pyrenaica Willd.*, *Q. faginea Lam*.) in the understory (80% of the burned area). Shrubs were common under the canopy, and also in open areas, where it formed shrublands (8% of the burned area). The fire also affected some smaller areas of broadleaved woodlands (8% of the total burned area) dominated *by Quercus pyrenaica* and *Q. faginea*. Finally, *Juniperus thurifera L*. woodlands occupied 4% of the burned area.
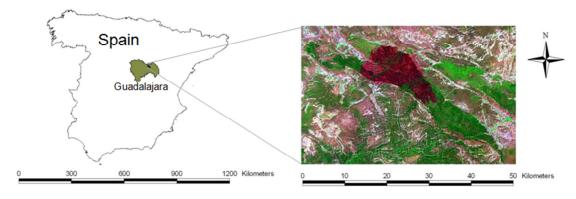
Figure 1. Location of the study area. False color composite of a Landsat TM image captured after the fire

Estimation of the response variable: fire severity

Fire severity was estimated using two Landsat 5 Thematic Mapper (TM) images, corresponding to July 1st, 2004 (pre-fire) and August 5th, 2005 (post-fire). The original Landsat 5 TM images were first scaled to radiance values using the procedure proposed by Chander y Markham

(2003). The atmospheric correction was performed using the dark object method proposed by Chavez (1996). A set of 70 ground control points was selected for the geometric correction of the pre-fire image, using a Landsat ETM+ ortho-image as reference (from the CORINE 2000 project, UTM 30 T European 1950 mean). A linear polynomial function and a cubic convolution re-sampling algorithm were chosen to minimize the loss of spatial accuracy of the data. The resulting Root Mean Square Error (RMSE) was under half a pixel (or 15 m). Then, pre- and post-fire images were co-registered (RMSE<15 m). The illumination correction was carried out using a digital terrain model (DTM, 10 m of resolution) and the method proposed by Civco (1989). The radiometric fitting between pre- and post-fire images was tested by comparing spectral signatures of the pixels corresponding to areas with low seasonal changes (asphalt and rock). The comparison of reflectance values returned a RMSE of 0.02.

Fire severity was estimated as the relative delta normalized burn ratio (RdNBR):

$$RdNBR = PreFireNBR - PostFireNBR)/(SquareRoot(ABS(PreFireNBR/1000)))$$

Where, NBR = (band4-Band7)/(Band4+Band7)

The RdNBR has previously shown good correlation with the Composite Burn Index (CBI), proposed by Key and Benson (2006) in order to provide consistent and comparable estimations of fire severity, as well as with the modified version of this index, called GeoCBI (De Santis and Chuvieco, 2009).

The explanatory variables

Twenty eight independent variables were considered for predicting fire severity in this large fire. They were classified into four major groups: (1) Vegetation-derived variables (pre-fire vegetation composition and structure), (2) Topography-derived variables, variables that are related to topographic wetness and topographic complexity, (3) Human variables, variables related to the level of accessibility and the management of the area; and (4) Burning condition variables, variables related to the weather conditions during the fire progression and position in relation to the fire front. These variables were derived from previously existing maps, extensive field work and geographic information systems.

Table 1. Contribution (in percentage) of the explained variance of the obtained BRT models for the explanatory variables. The variables that exceeded the expected contribution under an even distribution of explained variance are highlighted in bold.

			Fire severity model (BRT)				
			Vegetation	Topography	Human	Burning cond.	Combined
Variables	Vegetation	Forest type	**20.0**				4.1
		Basal area_Pinus	**28.2**				**6.5**
		Basal_area Qp	9.3				
		Basal_area Cistus	4.9				
		Number trunks_Pinus	7.2				
		Number trunks_Qp	**25.6**				**5.7**
		Number trunks_Cistus	4.8				
	Topography	Curvature		8.3			
		Elevation		**12.6**			**9.1**
		Flow		8.5			
		North		7.2			
		West		7.7			
		Radiation_summer		6.8			**6.2**
		Radiaton_winter		**9.3**			**6.0**
		Slope		**11.8**			9.4
		Stream		6.0			
		Topographic Wetness Index		**14.7**			**10.9**
	Human	Ownership			14.9		2.7
		Distance to Roads			**46.7**		**7.9**
		Distance to Villages			**38.4**		**6.1**
	Burning Cond.	Position within the fire perimeter				**24.3**	3.8
		Time of burning				6.6	
		Humidity during burning				10.9	
		Max temp during burning				5.5	
		Mean temp during burning				**14.1**	3.6
		Min temp during burning				8.7	
		Wind_direction during burning				**16.3**	3.6
		Wind_speed during burning				**13.6**	1.9
R²			0.24	0.50	0.20	0.17	0.76
NRMSE (%)			97.0	90.0	97.0	92.0	55.0

Statistical analysis

We assessed the relationship between fire severity (RdNBR) and the predictor variables by using Boosted Regression Trees (BRT) (Friedman et al., 2000) and Regression Tree Analysis (RTA) (Breiman et al., 1984). First, each group of variables was used independently to model fire severity (i.e., vegetation, topography, human-derived and burning condition variables); then, the significant variables from each group were combined in an independent fire severity model. BRT models were used for predictive purposes because of their ability to handle complex and non-linear interactions (boosting and cross-validation algorithms). RTA was applied for descriptive purposes, since it allows the analysis of hierarchical interactions and threshold predictor behaviours (Prasad et al., 2006).

Results and discussion

The results of the BRTs models are summarized in Table 1. When considered independently, the topography-related variables explained the greatest RdNBR variability (50%), followed by vegetation (24%), human-derived variables (20%) and burning conditions (17%). However, when all variables were considered together, the explained variance increased considerably

(76%). These results suggest that, although the environmental variables (i.e., topography and vegetation) explain the majority of variability in fire severity, information related to human activities and burning conditions can also aid to explain this variability.

For the combined BRT model, topographic wetness (soil humidity), topographic complexity (elevation and slope), vegetation structure (basal area of *Pinus pinaster* and number of trunks of *Quercus pyrenaica*), distance to roads, distance to villages and burning conditions (mainly, position in relation to the fire front) interacted in a hierarchical and non-linear way to explain variability in fire severity. Burning condition variables occupied the highest level of the hierarchical structure. Thus, high values of severity were associated with the fire front and the windward flank under high speed winds; whereas lower severities were found in the leeward fire flank and in areas that burned at night. Vegetation, topography and human-derived variables were responsible for the fine tuning of the fire severity model. Higher severities were found in areas with high solar radiation and medium to high soil humidity conditions, where forests of *Pinus pinaster* were dominant, and in areas with lower solar radiation and at high elevation, where the number of trunks of *Quercus pyrenaica* was higher; whereas low fire severity was found in the lowest illuminated areas and steep slopes, with a high density of deciduous species. Also, higher severities occurred near roads and at intermediate distances to villages, where there was greater fuel accumulation and high basal area of *Pinus pinaster*; whereas lower fire severities were found in areas very distant to roads and close or very far to villages, with greater presence of shrublands of *Cistus* sp. The application of the regression tree approach highlighted the relative importance of the studied variables for predicting fire severity. These results support the idea that fire severity is the result of complex and non-linear relationships between biophysical conditions, land management and specific burning conditions.

Acknowledgments

References

Alexander, J. D., Seavy, N. E., Ralph, C. J., Hogoboom, B. 2006. Vegetation and topographical correlates of fire severity from two fires in the Klamath-Siskiyou region of Oregon and California. *International Journal of Wildland Fire,* 15, 237-245.

Breiman, L., Friedman, J. H., Olshen, R. A., Stone, C. J. 1984. *Classification and Regression Trees,* Ney York, NY, USA, Chapman and Hall, Wadsworth Inc.

Civco, D. L. 1989. Topographic Normalization of Landsat Thematic Mapper Digital Imagery. *Photogrammetric Engineering and Remote Sensing,* 55, 1303-1309.

Chander, G., Markham, B. 2003. Revised Landsat-5 TM radiometric calibration procedures and postcalibration dynamic ranges. *IEEE Transactions on Geoscience and Remote Sensing,* 41, 2674 - 2677.

Chavez Jr., P. 1996. Image-based atmospheric corrections—revised and improved. *Photogrammetric Engineering and Remote Sensing,* 62, 1025– 1036.

De Santis, A., Chuvieco, E. 2009. GeoCBI: A modified version of the Composite Burn Index for the initial assessment of the short-term burn severity from remotely sensed data. *Remote Sensing of Environment,* 113, 554-562.

Friedman, J. H., Hastie, T. & Tibshirani, R. 2000. Additive logistic regression: a statistical view of boosting. *Annals of Statistics,* 28, 337-407.

Hammill, K. A., Bradstock, R. A. 2006. Remote sensing of fire severity in the Blue Mountains: influence of vegetation type and inferring fire intensity. *International Journal of Wildland Fire,* 15, 213-226.

Keeley, J. E. 2009. Fire intensity, fire severity and burn severity: a brief review and suggested usage. *International Journal of Wildland Fire,* 18, 116-126.

Key, C., Benson, N. C. 2006. Landscape assessment: sampling and analysis methods. In: D. C. LUTES, R. E. K., J. F. CARATTI, C. H. KEY, N. C. BENSON, S. SUTHERLAND, AND L. J. GANGI (Ed.) *FIREMON: Fire effects monitoring and inventory system.* USDA Forest Service Rocky Mountain Research Station. Ogden, UT, USA.

Odion, D. C., Frost, E. J., Strittholt, J. R., Jiang, H., Dellasala, D. A., Moritz, M. A. 2004. Patterns of fire severity and forest conditions in the western Klamath Mountains, California. *Conservation Biology,* 18, 927-936.

Prasad, A. M., Iverson, L. R., Liaw, A. 2006. Newer classification and regression tree techniques: Bagging and random forests for ecological prediction. *Ecosystems,* 9, 181-199.

Schoennagel, T., Veblen, T., Romme, W. H. 2004. The interaction of fire, fuels, and climate across Rocky Mountain forests. *BioScience,* 54, 661-671.

Thompson, J. R., Spies, T. A. 2009. Vegetation and weather explain variation in crown damage within a large mixed-severity wildfire. *Forest Ecology and Management,* 258, 1684-1694.

III - National to global applications of remote sensing in pre and during fire conditions

INTEGRATING GEOSPATIAL INFORMATION INTO GLOBAL FIRE RISK ASSESSMENT

Emilio Chuvieco

University of Alcala, Alcala de Henares, Spain. emilio.chuvieco@uah.es

Abstract

Fire risk assessment involves considering a wide range of variables, both related to estimate fire occurrence and potential fire effects. This lecture will focus on defining a comprehensive fire risk information system for global scales, although the basis may be adapted to different temporal and spatial scales.
Fire occurrence factors have been traditionally classified in three groups: Fuels, Heat source and Oxygen. In the case of wildland fires, heat source is mostly related to the starting of the fire (fire ignition), and can be further divided in natural-caused (lightning, volcano eruption) and human-caused. Oxygen is needed for combustion, and it is mostly related to fire propagation, being the critical parameters wind speed, direction and slopes. Fuels are both related to fire ignition (the drier, the more likely to ignite) and propagation (the more fuel load available, the more energy will be released and favour further ignition). Fuel moisture is associated to short-term weather factors, topographic conditions and soil characteristics, while fuel load and geometrical properties are related to climate, soil and land use patterns. In addition to these factors, fire risk assessment should also consider the potential damages caused by fires, which are very much dependent on fire characteristics (energy released, residence time, flame length, etc.). Even though some of the methods to derive the required variables for such a system have been derived in the last few years, still little experience is available on how to apply them to a global scale. In addition to, additional efforts should be invested on improving current integration tools, as well as providing a more consistent framework for accuracy assessment.

COMPLEMENTARITY OF REMOTE SENSING INDICATORS OF WILDFIRE DANGER WITH VEGETATION COMBUSTIBILITY MAPPING

V. Cheret[1], J-P. Denux[1], R. Savazzi[2], C. Piedallu[3], A. Jacquin[1], V. Drolon[2]

[1]*Université de Toulouse; Institut National Polytechnique de Toulouse, Ecole d'Ingénieurs de Purpan ; UMR 1201 DYNAFOR; 75, voie du TOEC, BP 57611, F-31076 Toulouse Cedex 03, France. veronique.cheret@purpan.fr*
[2]*ONF-Direction Territoriale Méditerranée ; 46, avenue Paul Cézanne, 13097 Aix-en-Provence, France*
[3]*AgroParisTech-ENGREF, LERFoB UMR INRA-ENGREF 1092 ; 14, rue Girardet, 54042 Nancy Cedex, France*

Abstract

In the framework of wildfire fighting in Mediterranean regions, fire risk planners need updated daily vegetation combustibility maps. Current research developed by both forest and meteorological services ("Office National des Forêts", "Météo-France") aims to map vegetation sensitivity to fire during drought period homogeneously for all French Mediterranean regions. This "static" combustibility map is based on an interpretation of a vegetation map, combustibility index values are assigned according to vegetation behavior and to bioclimatic zones. The next step will be to produce a "dynamic" mapping of vegetation sensitivity to fire risk merging vegetation charac-teristics and daily meteorological dryness maps. Concurrently, the authors have developed indicators of vegetation sensitivity to fire based on time series of re-mote sensing images (MODIS). This approach is based on the analysis of series of vegetation index values related to annual and inter-annual variations of chlorophyll activities and green biomass development, to map indicators linked to fuel dryness and to express fire danger:
- A spring greenness indicator to characterize the vegetation status at the end of spring;
- An annual greenness indicator that reflects vegetation drying up in summer and used for the analysis of spatial and temporal variations of vegetation fire susceptibility.
This paper aims to present the attempts made to identify the complementarity of the two approaches. Remote sensing indicators can be used on the one hand to express the spatial variability of the vegetation dryness, and on the other hand to be integrated into the regular update process of combustibility index calculated from meteorological data.

Keywords: fire risk mapping, NDVI time series, MODIS, annual RGRE

Introduction

In the framework of wildfire fighting in Mediterranean regions, fire risk planners need updated daily vegetation combustibility maps. Current research developed by both forest and meteorological services ("Office National des Forêts", "Météo-France") aims to map vegetation sensitivity to fire during drought period homogeneously for all French Mediterranean regions (Duché et al., 2011). A combustibility map is based on an interpretation of a vegetation map, combustibility index values are assigned according to vegetation behavior and to bioclimatic zones. Weekly maps of vegetation sensitivity to fire risk are produced merging vegetation characteristics and daily meteorological dryness maps.

Concurrently, the authors have developed indicators of vegetation sensitivity to fire based on time series of remote sensing images (MODIS) (Chéret and Denux, 2011). This approach is based on the analysis of series of vegetation index values related to annual and inter-annual variations of chlorophyll activities and green biomass development, to map indicators linked to fuel dryness forest fire susceptibility.

An yearly greenness indicator that reflects vegetation drying up in summer and used for the analysis of spatial and temporal variations of vegetation fire susceptibility (Chéret and Denux, 2007). For a given pixel, the annual RGRE is calculated from:

NDVImax: the maximum NDVI observed at the end of spring (June),
NDVImin Phase 1: the minimum measured before onset of spring greenness (March-April)
NDVImin Phase 2: the minimum NDVI attained during the driest period (August or September),

Annual RGRE = (NDVImin Phase 2 – NDVImin Phase 1) / (NDVImax – NDVImin Phase 1)

This work presents the attempts made to identify the complementarity of the two approaches. Remote sensing indicators can be used to express the spatial variability of the vegetation dryness. We focus on the analysis of the potential of the annual RGRE to improve the mapping of the spatial variability of the combustibility index.

The study area is Aude and Pyrénées-Orientales provinces, in the South of France, covering 10,255 km². The extent of forest and wildland is about 6,250 km². The Western part of the territory is under Mediterranean climate influence, characterized by a very dry and hot summer, and where spring is the wettest season, Mediterranean vegetation, mainly composed of evergreen sclerophyllous species, is very sensitive to fire. In the South-West, mountainous areas benefits from a cooler and wetter climate and the vegetation is dominated by mountainous species less sensitive to fire.

We processed a time series of MODIS Terra Normalized Difference Vegetation Index (NDVI) produced at 231x231 m spatial resolution and 16 day compositing periods (MOD13Q1) (Huete et al., 2002; Justice et al., 1998). The data set spans 9 years from March 2000 to December 2008, acquired from the Land Processes Distributed Active Archive System (http://edcimswww.cr.usgs.gov/). For each 16 day synthesis a mean synthesis was processed from these 9 years, in order to create a mean annual series of NDVI used to generate a mean annual RGRE.

The maps of figure 1 present the combustibility index, the mean annual RGRE and the limits of the biogeographic zones. These biogeographic limits plainly divide the combustibility index values. The mean annual RGRE values are consistent with the biogeographic zones but changes are more gradual than those of the combustibility index. In the mountain area, positive RGRE values match low combustibility values. Overall the study area, increasing combustibility and decreasing RGRE follow the succession of the biogeographic zones: mountains, hills, plain and Mediterranean lowland. However, in the Mediterranean area this gradient is reversed. Combustibility is low along the coast, covered mainly by shrubs, and increase from east to west, where Holm oak coppices are growing. Oppositely, the highest values of RGRE are found for the eastern Mediterranean shrubland. The annual RGRE showing summer decrease of vegetation activities can be interpreted as vegetation dryness and it can be related to inflammability rather than combustibility.

Mean annual RGRE value
- 100 - 30 : low drying intensity
- 30 - -30
- -30 - -150
- -150 - -450 : high drying intensity
- Biogeographic zone

Combustibility level
- 0 - 4 : low
- 4 - 5 : moderate
- 5 - 6 : high
- 6 - 9 : very high
- Biogeographic zone
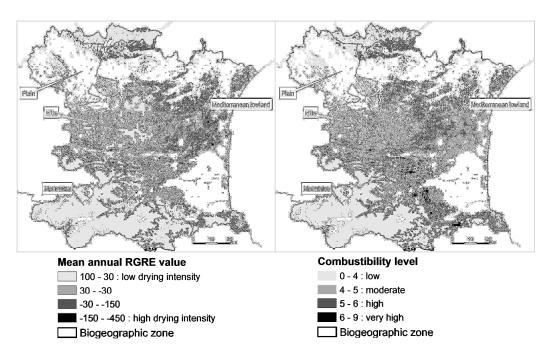
Figure1. Maps of the mean annual RGRE (left) and combustibility index (right) for Aude and Pyrénées-Orientales provinces (France)

Mean annual RGRE values were extracted for each forest types mapped for the study area. In mountainous and hilly zones dominated by deciduous oaks, beech and chestnut forest stands, RGRE values for each type are homogeneous, as illustrated in figure 2a for deciduous oaks coppices characterized by combustibility index value of 2 or 3. Most of the Mediterranean vegetation shows RGRE values widely spread. The histogram of RGRE values extracted for Mediterranean shrubland (figure 2b) covers the whole range of RGRE values meanwhile its combustibility index values rank from 5 to 6 with limited spatial variability. This can be understood as a lack of thematic precision in the forest map used, where not enough distinction was made between shrubs types. Furthermore, in Mediterranean lowland, local constraints linked to climatic conditions (localized rainfall or dry wind) and to edaphic factors (soil water content) can be highly variable.

Our hypothesis is that RGRE variability has the capability to take into account local vegetation dryness in the area where wildfire risk is the most important and could be used as complementary information of the combustibility index.
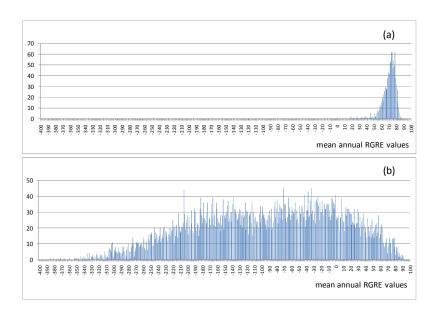
Figure2. Histograms of the mean annual RGRE values extracted for deciduous oak coppices (a) and for Mediterranean shrubland (b)

Method

The purpose is to evaluate the capability of RGRE to assess local variations of hydric constraints. To validate this interpretation in the Mediterranean lowland a regression analysis (Leblon et al., 2007) was made with climatic and edaphic factors newly designed to assess these local variations of water availability. Meteorological data (temperature and rainfall) acquired from weather stations network and soil parameters (soil water holding capacity) from national survey were interpolated over the study area with a spatial resolution similar to MODIS images. These data were available monthly from 2000 to 2008. They were used to process indices mapping climatic and edaphic factors (Lebourgeois and Piedallu, 2005; Piedallu and Gégout, 2008; Piedallu et al., 2011) to be used to analyze the spatial variability of RGRE (table 1). RGRE is designed to characterize vegetation behavior in summer. The indices were integrated over different period of time to take into account not only summer season and but potential effects of previous months on water availability.

Table 1. Climatic and edaphic factors used in this study (source: LERFOB)

Climatic index	definition	Soil index	definition
ST	sum of mean temperature	SWC	Soil water content
		SWHC	Soil water holding capacity
SR	sum of rainfall	REW	Relative Extractable Water: REW=SWC/SWHC
PET	sum of potential evapotranspiration	SI	Stress Index: SI=SWC/PET
HB	hydric balance: HB=SR-PET	AET	Actual evapotranspiration : AET=R-(SWC(t) − SWC(t-1))
BI	Bioclimatic index: BI= SR/PET	ED	Evaporation deficit: DE=PET-AET
IM	De Martonne index: IM=SR/(ST+10)	AI	Aridity index: AI=AET/PET

170

Results

Table 2 shows the Pearson coefficient of determination between the mean annual RGRE and climatic and edaphic indices. All the indices show significant correlation with the remote sensing indicator. The period of time allowing the best correlation covers spring and summer seasons for most of the indicators. Roughly, the indices using soil properties display higher r^2 values than those based only on meteorological data.

Table 2. Correlation analysis between annual RGRE and climatic and edaphic factors (all r^2 are significant at the .01 level)

Climatic index	period	r^2	Soil index	period	r^2
ST	March - August	0.33	SWC	March - August	0.30
SR	July - August	**0.50**	REW	March - August	**0.58**
PET	March - August	0.29	SI	March - August	0.37
HB	July - August	0.45	AET	July - August	**0.55**
BI	March - June	0.20	ED	March - August	**0.62**
IM	March - August	0.34	AI	March - August	**0.62**

The sum of rainfall alone expresses 50% RGRE variability. The three indices integrating actual evaporation estimates present the best r^2 values. This may validate the capability of the RGRE to express local variation of vegetation hydric status. The regression model presented could be improved using multiple linear regression tools. However some important climatic factors, like wind, cannot be easily included in the analysis.

These first results show that annual RGRE could be used to weight combustibility index to assess local variability at pixel resolution. Annual RGRE is an efficient way to take into account biogeographic conditions as a gradient rather than an abrupt limit. Next investigation will aim to use the potential of RGRE to provide yearly information on vegetation status and to include temporal variability in combustibility index calculation.

Aknowledgements

References

Chéret, V., Denux, J.P. 2007. Mapping wildfire danger at regional scale with an index model integrating coarse spatial resolution remote sensing data, J. Geophys. Res., 112. G02006, doi:10.1029/2005JG000125.

Chéret, V., Denux, J.P. 2011. Analysis of MODIS NDVI Time Series to Calculate Indicators of Mediterranean Forest Fire Susceptibility, GIScience & Remote Sensing of Environment, 48 (2): 171-194. DOI: 10.2747/1548-1603.48.2.171.

Duché, Y., Savazzi, R., Reymond, B. 2011. La cartographie de la sensibilité de la végétation aux incendies de forêt en région méditerranéenne - Apport et limites d'usage des images satellites, RDV techniques - ONF, 32.

Huete, A., Didan, K., Miura, T., Rodriguez, E.P., Gao, X., Ferreira, L.G. 2002. Overview of the radiometric and biophysical performance of the MODIS vegetation indices, Remote Sensing of Environment, 83: 195-213.

Justice, C.O., Vermote, E., Townshend, J.R.G., Defries, R., Roy, D.P., Hall, D.K., Salomonson, V.V., Privette, J.L., Riggs, G., Strahler, A.H., Lucht, W., Myneni, R.B., Knyazikhin, Y., Running, S.W., Nemani, R.R., Wan, Z., Huete, A., van Leeuwen, W., Wolfe, R.E., Giglio, L., Muller, J.-P., Lewis, P., Barnsley, M., J. 1998. The Moderate Resolution Imaging Spectroradiometer (MODIS): land remote sensing for global change research, IEEE Transactions on Geoscience and Remote Sensing, 36 (4): 1228-1249.

Leblon, B., García, P.A.F., Oldford, S., Maclean, D.A., Flannigan, M. 2007. Using cumulative NOAA-AVHRR spectral indices for estimating fire danger codes in northern boreal forests, International Journal of Applied Earth Observation and Geoinformation, 9 (3): 335-342. 10.1016/j.jag.2006.11.001.

Lebourgeois, F., Piedallu, C. 2005. Comment appréhender le niveau de sécheresse dans le cadre des études stationnelles et de la gestion forestière? Notion d'indices bioclimatiques, méthode d'estimation de l'évapotranspiration potentielle., Revue forestière Française LVII (4): 331-356.

Piedallu, C., Gégout, J.-C. 2008. Efficient assessment of topographic solar radiation to improve plant distribution models, Agricultural and Forest Meteorology, 148 (11): 1696-1706. 10.1016/j.agrformet.2008.06.001.

Piedallu, C., Gégout, J.-C., Bruand, A., Seynave, I. 2011. Mapping soil water holding capacity over large areas to predict potential production of forest stands, Geoderma, 160 (3-4): 355-366. 10.1016/j.geoderma.2010.10.004.

INTEGRATING GEOSPATIAL INFORMATION INTO FIRE RISK ASSESSMENT

E. Chuvieco[1], I. Aguado[1], S. Jurdao[1], M.L. Pettinari[1], J. Salas[1], J. de la Riva[2], P. Ibarra[2], M. Rodríguez[2], M. Echeverría[2], D. Azqueta[3], M.V. Román[3], A. Bastarrika[4], S. Martínez[5], C. Recondo[6], E. Zapico[6], F. J. Martínez-Vega[7], S. Martín[8]

[1]*Departamento de Geografía, Universidad de Alcalá. C/ Colegios, 2. 28801 Alcalá de Henares (Madrid). emilio.chuvieco@uah.es;* [2]*Departamento de Geografía y Ordenación del Territorio, Universidad de Zaragoza (Zaragoza);* [3]*Departamento de Fundamentos de Economía e Historia Económica, Universidad de Alcalá (Madrid);* [4]*Departamento de Ingeniería Topográfica, Universidad del País Vasco (Vitoria);* [5]*Departamento de Botánica-IBADER, Universidad de Santiago (Lugo);* [6]*INDUROT. Campus de Mieres, Universidad de Oviedo (Asturias);* [7]*Centro de Ciencias Humanas y Sociales (CCHS), Consejo Superior de Investigaciones Científicas (CSIC);* [8]*Departamento de Economía y Gestión Forestal. ETSI Montes, UPM (Madrid)*

Abstract

The conceptual definition of a fire risk assessment system should include the most relevant components associated to the fire process. Fire occurrence factors have been traditionally classified in three groups: Fuels, Heat source and Oxygen. In the case of wildland fires, heat source is mostly related to the starting of the fire (fire ignition), and can be further divided in natural-caused (lightning, volcano eruption) and human-caused. Oxygen is needed for combustion, and it is mostly related to fire propagation, being the critical parameters wind speed, direction and slopes. Fuels are both related to fire ignition (the drier, the more likely to ignite) and propagation (the more fuel load available, the more energy will be released and favour further ignition). Fuel moisture is associated to short-term weather factors, topographic conditions and soil characteristics, while fuel load and geometrical properties are related to climate, soil and land use patterns. In addition to these factors, fire risk assessment should also consider the potential damages caused by fires, which are very much dependent on fire characteristics (energy released, residence time, flame length, etc.).
Following these ideas, a comprehensive fire risk assessment system has been developed within the Fireglobe project (www.fireglobe.es), funded under the Spanish Program for Science and Research. To implement the proposed risk framework, the first phase focused on the generation of risk factors for the whole Spanish Iberian territory (both the Canary and the Balearic islands were not considered at this stage). Human factors, lightning probability, fuel moisture content of both dead and live fuels, and propagation have been considered. Additionally, fire vulnerability has been assessed by analyzing values at risk and landscape resilience. Once the variables were generated, the fire risk model was defined by integrating the input variables using statistical and physical approaches. Finally, the validation has been performed using fire statistics derived from the fire seasons of 2010 and 2011.

Keywords: Fire Risk, Fuel Moisture Content, Vulnerability, Human factors, Fire propagation

1.1   *Fire risk conceptual framework*

Forest fires are a major factor of environmental transformation in a wide variety of ecosystems (FAO 2007), while they also have important impacts at global scale, both in terms of land use transformation (affecting habitats and biodiversity) and gas emission (Chuvieco 2008). Recent impacts of severe fire seasons in Europe (Portugal, 2005; Greece, 2007; Russia, 2010) have made the importance of improving current fire risk assessment systems evident for alleviating the most negative effects of fire.

Any fire risk assessment system should aim to provide certain functions that are either not currently available or are unsatisfactory. In most operational fire risk assessment systems, the main objectives are to improve the pre-fire planning actions or improve the suppression actions. The end-users are fire managers at local or regional administrations. The conceptual definition of a fire risk assessment system should include the most relevant components associated to the fire process. Traditionally, fire ignition and propagation has been concerned

with three factors: Fuels, Heat source and Oxygen. The heat source can be either natural-caused (lightning, volcano eruption) or human-caused, being the latter the most extended worldwide. Oxygen is needed for combustion, and it is mostly related to fire propagation, being the critical parameters wind speed, wind direction and slope gradient. Fuels are both related to fire ignition (the drier, the more likely to ignite) and propagation (the more fuel load available, the more energy will be released and favour further ignition). Fuel moisture is associated to short-term weather factors, topographic conditions and soil characteristics, while fuel load and geometrical properties are related to climate, soil and land use patterns.

A comprehensive risk assessment system should also consider the potential damages that may be caused by a natural hazard. In the case of forest fires, the actual damages are very dependent on fire behaviour (energy released, residence time, flame length, etc.), which is not known before the fire. Therefore, the estimation of potential damages is based on expected scenarios, the worst-case and average conditions being the most common. Those conditions are commonly based on historical trends of weather variables for the target region, but modelling approaches are also very useful, especially when considering medium-term changes of weather or land use patterns as a result of climatic or socio-economic changes.

Figure 1 includes the components of a fire risk system that we have developed within the framework of the Fireglobe project, funded under the Spanish Science and Innovation program. It includes the physical probability that a fire starts or propagates, and the potential damages that it may cause. The former component is named fire danger throughout this document, whiles the latter, named vulnerability, includes damages related to socio-economic and ecological values.
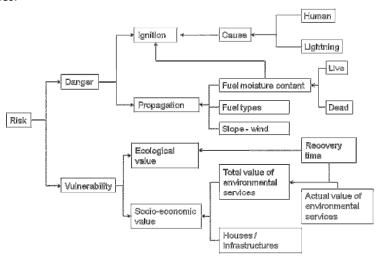
Figure 1. Proposed Framework for an integrated fire risk assessment system (adapted from Chuvieco et al. 2010)

To implement the proposed risk framework, the following steps should be carried out:
- Generation of risk factors, using a common geographical unit. A target scale and spatial resolution needs to be defined, in relation to the sources of data available.
- Model calibration. Input variables of the risk index are measured in a very different scale (%, m, m/s), and they must be integrated using a sound model that provides

objective assessment of risk conditions. This model should be properly parameterized for a wide set of input conditions.

- Validation. The proposed system should be compared with actual impacts of fire to quantify its performance for different ecosystem types and for various fire characteristics.
- Dissemination of risk information, defining the mechanisms to transfer the computed indices to the end-users, including temporal updating.

1.2 *Methods to generate risk factors*

There is a wide variety of studies published in the last decades on methods to generate relevant data for fire risk assessment. Table 1 provides a summary of the methods and input variables used in the Fireglobe project. All variables were mapped at 1 km^2 spatial resolution using the UTM as standard projection system.

Table 1. Sources for the main inputs of the Fireglobe risk assessment system

Factor	Methods	Input variables
Human factor	Spatial analysis. Statistical approach	Land use change, Population density, Income, Socio-economic conditions, Properties, Distances to roads or urban areas
Lightning	Statistical approach	Meteorological data, Lightning strikes, forestry maps
Live Fuel Moisture Content	Field work Meteo-models Statistical approach	Satellite images, simulation models
Dead FMC	Meteo-models	Meteorological data
Fuel types	Field work Classification techniques	Forestry maps. Corine Land Cover map. Digital terrain models
Socio-economic vulnerability	Economic analysis Sample studies	Wood and non-wood products statistics, Forestry inventory and maps, Hunting, Fishing and recreational use of forests statistics, Pastureland prices, CO2 prices, Housing prices
Ecological vulnerability	Field work Ecological/erosion models	Soil, Vegetation and land use maps, Protected areas, satellite images, Digital terrain data, Ecoregions, Climatic maps

The impacts of human factors on fires can be considered as both a cause and an effect. The former studies are more abundant, since human activities are the most common cause of fires. Identifying the most important factors of fire occurrence has been the main goal of a wide range of studies, commonly based on statistical approaches, which try to explain historical human-caused fire occurrence from a set of independent variables (Chou et al. 1993; Chuvieco et al. 2003; Martell et al. 1989; Martínez et al. 2009; Vega-García et al. 1995). The consideration of human values in fire risk assessment is more recent and only a few regional studies have identified that the main socio-economic damages potentially caused by wildland fires are associated to lives, properties, and environmental services (wood products, hunting, fungi, carbon stocks, recreational...).

Even though most fires are human-caused worldwide, the importance of fires caused by lightning cannot be underestimated, since they account for a significant part of all fires in low populated areas (> 30% in the Boreal forest, for instance). To include this variable in fire risk models, a good knowledge of spatial distribution of lightning strikes is required, as well as a

better understanding on why a strike becomes an ignition point (Dissing and Verbyla 2003; Larjavaara et al. 2005; Renkin and Despain 1992).

With respect to fuel moisture content status (FMC, commonly expressed as percentage of dry weight), the most common approach has been the estimation through moisture codes based on weather data. The spatial estimation of these indices is commonly based on interpolation techniques or on gridded forecasted data (Aguado et al. 2007). The FMC of live plants has been approached from satellite data, both using empirical and simulation methods (Chladil and Nunez 1995; Garcia et al. 2008; Yebra et al. 2008).

Fire propagation potential was modelled in this project using the Behave model (Rothermel 1983). As an approximation of fuel type mapping, the forestry map of Spain was used, and updated for some categories using the CORINE land cover map at 1:200.000.

For assessing the potential impacts of fire, and therefore which areas might be more affected if burned, two synthetic variables were derived. On one hand, the ecological vulnerability, which was based on an estimation of the number of years any cell in our study area would recuperate its pre-fire conditions, and on the other the socio-economic values at stake. This latter variable has in turn two components: values of houses that may be burned in case of fire (those close to the forest interface), and ecosystem services that may be affected (including wood prices, firewood, cork, pine nuts, pasture, hunting, CO_2 sinks, fishing and recreational services.

1.3 *Integration*

The integration of input variables is being based in statistical and physical approaches. Probabilistic scenarios are being considered for human and natural causes, while the propagation is based on fire behavior models and vulnerability is based on production and utility functions and expressed in monetary units.

The validation will be based on the fire seasons of 2010 and 2011. Preliminary results show significant differences between high and low risk areas in terms of fire occurrence.

References

Aguado, I., Chuvieco, E., Boren, R., & Nieto, H. (2007). Estimation of dead fuel moisture content from meteorological data in Mediterranean areas. Applications in fire danger assessment. International Journal of Wildland Fire, 16, 390-397.

Chladil, M.A., & Nunez, M. (1995). Assessing grassland moisture and biomass in Tasmania. The application of remote sensing and empirical models for a cloudy environment. International Journal of Wildland Fire, 5, 165-171.

Chou, Y.H., Minnich, R.A., & Chase, R.A. (1993). Mapping probability of fire occurrence in San Jacinto Mountains, California, USA. Environmental Management, 17, 129-140.

Chuvieco, E. (2008). Satellite observation of biomass burning: implications in global change research. In E. Chuvieco (Ed.), Earth Observation and Global Change (pp. 109-142). New York: Springer

Chuvieco, E., Aguado, I., Yebra, M., Nieto, H., Salas, J., Martín, P., Vilar, L., Martínez, J., Martín, S., Ibarra, P., de la Riva, J., Baeza, J., Rodríguez, F., Molina, J.R., Herrera, M.A., & Zamora, R. (2010). Development of a framework for fire risk assessment using remote sensing and geographic information system technologies. Ecological Modelling, 221, 46-58.

Chuvieco, E., Allgöwer, B., & Salas, F.J. (2003). Integration of physical and human factors in fire danger assessment. In E. Chuvieco (Ed.), Wildland Fire Danger Estimation and Mapping. The Role of Remote Sensing Data (pp. 197-218). Singapore: World Scientific Publishing

Dissing, D., & Verbyla, D.L. (2003). Spatial patterns of lightning strikes in interior Alaska and their relations to elevation and vegetation. Canadian Journal of Forest Research, 33, 770-782.

FAO (2007). Fire management - global assessment 2006. A thematic study prepared in the framework of the Global Forest Resources Assessment 2005. Rome: FAO Forestry Paper 151

Garcia, M., Aguado, I., & Chuvieco, E. (2008). Combining AVHRR and meteorological data for estimating live fuel moisture content in forest fire danger rating. Remote Sensing of Environment, 112, 3618-3627, doi:3610.1016/j.rse.2008.3605.3002.

Larjavaara, M., Pennanen, J., & Tuomi, T.J. (2005). Lightning that ignites forest fires in Finland. Agricultural and Forest Meteorology, 132, 171-180.

Martell, D.L., Bevilacqua, E., & Stocks, B.J. (1989). Modelling seasonal variation in daily people-caused forest fire occurrence. Canadian Journal of Forest Research, 19, 1555-1563.

Martínez, J., Vega-García, C., & Chuvieco, E. (2009). Human-caused wildfire risk rating for prevention planning in Spain. Journal of Environmental Management, 90, 1241-1252.

Renkin, R.A., & Despain, D.G. (1992). Fuel moisture, forest type, and lightning-caused fire in Yellowstone National Park. Canadian Journal of Forest Research, 22, 37-45.

Rothermel, R.C. (1983). How to predict the spread and intensity of forest and range fires. Ogden, UT: USDA, Forest Service, GTR INT-143

Vega-García, C., Woodard, T., Adamowicz, & Lee, B. (1995). A logit model for predicting the daily occurence of human caused forest fires. International Journal of Wildland Fire, 5, 101-111.

Yebra, M., Chuvieco, E., & Riaño, D. (2008). Estimation of live Fuel Moisture Content from MODIS images for fire risk assessment. Agricultural and Forest Meteorology, 148, 523-536.

A HIGH-RESOLUTION ANALYSIS OF FUEL SPATIAL STRUCTURE AND FIRE SPREAD IN SPAIN

Sergi Costafreda-Aumedes, Cristina Vega-Garcia

University of Lleida. scaumedes@gmail.com; cvega@eagrof.udl.cat.

Abstract

Fuel landscape structure determines wildfire occurrence and propagation. The pervasive abandonment the rural mountainous Mediterranean landscape has undergone in past decades has highly influenced fuel arrangements and loads in many areas. The relationship between landscape homogenization and increased hazard conditions has been studied before, using medium-resolution sources of remote sensing data (i.e. Landsat). High-spatial-resolution analyses of spatial fuel arrangements and their influence on local fire hazard are very scarce, though. We selected fires occurred between 2006 and 2010 in several Mediterranean regions in Spain: Aragón (1399 fires), Cataluña (1383), Castilla-La Mancha (144) and Comunidad Valenciana (1165). We analyzed local fuel structure by applying texture and several kernel measurements to blue, green, red and near infrared bands in 0.5 meters-resolution ortophotos acquired before the fires occurred. We then studied the relationship between the spatial configuration of the fuels in the burned area of each forest fire and the spatial configuration of the fuels in not-burned areas. Where developmental perimeters were available for each fire (perimeters at successive time steps of the fire spread until final burned area is reached), directional texture and kernel measures were computed and tested for agreement with propagation direction

Keywords: Fire spread, High spatial resolution, Fuels, Spatial pattern, Ortophotos

EVALUATING PRESENT AND FUTURE FIRE RISK IN GREECE

C. Giannakopoulos[1], A. Karali[2], A. Roussos[2], M. Hatzaki[2], G. Xanthopoulos[3], K. Kaoukis[3]

[1]Institute for Environmental Research and Sustainable Development, National Observatory of Athens, I. Metaxa & V. Pavlou, Palaia Pendeli, 15236, Athens, Greece. cgiannak@meteo.noa.gr
[2]Institute for Environmental Research and Sustainable Development, National Observatory of Athens, Athens, Greece. akarali@meteo.noa.gr , anargyrosroussos@yahoo.gr, marhat@phys.uoa.gr
[3]Institute of Mediterranean Forest Ecosystems and Forest Products Technology, National Agricultural Research Foundation, Athens, Greece. gxnrtc@fria.gr , kako@fria.gr

Abstract

The current climate change trend in the Mediterranean and more specifically in Greece causes longer summer droughts and intensification of these droughts even out of season. Also, extreme weather events, such as periods of high temperatures, strong air dryness and very strong winds, as well as sudden storms with heavy rainfall in only few hours are becoming frequent. As a result, the frequency of large-scale forest fires is on the rise and the same holds true about soil erosion which is aggravated when such fires are followed by heavy rains a few days later. When a period of drought and high temperatures is followed by a day of peak temperatures, low relative humidity and very strong winds, fire danger reaches extreme levels and multiple fires can easily get out of control creating havoc.

In order to investigate fire danger in correlation with meteorological conditions in Greece, the Canadian Fire Weather Index (FWI) was used in the context of the current study. FWI is a daily meteorologically-based index designed in Canada and used worldwide to estimate fire danger in a generalized fuel type. The FWI System provides numerical ratings of relative fire potential based on weather observations. FWI components depend solely on daily noon measurements of dry-bulb temperature, air relative humidity, 10 m open wind speed and 24 h accumulated precipitation. FWI consists of 6 standard components each measuring a different aspect of fire danger. The first three are fuel moisture codes that follow daily changes in the moisture contents of three classes of forest fuel with different drying rates. The remaining components are fire behavior indices representing the rate of spread, fuel weight consumed and fire intensity.

In this study, an evaluation of the index applied to current fire data for Greece is initially performed. Additionally, the index is correlated to observed meteorological data over a 7-year period, with particular emphasis on the most vulnerable region of Southern Greece. The study aims to establish whether FWI values and its components can adequately reflect fire risk as judged by actual fire occurrence and area burnt. New thresholds of elevated (FWI>15) and extreme (FWI>45) fire risk are established in accordance with previous studies.

Subsequently, a regional climate model with a high horizontal resolution of 25x25km is used to provide input for the FWI system in order to investigate the impacts of climate change on fire risk for two future time periods - 2021-2050 and 2071-2100. Days with extreme fire risk are expected to increase over the domain of interest with a maximum value of 30 days occurring by the end of the century, in Eastern Peloponnese and the Attica Peninsula.

Keywords: fire risk, forest fires, FWI, meteorological conditions, RCMs

Introduction

Forest fires have always been present in the Mediterranean ecosystems. Throughout history, human induced or naturally caused forest fires imposed their impact on natural environment. The last few decades though, the number of forest fires has significantly increased, as well as their severity and impact on the environment. An average of 50,000 fires sweep away from 700x103 to 1000x103 ha of Mediterranean forests per annum (FAO 2007), causing enormous economic and ecological destruction. In particular, the data collected reveal that, according to the average burnt area per fire, Greece has the most severe forest fire problems among the

European Union countries (EU 2001). It has been estimated that the average area burnt per fire was 39.4 ha in Greece, 28.47 ha in Spain, 19.74 in Italy and 15.29 in Portugal (Iliadis et al. 2002). Forest fires are highly sensitive to climate change because fire behavior responds immediately to fuel moisture (Weber and Flannigan 1997; Stocks et al. 2001). Thus, the projected increase in temperature will increase fuel dryness and reduce relative humidity and this effect will worsen in those regions where rainfall decreases. Accordingly, increases in climate extreme events are expected to have a great impact on forest fire vulnerability (Beniston 2003).

The contribution of meteorological factors to fire risk is simulated by various non-dimensional indices of fire risk. Viegas et al. (1999) validated several such indices in the Mediterranean against observed fire occurrence, with the Canadian Fire Weather Index (FWI, van Wagner 1987) amongst the best performers. The FWI model is non-dimensional, based on physical processes and has been used in many different locations, therefore it seems a sensible basis for exploring the mechanisms of fire risk change.

In this study, an evaluation of the index applied to current fire data for Greece is performed with particular emphasis on the most vulnerable region of Southern Greece. The study aims to establish whether FWI values can adequately reflect fire risk as judged by actual fire occurrence and to estimate the potential projected changes in fire risk.

Data and methods

In our study, the fire data were provided by the Forest Special Secretariat of the Ministry of Environment, Energy & Climate Change. Fire data concern inventory of forest fires that occurred in the period 1991-1997 throughout Greece.

Meteorological data covering the 7-year period (1991-1997) were obtained from the Hellenic National Meteorological Service. Mean daily values from two stations (Elliniko-37° 44' N. 23° 44' E, Kalamata-37° 04' N. 22° 10' E) were used in order to compute daily values of FWI.

Due to the different meteorological conditions prevailing in the eastern and western areas of Southern Greece, the domain of interest was split into two parts covering the eastern Peloponnese and the Attica Peninsula (Eastern Domain) and the western Peloponnese (Western Domain).
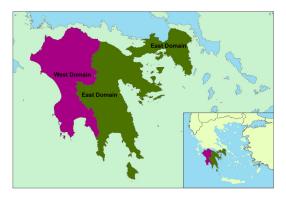

Figure 1. Map of Southern Greece, where the two domains are displayed.

Forest fire risk was assessed using the Canadian Fire Weather Index (FWI). FWI is a daily meteorological-based index used worldwide to estimate fire danger in a generalized fuel type.

Although it has been developed for Canadian forests, several studies have shown its suitability for the Mediterranean basin (Moriondo et al. 2006). The FWI System provides numerical ratings of relative fire potential based solely on weather observations. FWI components depend on daily noon measurements of dry-bulb temperature, air relative humidity, 10m open wind speed and 24 h accumulated precipitation and are described in detail in van Wagner (1987). FWI consists of 6 standard components each measuring a different aspect of fire danger. The first three are fuel moisture codes that follow daily changes in the moisture contents of three classes of forest fuel with different drying rates. The remaining components are fire behavior indices representing the rate of spread, fuel weight consumed and fire intensity.

Results

1.1   *Forest fire records and FWI validation*

The following table concerns cumulative data on burnt area and the number of fires occurred in the eastern and western domain respectively on each year in the period 1991-1997.

Table 1. Burnt area and number of fires per year for the Eastern and the Western Domain during 1991-1997 period.

	Burnt Area (ha)		Number of fires	
	Eastern Domain	Western Domain	Eastern Domain	Western Domain
1991	2668,9	570,6	119	91
1992	28436,5	5652,8	312	224
1993	13486,6	6754	301	292
1994	3567,1	2495,7	212	182
1995	4367,3	3768,2	188	214
1996	4643,2	1040,9	162	146
1997	2307	3355,8	138	239
Total	**59476,6**	**23638**	**1432**	**1388**

The table depicts an almost total predominance in burnt area and the number of fires of the Eastern Domain. That is due to several factors, such as the larger extent of the Eastern Domain, population, the density of infrastructure and the climate. Most fires are caused by human activities, deliberately or by negligence (Pausas & Vallejo, 1999), and in this way it is expected to have more fire events on a highly populated area.

The FWI was classified in categories of bin with size 1 and the average value of the number of fires that occurred at each category was calculated for both domains (Figure 2). It should be noted that the increased variability in high FWI values results from the decrease in the frequency of occurrence of high index values. The best estimated polynomial fit was applied on the data. The turning points of both fitted equations were calculated at FWI ≈ 15 and FWI ≈ 45. This implies that at FWI ≈ 15 the fire risk is starting to increase and one fire in two days occurs when FWI ≈ 15. The FWI ≈ 45 value indicates extreme fire risk, while one fire occurs in each day with FWI ≈ 45. These values are in accordance with Moriondo et al. (2006) and Good et al. (2008) that resulted at the same threshold values with different methodologies. Therefore, FWI ≈ 15 and FWI ≈ 45 are set as thresholds for elevated and extreme fire risk, respectively.
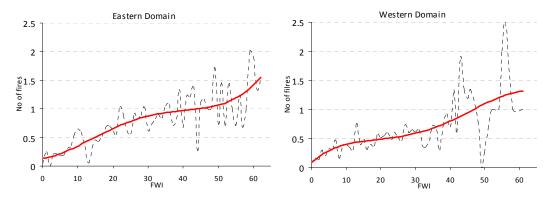
Figure 2. Mean number of fires per day against FWI (black line) and the respective polyonimal fit (red line) for the Eastern (left) and the Western Domain (right) for 1991-1997 period.

1.2 *Future Projections*

Present and future model data from the Regional Climate Model RACMO2 were used in this study. The model was developed within the framework of the ENSEMBLES Project, by the Royal Netherlands Meteorological Institute (KNMI), at 25km horizontal resolution. The control run represents the base period 1961-1990 and is used here as reference for comparison with future projections for the periods 2021-2050 and 2071-2100. For the study region, maps produced illustrating the change in the number of days with extreme fire risk (FWI>45) between the reference and the two future periods (Figure 3).

In the near future, namely 2021-2050, the most considerable increases are estimated in the eastern part of Peloponnese and the greater part of Attica with up to7 and 10 more days of fire risk per year, respectively (Fig 3a).On the other hand, by the end of the century (2071-2100), most part of the Eastern Domain may experience increases of up to 30 days per year, with the Attica Peninsula being the most vulnerable part of the domain. Smaller increases of up to 12 days may occur on the Western Domain (Fig 3b).
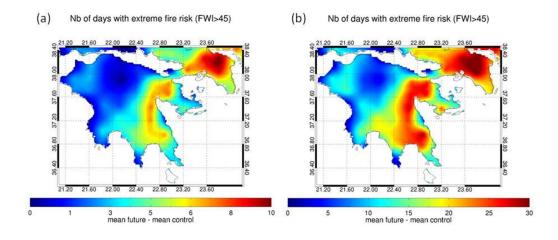
Figure 3. Projected changes in the number of days with extreme fire risk (FWI>45) during (a) the first future period (2021-2050) and (b) the second future period 2071-2100.

Conclusions

FWI was confirmed to be skillful in predicting fire occurrence for the vulnerable area of Southern Greece. The resulted thresholds FWI ≈ 15 and FWI ≈ 45 for elevated and extreme fire risk, respectively, are in accordance with Moriondo et al. (2006) and Good et al. (2008).

The future projections suggest a general increase in fire risk over the domain of interest with a very strong impact in the eastern Peloponnese and Attica. For the near-future period 2021-2050, the number of days with extreme fire risk increases up to 10 more days per year in the eastern part of the study area. By the end of the century (2071-2100), the increase is 12 and 30 days in the Western and Eastern Domain, respectively.

Acknowledgements

References

Beniston M. 2003. Climatic change in mountain regions: a review of possible impacts. Climatic Change 59: 5–31.

EU, European Union 2001. Report No 1: Forest Fires in southern Europe. Brussels, Belgium, European Commission, 45 p.

FAO, Food and Agriculture Organization 2007. Fire management - Global assessment 2006. FAO Forestry Paper No. 151 Rome, Italy, 121 p.

Good, P., Moriondo, M., Giannakopoulos, C., Bindi, M., 2008. The meteorological conditions associated with extreme fire risk in Italy and Greece: relevance to climate model studies. International Journal of Wildland Fire 17,155–165.

Iliadis L.S., Papastavrou A.K., Lefakis P.D. 2002. A computer-system that classifies the prefectures of Greece in forest fire risk zones using fuzzy sets. Forest Policy and Economics 4: 43–54.

Moriondo, M., Good. P., Durao, R., Bindi, M., Giannakopoulos, C., Corte-Real, J. 2006. Potential impact of climate change on fire risk in the Mediterranean area. Climate Research 31: 85–95.

Pausas, J. G., & Vallejo, V. R. 1999. The role of fire in European Mediterranean ecosystems. In E. Chuvieco (Ed.), Remote sensing of large wildfires (pp. 3– 16). Berlin, Springer-Verlag.

Stocks B.J., Wotton B.M., Flannigan, M.D., Fosberg, M.A., Cahoon, D.R., Goldammer, J.G. 2001. Boreal forest fire regimes and climate change. In M.Beniston and M.M. Verstraete (Eds.), Remote Sensing and Climate Modeling: Synergies and Limitations (pp. 233-246). Advances in Global Change Research, Kluwer Academic Publishers, Dordrecht and Boston.

Van Wagner, C.E. 1987. Development and structure of a Canadian forest fire weather index system, Forestry Technical Report 35. Canadian Forestry Service, Ottawa.

Viegas D.X., Bovio G., Ferreira A., Nosenzo A., Sol B. 1999. Comparative study of various methods of fire danger evaluation in southern Europe. International Journal of Wildland Fire 9, 235–246.

Weber M.G., Flannigan M.D. 1997. Canadian boreal forest ecosystem structure and function in a changing climate: impact on fire regimes. Environ. Rev. 5: 145-166.

A NEW METHODOLOGY FOR NEAR-REAL TIME ESTIMATION OF SMOKE PLUME EMISSIONS FROM FOREST FIRES IN THE EUROPEAN FOREST FIRE INFORMATION SYSTEM

B. Guillaume[1*], C. Liousse[1], J. San-Miguel Ayanz[2], A. Camia[2]

[1]Laboratoire d'Aérologie, France. guib@aero.obs-mip.fr; [2]Joint Research Centre, IES, Italy

Abstract

This article presents the new forest fire emissions module in the European Forest Fire Information System (EFFIS). The European Forest Fire Information System (EFFIS) systematically delivers since 2000 series of burnt area statistics mapped from satellite imagery. A previous emission module in EFFIS, built on classical methodologies of fuelmap-based emission estimation, has been revisited here. Since 2009, the Rapid Damage Assessment module in EFFIS provides daily increases of the burnt areas and perimeters based on MODIS imagery. This improvement made EFFIS a unique system, with no equivalent in accuracy for both local (fire-by-fire) and regional (covering whole Europe) scales. The new methodology exposed here makes use of this near-real time fire information, and additionally implements a more detailed module to better assess the burning efficiency, a key parameter impacting largely the fire emission estimation. The main improvement concerning burning efficency modelling in respect to the previous European emission estimates is the modelling of the burning efficiency not only with fuelmap-dependency, but also accounting both for the fuel moisture damping effect and the feedback of the fire intensity itself. Results on the application of the new EFFIS emissions module for a Greek large fire in 2009 and for the entire 2009 fire season are presented and compared to previous estimates in the system. A sensitivity test to different burning efficiency models has been performed, showing the large differences with models where only the fuel-dependency is considered, or when a coarser empirical model of moisture damping effect is used. The systematic application of the methodology will start in EFFIS operational system in 2011 and will lead to an enhanced estimate of forest fire emission over Europe.

Keywords: European Forest Fire Information System, forest fire smoke plume emissions

Introduction

Biomass burning events are large sources of gases, particles and heat releases in the atmosphere. These fires widely vary in three aspects: which pollutants are emitted, in what proportions and with which energy. These direct or immediate consequences of forest fires are a major issue for air pollution (Miranda et al., 2004; Goldhammer, 2009), climate and health (Liousse *et al.*, 1996; Wu *et al.*, 2007)

For almost three decades the estimation of trace gases emissions from vegetation fires has been based on the "fuel map" –based method proposed by Seiler and Crutzen (1980). This approach is based on information on the burnt surface extent, the amount and type of biomass burnt (fuel types, fuel loads), and the conditions under which fires take place (combustion efficiencies); finaly emission factors are used to estimate the amount of emissions of each species (gases and particles). All these variables are affected by high uncertainties, often reaching more than 50% in the final emission estimates at the global scale (Liousse *et al*., 2004). Currently, large use is made of detailed space borne data to help reduce such uncertainties, as shown by recent comparison exercise at global scale (Jain*,* 2007; Stroppiana *et al*., 2010).

A new alternative approach to this "fuelmap"-based approach has emerged recently (Wooster, 2002; Wooster *et al.*, 2005; Roberts *et al.*, 2005). Burned biomass is directly retrieved from the

fire radiative power/energy provided by satellite products, without any assumptions on burning fuel types. This approach is actively tested all over the world (Kaiser *et al.*, 2011). One of the main uncertainties in this approach is linked to the relationship between energy and emitted masses of pollutants and for instance, Kaiser *et al*. finally calibrates their estimates using estimates from the fuelmap-based approach.

In spite of all these uncertainties and because real-time information are now increasingly needed for operational use in rapid fire damage assessment, operational fire emission systems have been recently developed both at the global (MACC system) (Kaiser *et al*., 2011) and regional scales (EFFIS system) (San Miguel *et al*., 2011). The European Forest Fire Information System (EFFIS) provides one of the finest resolution fuelmap-based operational system, allowing to retrieve the required spaceborne information for estimating forest fire emissions over Europe. Since 2000, burnt area information over Europe is mapped from satellite imagery at the highest available resolution. Additionally, information on fuels is also available, with fuel types identified at 250m resolution (Sebastian-Lopez *et al* , 2002). Based on this information, fire emission estimations are performed (Barbosa *et al*, 2009; San-Miguel-Ayanz *et al.* 2011). More recently, in 2009, the sytem has gained in accuracy with retrieval of daily increases of the burnt areas and burning perimeters using MODIS imagery. This improvement makes EFFIS a unique European system, with no equivalent in spatial and temporal resolution to retrieve in near-real time, with precise fire information, both at local scale (for each fire) and at continental scale burnt area information covering the entire Europe.

The present article reports on new improvments on the classical "fuelmap"-based approaches, especially on revisiting the burning efficiency estimations and the choice of emission factors, and on the use of the near-real time fire information. After detailing the methodology in section 2, results are shown both at single fire scale and for whole Europe in section 3. A sensitivity test (section 4) has been conducted by degrading the estimation of burning efficiencies, with more classical approaches to evaluate the impact of such variations upon the data set. Results and prospects are then discussed in section 5.

Methodology

The key factors influencing the European forest fire emissions are fuel types, meteorological conditions, topography, and the fire itself (fire intensity evolving during the combustion phases). Typically, here in the approach, these key factors are taken into account in the following steps: (1) retrieval of information on fire location (position of fire fronts and backfires, or location of burnt areas if the fire history cannot be reconstituted finely enough in real time), (2) identification of topography, meteorological fields and fuel composition at that site, (4) evaluation of two key variables: fuel moisture (% of relative humidity in fuel) and fire intensity (kW/m^2), (5) assessment of burning efficiencies and amounts of fuel burnt (or fuel consumptions) during the different combustion phases (smoldering/flaming), and finally, (6) evaluation of emissions from burnt fuel loadings. The main improvements from previous methods are thus: (1) a more precise estimation of the burning efficiency, accounting not only for fuel properties, but also for meteorological factors and for the fire intensity itself, (2) an update of the emission factors from the most recent literature, and (3) the use of the most

recent fire information (daily updates of burnt areas and perimeters from MODIS imagery). In the EFFIS system, the current fuelmaps are from Sebastian-Lopez *et al*. (2002), which are compatible with the US-NFDRS fuel nomenclature, using standard fuel properties (fuel loads, fuel depth,...) (Deeming *et al.*, 1978). Use was also made of canopy forest type classes from the most recent high resolution forest type maps (Kempeneers *et al.*, 2011). A new fuelmap is under development in the EFFIS system which will be incorporated in a near future.

1.1 *Burning efficiency estimations*

The simplest method to estimate burning efficiency is a fuel-dependent (Leenhouts, 1980; Liousse et al 1996; Barbosa et al., 2009) method, clearly more suited for emission inventories at lower time resolution (mainly for monthly estimates in climate models). More developed approaches required for high temporal resolution systems do also involve a fuel moisture damping effect and an estimation of fire intensity, crucial factors of short-term variability of burning efficiency. Two types of models (propagating and non-propagating) do take into account such dependency. The propagating models spatially reconstitute the fire behaviour and the associated burning efficiency, like the mathematical model FARSITE (Finney *et al.*, 2004) or the physically-based models WFDS (Mell *et al.*, 2005) and FIRETEC (Linn *et al.*, 2002). Non-propagating models include the emipirical relationships of the CFFDRS Canadian model (CFFDRS, 2007), providing both fire behaviour (fire intensity, rate of srpead) and fire effects (burning efficiency, fire emissions). They also include models for fire behaviour like NEXUS (Scott and Reinhardt, 2001), separated from models for fire effects model like FOFEM5 (Reinhardt, 2003) or FEPS (Anderson *et al*., 2004).

Propagating models, though particularly promising, are not yet able to assimilate measurements of burnt areas and burnt perimeters. Thus, in this paper, a non-propagating approach was developed. The Canadian CFFDRS system has been discarded for use in Europe, mainly due to the shrub class lack. A coupling between the fire behaviour and fire effects modelling has been developed here including the NEXUS model for fire behaviour calculations, the FOFEM5 model for fire effects of woody fuels, and the CONSUME3 model for fire effects of non-woody fuels. This model was preferred to the FOFEM5 for non-woody fuels since, in FOFEM5, additional distinction is made on regionalisation in the US continent, a refinement not adapted to the European region. Let us note that the FOFEM5 system has recently been shown to be well adapted to European woody fuels by Bacciu *et al.* (2009) for Mediterranean bush fires in Sardinia (Italy) during 2007.

The large variability in a day of the fuel moisture content (FMC) of fine dead fuels, mainly due to the variability in a day of the meteorological factors, is taken into account in our system: this parameter is known to be largely impacting the burning efficiency. Meteorological fields are from the COSMO-EU model, at 3hour and 7km resolutions, provided by the German meteorological institute DWD German Meteorological model. The FMC for other dead and living fuels than the fine dead fuels are estimated on the basis of a lower temporal resolution (daily at best) : (1) the FMC of large dead fuels are derived from the fire danger assessment module in EFFIS (San-Miguel-Ayanz *et al.*, 2011), (2) the FMC of living herbaceous fuels are derived from the method proposed by Yebra et al. (2008) for MODIS vegetation indices, which has shown to give coherent FMC values in Europe, (3) the FMC for shrub fuels, quite variable

between European sites, cannot be easily derived from satellite products on a continental scale (Chuvieco *et al.*, 2004). In this case, a more validated approach considering meteorologically-based indices (drought code), has been used here (Viegas *et al.*, 2001; Pellizzaro *et al.*, 2007). Finally, (4) the FMC of canopy in the model follows a seasonal variation (Alexander *et al.*, 2010) from a set of empirical data (Dimitrakopoulos *et al.*, 2003; Mitsopoulos, 2010). Note that the curing effect (transition from living to dead fuels in dry season) has not been considered: its implementation in the EFFIS fire danger assessment module is currently under development. Finally, the common problem in non-propagating models of the not accessible precise location of the fire front, was raised here, with a need to manage together (1) the 3hr resolution of the fine dead fuel FMC with the coarser daily resolution of the burnt area and perimeter increase, and (2) the fine spatial resolution (250m) of the fuelmap with the coarser daily increase in fire area and perimeter. This problem has been handled with the use of an additional assumption: an hypothesis has thus been made of equiprobable events of burning one particular fuel type or the other within one given fuelmap cell in by daily burnt areas. Consequently, as a first step, for each fuel type encountered in the daily burnt area increase, a disaggregation of the burning efficiency from the day to a 3-hr evolution has been performed, proportionally to the 3-hr intensity of the rate of spread. Then, averaging has been made over all fuel types, using individual fuel type burning efficiencies weighted by the percentages of surface coverage by such fuel type in burnt areas.

1.2   *Emission estimations*

Emissions were estimated for the main pollutants emitted by fires, namely CO_2, CO, CH_4, PM2.5, PM10, NMHC, VOC, NOx, BC, OC, SO_2, NH4, BaP and levoglucosan. The emission factors in the existing fire literature are often relative to large ecosystems (temperate, tropical forests) (Andreae and Merlet, 2001), but they are not provided by individual fuel components (living grass, shrubs, small, medium, large dead fuels, canopy,...) in the fuel models. A few papers however present more details by fuel components, but either for a restricted list of fuel componenrts (Battye and Battye, 2002; Miranda *et al*., 2005), or from more ancient literature for the entire list of fuel components (Leenhouts, 1998). They all provide differentiated emission factors for flaming and smoldering combustion phases, but only Miranda et al. (2005) (MI2005) provide emission factors for combustion phases adapted to European biomass burning. However, MI2005 does not provide emission factors for duff and for dead woody fuels, and does not include emission factors for SO_2, NH3, BaP and levoglucosan. Thus, EF values were first taken here from MI2005 for grasslands, shrublands and canopy, and then complemented for fine dead fuels by values from Battye and Battye (2002) and Leenhouts (1998) and, for medium/large dead fuels from Leenhouts (1998) only. Missing EF for some species (SO_2, NH3, BaP, levoglucosan) were adapted from Andreae and Merlet (2001).

Results

Zoom on a Greek fire in 2009

The method was tested in the largest fire of the 2009 fire season occurred in the Attiki region (Greece) between August 22nd and 23rd, with final burnt areas of 20,520 ha and more than 80%

burnt the first day (Figure 1). This fire had a behaviour typical of very large fires, with estimated plume injection height of about 6km, clearly visible (not shown here) in IASI-CO satellite products (Clerbaux et al., 2009). This contrasts with highermost injection height of 4km traditionally observed for Mediterranean fires (Lavoue et al., 2000). Modelled fire intensity (Figure 1 center right) is found quite different between August 22nd and 23rd. This is largely due to differences in burnt areas (Figure 1 center left) whereas meteorological factors and fuel moisture only poorly differ from one day to the other. Total CO emissions every 3hour display a diurnal cycle with large differences between August 22nd and 23rd.
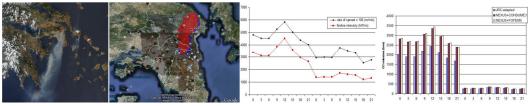
Figure 1. MODIS imagery of the fire (left), MODIS-based burnt area increases between August 22nd and 23rd (center left), fireline intensity and rate of spread (values multiplied by 100) (center right), comparison of results of the three simulations for CO emissions (left).

Biomass burning emissions during the 2009 fire season

We have focused on the five European Mediterranean most fire affected countries: France, Greece, Italy, Portugal and Spain. In 2009, the other countries with significant fires were Albania, Bulgaria and Sweden, but with less than 4% cotntribution in the 2009 burnt area total of the European Union.

Burnt areas in the five quoted countries amount to 238000 ha. In our system, the CO emission total amounts to 260Gg, with 32%, 30% and 22% of this total respectively for Spain, Portugal and Greece, the most fire affected countries. Greek CO fire emissions are issued for 40% from 22nd-23rd August fire in Attiki region.

CO emission amount was compared to other emission inventories in the context of collaborations during the intercomparison exercise BBSO-2 (Stroppiana et al., 2010) and from JRC previous estimate (San Miguel et al., 2011). These emission inventories were provided at global scale, with different grid resolutions, all about 1°x1° resolution. Total amounts were derived from these inventories for the five EU Mediterranean countries mostly affected by fires. As seen in Table 1, our estimate for the year 2009 is slightly higher but of the same order than the previous JRC estimate (San Miguel et al., 2011). As shown by San Miguel *et al*., the 2009 emission amount is among the lowest in the period 2003-2009, whereas the 2003 one is the highest. The comparison for the year 2003 shows a very high range of uncertainty in Europe. In 2003, MODIS-based data let appear two different types of results: the previous JRC estimate, relying on purely MODIS burnt area products, show lower values than the Chin et al. (2002) estimate, based on composite MODIS active fire and burnt area products. GFED v2 and v3 are more tightly linked to MODIS burnt areas than to active fires (resp. Giglio *et al.*, 2006 and Giglio, 2010) and their estimates are quite comparable to the ones from San Miguel *et al*. The MOPITT-based approach, an independent method relying on inverse source modelling from EO-based CO column retrievals, provides estimates in the middle range. The highest estimates are basically relying on active fire data, e.g. ones from Mieville *et al*. (calibrated by GBA2000 BA

product) and from Chin *et al*. The L3JRC product exhibit highly different results (Stroppiana et al., 2010), mainly due to problems of threshold in the burnt area retrieval, particularly over temperate regions.

Table 1. Comparison of CO total amounts from various emission inventories

	CO emission amounts	Region	Reference
EFFIS system	0.644 (2003), 0.299 (2004), 0.523 (2005), 0.264 (2006), 0.384 (2007), 0.104 (2008), 0.147 (2009)	Whole EU Mediterranean Region	*San Miguel et al.
GBA-ATSR 1	2.7 (2003)	5 countries	Mieville etal., 2010
L3JRC	13.3 (2003)	5 countries	Tansey et al., 2008
MODIS-based	3.7 (2003)	5 countries	Chin et al. 2002
GBA-ATSR 2	0.217 (2003)		Ito and Penner, 2004
MOPITT inverse	1.2 (2003)	5 countries	Petron et al., 2005
GFED v2	1.16 (2003)	5 countries	Van der Werf et al., 2006
GFED v3	0.63 (2003)	5 countries	Van der Werf, pers. comm.
This study	0.261 (2009)	5 countries	This study

Sensitivity to the burning efficiency model

Burning efficiency (BE) is a key parameter in fire emissions. As already stated, major inventories at large spatial and temporal scales only display model fuel-dependent BE. Let us denote S0 the current inventory here. In a S1 scenario, the same BE model as in San Miguel *et al.* (2011), with only fuel-dependent BE, has been considered, whereas in a S2 scenario, the complex physcially-based FOFEM5 model for woody fuels has been replaced by the more simple empirical relationships for woody fuels provided by CONSUME3. Five different test areas in Europe have been selected for throrough comparison: two large fire zones in Portugal, other zones being located in Corsica, Sardinia and Greece. These zones were chosen because they totalize large amounts of fires in 2009, while clearly showing different fuel type patterns from zone to zone, with grassland/shrublands being the largely dominant fuel type in western Portugal, eastern Portugal and Greece, against transitional shrublands/woodlands in Corsica and perennial grasslands and agricultural grasslands in Sardinia. About forest type coverage of burnt areas in test zones, non forested areas largely dominate. Relatively to other zones, high coniferous proportions are found in the eastern Portuguese zone and in Greece (mostly mixed with shrubs) and high broadleaved proportions are found in Sardinia.

Comparing the three scenarios on the basis of resulting burnt biomass amounts by fuel type and combustion phases (Figure 2), the highest amounts are found for the S0 and S1 scenarios, as compared to S2, showing the large differences obtained when moisture damping is considered. We note that S2 does not account for canopy fires, but impact of canopy is relatively small in each region when compared to other fuel components, mainly due to poor relative representation of this fuel stratum. The difference of BE modelling in S0 and S1 bearing on dead woody fuels (brown color in Figure 2), the former generally exhibits lower CO amounts, and significantly larger amounts in the smoldering phase relatively to the flaming ones. This also reveals the strong sensitivity of flaming/smoldering relative emission contributions to the BE modelling.
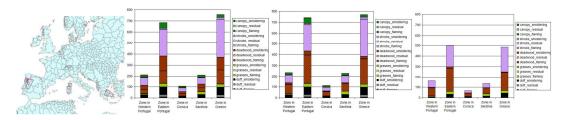
192

Figure 2. Evolution of burnt biomass (tons/year) in the five selected regions (left), according to fuel types and combustion phases. Left: chosen regions, center left : S0 scenario, center right: S1, right: S2

Conclusion

A new methodology been applied to evaluate fire-by- fire the emissions in the European zone covered by the EFFIS system. Main improvements in respect to other emission inventories are on burning efficiency modelling, considering not only fuel type-dependence, but also moisture damping and the impact of fire intensity itself on the distribution of emissions during the different combustion phases. These parameters have been found largely impacting burnt biomass. Improvements also include the updating of emission factors using recent literature data. The systematic application of the methodology will start in EFFIS operational system in 2011 and will lead to an enhanced estimate of forest fire emission over Europe. Prospects for this new emission model are numerous and diverse, with future developments on dead/living grassland/shrubland curing, but also distinction between broadleaf deciduous and broadleaf evergreen in the canopy coverage, since variability exists in the fuel parameters between these two canopy classes. Moreover, implementation of a new European fuel map is presently ongoing in EFFIS. This emission model is already adapted to associated fuel properties which may replace the US-NFDRS default properties currently used. Finally, an approach combining a fire propagation model and the EO-based fire evolution burnt areas from EFFIS could make better use of fine spatial scales availalable for most fields (forest maps, topography, fuelmaps) to improve emission estimates.. This approach would improve current emission schemes and also results in short-term forecasting of fire propagation risks, using 3-hr meteo predictions.

References

Alexander M. 2010. Foliar moisture content input in the Canadian Forest Fire Behavior Prediction System for areas outside of Canada, VI International Conference on Forest Fire Research, D.X. Viegas (Ed.).

Anderson, G.K.; Sandberg, D.V; Norheim, R.A., 2004. Fire Emission Production Simulator (FEPS) User's Guide. Available at http://www.fs.fed.us/pnw/fera/feps/FEPS_users_guide.pdf

Andreae, M. O. and Merlet P. 2001. Emission of trace gases and aerosols from biomass burning. Global Biogeochemical Cycles, 15: 955-966, 2000GB001382.

Arino, O. and Plummer, S. 2001. The Along Track Scanning Radiometer World Fire Atlas – Detection of night-time fire activity, IGBP-DIS Working Paper #23. Postdam, Germany

Arroyo L., Pascual C., Manzanera J.A. 2008. Fire models and methods to map fuel types: the role of remote sensing, Forest Ecology and Management, 256, 1239-1252.

Bacciu V., M. Salis, D. Spano, B. Arca, G. Pellizzaro, Duce P. 2009. Assessment of Smoke Emission and Carbon Estimates from Mediterranean Maquis Fire Events, Eight Symposium on Fire and Forest Meteorology, P15.

Barbosa P., Camia A., Kucera J., Liberta G.`, Palumbo I., San-Miguel-Ayanz J., Schmuck G. 2009. Assessment of Forest Fire Impacts and Emissions in the European Union Based on the European Forest Fire Information System, Developments in Environmental Science, Volume 8 197, A. Bytnerowicz, M. Arbaugh, A. Riebau and C. Andersen (Editors).

Battye, W., Battye R. 2002. Development of Emissions Inventory Methods for Wildland Fire. U.S. Environmental Protection Agency Contract No. 68-D-98-046. Online Link: http://www.epa.gov/ttn/chief/ap42/ch13/related/c13s01.html.

Brown J.K., Marsden M.M., Ryan K.C., Reinhardt E.D. 1985. Predicting duff and woody fuel consumed by prescribed fire in the northern Rocky Mountains, USDA Forest Service Res. Pap., INT-337.

Canadian Forest Service 2007. Canadian Wildland Fire Information System: Canadian Forest Fire Behavior Prediction (FBP) System, available at: http://cwfis.cfs.nrcan.gc.ca/en/background/bi_FBP_summary_e.php (accessed 23/07/2007).

Chin, M., Ginoux, P., Kinne, S., Torres, O., Holben, B. N., Duncan, B. N., Martin, R. V., Lo-gan, J. A., Higurashi, A., and Nakajima, T. 2002. Tropospheric aerosol optical thickness from the GOCART Model and comparisons with satellite and sun photometer measurements, J. Atmos. Sci., 59, 461–483.

Chuvieco E., Cocero D., Riaño D., Martin P., Martinez-Vega J., de la Riva J., Pérez F. 2004. Combining NDVI and surface temperature for the estimation of live fuel moisture content in forest fire danger rating. Remote Sensing of Environment, volume 92, issue 3, pp. 322-331.

Deeming, J. E., Burgan, R. E. and Cohen, J. D. 1978. The National Fire Danger Rating System 1978, INT-39, US Department of Agriculture, Ogden, UT.

Dimitrakopoulos A.P., I.D. MItsopoulos, E.A. Samara. 2003. Seasonal variation of forest species flammability as a reforestation criterion. In: I. Takos (Ed.), Plant species selection for afforestation, reforestation and improvement of rural and natural landscapes. Proceedings of a conference in Drama, Greece, 6 June 2003. pp. 157-174. (in greek).

Finney M.A. 2004. FARSITE; fire area simulator – model development and valuation. Rep. No. Paper RMRS-RP-4. USDA Forest Service, Ogden, UT.

Finney M.A. 2004. FARSITE; fire area simulator – model development and valuation. Rep. No. Paper RMRS-RP-4. USDA Forest Service, Ogden, UT.

Giglio L. 2010. 'MODIS Collection 5 Active Fire Product User's Guide Version 2.4.' (University of Maryland: College Park, MD).

Giglio, L., van der Werf, G. R., Randerson, J. T., Collatz, G. J., Kasibhatla, P. 2006. Global estimation of burned area using MODIS active fire observations, Atmos. Chem. Phys., 6, 957-974.

Goldammer, J.G. 2009. Impact of Climate Change, Socio-economic and Land-use Changes on Fire Regimes in the Asian Region. In: Proceedings of the International Symposium "Regional / National Impact of Climate Change on Fire Regimes" (Korea Forest Service, Korea Forest Research Institute, Inje University and Global Fire Monitoring Center, eds.), 3-22. Busan. South Korea, 2-6 February 2009, 329 pp.

Jain, A. K. 2007. Global estimation of CO emissions using three sets of satellite data for burned area, Atmos. Environ., 41, 6931–6940.

Kaiser, J. W., Heil, A., Andreae, M. O., Benedetti, A., Chubarova, N., Jones, L., Morcrette, J.-J., Razinger, M., Schultz, M. G., Suttie, M., and van der Werf, G. R. 2011. Biomass burning emissions estimated with a global fire assimilation system based on observed fire radiative power. BGD, **8**(4):7339–7398.

Kempeneers, P., Sedano, F., Seebach, L., Stobl, P., San-Miguel-Ayanz, 2011. IEEE Transactions on Geoscience and Remote Sensing, in press.

Leenhouts, B. 1998. Assessment of biomass burning in the conterminous United States. Conservation Ecology [online] 2(1): 1. Available from the Internet. URL: http://www.consecol.org/vol2/iss1/art1.

Linn, R., Reisner, J., Colman, J.J., Winterkamp, J. 2002. "Studying wildfire behavior using" FIRETEC, Int. J.Wildland Fire, 11: 233-246.

Liousse, C., Andreae, M. O., Artaxo, P., Barbosa, P., Cachier, H., Grégoire, J. M. , Hobbs, P., Lavoué, D., Mouillot, F., Penner, J., and Scholes, M. 2004. Deriving global quantitative estimates for spatial and temporal distributions of biomass burning emissions, in: Emissions of Atmospheric Trace Compounds, edited by: Granier, C., Artaxo, P., and Reeves, C., Kluwer 10 Academic Publishers, Dordrecht, The Netherlands, pp.544.

Liousse, C., Guillaume, B., Grégoire, J. M., Mallet, M., Galy, C., Pont, V., Akpo, A., Bedou, M., Castéra, P., Dungall, L., Gardrat, E., Granier, C., Konaré, A., Malavelle, F., Mariscal, A., Mieville, A., Rosset, R., Serça, D., Solmon, F., Tummon, F., Assamoi, E., Yoboué, V., and Van Velthoven, P. 2010. Western African aerosols modelling with updated biomass burning emission 15 inventories in the frame of the AMMA-IDAF program, Atmos. Chem. Phys. Discuss., 10, 7347–7382, doi:10.5194/acpd-10-7347-2010.

Liousse, C., J. E. Penner, C. Chuang, J. J. Walton, H. Eddleman, Cachier, H. 1996. A global three-dimensional model study of carbonaceous aerosols, /J.Geophys. Res., / *101* 19411–32.

Mell, W., Jenkins, M.A et al. 2005. "A physics based approach to modeling grassland fires", to be submitted to Int. J. Wildand Fire.

Mieville, A., Granier, C., Liousse, C., Guillaume, B., Mouillot, F., Lamarque, J.-F., Grégoire, J.-M., Pétron, G. 2010. Emissions of gases and particles from biomass burning during the 20th 25 century using satellite data and an historical reconstruction, Atmos. Environ., 44, 1469–1477.

Miranda, A.I. 2004. An integrated numerical system to estimate air quality effects of forest fires. Int. J. Wildland Fire 13(2); pp. 217-226.

Miranda, A.I.; Ferreira, J.; Valente, J., Santos; P., Amorim, J.H.; Borrego, C. 2005. Smoke measurements during Gestosa 2002 experimental field fires. International Journal of Wildland Fire 14, 107–116.

Mitsopoulos I. 2010. Seasonal variation of live fuel moisture content of several Mediterranean plant species. Unpublished manuscript, pers. comm.

Ottmar, Roger D., Prichard, Susan J., Vihnanek, Robert E., Sandberg, David V.. 2006. Modification and validation of fuel consumption models for shrub and forested lands in the Southwest, Pacific Northwest, Rockies, Midwest, Southeast, and Alaska. JFSP Final Report 98-1-9-06. Online at: http://www.fs.fed.us/pnw/fera/research/smoke/Consume/Consume30_users_guide.pdf

Pellizzaro G., Cesaraccio C., Duce P., Ventura A., Zara P. 2007. Relationships between seasonal patterns of live fuel moisture and meteorological drought indices for Mediterranean shrubland species, Int. J. Wildland Fires, 16, 232-241.

Reinhardt, E.D. 2003. Using FOFEM 5.0 to estimate tree mortality, fuel consumption, smoke production and soil heating from wildland fire. Missoula, MT: USDA Forest Service, Missoula Fire Sciences Lab. 7 p.

Roberts, G., Wooster, M. J., Perry, G. L. W., Drake, N., Rebelo,, L. M., Dipotso, F. 2005. Retrieval of biomass combustion rates and totals from fire radiative power observations: Application to southern Africa using geostationary SEVIRI imagery, J. Geophys. Res., 110, D21111.

San-Miguel-Ayanz, J., Schulte, E., Schmuck, G., Camia, A., Strobl, P., Liberta, G., Giovando, C., Boca, R.,   Sedano, F., Kempeneers, P., McInerney, D., Withmore, C., Santos de Oliveira, S., Rodrigues, M., Durrant, T., Corti, P., Oehler, F., Vilar, L., Amatulli, G. 2011. Comprehensive monitoring of wildfires in Europe: The European Forest Fire Information System (EFFIS), in Tiefenbacher, J. (Ed.) "Disaster Management", ISBN 978-953-307-651-5, in press.

Scott J.H., Reinhardt, E.D. 2001. Assessing crown fire potential by linking models of surface and crown fire behaviour, USDA For. Serv. Res. Pap., RMRS-RP-29.

Sebastian L. A., San-Miguel-Ayanz, J., Burgan, R. E. 2002. "Integration of satellite sensor data, fuel type maps and meteorological observations for evaluation of forest fire risk at the pan-European scale", International Journal of Remote Sensing, vol. 23, no. 13, pp. 2713-2719.

Seiler, W., Crutzen, P.J. 1980. Estimates of gross and net fluxes of carbon between the biosphere and the atmosphere from biomass burning. Climatic Change, *2*, 207-247

Stroppiana D., Brivio P.A., Grégoire J.-M., Liousse C., Guillaume B., Granier C., Mieville A., Chin M., Pétron G. 2010. Comparison of global inventories of monthly CO emissions derived from remotely sensed data, Atmos. Chem. Phys. Discuss., 10, 17657-17697, doi:10.5194/acpd-10-17657-2010, 2010.

Tansey, K., Grégoire, J. M., Stroppiana, D., Sousa, A., Silva, J., Pereira, J. M. C., Boschetti, L., Maggi, M., Brivio, P. A., Fraser, R., Flasse, S., Ershov, D., Binaghi, E., Graetz, D., and Peduzzi, P. 2004. Vegetation burning in the year 2000: global burned area estimates from SPOT vegetation data, J. Geophys. Res., 109, D14S03, doi:10.1029/2003JD003598.

Tansey, K., Gregoire, J.M.C., Defourny, P., Leigh, R., Pekel, van Bogaert, E., Bartholomé, E., Bontemps, S. 2008. A new, global, multi-annual (2000-2007) burned area product at 1 km resolution and daily intervals. Geophysical Research Letters, vol. 35, L01401, doi:10.1029/2007GL031567

Viegas D.X., Pinol J., Viegas M.T., Ogaya R. 2001. Estimating live fine fuels moisture content using meteorologically-based indices, Int J Wildland Fires, 10, 223-240.

Wooster, M. J., Roberts, G., Perry, G. L. W. 2005. Retrieval of biomass combustion rates and totals from fire radiative power observations: FRP derivational and calibration relationships between biomass consumption and fire Radiative Energy Release, J. Geophysical Research, Vol 110, D24311.

Wooster, M.J., 2002. Small-scale experimental testing of fire radiative energy for quantifying mass combusted in natural vegetation fires, Geophysical Research Letters, 29(21) 2027.

Wu W, Lynch A.H., Drobot S., Maslanik J., McGuire A.D., Herzfeld U. 2007. Comparative Analysis of the Western Arctic Surface Climate with Modeling and Observations, Earth Interactions, 11, pp.24.

Yebra M., Chuvieco E., Riaño D. 2008. Estimation of live fuel moisture content from MODIS images for fire risk assessment. Agricultural and Forest Meteorology, volume 148, pp. 523-536.

FIRE OCCURRENCE ZONES FROM LOCAL TO GLOBAL SCALE IN THE MEDITERRANEAN BASIN: IMPLICATIONS FOR MULTI-SCALE FIRE MANAGEMENT AND POLICY

N. Koutsias[1], B. Allgower[2], K. Kalabokidis[3], G. Mallinis[4], P. Balatsos[5], J. G. Goldammer[6]

[1]Department of Environmental and Natural Resources Management, University of Ioannina, G. Seferi 2, GR-30100 Agrinio, Greece. nkoutsia@cc.uoi.gr; [2]Science City Davos, Rathaus, Berglistutz 1, CH-7270 Davos Platz, Switzerland. britta.allgoewer@wissensstadt.ch; [3]Department of Geography, University of the Aegean, University Hill, 81100 Mytilene, Greece. kalabokidis@aegean.gr; [4]Department of Forestry & Management of the Environment and Natural Resources, Democritus University of Thrace, Pantazidou 193, GR-68200 Orestiada, Greece. gmallin@for.auth.gr; [5]Ministry of Environment, Energy and Climatic Change , Special Secretariat of Forests, General Direction for Development and Protection of Forests and Natural Environment, Direction of Protection of Forests and Natural Environment, Department of Forest Fire Prevention & Suppression, Chalkokondili 31, 10164, Athens, Greece. pbalatso@yahoo.co ; [6]Global Fire Monitoring Center (GFMC), Max Planck Institute for Chemistry, c/o Freiburg University / United Nations University, Georges-Koehler-Allee 75, D-79110 Freiburg, Germany. fire@fire.uni-freiburg.de

Abstract

In 2007, Greece faced the worst natural disaster recorded in recent history as 67 people (fire-fighting personnel and civilians) lost their lives; and according to the Greek Fire Brigade, 189,952 ha of forested and agricultural lands were burned in the Peloponnese (south Greece). More recently, in February of 2009 more than 170 people died and 4,500 square kilometers were burned by wildfires in Australia. During the wildfires in Russia in 2010 more than 60 people were killed directly by fire, and the possible premature deaths due to heat and smoke effects in western Russia was probably in the magnitude of 55,000 people. The magnitude of the problem emphasizes the need to develop fire management strategies, and in particular efficient fire prevention policies and methods. Fire danger evaluation is a critical part of fire prevention, since fire planning resources require objective tools to monitor areas where a wildfire is more prone to occur. Based on this information, an optimization of the alternative fuel treatments, fire-fighting personnel dispatching, infrastructure development, etc. can be achieved. Many factors such as requirements, labour, specialized personnel, availability of necessary means, and usually limited economic recourses compete to optimize such efforts and actions.

The focus of this study is to present a method for multi-scale fire risk zoning in the Mediterranean basin. The proposed method is based on historical wildfire ignition observations and uses a kernel density estimation. Kernels have the advantage of directly producing density estimates that are not influenced by grid size and localization effects. Within this scheme, kernel density surfaces have been created and reclassified to construct fire risk zones from local to global scale in the Mediterranean Basin. Specifically, fire risk zones were created for the Eu-ropean scale (European Mediterranean Basin), for National scale (Greece), for regional scale (Peloponnese, Greece) and for local scale (Chalkidiki, Greece). For the evaluation of the value of fire risk zones, we compared the observed with the expected number of fires. In all cases, these numbers were statistically different, as devia-tions from the expected distributions towards the high risk zones indicated a successful assessment and value of fire risk zoning. In this paper, we further discussed the value of these risk zones for multi-scale fire management and fire policy.

Keywords: kernel density interpolation, fire mapping, fire management and policy, Mediterranean

Introduction

In 2007, Greece faced the worst natural disaster recorded in recent decades as 67 people (fighting personnel and other civilians) lost their lives and according to Hellenic Fire Brigade 189,952 ha of forested and agricultural areas was burned in the Peloponnese (south Greece). More recently, in February 2009 more than 170 people died and 4500 square kilometers were burned by wildfires in Australia. During the wildfires in Russia in 2010 more than 60 people were killed directly by fire, and the possible premature deaths due to heat and smoke effects in Western Russia was possibly in the magnitude of 55,000 people (Goldammer 2010, 2011). The

magnitude of the problem sets up the need to develop fire management strategies and in particular efficient fire prevention policies and methods. Fire danger evaluation is a critical part of fire prevention, since pre-fire planning resources require objective tools to monitor areas where a fire is more prone to occur (Chuvieco et al. 2009). Based on this information an optimization of the alternative fuel treatments, fire-fighting personnel distribution, infrastructure development etc. can be achieved.

Precise detection of the actual ignition points is difficult and the recorded fire ignition locations contain positional inaccuracies, due to fire characteristics and logistic problems. Positional as well as attribute uncertainties may result from factors such as small-scale or inaccurate, non-updated maps used to read the x and y coordinates or large interval resolutions (e.g., coordinates given only in degrees and minutes) (Koutsias et al. 2004). If the aim is to explain the spatial pattern of landscape fire regimes and/or the underlying causal factors these inaccurate point records may introduce substantial errors. Especially, if explanatory variables are extracted from other geo-referenced data layers using spatial overlay techniques, these records may lead to serious inaccuracies.

In our study, fire risk zoning is implemented by using the kernel density estimation in an attempt to overcome information loss and aggregation constraints (Bailey and Gatrell 1995). In addition, definition of fire risk zones based on fire occurrence density mapping could allow more effective communication with decision makers and improved public information dissemination.

Kernel density estimation

Kernel density has been originally introduced in wildfire occurrence mapping by Koutsias et al. (2004), as a method to address the inherent positional inaccuracies of recorded wildland fire ignition points. The basic principle of this concept is the assumption that wildland fire ignition points do not constitute exact point locations but fuzzy ones that define a broader area, where the actual point location lies inside. De Riva et al. (2004) and Amatulli et al. (2007), further extended the utility of the developed concept in wildfire research.

An important issue, however, and rather difficult to define when implementing kernel density interpolation, is the choice of the smoothing parameter of the kernel. Narrow bandwidths allow nearby observations to dominate the density estimate, while wide bandwidths favor distant locations (Seaman and Powell 1996; Worton 1989). According to Silverman (1986), the choice of the bandwidth depends mostly on the purpose for which the density estimate is used. If the aim is to explore the data and suggest models and hypotheses about them, it would be sufficient to choose the smoothing parameter subjectively by visual inspection.

Materials and Methods

1.1 *Study area and fire observations*

To apply and explore the kernel density interpolation in fire risk zones assessment we established four study cases corresponding to four different study scales. The European Mediterranean Basin for the global scale, Greece for the National scale, Peloponnese (Greece) for the regional scale and Chalkidiki (Greece) for the local scale. The fire database consists of

the fire ignition points occurred between 1985 and 1995 in Greece as well as the number of fires occurred in municipality level in European Mediterranean countries between 1990 and 2000. The latter data come from the SPREAD[2] project. For the Greek database the fire events with x and y coordinates have been recorded in latitude and longitude using degrees and first minutes resulting in positional uncertainty of about ±700 to ±925 meters in x and y axes.

1.2 *Methods*

To implement kernel density estimation in fire risk zoning, the fixed mode approach has been adopted in order to keep the smoothing parameter of the kernel constant over the entire study area. The incentive behind this decision was to avoid different treatments of the point observations over the areas with different degrees of concentration. In addition to the choice of the kernel type, which might not be so important, the choice of the smoothing parameter is very crucial since it controls the amount of variation of the estimates (Worton 1989). To define the size of the bandwidth the mean nearest distance of fire ignition points was considered. Kernel density interpolation was applied also to control points established using random design sampling restricted by the constraint of distance. Since, the kernel density estimation of control points refers to points, where no fires have been observed, the estimation was inverted to a negative scale by multiplying the original densities times the value of -1. The inversion to a negative scale preserves the general shape of the data distribution with a mirror effect, however. Finally, the kernel density estimates of both, the fire ignition events and the control points, were combined into one layer using spatial overlay functions.

Results

The kernel density surfaces of both, fire ignition points and control points, were reclassified to create fire risk zones using the criterion of "equal areas" (Figure).

For the evaluation of the value or fire risk zones we compared the observed with the expected number of fires. In all cases these numbers are statistical different while the deviations from the expected distribution towards the high risk zones indicates a successful assessment and value of fire risk zones.

Discussion

Fire fighting organizations design and implement operational projects to successfully face forest fires for prevention, forecast and suppression. Many factors such as availability of labor, specialized firefighter personnel, availability of technical firefighting resources, and usually limited economic recourses compete to optimize such efforts and actions. Wildland fire risk zoning helps to orient *a priori* the managers towards proper action for forest fire and civil protection. Fire risk zoning might be a strategic operational advantage for the proper development of a Decision Support System, since such actions can be applied with priority (spatial and temporal) inside the zones of high risk. Reduction of the necessary costs and maximization of the benefits and outcomes can be considered. Fire risk zoning based on

---

[2] EC project 'Forest Fire Spread and Mitigation (SPREAD), EC-Contract Nr. EVG1-CT-2001-00027, and the Federal Office for Education and Science of Switzerland (BBW), BBW-Contract Nr. 01.0138

historical fire observations can contribute further for the proper and documented use and distribution of available resources. The diachronic value of those fire risk zones is a challenge and on the same time a requirement so that to become a real strategic operational tool for prevention and suppression. Our results can be used at the Euro-Mediterranean level by policy-makers and at national, regional and local scales by national public bodies, planners and managers to prioritize projects and investments to reduce wildfire risk and manage fire prone areas.
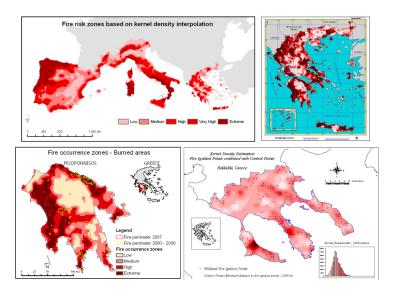
Figure 1. Fire risk zones in a. European Mediterranean scale b. national scale in Greece, c. regional scale in Peloponnese, Greece and d. local scale in Chalkidiki, Greece

| a. Mediterranean | b. Greece | c. Peloponnese |
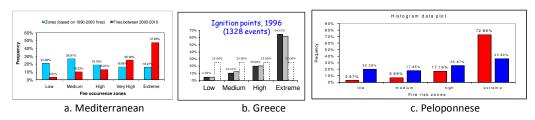
Figure 2. Evaluation statistics.

At local scale fire risk zoning could be used as part of a Decision Support System for vegetation and fuels treatment, wildland fire early warning, development of fire management plans, etc..

At national scale fire risk zones could be used as a standard component of a daily, national scale fire risk index. Also, the distribution of fire risk could be used for spatial allocation of human and economic resources throughout the year, for planning and regional development as well as for implementing environmental policies and laws and educational activities.

At Euro-Mediterranean scale, risk zoning could serve first of all as means for the establishment of inter-national forest fire information systems. Also, fire risk zones could indicate regions where common awareness raising campaigns and scientific and research networks and institutions should be introduced. EU member states could introduce new rural policies and regulations or modify existing ones (i.e. subsidies policies of Common Agricultural Policy) in

regions highly threatened by forest fires. Also, the fire risk zone information could be used as part of a financing instrument which could promote transboundary collaboration between countries in fire management.

References

Amatulli, G., Peréz-Cabello, F., De la Riva, J. 2007. Mapping lightning/human-caused wildfires occurrence under ignition point location uncertainty. Ecological Modelling 200: 321-333

Bailey, T.C., Gatrell, A.C. 1995. Interactive Spatial Data Analysis. Essex: Longman Scientific & Technical

Chuvieco, E., Aguado, I., Yebra, M., Nieto, H., Salas, J., Martín, M.P., Vilar, L., Martínez, J., Martín, S., Ibarra, P., de la Riva, J., Baeza, J., Rodríguez, F., Molina, J.R., Herrera, M.A., Zamora, R. 2009. Development of a framework for fire risk assessment using remote sensing and geographic information system technologies. Ecological Modelling 221: 46-58

Goldammer, J.G. 2010. Preliminary Assessment of the Fire Situation in Western Russia. Analysis of 15 August 2010. presented at the State Duma, Moscow, 23 September 2010. International Forest Fire News No. 40, 2-23. Online publication: http://www.fire.uni-freiburg.de/intro/about4_2010-Dateien/GFMC-RUS-State-DUMA-18-September-2010-Fire-Report.pdf and

Goldammer, J.G. 2011. Wildland Fires and Human Security: Challenges for Fire Management in the 21st Century. In: Proceedings of the International Forest Fire Symposium Commemorating the International Year of Forests 2011, Sol Beach, Gangwon-do, Republic of Korea, 7-8 June 2011, p. 36-49. Korea Forest Research Institute, Seoul, Korea, 461 p. – Online publication: http://www.fire.uni-freiburg.de/GlobalNetworks/Northeast-Asia/Korea-Fire-Symposium-2011-Proceedings.pdf

de la Riva, J., Pérez-Cabello, F., Lana-Renault, N., Koutsias, N. 2004. Mapping forest fire occurrence at a regional scale. Remote Sensing of Environment 92: 363-369

Koutsias, N., Kalabokidis, K.D., Allgöwer, B. 2004. Fire occurrence patterns at landscape level: beyond positional accuracy of ignition points with kernel density estimation methods. Natural Resource Modeling 17: 359-375

Seaman, D.E., Powell, R.A. 1996. An evaluation of the accuracy of kernel density estimators for home range analysis. Ecology 77: 2075-2085

Silverman, B.W. 1986. Density Estimation for Statistics and Data Analysis. London, England: Chapman and Hall

Worton, B.J. 1989. Kernel methods for estimating the utilization distribution in home-range studies. Ecology 70: 164-168

MODELLING FIRE OCCURRENCE FACTORS IN SPAIN. NATIONAL TRENDS AND LOCAL VARIATIONS

J. Martínez-Fernández[1], N. Koutsias[2]

[1]*Forest Research Center, INIA (National Institute for Agricultural and Food Research and Technology), Carretera de La Coruña, Km. 7,5 28040 Madrid. Spain. martinez.jesus@inia.es*
[2]*Department of Environmental and Natural Resources Management, University of Ioannina, G. Seferi 2, GR-30100 Agrinio, Greece. nkoutsia@cc.uoi.gr*

Abstract

In this study we compared global and local models to identify driving factors of occurrence of human-caused forest fires in Spain. The number of human-caused fires occurred within a 25 years period (1983-2007) were computed for each one of the 7.638 municipalities of the Spanish peninsula that were analyzed. We created a binary variable (fire/no fire) to develop logistic models, and a continuous variable (log transformed fire density to account for normality) to build linear regression models. For the linear regression, we selected 6.993 municipalities in which one or more fires were registered during the study period. The independent variables are composed by socio-economic and demographic indicators together with land cover and agricultural statistics. The 29 of those variables were compiled from a previous study while 6 new variables were introduced referring to topographic and climatic parameters.

The binary logistic model, which estimates the probability of having or not a fire, classified successfully 76.4% of the total observations. Nine explanatory variables were identified as critical by the analysis, while the most influ-enced variables were the forest surface, population decrease and forest-cultivated land interface. Mean annual precipitation and mean summer temperature were also important. For the linear regression that has been used to explain long-term fire density patterns, 12 of the original variables was selected after a stepwise process which explain 53% of the variation of the dependent variable (adjusted R2 0.53). Among them mean annual precipita-tion, density of agricultural properties, mean altitude, population decrease and non tree-covered forest surfaces seem to be the most important ones. Only 2 variables (precipitation and population decrease) were common by both modeling approaches. In addition to forest properties and climatic variables, our results confirm the im-portance of variables related with agrarian activities, land abandonment, rural exodus and development processes, as underlying factors of fire occurrence.

To overcome the constraints of these traditional global regression models (linear and logistic) which assume sta-tionary processes, we applied geographically weighted regression (GWR) models using the same independent variables previously selected, both for the linear and the logistic approach. The GWR logistic model, using a fixed bandwidth of 209 km, selected by an automatic process based on AICc minimization, classified correctly 80.00% of the observations while the deviance (-2Log Likelihood) improved from 3431.2 to 3261.4. For the line-ar approach, the explanatory power of the OLS model increased from 53% to 67% in the case of an adaptive GWR linear model, using a bandwidth of 1300 nearest neighbors, and 62%, in the case of a fixed GWR using a bandwidth of 154 km. Apart from these slight fitting improvements of the models, local approaches like GWR seems to be a valuable approach for exploring non-stationary relationships between the response and explanatory variables. In fact, the results of a Monte Carlo test on the local estimates indicate that there is significant spatial variation in the local parameter estimates for all the variables. These local coefficients were mapped in order to better understand local variations of the fire occurrence causal factors in Spain.

Keywords: Fire occurrence, Fire Factors, Geographically Weighted Regression, Logistic Regression, OLS Regression

Introduction

In fire occurrence modeling, regression techniques are applied frequently at several scales (Vega-García et al., 1995; Vasconcelos et al, 2001;Martínez et al., 2009), assuming that the model parameters are valid for the entire study area from which the data are sampled.

However, especially when the geographical extent of the study area is large it would be more reasonable to find varied rather than constant relationships. Koutsias et al. (2010) observed that the explanatory power of traditional regression (linear or logistic) increased considerably when it assumed varying relationships instead of constant ones, because region-specific factors might affect fire occurrence patterns locally.

In this study, carried out with Spanish data, we built predictive models at national scale using classical regression, both linear Ordinary Least Squares (OLS) and binary logistic regression, and both were compared with local models based on Geographically Weighted Regression (GWR). Specifically, the objectives of the analysis are to identify the main driving factors of human-caused forest fires in Spain and to explore which factors or variables vary spatially. We hypothesize that some region-specific factors deviate from global or national trends.

Materials and Methods

1.1   *Study Area and Database*

The independent variables used in the analysis are composed by socio-economic and demographic indicators together with agricultural and land cover statistics. The 29 of those variables were compiled from a previous study (Martínez et al., 2009) while 6 new variables were introduced referring to topographic (mean altitude and slope), climatic parameters (summer temperature and mean annual precipitation) and forest vegetation (forest surface and non tree-covered forest surfaces), selected after an analysis to avoid multi-collinearity. All the variables were compiled at municipality level for the Spanish peninsula.

The number of human-caused fires occurred within a period of 25 years (1983-2007) were computed for each one of the 7.638 municipalities that were analyzed, with the exception of the region of Navarre. We created a binary variable (fire/no fire) to develop logistic models, and a continuous variable (log transformed fire density to account for normality) to build linear regression models. For the linear regression, we selected 6.993 municipalities in which one or more fires were registered during the study period.

1.2   *National models using classical regression*

We used different regression methods to obtain predictive models of ignition. OLS linear regression has been used to explain long-term fire density patterns, using only a database with 6.993 municipalities. Despite the fact that the distribution of the dependent variable indicates a negative binomial or a Poisson model as most appropriated, we used a linear model after applying a logarithmic transformation to the dependent variable to convert their values to an approximate normal distribution.

Additionally, as a complement of the fire density model, a binary logistic model tries to estimates and explains the probability of having or not a fire. Logistic regression is one of the most popular mathematical modeling approaches than has been used successfully in similar studies. The assumption of multivariate normality is not presupposed in logistic regression.

Cut-off points in binary logistic regression are used to convert probability of ignition to dichotomous 0-1 data. Cases with predicted values that exceed the classification cutoff are classified as positive (fire), while those with predicted values smaller than the cutoff are

classified as negative (no fire). In order to select the optimal cut-off point we constructed tables with classification error rates for varying cut-off points, computing for each one two statistics: sensitivity and specificity. Sensitivity is the proportion of true positives that were predicted as fire and specificity is the proportion of true negatives that are predicted as no fire. The optimal cut-off point corresponds to the intersection of the two lines, in which sensitivity and specificity are equal (Vasconcelos et al, 2001). Figure 1 show the calculation of the statistics, being the best cut-off point in this case 0.91.

The final multivariate models were obtained in SPSS using automatic stepwise forward procedures for variable selection in combination with manual modification or selection using "introduce method". In all cases we checked for potential collinearity problems of the selected variables calculating the correlation matrix and other common statistical tests such as the tolerance coefficient, the variance inflation factor (VIF) and eigenvalue analysis. In the case of logistic model we selected a stepwise model with 10 variables, but after collinearity analysis we removed the variables "slope" and "population occupied in agriculture" and we introduced the variable "agricultural areas but with significant areas of natural vegetation". In the case of OLS model we selected with stepwise a model with 9 variables, but in a second process we introduced manually another 3 variables of interest (decrease in number of owners of agrarian holdings, % owners of agrarian holdings >55 years and density of agricultural machinery), so the final model has 12 variables. Models have been built using standardized Z scores for dependent and independents variables.

To evaluate the influence of individual variables in the models, several criteria were computed and analyzed globally; (i) a simple calculation of the standardized coefficients according to Menard (2010 p.89), (ii) the t statistic and its level of significance, but in the case of the logistic regression we used the Wald statistic, (iii) the step at which the variable was input into the model, (iv) the change in the R^2 when the variable was removed from the model (the greater the change, the more important the variable). In the case of logistic regression we used the change in logarithm of likelihood (-2LL), (v) only in the case of logistic, the Odds ratio or the exponential of the logit coefficient B (Exp(B)).

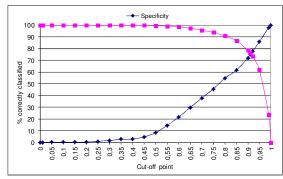Figure1. Sensitivity and specificity graphs of the binary logistic model for select optimal cut-off point

1.3 Local models using GWR

Traditional statistical methods like logistic and linear regression assume independent observations, spatial stationarity and no autocorrelation. To overcome these limitations we applied GWR models using the same independent variables previously selected, both for the

linear and the logistic approach. GWR considers that the relationships between the response and explanatory variables vary in space according to their location and allows local variations to be taken into account. At each data point, GWR fits a regression model by weighting all observations from that point as a function of distance. GWR adopt a kernel function controlled by the bandwidth size of the kernel to implement this geographical weighting. In our study, we used both the adaptive (nearest neighbors) and the fixed (distance) kernel types, while the minimization of the corrected Akaike Information Criterion (AICc) served to determine the bandwidth size. We used GWR 3.0.1 software for Windows (Fotheringham et al., 2002).

Results

National Models

The binary logistic model classified successfully 76.4% of the total observations. Nine explanatory variables were identified as critical by the analysis, while the most influenced variables were the forest surface, population decrease and forest-cultivated land interface. Mean annual precipitation and mean summer temperature were also important (Table 1). For the linear regression 12 of the original variables was selected after a stepwise process which explain 53% of the variation of the dependent variable (adjusted R^2 0.53). Among them mean annual precipitation, density of agricultural properties, mean altitude, population decrease and non tree-covered forest surfaces seem to be the most important ones. Only 2 variables (precipitation and population decrease) were common in both approaches. In addition to forest properties and climatic variables, our results confirm the importance of variables related with agrarian activities, land abandonment, rural exodus and development processes (Moreira et al., 2011).

GWR models

The GWR logistic model, using a fixed bandwidth of 209 km, selected by an automatic process based on AICc minimization, classified correctly 80.00% of the observations while the deviance (-2Log Likelihood) improved from 3431.2 to 3261.4. For the linear approach, the explanatory power of the OLS model increased from 53% to 67% in the case of an adaptive GWR linear model, using a bandwidth of 1300 nearest neighbors, and 62%, in the case of a fixed GWR using a bandwidth of 154 km.

Table 1. Results of the sensitivity analysis for logistic model: ranking of influence of the input variables (the lower the ranks, the more important)

Variable Name	(i) Std. Coef. B	(ii) Wald	(iii) Stepwise	(iv) Change in -2LL	(v) Exp(B)	Global Score (sum)	B_Std	Wald	Stepwise	Change in -2 LL	Exp(B)
FOR_P	1	1	1	1	3	4	0,979	160,661	1	200,84	1,034
DIS_50_91	3	2	2	2	4	9	0,588	89,756	2	98,27	1,021
ICFSUP_P	4	4	3	3	2	14	0,506	55,005	3	59,71	1,104
NOGES_PF	6	3	4	4	7	17	0,327	58,114	4	55,47	1,011
T_SU	5	6	7	6	1	24	0,687	40,574	6	48,09	1,003
P_A	2	5	6	5	8	18	0,386	37,395	7	38,58	1,171
DIS_SAU	7	7	5	7	6	26	0,247	23,797	5	22,09	1,012
CL21_PM	8	9	9	9	5	35	-0,155	17,730	8	18,54	1,000
POT_DEN	9	8	8	8	9	33	0,163	7,422	9	8,59	1,015

Regional-local variations

The results of a Monte Carlo test on the local estimates indicate that there is significant spatial variation in the local parameter estimates for all the variables. These local coefficients were mapped in order to better understand, in the subsequent analysis, local variations of the fire occurrence causal factors in Spain (Figure 2). Negative coefficients were mapped with cold colors (green to blue) and positive with warm colors (orange to red).
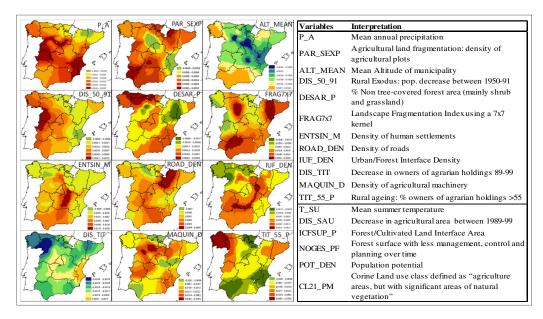

Variables	Interpretation
P_A	Mean annual precipitation
PAR_SEXP	Agricultural land fragmentation: density of agricultural plots
ALT_MEAN	Mean Altitude of municipality
DIS_50_91	Rural Exodus: pop. decrease between 1950-91
DESAR_P	% Non tree-covered forest area (mainly shrub and grassland)
FRAG7x7	Landscape Fragmentation Index using a 7x7 kernel
ENTSIN_M	Density of human settlements
ROAD_DEN	Density of roads
IUF_DEN	Urban/Forest Interface Density
DIS_TIT	Decrease in owners of agrarian holdings 89-99
MAQUIN_D	Density of agricultural machinery
TIT_55_P	Rural ageing: % owners of agrarian holdings >55
T_SU	Mean summer temperature
DIS_SAU	Decrease in agricultural area between 1989-99
ICFSUP_P	Forest/Cultivated Land Interface Area
NOGES_PF	Forest surface with less management, control and planning over time
POT_DEN	Population potential
CL21_PM	Corine Land use class defined as "agriculture areas, but with significant areas of natural vegetation"

Figure 2. Local coefficients for adaptive GWR lineal model using a bandwidth of 1300 nearest neighbors

Conclusions

Apart from some of the slight fitting improvements of the models presented in this study, local approaches like GWR, an alternative to global regression modeling, seems to be a valuable complement for exploring non-stationary relationships between the response and explanatory variables and thus to better understand changes in spatial resolution and scale, possible regional variations and other spatial processes in wildland fire occurrence. All factors analyzed show significant spatial variations in Spain.

References

Fotheringham, A. S., Brunsdon, C., and M. Charlton, 2002. Geographically WeightedRegression: The Analysis of Spatially Varying Relationships, New York, NY: JohnWiley & Sons, 269 pp.

Koutsias, N., Martínez-Fernández, J; Allgöwer, B. 2010. Do factors causing wildfires vary in space? Evidence from geographically weighted regression.GIScience & Remote Sensing. Volume 47, Number 2, 1548-1603

Martínez, J., Vega-García, C., and Chuvieco. E. 2009. Human-Caused Wildfire RiskRating for Prevention Planning in Spain," Journal of Environmental Management,90(2):1241–1252.

Menard, S.W. 2010.Logistic regression: From introductory to advanced concepts and applications. London. Ed. SAGE.377 pp.

Moreira, F., Viedma, D., Arianoutsou, M., Curt, T., Koutsias, N., Mouillot, F., Vaz, P., Barbati, A., Co-rona, P., Rigolot, E., Xanthopoulos, G., Bilgili, E. 2011. Landscape - wildfire interactions in Southern Europe: implications for landscape management. Journal of Environmental Management 92: 2389-2402

Vasconcelos, M.J.P., Silva, S., Tome, M., Alvim, M., Pereira, J.M.C. 2001. Spatialprediction of fire ignition probabilities: comparing logistic regressionand neural networks. Photogrammetric Engineering and Remote Sensing 67,73–8

Vega-García, C., Woodard, P., Titus, S. J., Adamowicz, W. L., and B. S. Lee. 1995. A Logit Model for Predicting the Daily Occurrence of Human-Caused ForestFires," International Journal of Wildland Fires, 5(2):101–111.

THE ROLE OF REMOTE SENSING IN THE IMPLEMENTATION OF LEBANON'S NATIONAL STRATEGY FOR FOREST FIRE MANAGEMENT

G. H. Mitri[1], I. Z. Gitas[2]

[1]*Biodiversity Program, Institute of the Environment, University of Balamand; Faculty of Sciences, University of Balamand - P.O.Box: 100, Tripoli, Lebanon. george.mitri@balamand.edu.lb*
[2]*Laboratory of Forest Management and Remote Sensing, School of Forestry and Natural Environment, Aristotle University of Thessaloniki, Thessaloniki, Greece. igitas@for.auth.gr*

Abstract

Among the factors that threaten the forests in Lebanon, fire constitutes the most dangerous one and causes severe ecological and economic losses and, sometimes, human injuries and death. Recently, a National strategy for forest fire management was developed and endorsed by the Lebanese Council of Ministers. The aim of the Strategy is to reduce the risk of intense and frequent forest fires whilst allowing for fire regimes that are socially, economically and ecologically sustainable. The Strategy acknowledged that decisions about fire management are best made within a risk-management framework, known as the 5Rs, namely (1) Research, information and analysis; (2) Risk modification, including fire vulnerability reduction and prevention of harmful fires; (3) Readiness, covering all provisions intended to improve interventions and safety during a fire event; (4) Response, including all means of intervention for fire suppression; and (5) Recovery, including the rehabilitation and ecological restoration of healthy forest conditions, and the support to individuals and communities in the short- and medium term aftermath of the fire. Although satellite remote sensing is reported to be an effective tool for conducting different studies related to forest fire management, only a small number of them have been conducted in Lebanon. The aim of this work was define which satellite remote sensing applications can help in forest fire management in Lebanon by identifying the role of remote sensing in each of the previously mentioned components, i.e. the 5Rs. The methodology of work included reviewing all items under each strategic component to define priorities in the implementation of remote sensing in the different phases of fire management. The work included a presentation of operational examples from the Mediterranean illustrating the practical use of remote sensing within a strategic framework. Overall, the review of literature proved that remote sensing can provide very useful support to fire managers and planners who are involved in the implementation of the Strategy. It is expected that the use of remotely sensed information will result in improved fire management at both levels, local and National.

Keywords: Remote Sensing, forest fire management, National Strategy, the Mediterranean

Introduction

Forests in Lebanon are a unique feature in the arid environment of the Eastern Mediterranean. Increasingly, Lebanon's forests, which include remnants of valuable broad-leaved trees, conifer forests and evergreen trees that cover the Lebanese mountains in patches, are exposed to degradation due to urbanization, pests and diseases, fires, wars, climate change, human neglect, improper management, outdated laws, and poor law enforcement (Mitri 2009). Like other Euro-Mediterranean countries, forest fires have been especially damaging Lebanon in recent years, representing one of the most important elements that destroy Lebanon's natural resources (Mitri and Elhajj 2008).

Recently, the fires in Lebanon have harvested large green areas, noting that the percentage of forest cover has declined in a short period of time in Lebanon in recent years to 13% of its total area (MOE/UNDP/ECODIT 2011), after it had constituted around 35% in the years 1960-1965. This has given rise to concern at the national and international levels resulting from the risk of loss to forest cover. Despite the increased efforts, fire issues increasingly threaten forest

ecosystems and economic development in Lebanon. Reports accuse increases in fire frequency and severity; thus, affecting tree growth and survival as well as yield and quality of wood and non-wood forest products, wildlife habitat and the recreational, scenic, environmental and cultural value of forests. Serious fires can also cause human injuries, death, and losses in properties.

Most recently, a National strategy for forest fire management was developed and endorsed by the Lebanese Council of Ministers (Mitri 2009). The aim of the Strategy is to reduce the risk of intense and frequent forest fires whilst allowing for fire regimes that are socially, economically and ecologically sustainable. The Strategy acknowledges that decisions about fire management are best made within a risk-management framework, known as the 5Rs, namely, (1) Research, information and analysis; (2) Risk modification, including fire vulnerability reduction and prevention of harmful fires; (3) Readiness, covering all provisions intended to improve interventions and safety in the event of fire; (4) Response, including all means of intervention for fire suppression; and (5) Recovery, including the rehabilitation and ecological restoration of healthy forest conditions, and the support to individuals and communities in the short- and medium term aftermath of the fire.

The implementation of the Strategy requires strengthening the capacity of the concerned authorities in order to address the different issues related to forest fires. However, Lebanon lacks the necessary technological measures and management capacities to address a number of measures related to fire management including monitoring, prediction (early warning), preparedness, prevention, suppression and restoration. Also, experience has shown over a number of years that forest fire reporting systems in Lebanon are weak and do not reflect the reality of the problems.

Although Remote Sensing (RS) is reported to be an effective tool for conducting different studies related to forest fire management (Chuvieco 2009), only a small number of them have been conducted in Lebanon. Today, the development of new remote sensing instruments provides an opportunity to advance studies and researches on forest fire management in Lebanon.

The aim of this work was define which RS applications can help in forest fire management in Lebanon by identifying the role of RS in each of the previously mentioned components, i.e. the 5Rs. The methodology of work involved reviewing all items under each strategic component to define priorities in the implementation of RS in the different phases of fire management. The work included the presentation of operational examples from the Mediterranean illustrating the practical use of remote sensing within a strategic framework.

1.1 *Potential use of Remote Sensing in the National Strategy*

Satellite remote sensing data and techniques are used in all the phases of wildland fire monitoring at the regional and national levels in a number of European Mediterranean countries. The use of RS in forest fire management has been a relevant research topic of several European Union research projects in the last 15 years (e.g. MEGAFIRES, SPREAD, EUFIRELAB, among others). Other EU funded projects such as PREVIEW and RISK-EOS aimed at providing operational use of existing methodologies in the context of the Global Monitoring for Environment and Security (GMES) joint initiative of the European Commission and the

European Space Agency. This section included 1) a general review of all items under each component of Lebanon's National Strategy for forest fire management, and 2) an identification of the role of satellite Remote Sensing in each component.

1.2 *Research, Information and Analysis*

The strategic objective of this component is to support and promote the improvement, know-how sharing, monitoring and dissemination of knowledge on fire ecology, fire management and post-fire vegetation dynamics among all relevant actors (science/research, policy makers, land managers, grassroots' groups), bridging science and traditional knowledge. In general, satellite remote sensing can provide valuable data for "Research, Information and Analysis" in fire management. This includes 1) the development of effective fire monitoring systems, 2) the development of daily danger indices based on vegetation types, and thus, developing a comprehensive danger-rating system (Chuvieco and Salas 1996, Camia et *al*. 2006), and 3) development of an annual comprehensive database on forest fires for analytical use (Barbosa et *al*. 2006, San-Miguel-Ayanz et *al.* 2009, Camia et *al.* 2010). The European Forest Fire Information System (EFFIS) provides standardized European forest fire danger forecast and burned area maps for the EU Mediterranean region (San-Miguel-Ayanz et *al.* 2009). The system RISICO (RISchio Incendi & COordinamento) which involves remote sensing data has been used since 2003 by the Italian National Civil Protection for daily dynamic forest fire risk assessment (D'Andrea et *al*. 2008). In Greece, a daily forest fire risk map involving up-to-date satellite data of vegetation greenness is published by the civil protection (Gitas et *al.* 2004).

1.3 *Risk modification (fire vulnerability reduction and prevention of harmful fires)*

The strategic objective of this component is to develop effective measures intending to reduce fire vulnerability, to increase ecological and social resilience to fire, and to prevent the occurrence of harmful fires and unsustainable fire regimes. Remote sensing is considered a useful tool for sustaining prevention activities (Chuvieco 2009). Remote sensing proved to provide valuable data on type (e.g. distribution and amount of fuels) and status of vegetation in a consistent way and at different spatial and temporal scales (Riano et *al.* 2002, Arroyo et *al.* 2006, Lasaponara et *al*. 2006, Lasaponara and Lanorte 2007). Also, satellite remote sensing proved to assist in the detailed analysis of forests status and the improvement of pre-fire management plans (Hernandez-Leal et al. 2006).

1.4 *Readiness or pre-suppression*

The strategic objective of this component is to undertake all possible provisions by individuals, communities and fire and land management agencies to be prepared before a fire event occurs, and improve interventions and safety in monitoring the probability of fire and detecting the event of fire. Satellite remote sensing data has contributed to the conduction of a proper distribution at the landscape level of fire control infrastructures such as fire lookout towers (Nogueira et *al.* 2002, Catry et *al.* 2007), water reservoirs, forest strips with low tree density and low shrub cover, fire break areas of first and second level, forest tracks with fire break lines along them, and protection perimeters in urbanized areas (Chuvieco and Salas 1996, Jaiswal et *al* 2002).

1.5 *Response*

The strategic objective of this component is to quickly suppress and limit the extension of fires through the development of methods and techniques coupled with appropriate material and very well trained personnel. Satellite remote sensing has helped in the development of fire behaviour models and/or combustibility models to allow fire-fighting brigades to better predict the fires and better manage them, thus avoiding the expansion of fires (Dimitrakopulos 2002, Stergiadou et *al*. 2007). Also, spatial information such as, the vegetation cover density and the location and defensible space of buildings, can contribute to the improvement of forest fire suppression planning. Satellite remote sensing are tools that can be implemented to extract, store and process relevant information (Tsakalidis and Gitas 2007). In Spain, the EMERCARTO mapping viewer involving satellite remote sensing data proved to be a powerful GIS tool for the optimization and control of resources during forest fire suppression (Aguirre et *al.* 2007). Today, Lebanon is in the process of developing a similar system. Also, it is possible for Lebanon like other countries to submit official requests to the International Space Charter which can provide available data from a series of satellites such as RADARSAT, ERS, EMVISAT, SPOT, LANDSAT, and DMC in order to obtain data and information on a disaster occurrence.

1.6 *Recovery, Post-fire Management and Rehabilitation*

The strategic objective of this final component is to provide support for individuals and communities in the immediate aftermath of the fire as well as in the medium and longer term efforts of community and economic renewal, and restore healthy ecological conditions of burned forest land to facilitate the natural recovery of vegetation and increase forest resilience against future fires. Remote sensing satellite data has previously assisted in 1) mapping fire affected areas and assessing the impact of fire on different vegetation types (Mitri and Gitas 2004), 2) mapping fire type (Mitri and Gitas 2006) and fire severity (Mitri and Gitas 2008, Gitas et *al*. 2009). Also, remote sensing data has helped in implementing activities aiming at the reduction of soil erosion, and mapping forest regeneration and vegetation recovery (Diaz-Delgado et *al*. 2003, Twele and Barbosa 2004, Hernandez-Clemente et *al*. 2009, Gouveia et *al.* 2010, Mitri and Gitas 2010, Vila and Barbosa 2010, Gitas et *al.* 2011, Veraverbeke et *al*. 2011) for the development of post-fire active restoration/rehabilitation activities (forest landscape restoration). Eventually, RS data contributed to the development of national reporting systems based on fire statistics, expanding national databases on forest fires, their occurrence, and the ecosystems where they occur (Viedma et *al.* 1997, Roder et *al*. 2008). For instance, Portugal has an operational system for mapping burned areas from satellite remote sensing imagery (Pereira and Santos 2003, San-Miguel-Ayanz et *al*. 2009).

Conclusions

The review of the literature proves that satellite remote sensing can provide very useful support to fire managers and planners who are involved in the implementation of Lebanon's National strategy for forest fire management. However, there are many factors that should be taken into account to decide on which of the different operational RS applications in the forest fire sector should be given a priority in Lebanon. Such factors include the degree of maturity to acquire,

pre-process and process satellite data, the existing level of expertise, the capability to disseminate results in an efficient way, and the availability of financial resources.

Accordingly, priorities for use of RS applications in the different phases of fire management can be focused on 1) advancing current academic and public research for the development of a national forest fire monitoring system and daily danger indices with the use of RS data, 2) producing accurate maps showing the distribution and amount of forest fuels at the national level, 3) developing proper forest management plans and infrastructure, 4) optimizing and controlling resources during forest fire suppression, and 5) expanding the national databases on forest fires, their occurrence, their locations, and their impact on the vegetation cover.

It is expected that the use of remotely sensed information and techniques in each of the Strategy's components will result in strengthened capacities of public authorities and units involved in forest fire management (mainly, the Central Operations Room of forest fire management which is currently managed by the Directorate of Civil Defence, the General Directorate of Environment, and the Directorate of Rural Development and Natural Resources at the Ministry of Agriculture).

References

Arroyo, L., Healy, S., Cohen, W. and Manzanera, J. 2006. Using object-oriented classification and high-resolution imagery to map fuel types in a Mediterranean region. Journal of Geophysical Research 11: 1-10.

Aguirre, F., Fernandez, J., Aragoneses, D., Gomez, R, Quesada, C., Alferez, C. 2007. Herramientas para la gestión de la extinción de incendios forestales. Visor de cartografía para Emergencias: EMERCARTO. International Wildland Fire Conference, Seville, Spain, 13-17

Barbosa, P., Kucera, J., Strobl, P., Vogt, P., Camia, A., San-Miguel-Ayanz, J., 2006. European forest fire information system (EFFIS) - rapid damage assessment: appraisal of burnt area maps in southern Europe using modis data (2003 to 2005), Proceedings of the 5th International Conference on Forest Fire Research, 27-30, Portugal.

Camia, A., Barbosa, P., Amatulli, G., San-Miguel-Ayanz, J., 2006. Fire danger rating in the European Forest Fire Information System (EFFIS): current developments. Proceedings of the 5th International Conference on Forest Fire Research, 27-30 Figueira da Foz, Portugal, Elsevier.

Camia, A., Durrant, T., San-Miguel-Ayanz, J. 2010. The European Fire Database: development, structure and implementation. In: Viegas D.X. (Ed.) VI International Conference on Forest Fire Research, Coimbra.

Catry, F.X., Rego, F.C., Santos, T., Almeida, J and Relvas, P. 2007. Forest fires prevention in Portugal-Using GIS to help improving early fire detection effectiveness, Wildfire 2007, Seville, Spain.

Chuvieco, E. 2009. Earth Observation of Wildland Fires in Mediterranean Ecosystems. Springer Heidelberg Dordrecht London, New York

Chuvieco, E., and Salas, J. 1996. Mapping the Spatial distribution of Forest Fire Danger Using GIS. International Journal of Remote Sensing, 10 (3), pp. 333-345.

D'Andrea, M., Dal Pra, S., Angelini, F., Fiorucci, P., Gaetani, F. Mazzetti, P., and Verlato, M. 2008. G.RISICO: a grid architecture for high resolution nation-wide forest fire risk assessment. Geophysical Research Abstracts, Vol. 10, EGU2008-A-07307, 2008

Diaz-Delgado, R., Lloret, F., and Pons, X. 2003. Influence of fire severity on plant regeneration through remote sensing imagery. International Journal of Remote Sensing, 24 (8), 1751-1763.

Dimitrakopoulos, G. 2002. Mediterranean fuel models and potential fire behaviour in Greece. International Journal of Wildland Fire, 11, 127-130

Gitas I., Mitri G., Avyikou I and Diamanti E. 2004. Vegetation greenness mapping of Greece using MODIS imagery. MODIS workshop, June 24-25, University of Valladolid, Spain.

Gitas, I., De Santis, A., and Mitri, G. 2009. Remote Sensing of Burn Severity. In. Earth Observation of Wildland Fires in Mediterranean Ecosystems (Ed. Chuvieco, E.). Springer-Verlag Berlin Heidelberg, pp. 129-148.

Gitas, I., Mitri, G. Veraverbeke, S. and Polychronaki, A. 2011 Advances in Remote Sensing of Post-Fire Monitoring (a Review). Remote Sensing of Biomass: Principles and Applications/Book 1. Ed. T. E. Fatoyinbo, INTECH publisher: In press ISBN 978-953-307-315-6.

Gouveia, C., DaCamara, C. & Trigo, R., 2010. Post-fire vegetation recovery in Portugal based on spot/vegetation data. Natural Hazards and Earth System Sciences 10, 673-684

Hernandez-Leal, A., Arbelo, M., Gonzalez-Calvo, A. 2006. Fire Risk assessment using satellite data, Advances in Space research, (37(4), 741-746.

Hernandez-Clemente, R., Navarro, R., Hernandez-Bermejo, J., Escuin, S. & Kasimis, N. 2009. Analysis of postfire vegetation dynamics of Mediterranean shrub species based on terrestrial and NDVI data. Environmental Management 43, 876-887

Jaiswal, R.Ki, Mukherjee, S., Raju, K.D., Saxena, R. 2002. Forest fire risk zone mapping from satellite imagery and GIS, International Journal of Applied Earth Observation and Geoinformation 4, 1-10.

Lasaponara, R., A. Lanorte, and Pignatti, S. 2006. Characterization and Mapping of Fuel Types for the Mediterranean Ecosystems of Pollino National Park in Southern Italy by Using Hyperspectral MIVIS Data. Earth Interactions 10(13): 1-11.

Lasaponara, R. and Lanorte, A. 2007. Remotely Sensed characterization of forest fuel types by using satellite ASTER data. International Journal of Applied Earth Observations and Geoinformation, 9, 225-234.

Mitri, G. (Ed.). 2009. Lebanon's National Strategy for Forest Fire Management. Beirut: MOE-AFDC

Mitri, G. and Elhajj, R. 2008. State of Lebanon's Forests. Beirut, AFDC.

Mitri G., Gitas I., 2004. A semi-automated object-oriented model for burned area mapping in the Mediterranean region using Landsat-TM imagery. International Journal of Wildland Fire, 13 (3): 367–376.

Mitri, G. and Gitas I. 2006. Fire type mapping using object-based classification of IKONOS imagery. International journal of wildland Fire, 15 (4): 457-462.

Mitri, G. and Gitas, I. 2008. Mapping the severity of fire using object-based classification of Ikonos imagery. International Journal of Wildland Fire, 17 (3): 431-442.

Mitri, G. and Gitas, I. 2010. Mapping post-fire vegetation regeneration using EO-1 Hyperion. IEEE Transactions on Geoscience and Remote Sensing. Volume 48, Number 3, pp. 1613-1618

MOE/UNDP/ECODIT, 2011. State and trends of the Lebanese Environment 2010.

Nogueira, G.S., Ribeiro, G.A., Ribeiro, C.A.A.S, Silva, E.P. 2002. Installation of fire detection towers using the GIS system, R. Árvore, Viçosa-MG, v.26, n.3, p.363-369.

Pereira, J. and Santos, M. 2003. Fire risk mapping and burned area mapping in Portugal. Direccao Geral das Florestas, Lisboa, p.64.

Riaño, D., E. Chuvieco, Salas, J., Palacios-Orueta, A. and Bastarrika, A. 2002. Generation of fuel type maps from Landsat-TM images and auxiliary data in Mediterranean ecosystem. Can. J. For. Res. 32: 1301–1315.

Roder, A., Hill, J., Duguy, B., Alloza, J., Vallejo, R., 2008. Using long time series of Landsat data to monitor fire events and post-fire dynamics and identify driving factors. A case study in the Ayora region (eastern Spain). Remote Sensing of Environment 112, 259-273

San-Miguel-Ayanz J, Pereira J, Boca R, Strobl P, Kucera J, Pekkarinen A. 2009. Forest Fires in the European Mediterranean Region: Mapping and Analysis of Burned Areas. In: Chuvieco Emilio (Ed.). Earth Observation of Wildland Fires in Mediterranean Ecosystems. Berlin (Germany): Springer Berlin Heidelberg, p. 189-204.

Stergiadou, A., Valese, E. and Lubello, D. 2007. Detailed Cartography System of fuel types for preventing forest fires. Proceedings of the 6th workshop on forest fires, EARSeL. 120-124.

Tsakalidis, S. and Gitas, I. 2007. Use of Remote Sensing and GIS in forest fire suppression planning. Proceedings of the 6th workshop on forest fires, EARSeL. 91-95.

Twele, A. and Barbosa, P., 2004, Monitoring vegetation regeneration after Forest Fires using satellite imagery, In: Proc. of the 24th Symp. of EARSeL, Dubrovnik, Croatia, May 25-27, 2004.

Veraverbeke, S., Lhermitte, S., Verstraeten, W. and Goossens, R., 2011. A time-integrated MODIS burn severity assessment using the multi-temporal differenced Normalized Burn Ratio (dNBRMT). International Journal of Applied Earth Observation and Geoinformation 13, 52-58

Viedma, O., Melia, J., Segarra, D. and García-Haro, J. 1997. Modeling Rates of Ecosystem Recovery after Fires by Using Landsat TM data. Remote Sensing of Environment 61: 383-398.

Vila, G., Barbosa, P. 2010. Post-fire vegetation regrowth detection in the Deiva Marina region (Liguria-Italy) using Landsat TM and ETM+ data. Ecological Modelling 221, 75-84

AN INSIGHT INTO THE UNDERLYING CAUSES OF TEMPORAL/SPATIAL TRENDS OF FIRES AND BURNED AREAS IN THE EUROPEAN MEDITERRANEAN COUNTRIES

M. Rodrigues[1,2], J. San-Miguel Ayanz[1], S. Oliveira[1,3], F. Moreira[4], A. Camia[1]

[1]Institute for Environment and Sustainability, Joint Research Centre, European Commission; [2]GEOFOREST Group, Department of Geography and Land Management, University of Zaragoza. r.marcos.1980@gmail.com
[3]Centre of Forestry Studies, Institute of Agronomy, Technical University of Lisbon; [4]Centre of Applied Ecology, Institute of Agronomy, Technical University of Lisbon

Abstract

This paper presents an analysis of the fire regimes in Southern European countries, where forest fires are a major hazard. Data on number of fires and burned area size available from 1985 until 2009 were retrieved from the European Fire Database and were used to study the temporal and spatial variability of fire occurrence, at three different spatial scales: for the whole region, at country level and at province level. The temporal trends were assessed with the Mann-Kendall test and Sen slope and two periods were compared: the whole time-series (1985-2009) and the last 10 years (2000-2009). At regional (supranational) level, results suggest that in the last 10 years there was a significant decreasing trend in the number of fires and in relation to the burned area the decrease occurs for the whole study period. At country level, the trend varies by country but there is a general decrease in burned area and the same decreasing trend was found for almost all the provinces in the last decade. These results provide an important insight into the spatial distribution and temporal evolution of fires, a crucial step to investigate the underlying causes and impacts of fire occurrence in this region.

Introduction

The Mediterranean region of Europe is strongly affected by forest fires. Particularly the countries of Portugal, Spain, Italy, Greece and southern France, are by far the most affected by wildfires. According to European Statistics (EC 2010), from 1980 until 2009 fires have burned an average of circa 480,000 hectares of land per year in this region alone, with an annual average of 50,000 occurrences. Data on the number of fires and burned area in this region have been collected since the 80's by each country and compiled in the European Fire Database of the European Forest Fire Information System (Camia et al., 2010). The analysis of the spatial and temporal trends of fires is crucial to understand the underlying causes of the fires and their environmental and socio-economic impacts, assuming a key role in fire prevention and management. The purpose of this work was to analyze the spatial and temporal trends of fire frequency (number of fires) and burned area size, two essential components of the fire regimes, and to draw conclusions on the main factors affecting fire regimes in the European Mediterranean region.

Methods

The analysis was carried out at three different spatial levels: (i) at regional (supranational) level, considering the Euro-Mediterranean region as a whole, with the purpose of characterizing its fire regimes, known to be markedly different from the rest of Europe. The region under study,

shortly referred to as EUMed in what follows, comprises Portugal, Spain, France, Italy and Greece; (ii) at country level, by analyzing the data of each country individually in order to assess differences between countries that may depend on national settings and policies; and (iii) at province level (NUTS3), to investigate the potential influence of local environmental and socio-economic conditions. Temporal trends were analyzed separately for the whole study period (1985 – 2009) and for the last 10 years (2000 – 2009). These trends were compared using the Mann-Kendall test, a non-parametric statistical test used to identify trends in time series data (Kendall 1975). In addition, seasonal trends were also characterized both at regional and country levels, by examining separately the months corresponding to the main fire season (June to October) and the other months.

Results and discussion

Our results suggest that, compared with the overall period 1985 – 2009, changes in the fire regime have been observed in the last 10 years (2000 – 2009) in Southern Europe. The long-term trend for the number of fires in the EUMed region was an increase (Figure 1), but non-significant according to the Mann-Kendall test; however, this trend was reversed in the last 10 years, showing a significant decrease (S=-25, p=0.032). This increase was particularly high in the 90's, which can be partly due to the changes in the reporting systems in the countries that occurred during this time, mostly driven by EC regulations. Besides, the tendency for the abandonment of agricultural land verified in the last decades in this region, which causes an increase in fuel accumulation and the expansion of shrublands, may also explain this trend (Carmo et al., 2011; Lloret et al., 2002; Romero-Calcerrada et al., 2010).

The burned area, on the other hand, shows a decreasing trend since 1980 (Figure 1), with strong annual fluctuations. The results of the Mann-Kendall test show that, for both periods, the general trend is a decrease, but only significant when considering the entire time series (S= -88, p=0.042). This decrease is likely related to the implementation of fire prevention strategies and to the improvement in fire detection and fire-fighting techniques verified in the last years.
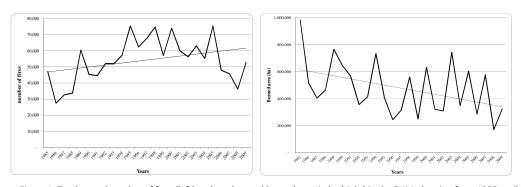

Figure 1. Total annual number of fires (left) and total annual burned area in ha (right) in the EUMed region from 1985 until 2009

However, downscaling the analysis at national and province (NUTS3) level reveals the existence of certain spatial variation in the trends concerning the number of fires and burned area. At country level, Portugal, Spain and Greece show an increasing trend in the number of fires for the whole study period, while France and Italy had a general decrease (Table 1). Both the

increasing trend observed for Portugal and the decreasing trend of Italy are significant. In the last decade, a decrease was observed for all the countries, significant only for Portugal, which had a median decrease of over 1500 fires per year (Sen slope). In relation to the burned area, results of the Mann-Kendall test show a decreasing trend in all countries during both periods (Table 2), with the exception of Greece, where an increasing trend was observed for the last decade. The decreasing trend for the whole time series was significant only for Spain and Italy, which show a higher score and a median annual decrease in area burned of 5175 ha for Spain and 3243 ha for Italy, according to the sen slope.

Table 1 –Results of the Mann-Kendall test and Sen slope for the number of fires by country in both periods. Negative values mean a decrease and positive values mean an increase.

Number fires 1985-2009	Portugal	Spain	France	Italy	Greece
Mann-Kendall score (S)	110	82	-28	-164	22
p value	0.010906	0.058524	0.52831	0.000141	0.62381
sen slope	801.9	396.9	-33.04	-346.2	5.969

Number fires 2000-2009	Portugal	Spain	France	Italy	Greece
Mann-Kendall score (S)	-27	-21	-7	-7	-17
p value	0.020045	0.073638	0.5915	0.5915	0.15241
sen slope	-1554	-1134	-157.5	-201.2	-118

Table 2 –Results of the Mann-Kendall test and Sen slope for the burned area by country in both periods. Negative values mean a decrease and positive values mean an increase.

Burned area 1985-2009	Portugal	Spain	France	Italy	Greece
Mann-Kendall score (S)	-6	-100	-52	-96	-68
p value	0.90704	0.02077	0.23361	0.026506	0.11763
sen slope	-101.6	-5175	-473.5	-3243	-1703

Burned area 2000-2009	Portugal	Spain	France	Italy	Greece
Mann-Kendall score (S)	-19	-9	-21	-5	11
p value	0.1074	0.47427	0.073638	0.72051	0.37109
sen slope	-14016	-6232	-2215	-1443	2127

At NUTS3 level, the trend in the number of fires is very irregular depending on the province, although general patterns can be observed by country (Figure 2). Portugal and Spain have the majority of provinces with a significant increasing trend, while Italy and Greece have more provinces with a significant decreasing trend. However it should be noted that the in Greece data at NUTS3 level after 1998 are partial, because of changes in the reporting system in the country. In the case of Italy, an exception occurs in Sicily, where all provinces show increasing trend or no trend, while in Sardinia almost all the provinces had a decreasing trend. In France, most of the provinces with available data indicate no trend or decreasing. The situation changes when considering only the data between 2000 and 2009. There are few provinces in the whole study area with a significant trend, either increasing or decreasing, possibly because the time series is too short at this scale of analysis.

The burned area, on the other hand, evidences a general significant decreasing trend for the provinces of all countries, except Portugal and the region of Sicily in Italy, between 1985 and 2009 (Figure 3). In the last years, however, the general tendency is a decrease (significant or not) for almost all the provinces.
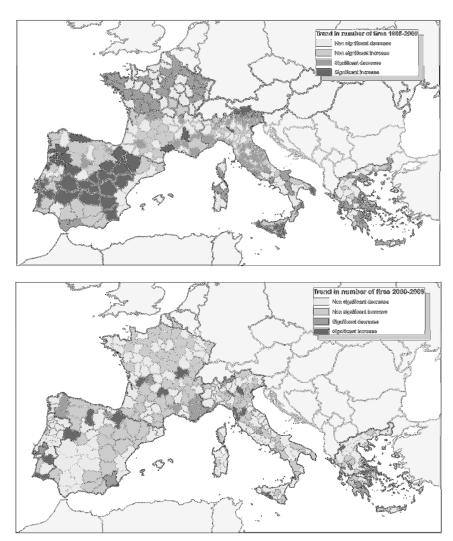
Figure 2. Trend in the number of fires by province in the EUMed region between 1985 - 2009 (top) and between 2000-2009 (bottom) obtained from the Mann-Kendall test.
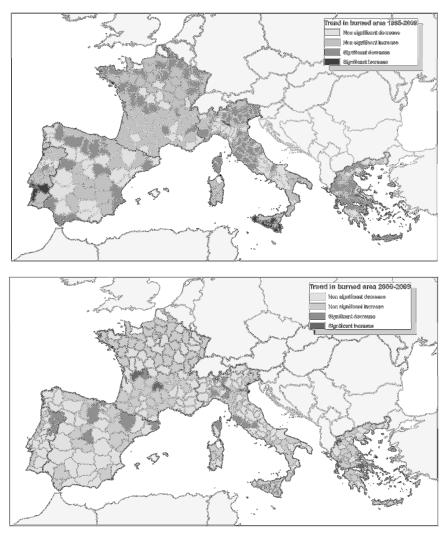
Figure 3. Trend in the burned area (ha) by province in the EUMed region between 1985 – 2009 (top) and between 2000 – 2009 (bottom), obtained from the Mann-Kendall test.

The variation found between countries and provinces in burned area is potentially related to the influence of physical parameters like the topography or the weather conditions, which vary spatially and/or seasonally, and to the diversity of the environmental and socio-economic conditions found throughout the study area, which set the availability of ignition agents (population) and the possibility of fire spread. However, the fire recording process, which is different in each country, and in some cases even in each NUTS2 region (Spain) and has been improved through time, can also have influence in the datasets, especially in the number of fires, and consequently in the results.

In any case, our findings suggest that the general tendency in the EUMed region is a decrease in the total amount of burned area, while the total number of fires seems to be increasing. Nevertheless, trend comparison between the whole period and the last ten years reveals that the increasing trends in number of fires is reversing, or at least losing its significance in recent years.

References

Camia, A., Durrant Houston, T., San-Miguel-Ayanz, J., 2010 The European Fire Database: Development, Structure and Implementation. In: D.X. Viegas (Ed.) Proceedings of the VI International Conference on Forest Fire Research, Coimbra, Portugal.

Carmo, M., Moreira, F., Casimiro, P., Vaz, P. 2011. Land use and topography influences on wildfire occurrence in northern Portugal. Landscape and Urban Planning 100: 169–176

EC, European Commission (2010). Forest Fires in Europe 2009, Report nr. 10. EUR 24502 EN – Joint Research Centre, Institute for Environment and Sustainability, 84 pp. Office for Official Publications of the European Communities, Luxembourg. ISSN 1018-5593

Lloret, F., Calvo, E., Pons, X., Diaz-Delgado, R. 2002. Wildfires and landscape patterns in the Eastern Iberian Peninsula. Landscape Ecology 17: 745-759

Mann, H.B. ,1945. Non-parametric tests against trend, Econometrica 13, 245–259.

Romero-Calcerrada, R., Novillo, C.J., Millington, J.D.A., Gomez-Jimenez, I. 2008. GIS analysis of spatial patterns of human-caused wildfire ignition risk in the SW of Madrid (Central Spain), Landscape Ecology 23, pp. 341–354

LEVEL OF AGREEMENT ON FOREST FIRE STATISTICS FROM NATIONAL SOURCES AND REMOTE SENSING IN THE EFFIS

L. Vilar, J. San-Miguel Ayanz, A. Camia

Institute for Environment and Sustainability, Joint Research Centre, European Commission. lara.vilar@jrc.ec.europa.eu, jesus.san-miguel@jrc.ec.europa.eu, andrea.camia@jrc.ec.europa.eu

Abstract

The impact of forest fires in Europe is assessed in the European Forest Fire Information System (EFFIS) from two different information sources: (1) field data collected at regional and national level by the fire services of the countries, and (2) remote sensing.

Forest fire statistics have been stored in the European Forest Fire Database (EFFD) of EFFIS since 2000. These statistics go back to the 80s for some of the Mediterranean countries. Additionally, the area burnt by forest fires in the European countries has been monitored in EFFIS since the year 1998 by remote sensing techniques. Data from RESURS, WiFS and MODIS satellite sensors have subsequently been used for this purpose. Since 2003 MODIS daily images of 250 m spatial resolution are used to map burnt areas in the so-called Rapid Damage Assessment (RDA) module of EFFIS. The RDA provides a daily update of the perimeters of burnt areas in Europe for fires of 40 ha or larger. Both information sources, EFFD and RDA, are considered reliable and the basis for official statistics for the countries and for the European Institutions e.g. the European Parliament and the European Commission. However, it acknowledged that these information sources contain inherent errors due to the methodologies used in assessing fire size. On the one hand, in country statistics, fire sizes are often derived by ocular estimation of the burnt area on the ground; in some occasions GPS tools are used to determine fire perimeters. Although this methodology may be considered very precise for small fires, it introduces errors when mapping fires of large size. On the other hand, remote sensing is considered very reliable for mapping large fires, while less precise when mapping fires of small size which may be omitted in the process of automatic classification of remote sensing imagery. It is thus important to assess the coherence and consistency of the reported fires and fire statistics drawn from these sources.

The present study focuses on the analysis of the agreement between the above-mentioned sources: EFFD and RDA. The comparison is performed for all the fires recorded between 2000 and 2009 in the 5 most affected countries, those of the Mediterranean basin. The first stage of the analysis uses common variables recorded in the EFFD and the RDA such as date, location and fire size to match fire records. In a second stage, when the exact date or location was unknown, ranges of time (7-10 days) and fire size were used; additionally, spatial cross checking with different administrative unit levels (NUTS5-municipality-, NUTS3-province) was performed. For those fire perimeters (in the RDA) that were not automatically matched to records in EFFD a manual quality check was carried out. The reasons for mismatching were manifold e.g. assignment of spatial location to a fire within an administrative unit using different criteria, not reported fires, reporting of some events more than once, different fire sizes in RDA and EFFD.

The perimeters of the big fires (more than 500 ha) matched in most countries, around 94% of the total (over 95% for all countries except for Greece, 68%). However, taking into account all fires bigger than 50 ha, the agreement decreased to around 15-20%. This analysis made it possible to explore the level of accuracy of the main two sources of information on forest fires at the European level. Although remote sensing can be considered the most reliable method for mapping large fires, the analysis performed suggests that its reliability may decrease as fires decrease in size approaching the threshold of 40 ha in the RDA.

Keywords: burnt area, Euro Mediterranean, fire occurrence, GIS, MODIS

Introduction

In the European Mediterranean region on average 60 000 fires occur every year, burning approximately half a million ha of forest areas (European Commission, 2010). Mediterranean ecosystems cannot be fully understood without the role of fires. Natural fires have been

essential to maintain biodiversity. Fire has been also a widely used tool to manage the territory. However, in the last decades, natural fire regimes have experienced significant alterations (fire frequency, intensity and severity), which have aggravated their ecological, social and economic consequences (Westerling et al., 2006; FAO, 2007). The first steps to create a European forest fire database were taken under the Regulation EEC No 2158/92, now expired, followed by the Regulation EEC No 804/94 and the Forest Focus Regulation (EC) No 2152/2003. The forest fire data of the European members is collected every year through the above-mentioned regulations. Since 2000 this data has been checked and stored by the European Forest Fires Information System (EFFIS) through the database known as the European Fire Database. In this harmonised database, the numbers of fires, burnt area and fire cause, among other variables, are stored since the 80s for some member states (European Commission, 2010). The burnt area of the European territory has been monitored since the year 1998 by means of remote sensing techniques. After carrying out tests and obtaining sub-regional results, EFFIS produced in 2000 a burned area product from WiFS data. This product was obtained by the end of each summer season on the basis of a single image mosaic. Classification was obtained through thresholding and post-classification visual interpretation. From 2003 onwards, MODIS daily images with 250 m spatial resolution have been used. Daily two full sets of tiles covering Europe are pre-processed, providing radiometry, geolocation and atmospheric corrected reflectances. Also the MODIS thermal activity product is processed and the active fire product is used for the automatic geo-location of active fires. The EFFIS Rapid Damage Assessment provides the daily update of the perimeters of burnt areas in Europe for fires of about 40 ha or larger (San-Miguel Ayanz et al 2009).

Methods

Study area

EUMED comprises the Southern European countries Portugal, Spain, Italy, Greece and the Mediterranean provinces of France, with an area of more than 1 million km^2. The climate in much of this region is Mediterranean, with mild, rainy winters and hot, dry summers (Merlo and Croitoru, 2005), which supports characteristic Mediterranean forests. Forests cover about 50% of its area, including shrub formations and other semi-natural categories (e.g. transitional woodlands, sclerophyllus vegetation) (CLC 2000). Reflecting the prevailing climate, Mediterranean forests are frequently characterized by fire climax species, i.e. those dependent on the presence on fire in the reproductive cycle (FAO, 2006). In this populated area of about 137 million people (Eurostat 2011; Insee 2009) most of the fires are directly or indirectly linked with human activity.

Data

The European Forest Fire Database (EFFD) contains fire statistics going back to the 1980s for some of the Mediterranean countries. For the study period 2000-2009, in the EUMED countries, the total number of fires was 541 324 and the burnt area 4 253 207 ha. In Portugal there were 254 542 fires with 1 608 558 ha of burnt area. In Spain 182 761 fires occurred and 1 269 074 ha of forest area was burnt. In the EUMED provinces of France there were 22 145 fires burning 164

438 ha. In Italy, there were 73 021 fires and 844 993 ha of burnt area. Finally, in Greece, there were 8855 fires burning 366 142 ha. Figure 1 illustrates the percentage of burnt area by fire size class for the whole EUMED and by country in the study period 2000-2009.
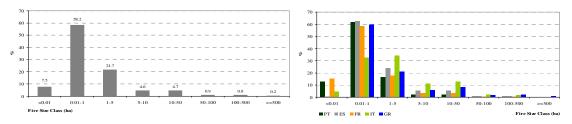

Figure 1. EFFD Percentage of fires by Fire Size Class at EUMED level and by country (2000-2009)

The Rapid Damage Assessment (RDA) provides a daily update of the perimeters of burnt areas in Europe for fires of 40 ha or larger. The methodology for its calculation is further explained in San-Miguel Ayanz et al 2009. In the study period 2000-2009 8890 fires were mapped, with a total burnt area of 2 814 264 ha. In Portugal, there were 4003 fires, burning 1 116 393 ha. In Spain, 2575 fires were mapped with 745 031 ha of burnt area. In the EUMED provinces of France, 313 fires were mapped giving a total burnt area of 104 433 ha. In Italy there were 1566 fires, burning 360 252 ha. Finally, in Greece, 433 fires were mapped with a total burnt area of 479 265 ha. The burnt area was calculated by the end of the season for 2000-2005 and daily for 2006 onwards, as the exact date of the fires was known for this latter period. Figure 2 shows the percentage of burnt area by fire size class for the whole EUMED and by country, in the study period 2000-2009.
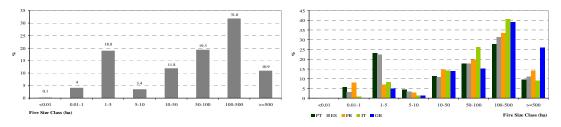

Figure 2. RDA Percentage of fires by Fire Size Class at EUMED level and by country (2000-2009)

Method

The present study focuses on the analysis of the agreement between the above-mentioned sources: EFFD and RDA. The comparison is performed for all the fires recorded between 2000 and 2009 at the EUMED level. The first stage of the analysis uses common variables recorded in the EFFD and the RDA such as date, location and fire size to match fire records. In a second stage, when the exact date or location was unknown, ranges of time (7-10 days) and fire size were used; additionally, spatial cross checking with different administrative unit levels (NUTS5-municipality-, NUTS3-province) was performed by using GIS tools. For those fire perimeters (in the RDA) that were not automatically matched to records in EFFD a manual quality check was carried out.

223

Results and discussion

The level of agreement between the two fire data sources is summarized in Table 1. On one hand, at the EUMED level, about 56% of the big fires (equal to or bigger than 500 ha) of the EFFD were linked to the burnt mapped area (RDA). On the other hand, the big fires from the RDA database were linked to the records in the EFFD in 94% of cases. By country, large fires were linked in the EFFD in about 70% in Spain and Greece, around 60% in France, while 55% and 45% in Italy and Portugal respectively. In the RDA, in all countries, except for Greece (68%), all big fires were linked in more than 90% of the cases.

Table 1. Percentage of linked fires by Fire size class in EFFD and RDA at EUMED level and by country in 2000-2009

	Linked fires (%)											
	EUMED		ES		FR		GR		IT		PT	
Fire size class (ha)	EFFD	RDA	EFFD	RDA	EFFD	RDA	EFFD	RDA	EFFD	RDA	EFFD	RDA
<0.01	0.1	0.0	0.0	0.0	0.0		0.0		0.0		0.2	0.0
0.01-1	0.1	0.0	0.0	0.0	0.0	0.0	0.0		0.0	0.0	0.2	0.0
1-5	0.1	0.0	0.0	0.0	0.0	0.0	0.1	0.0	0.0	0.0	0.2	0.0
5-10	0.1	0.0	0.0	0.0	0.1	0.0	0.2	0.0	0.0	0.0	0.4	0.0
10-50	0.7	13.5	0.5	11.6	0.3	2.2	2.0	6.7	0.8	16.4	0.7	15.4
50-100	3.7	14.8	2.8	10.5	7.9	29.0	11.4	33.3	3.8	12.2	2.9	16.2
100-500	13.8	22.0	14.9	18.1	14.9	40.0	30.2	32.5	14.5	27.6	9.6	18.4
>=500	56.1	94.0	68.9	99.0	62.9	97.7	73.3	67.9	54.8	96.4	45.6	96.6

Regarding the periods in the RDA database source in which the exact date of the fire was known (2006-2009) or not (2000-2005), table 2 illustrates the level of agreement in percentage of the linked mapped fires with the EFFD database by period and by country. As the table shows, for the smaller fires (10-50 and 50-100 ha), the success in linking cases is higher in the period 2006-2009, where the date of each event is available (except for Greece). In fires of size 100-500 ha, the agreement is higher in Spain, Italy and Portugal. Finally, for the largest fires, the percentage is quite similar in both periods.

Table 2. Percentage of linked fires by Fire size class in RDA by country in 2000-2005 and 2006-2009

	Linked fires (%)									
	ES		FR		GR		IT		PT	
Fire size class (ha)	00-05	06-09	00-05	06-09	00-05	06-09	00-05	06-09	00-05	06-09
<0.01	0.0	-	-	-	-	-	-	-	0.0	-
0.01-1	0.0	0.0	0.0	-	0.0	-	0.0	-	0.0	-
1-5	0.0	0.0	0.0	-	0.0	-	0.0	-	0.0	-
5-10	0.0	-	0.0	-	0.0	-	0.0	-	0.0	-
10-50	0.0	55.2	0.0	14.3	12.5	6.5	0.0	32.7	0.6	53.5
50-100	0.0	46.2	23.3	50.0	57.7	15.8	0.0	25	1.7	61.6
100-500	0.3	68.5	40.9	31.3	45.3	24.8	0.0	47.8	3.5	71.7
>=500	98.9	99.0	97.3	100.0	62.8	71	97.7	95.7	98.8	85

The main difficulties found in analyzing the agreement between the two databases were: (1) lack of coincidence in the date of the event; (2) fires that were not reported in the EFFD; (3) exact location of the fire not reported in the EFFD database; (3) fires that happened in border areas in between countries or regions; (4) fires in which the burnt area covered more than one municipality unit (NUTS5) and which appear in the EFFD as more than one different record according to the municipalities where they have happened; (5) big differences in burnt area size.

Conclusions

This analysis explores the level of accuracy of the main two sources of information on forest fires at the European level. For the big fires, most of them have been reported in both databases and are coincident in more than 95% of cases, with the exception of Greece (70%). This lower level of agreement may be related to changes in the Greek services in charge of collecting and reporting forest fire statistics. Regarding smaller fires, the reliability decreases. It might be due to the lack of information related to the spatial location, time of the event, or more precise burnt area data in the EFFD. Although there are decreases in the level of agreement between RDA and EFFD with decreasing burnt area size, remote sensing allows the enrichment of the fire data reported in the EFFD as it provides explicit detailed positioning of the burnt areas in the countries.

References

European Commission. 2010. Forest Fires in Europe 2009. JRC Scientific and Technical Reports. EUR 24502 EN – 2010. Publication Office of the European Union. Luxembourg. p. 83. doi:10.2788/74089.

Eurostat Basic Figures on the EU. First quarter 2011. Total population at 1/01/2009. Available at: http://epp.eurostat.ec.europa.eu/portal/page/portal/eurostat/home/

Food and Agricultural Organization of the United Nations (FAO). 2006. Fire management global assessment 2006. FAO Forestry Paper 151.

Food and Agricultural Organization of the United Nations (FAO). 2007. Fire Management Global Assessment. A thematic study prepared in the framework of the Global Forest Resources Assessment 2005. FAO Forestry Paper 151. 320 pp. http://www.fao.org/forestry/fra2005/en/.

Insee (Institut national de la statistique et des études économiques, France) 2009. Estimation de population au 1er janvier, par région, sexe et grande classe d'âge. Available at: http://www.insee.fr/fr/default.asp

Merlo, M., Croitoru, L. (Eds.) 2005. Valuing Mediterranean Forest. Towards Total Economic Value. CABI Publishing. UK.

San-Miguel Ayanz, J., Pereira, J.M.C., Boca, R., Strobl, P., Kucera, J., Pekkarinen, A. 2009. Forest Fires in the European Mediterranean Region: Mapping and Analysis of Burned Areas. In Chuvieco, E. (Ed.) Earth Observation of Wildland Fires in Mediterranean Ecosystems. Springer-Verlag Berlin Heidelberg 189-203.

Westerling, A.L., Hidalgo, H.G., Cayan, D.R. and Swetnam, T.W. 2006. Warming and earlier spring increase western US forest wildfire activity. Science 313: 940-943.

IV - National to global applications of remote sensing in post-fire assessment

MODIS-LANDSAT DATA FUSION FOR CONTINENTAL SCALE 30M RESOLUTION BURNED AREA MAPPING

L. Boschetti[1], D. Roy[2]

[1]*Department of Geography, University of Maryland, 2181 LeFrak Hall, College Park MD20740 (USA), luigi@hermes.geog.umd.edu;* [2]*GisCE, South Dakota State University, Brookings SD 57007, david.roy@sdstate.edu*

Abstract

Satellite data have been used to monitor fire for more than two decades using computer algorithms that detect the location of active fires at the time of satellite overpass, and in the last decade using burned area mapping algorithms that map the spatial extent of the areas affected by fires (Lentile et al. 2006; Roy et al. 2008). Until the successful launch of the polar-orbiting NASA Moderate Resolution Imaging Spectroradiometer (MODIS) sensors there were no environmental satellite systems with dedicated fire monitoring capabilities (Justice et al. 2003). The MODIS design includes bands specifically selected for fire detection and MODIS data are being used to systematically generate the daily global 1km active fire (Giglio et al. 2003) and the monthly 500m burned area products (Roy et al. 2005). However, neither MODIS product can detect fires reliably at the scale of 10's of meters. The recent USGS 2008 free Landsat data policy now provides the opportunity for continental to global scale Landsat 30m resolution processing

This paper presents a multi-temporal methodology to fuse the MODIS active fire and burned area products with Landsat data to map burned areas at 30m on a temporally rolling basis. To demonstrate the fusion methodology, 30m burned area maps of the conterminous United States (CONUS) are generated using the freely available Web Enabled Landsat (WELD) ETM+ mosaics (Roy et al. 2010, http://landsat.usgs.gov/WELD.php). Validation is conducted by systematic comparison with the fire perimeter vectors provided by the USGS Monitoring Trends in Burn Severity project (Eidenshenk et al. 2007). Prospects for future developments and continental application are discussed. The presented methodology demonstrates the potential for the fusion of the planned NPP/NPOESS VIIRS active fire product with reflectance data sensed by the planned Landsat Data Continuity missions.

Keywords: MODIS, Landsat, Data Fusion, Unsupervised Burned Area Detection

COMPARATIVE EVALUATION OF RESTORATION PRACTICES APPLIED TO MEDITERRANEAN FOREST ECOSYSTEMS USING REMOTE SENSING AND GIS: NATURAL REGENERATION VERSUS REFORESTATION

P. Christakopoulos[1], D. Paronis[2], M. Scarvelis[3], K. Kalabokides[4], I. Hatzopoulos[4]

[1]*Decentralized Administration of Attica, F. Negri 5, 19500 Lavrio, Greece. paulchri@hol.gr*

[2]*Institute for Space Applications & Remote Sensing, National Observatory of Athens, Vas. Pavlou & Metaxa, 15236 Palaia Penteli, Greece. paronis@noa.gr*

[3]*Technological Educational Institute of Larissa, 43100 Karditsa, Greece. skarvelis@teilar.gr*

[4]*Faculty of Environmental Studies, Aegean University, Lofos Panepistimiou, 81100 Mytilene, Greece. kalabokides@aegean.gr, ihatz@aegean.gr*

Abstract

The evaluation of the restoration practices applied to burnt Mediterranean forest ecosystems is an essential element of any restoration project and it refers both to the restoration by natural regeneration and by artificial reforestation as well.

The objective of the research was to study the forest post-fire dynamics for the two restoration practices under various fire regimes as regards the frequency of fire breakouts. This work was carried out in Pendeli mountain (Attica, Greece) that has been repeatedly burnt by fires. In-situ measurements were performed in 2008 in one hundred and three burnt surfaces which were identified in the territory. In each surface, all kind of plants (physical regeneration-artificial reforestation) as well as incremental data were measured and were subsequently used for the determination of the total aboveground biomass using suitable allometric equations. The analysis was based on appropriate satellite time-series of a modified Normalized Difference Vegetation Index retrieved from SPOT series satellites which were used for the determination of the forest recovery empirical model.

The results concluded that reforestation performed on surfaces that were burnt once in the year 1995 was comparable to natural regeneration. In fact, ten years after the fire, it was superior in terms of total biomass. The reforestation made after the year 1995 in areas that were burnt also in 1982, was superior than the corresponding natural regeneration. Those findings were confirmed by the assessment of the degree of natural regeneration of Pinus halepensis Mill in each surface and the measurement of the average value of biomass for year 2008.

Keywords: Restoration, Natural regeneration, Reforestation, Evaluation, SPOT

Introduction

Restoration of burned Mediterranean forest ecosystems with natural regeneration is ensured after a single incident (Trabaud 1982, Daskalakou 1996, Thanos et al. 1996). On the other hand, recurrent wildfires significantly impede or even eliminate the natural regeneration process of those ecosystems. As pointed out in the relevant literature, natural regeneration of *Pinus halepensis Mill* is not possible in the case of multiple fires occurring within a short period of time. For this reason, artificial reforestation is extensively adopted for restoration in Greece and other Mediterranean counties as well. (Christakopoulos et al. 2007).

The evaluation of the restoration practices is an essential element of any restoration project applied to burnt Mediterranean forest ecosystem and it refers both to the restoration by natural regeneration and by artificial reforestation. Benchmarking of the two practices may lead to useful findings, regarding restoration success. Towards this direction, the above-ground biomass is considered as one of the essential ecological indicators of restoration success (Aronson et al. 1993). In the literature, various biomass estimation methods based on

allometric equations are found (Blanco and Navarro 2003, Christakopoulos 2010). Alternatively, the assessment of the restoration success can be based on remote sensing indicators, such as the Normalized Difference Vegetation Index (NDVI) (Diaz-Delgado et al. 2002, Gouveia et al. 2010), the SWIR/NIR index (Vogelmann et al. 2009), pRI(Lhermitte et al. 2010), Green Vegetation Cover (Röder et al. 2007) and other indices derived from data acquired by existing sensors (e.g. LANDSAT TM and ETM+, ASTER, IKONOS, SPOT). In general, NDVI exhibits a strong relationship with a number of vegetation characteristics, notably green leaf area index (LAI), green biomass, and fractional absorbed photosynthetically active radiation, FPAR. In particular, and because of its general response to levels of green biomass irrespective of plant species, it has been used to quantify the total vegetation cover. It corresponds well to the levels of the total above-ground biomass, especially during the first stages of post-fire restoration before reaching its saturation level (Anderson et al. 1993).

This paper focuses on the evaluation of restoration success of a burnt forest ecosystem in Greece. The proposed research is based on the determination of an empirical restoration model using the post-fire trends as determined by a modified NDVI index derived from a series of high resolution SPOT multispectral images. The specific model is used in conjunction with estimations of the total above-ground biomass, for the comparative evaluation of the two restoration practices namely natural regeneration and artificial reforestation.
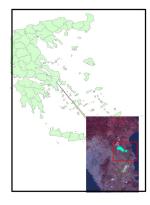
Data and methodology

The study took place in the area of mountain Pendeli near Athens, the capital city of Greece (Figure 1). Some parts of the area have been burnt once in 1995 while some other parts have been burnt by recurrent wildfires in 1982 & 1995. The former have been restored mainly by natural regeneration while a small part has been restored by artificial reforestation. The parts of the area burnt twice have been mainly restored with reforestation.

In-situ measurements were performed during 2008 in 103 burned surfaces (control surfaces) identified in the territory. In each surface, the number of plants (natural regeneration-artificial reforestation) as well as incremental data (height, basal diameter, canopy cover) were measured. Using suitable allometric equations suggested by Blanco and Navarro (2003) and Christakopoulos (2010) the total above-ground biomass was estimated in each area.

An extended set of images comprising twenty high resolution images from SPOT series satellites (SPOT 1, 2, 3, 4) covering the years 1986-2008 and corresponding to summer acquisitions was used. Prior to the analysis, all images were corrected for geometric, topographic and atmospheric effects. For each one of the identified control surfaces, the spatially average values of the Normalized Difference Vegetation Index (NDVI) were determined. Those values were normalized by the average NDVI values of some unburned areas identified in the area. This modified NDVI, called Resilience (R), has proven to be insensitive to factors such as moisture, visibility, and temperature variations (Diaz-Delgado et al. 2002).

The analysis of the satellite time-series showed that the post-fire response can be approximated via a logistic or sigmoid curve (Figure 2) expressed in general as $f(x)=a \cdot [(1+b \cdot exp(-c \cdot x)]-1$. Using the above mentioned curves, four different scenarios were examined in terms of frequency of fire occurrence and the restoration practice applied: a) Fire in year 1995-natural

regeneration, b) Fire in year 1995-artificial reforestation, c) Fires in years 1982 and 1995-natural regeneration and d) Fires in years 1982 and 1995- artificial reforestation.
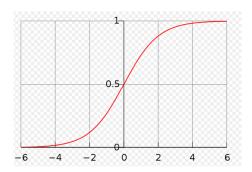

Figure 1. Areas of study in Pendeli mountain

Figure2. The general form of the logistic or sigmoid curve adopted

Results and discussion

Single-fire (1995)

In Figures 3 and 4 the graphs of the temporal evolution of the modified NDVI index (R) (in blue) and its post-fire logistic curves (in red) for natural regeneration and artificial reforestation are shown for the case of a single-fire occurred in 1995. The comparative graph of the post-fire trends is shown in Figure 5 reveals that soon after the fire, the curve of natural regeneration (in blue) is higher than the respective curve of reforestation (in green). This happens because in general, the areas restored with reforestation present low levels of natural regeneration. As it can be inferred from the slope of the two curves, reforestation is growing slightly faster than natural regeneration. As a result, at the tenth year, the two curves cross each other. From this point on though, a decrease of natural regeneration speed is observed. The average above-ground biomass values estimated from the allometric equations for year 2008 as given in Figure 5, are in agreement with the above findings. More precisely, the biomass estimates for reforestation (18.376 ton/Ha) and natural regeneration (17.709 ton/Ha) indicate a higher performance of the former by 4%.
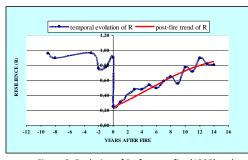

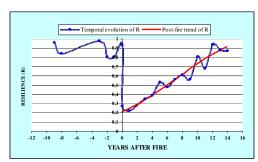Figure 3. Evolution of R after one fire (1995) and natural regeneration

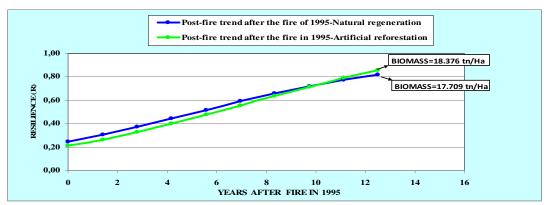Figure 4. Evolution of R after one fire (1995) and artificial reforestation

233

Figure 5. Post-fire trends after one fire in 1995. Natural regeneration versus Reforestation

Recurrent fires (1982, 1995)

Figure 6 depicts the temporal evolution of R as a function of time elapsed from the last fire incident (in 1995) in the case of two recurrent fires, for the two restoration practices.

As it is observed, the reforestation curve (in green) presents higher slope throughout the entire period than the natural regeneration curve (in blue), a fact indicating the higher restoration speed with reforestation. It is characteristic that although the two sample areas present almost identical values immediately after the second fire (R≈0.25) and thus similar initial conditions, the value of R for artificial regeneration is higher by approximately 20% (R≈0.90 and R≈0.75 respectively). The average above-ground biomass values for the areas with natural regeneration and reforestation in the year 2008 are respectively 19.638 ton/Ha and 17.798 ton/Ha, a difference equal to around 10%. According to Christakopoulos (2010), the plant density for natural regeneration of *Pinus halepensis Mill* for the specific case, is moderate (600 plants /Ha) while the relevant density of artificial reforestation is high (about 1400 plants/Ha). Thus, also in the specific case of two recurrent wildfires, artificial reforestation is superior to natural regeneration in terms of total above-ground biomass.
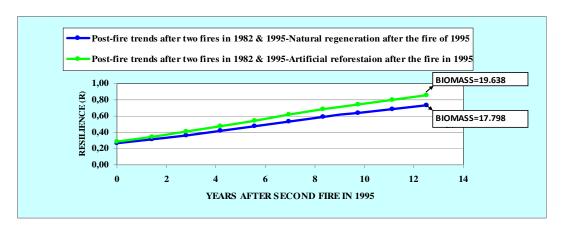

Figure 6. Post-fire trends after the two fires in 1982 and 1995. Natural regeneration versus Reforestation

Conclusion

In the specific work, appropriate sigmoid curves were fitted to the time-series of a Resilience (R) index derived from SPOT high resolution multispectral images to study the post-fire response of a Mediterranean forest ecosystem. The analysis, showed that for the specific cases examined, the post-fire response depends on the restoration practice applied. Reforestation in Pendeli mountain after one incident of fire in 1995 was slightly superior than restoration with natural regeneration while in the case of two fire incidents (in 1982 and 1995), restoration with reforestation was significantly superior to restoration with natural regeneration. The trends identified by the analysis of the satellite time-series were consistent with estimations of the total above-ground biomass made in 2008.

References

Anderson, G., Hanson, J., haas, R. 1993. Evaluating Landsat thematic mapper derived vegetation indices for estimating above ground biomass on semiarid rangelands. Remote Sensing of the Environment 45: 165-175.

Aronson, F., Floret, C., Le Floch, E., Ovalle, C., Pontanier, R. 1993. Restoration and rehabilitation of degraded ecosystems in arid and semi-arid lands. I. A review from the South. Restoration Ecology 1: 8-17.

Blanco Oyonarte, P., Navarro Cerrillo, M. 2003. Aboveground phytomass models for major species in shrub ecosystems of Western Andalusia. Invest. Agrar.: Sist. Recur. For. (2003): 47-55.

Christakopoulos, P., Hatzopoulos, I., Kalabokidis, K., Paronis, D., Filintas, A. 2007. Assessment of the response of a Mediterranean-type forest ecosystem to recurrent wildfires and to different restoration practices using Remote Sensing and GIS techniques. Proceedings of the 6th international workshop of the EARSel special interest group on forest fires: 213-216.

Christakopoulos, P. 2010. Assessment of the ecological restoration of repeatedly burnt Mediterranean-type forest ecosystems with the combined use of field data, GIS and Remote Sensing methods. Ph.D. Thesis, Aegean University (in Greek).

Daskalakou, E. 1996. Eco-physiology of post fire regeneration of Pinus halepensis, Ph.D. Thesis, University of Athens, Biology Department, Sector of Botanic (in Greek).

Diaz-Delcado, R., Lloret, F., Pons, X.,Terradas, J. 2002. Satellite evidence of decreasing resilience in Mediterranean plant communities after recurrent wildfires. Ecology 83: 2293-2303.

Gouveia, C., Da Camara, C., Trigo, R. 2010. Post-fire vegetation recovery in Portugal based on spot/vegetation data. Nat. Hazards Earth Syst. Sci., 10: 673–684.

Lhermitte,S., Verbesselt, J., Verstraeten,W., Veraverbeke,S., Coppin,P. Assessing intra-annual vegetation re-growth after fire using the pixel based regeneration index. International Journal of Photogrammetry and Remote Sensing, v. 66, iss. 1: 17-27.

Röder, A., Hill, J., Duguy, B., Alloza, J.,A., Vallejo, R. 2008. Using long time series of Landsat data to monitor fire events and post-fire dynamics and identify driving factors. A case study in the Ayora region (eastern Spain). Remote Sensing of Environment 112: 259–273.

Thanos, C., Daskalakou, E., Nikolaidou, S.1996. Early post-fire regeneration of a Pinus halepensis forest on Mount Parnis, Greece. Vegetation Science 7: 273-280.

Trabaud, L.1982. Effects of past and present fire on the vegetation of the French Mediterranean region. Symp. Dynamics Manage. Medit. Type Ecosyst. USDA Forest Serv.Gen. Tech. Rep. PSW-58:450-457.

Vogelmann, J., Tolk, B., Zhu, Z. 2009. Monitoring forest changes in the southwestern United States using multitemporal Landsat data. Remote Sensing of Environment 113: 1739–1748.

GLOBAL BURNED AREA MAPPING FROM EUROPEAN SATELLITES: THE ESA FIRE_CCI PROJECT

E. Chuvieco[1], Christopher Sandow[2], K. P. Guenther[3], F. González-Alonso[4], J.M. Pereira[5], O. Pérez[6], K. A. Bradley[7], M. Schultz[8], F. Mouillot[9], P. Ciais[10]

[1]Departamento de Geografía, Universidad de Alcalá. C/ Colegios, 2. 28801 Alcalá de Henares, Spain. emilio.chuvieco@uah.es; [2]GAF AG, Arnulfstr. 197, 80634 Munich, Germany. christopher.sandow@gaf.de
[3]German Aerospace Center (DLR), German Remote Sensing Data Center (DFD), 82234 Oberpfaffenhofen, Germany. Kurt.Guenther@dlr.de; [4]Centro de Investigación Forestal (CIFOR). INIA. Crta. Km7 28040. Madrid. Spain. alonso@inia.es; [5]Instituto Superior de Agronomia, Universidade Técnica de Lisboa, Tapada da Ajuda, 1349-017 Lisboa, Portugal; [6]GMV AEROSPACE AND DEFENCE, S.A., Isaac Newton, 11, E-28760 Madri. operez@gmv.com
[7]Department of Geography, University of Leicester, University Road LE1 7RH. UK. avb4@leicester.ac.uk; [8]Forschungszentrum Juelich GmbH, 52425 Juelich, Germany. m.schultz@fz-juelich.de; [9]IRD,1919 Route de Mend, 34293 Montpellier Cedex 5, France. mouillot@cefe.cnrs.fr; [10]IPSL – LSCE,CEA CNRS UVSQ, 91191 Gif sur Yvette France. philippe.ciais@lsce.ipsl.fr

Abstract

In 2010 the European Space Agency initiated the Climate Change Initiative, a relevant effort to provide long and consistent essential climate variables (ECV) time series data for improving global climate modelling. The program is part of the European effort to accomplish the Global Observing Climate System (GCOS) requirements. Within this program, ten ECVs are being generated, including atmospheric variables (ozone, greenhouse gasses, aerosols, clouds), oceanic variables (ocean colour, height and temperature), and terrestrial (fire, glaciers and land cover). This paper presents the goals and current developments of the fire ECV.

Keywords: Burned Area, Climate Change, MERIS, ATSR, VEGETATION, European Space Agency

Introduction

The European Space Agency (ESA) Climate Change Initiative (CCI) is part of the European contribution to the Global Observing Climate System (GCOS) program. In particular, the objective of this initiative is producing consistent and accurate time series of Essential Climate Variables (ECV), which can be used by climate, atmospheric and ecosystem scientists for their modeling efforts (Plummer 2009). The CCI stresses the importance of improving scientific impact of data acquired by ESA sensors, while maintain close links with key science bodies and other agencies currently generating ECV data. The first call of the CCI program includes ten ECVs covering atmospheric products (ozone, greenhouse gasses, aerosols, clouds), oceanic variables (ocean colour, sea ice, height and temperature), and terrestrial (fire, glaciers, and land cover). A Climate Modelling User Group (CMUG) is also part of the program, to help the interaction of ECVs data production with end-users.

Fire disturbance is one of the ECVs included in the ESA CCI program. It shall focus on mapping burned area (BA) using (A)ATSR, VEGETATION and MERIS data, and in comparing the performance of those products with other algorithms and external equivalents datasets (e.g. MODIS and VEGETATION products). The project aims at developing and validating algorithms to meet GCOS ECV requirements (Global Climate Observing System (GCOS) 2009), which require consistent, stable, error-characterized global satellite data products from multi-sensor data archives. The project also includes developing algorithms for pre-processing of (A)ATSR, VEGETATION and MERIS (both Full and Reduced resolution data), to improve geometrical accuracy and remove atmospheric effects that may lead to potential confusions with burned

areas (clouds, smoke, cloud shadows, water, snow, topographic shadows), as well as algorithms to merge BA from different sensors and adapting the outputs to the needs of the climate modelling community (for technical information on the fire_cci project, see http://www.esa-fire-cci.org/).

From a conceptual point of view, the project tries to answer the following scientific questions: What is the actual magnitude of fire impacts? How much area is burned annually worldwide?, What are the recent trends in fire activity? These questions are the basis for other aspects of global fire science, such as the amount of biomass actually consumed by the fires and their associated GHG emissions, the departure of current fire occurrence from natural fire regimes, the role of fire in world deforestation (REDD+), or the main factors behind fire occurrence trends, on whether they are mostly socio-economic (land-use transformation, for instance), political (fire suppression policy) or climatic.

1.1   *ORGANIZATION OF THE FIRE_CCI PROJECT*

The fire-cci project is developed by a consortium of ten teams from five different European countries (fig. 1): University of Alcalá, CIFOR-INIA and GMV (Spain); GAF, DLR and Julich (Germany), IRD and LSCE-CEA (France), ISA (Portugal), and University of Leicester (UK). These groups cover the different specialities required for the project: Earth Observation scientists, Climate-atmospheric-vegetation modellers, and System engineers.
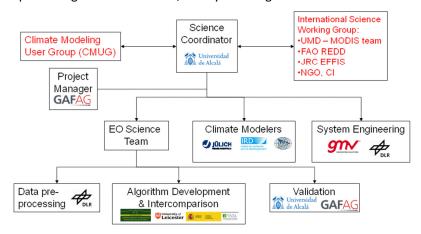

Figure 1. Fire_cci project composition

1.2   *PROJECT PHASES*

The fire_cci project includes the following main phases (fig. 2):

•   User requirement and definition of Product Specifications.

•   Geometric and radiometric processing of input images.

•   BA detection and merging algorithms

•   Validation and error characterization.

•   Testing BA data within climate-vegetation models.

In order to generate a long and consistent time series of BA products, which can be used by the climate, atmospheric and ecosystem scientists for their modelling efforts, it is necessary to understand in detail their needs. For that purpose a user requirement survey was carried out,

both considering the scientists potentially interested in the BA product and the literature references describing actual uses of global BA information.

From that analysis, the product specifications were generated, taking into account as well the limitations of the input data and the CMUG and GCOS requirements. As a result of this analysis, it was compromised that the fire_cci project would include two BA products, one at pixel level, merging the outputs of (A)ATSR, VEGETATION and MERIS sensors, and another one at grid level, at a 0.5 degree resolution, which is the most standard climate grid modelling (CGM) size. The BA information shall be provided at daily resolution, with temporal composites of 1 month for the pixel product and 15 days for the grid product. Each of the two products will be properly documented, including quality layers.
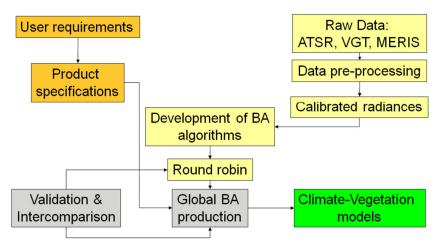

Figure 2. Modules of the fire_cci project

In terms of pre-processing, the BA products of the fire_cci project will be based on level-1B and level-2 calibrated radiances from (A)ATSR, VEGETATION and MERIS (Reduced and Full Resolution). To derive corrected level2 products advanced image geometrical matching has been introduced by DLR, which have also developed dedicated algorithms for removing atmospheric effects, improving cloud, water and snow masking, and topographic shadow removal. . Additional, long term drift effects will be investigated and corrected using CEOS-reference sites. The pre-processing chain has been mostly focused on ten 500x500 km study sites (fig. 3), with the full temporal series (1995-2009) that will be included in the project. They cover the major ecosystems affected by fires, as well as areas previously reported as problematic for burned area mapping.

Burned area algorithms adapted to the three target sensors and considering the diversity of burned area conditions at global scale are being developed. They will primarily aim at the ten study sites to demonstrate the consistency in the processing chain for the BA product outputs. Algorithms currently tested by the UAH-INIA and ISA teams are based on multitemporal change detection, contextual-regional analysis and fire seasonality. A Round-Robin exercise will be conducted between October and December 2011 to check the most relevant existing algorithms applicable to the three sensors against the same reference information. The goal of this exercise is to select the best performing algorithm for global production of burned area

maps. The exercise will be open to participation of any scientists interested in these issues. Once the best performing algorithm is selected, a merging process will be developed to create a synthetic BA product from the three sensor BA products (ATSR, VGT and MERIS). Finally, the complete processing chain will be applied at global scale for five selected years (1999, 2000, 2002, 2003 and 2005), to demonstrate the operational conditions of both the pre-processing and BA algorithms.
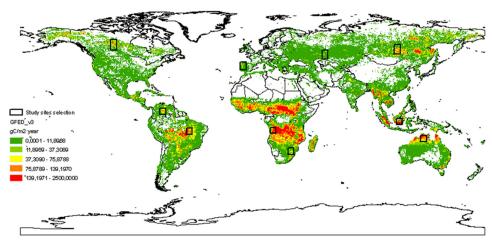

Figure 3. Location of study sites for the fire_cci project

Validation of the BA product will be performed by comparing BA outputs with reference fire perimeters generated from Landsat-TM/ETM+ multitemporal images. A standard protocol based on the CEOS LPV recommendations was generated and agreed between UAH and GAF validation teams to extract fire perimeters from Landsat data, based on a semi-automatic algorithm (Bastarrika et al. 2011). The validation exercise will aim to measure both spatial and temporal accuracy and precision. The spatial assessment will be based on a sample of 110 multitemporal Landsat images acquired in 2005, while the temporal stability will be measured from a temporal series of one Landsat scene for each of the ten study sites. Reference perimeters for these sites are already completed.

BA information generated by the fire_cci project will be compared with other global BA products currently available (GFED3 and MCD45), to check common trends and potential problems. Modellers within the fire_cci consortium will test the BA information in atmospheric and carbon cycle models to analyze its advantages and limitations.

References

Bastarrika, A., Chuvieco, E., & Martín, M.P. 2011. Mapping burned areas from Landsat TM/ETM+ data with a two-phase algorithm: balancing omission and commission errors. Remote Sensing of Environment, 115, 1003-1012.

Global Climate Observing System (GCOS) 2009. Guidelines for the generation of satellite-based datasets and products meeting GCOS requirements. Geneva: World Meteorological Organization.

Plummer, S. 2009. The ESA Climate Change Initiative. Description. Frascati: ESA-ESRIN.

A COMPREHENSIVE AND OPERATIONAL APPROACH TO FOREST FIRE MANAGEMENT

A. De Santis, R. Fabrizi

INSA, Ingeniería y Servicios Aeroespaciales S.A.,Calle Quintana 2, 28008 Madrid (Spain). angela.de.santis@insa.org;
roberto.fabrizi@insa.org

Abstract

Forest fires can be a major ecological disturbance agent that modifies landscapes, especially when normal fire frequencies and /or intensities are modified. The main negative fire effects are vegetation biomass loss, soil degradation, and greenhouse gas emissions. In the worst cases, fires cause not only natural and econom-ical but also human losses (for example, 2007 fire season in Greece). A comprehensive study of a fire event re-quires early warning, crisis monitoring and, after the fire occurs, the interpretation of causal factors, fire effects and ecosystem responses, in a wide range of spatial (local to regional) and temporal (short to long term) scales. However, the lack of data, standard methodologies and economic resources makes this assessment often difficult and/or incomplete. Therefore, analysis of a fire event is usually centered in a post-fire evaluation of the burnt area and, in some cases, in the fire risk estimation. Wildfires show marked seasonal and diurnal cycles and can vary widely in its spatial location. Satellite Earth Observation is actually the only method able to provide repetitive data at the spatial and temporal scales necessary for detecting, quantifying and monitoring this activity, and for understanding the regional and inter-annual variations involved. Therefore, INSA proposed several fire products in order to support the crisis management, integrated in a geoportal (www.insageoservices.com) and provided in the mark of the GMES/SAFER project:

- Fire monitoring -the geographic location of the hot spots and associated parameters, and cloud mask. Fire detection algorithm has been developed in order to detect actives fires in the Iberian Peninsula with MSG SEVIRI (5 min and 15 min- delivery frequency) and MODIS (8 times per day). The algorithm is based on contextual approach selecting pixels which could potentially be fires and afterwards confirms the pixels by comparing the potential fires with their immediate neighbors. In addition, the algorithm re-trieves temperature and burning area of hotspots following the Dozier's approach and the fire radiative power.
- Rapid burned area mapping -by the daily MODIS acquisition and processing, between 1 and 7 day after fire extinction.
- Recovery: Recovery products are intended for an in-depth analysis of fire event, e.g. damage assess-ment or a synthesis of the fire event. High resolution fire perimeter can be provided at the end of the fire season, for fire inventory. Fire severity product is the estimation of damage levels in the different vegetation strata, obtained using a simulation model.

All products have been validated using ground truth data and independent expert validation and have been con-sidered as fully operational.

Keywords: forest fires, active fires, burned area, fire severity, hot spots

Introduction

Forest fires can be a major ecological disturbance agent that modifies landscapes, especially when normal fire frequencies and /or intensities are modified. The main negative fire effects are vegetation biomass loss, soil degradation, greenhouse gas emissions and, in the worst cases, the loss of lives.

A comprehensive study of a fire event requires prevention, early warning, crisis monitoring and, after the fire occurs, the interpretation of causal factors, fire effects and ecosystem responses, in a wide range of spatial (local to regional) and temporal (short to long term) scales. Often, this assessment is incomplete due to economic reasons, the lack of data or the use of standard methodologies that are not efficient.

SAFER project proposed several fire services in order to support all phases of crisis management:

Preparedness/Prevention: *Global Fire Risk Service (GRF)* provides fire danger forecast on the basis of meteorological weather forecasts. Information content includes the identification of the area that can be under risk classified into 5 classes (from very low to very high risk)

Emergency Response: *Fire monitoring (FMM-1)* – They contain the continuous near-real time monitoring of active fires. This product includes fire location and several associated parameters: estimated fire power, fire temperature, size of burning area and background temperature. In addition, cloud cover is provided per each satellite image- and *Rapid burned area mapping (FMM-2)* – fire perimeters at medium resolution by the daily MODIS acquisition and processing can be provided, between 1 and 7 day after fire extinction.

Recovery: Recovery products are intended for an in-depth analysis of fire event, e.g. damage assessment or a synthesis of the fire event. *High resolution fire perimeter (BSM-1)* can be provided at the end of the fire season, for fire inventory. *Fire severity (BSM-2)* product is the estimation of damage levels in the different vegetation strata. A detailed and rapid knowledge of the level of damage and its spatial distribution is essential to: quantify the impact of fire on landscape; select and prioritize treatments applied on site; plan and monitor restoration and recovery activities; provide baseline information for future monitoring.

INSA leads the European forest fire platform of SAFER project (www.emergencyresponse.eu), coordinating the activities of Spain, Portugal, France, Italy and Greece.

Between all this services proposed by SAFER, INSA is service provider of FMM-1 and FMM-2 (in collaboration with the University of Valladolid -LATUV, Spain), BSM-1 (in collaboration with the University of Alcalá- UAH, Spain) and BSM-2. All these services are provided using a dedicated GeoPortal (www.insageoservices.com).

SAFER fire products have a strong scientific base, demonstrated by the number of scientific papers published in high impact journals and PhD thesis related to their development and testing. On the other hand, the methodologies developed are automatic or semi-automatic, what confirms the operational generation of fire products.

All fire services were selected among the most mature products provided in previous GMES projects. During 18 months, the products were tested and improved, taking into account both the validation results and users' feedback. In 2010, all products, except for GFR, were independently validated and checked by other partners and users of the project in order to evaluate their incorporation in the portfolio of operational services. User feedback results quantified the overall agreement with an average value of 4.15 over 5 (where 1 corresponds to "very low" and 5 to "very high" agreement), with a homogeneous trend for all products.

After this validation process, the SAFER fire services have been considered fully operational and have been included to the core SAFER services (since July 2011). Any authorized user can now activate SAFER and ask for our products in case of natural disaster.

Active fire location and rapid burned area mapping (FMM-1 and FMM-2 products) will be provided in "emergency" mode within 8 hours from the receipt of the first suitable satellite image of the disaster, whereas detailed burned area mapping and fire severity will be delivered within 45 days ("emergency support" mode).

The distribution of these products to a wide number of users will contribute to better understand and forecast fire behavior, to manage the crisis in a more cost-effective way, to reduce the impacts and to plan and monitoring the mitigation and recovery activities.

Description of fire product provided by INSA

FMM-1: Active fire detection

Active fire detection is obtained by means of MSG-Seviri and MODIS sensors, using sensor-specific processing chains and provided in collaboration of the University of Valladolid (LATUV, Spain).
In both cases (MSG and MODIS), the hot spot product is provided with the following associated parameters: Date (GMT), Reliability (%), Fire Temperature (Kelvin), Fire Released Power (W/m2), Fire Area (Pixel proportion, %).

MSG-Seviri Chain

The fire detection algorithm runs every 15 minutes, which is the temporal resolution of MSG-Seviri, and analyzes the pixels not covered by clouds (see CLM-cloud mask product) and catalogued (totally or partially) by Corine Land Cover as "forest". Further, the algorithm considers data from previous scenes in order to improve the consistency and persistency of the product.
The CLM cloud mask product is the most onerous process in term of processing time in the MSG-Seviri chain. Therefore, in order to reduce the fire detection processing time, the algorithm takes the previous 15 minutes cloud mask with respect to the actual image. The processing and delivery time of the fire product is about 4 minutes. The geographic coordinates associated to the pixel detected as a fire correspond to the centre of the MSG-Seviri pixel. The MSG spatial resolution at nadir is 3x3 kilometres and it is decreasing as we moved away from the nadir position, for example the pixel size is about 4.3 km x 3.1 km over Spain and 4.4 km x 3.5 km over Greece.

MODIS Chain

The temporal resolution of the MODIS sensor is about 6 images per day. Fire detection is performed through the Active Fire algorithm by NASA (Product MOD14). The time associated to the fire product is the time (UTC) at the acquisition of the image. The processing and delivery time of the fire product is between 45 and 120 minutes from image acquisition. The geographic coordinates associated to fire product correspond to the centre of the pixel (1x1 kilometres). The last steps for the active fire algorithm is to filtering through the cloud mask (product MOD35) by NASA and the Corine Land Cover forest mask.

FMM-2: Rapid Burned Area mapping

FMM-2 Burned area product is a vectorial fire perimeter obtained using MODIS data (250 m-spatial resolution). The burned area methodology is based on a contextual algorithm which takes into account the differences between the Normalized Difference Vegetation Index (NDVI)

values obtained before and after de fire. This methodology is applied twice: 7 and 16 days after the last hotspot detected. A forest mask based on GlobCover MERIS v2.2 is applied.

Every polygon of the product represents a MODIS pixel catalogued as burnt. The product fields provided through the GeoPortal are: Date (GMT), Name, Quality product (7 or 16, which correspond to the time since hotspot detection), Central Latitude, Central Longitude,Start Date, End Date, Area (ha), Product Creation Date.

Cloud mask

The cloud mask algorithms are based on temporal and spectral filters applied on MSG-Seviri data.

There are two combined windows for Europe:

Spain and Portugal: the algorithm takes into account high resolution visible (HRV), 0.6, 0.8, 1.6, 3.9, 10.8, and 13.4µm channels.

Europe without Spain and Portugal (faster product, lower processing time): the algorithm takes into account only 0.6, 0.8 and 10.8 µm channels.

The cloud masks for both windows are calculated in the MSG view geometry, and then a mosaic with both masks is created. The product is re-projected to Geographic longitude-latitude projection.

BSM-1: Detailed Burned Area mapping

UAH produces BSM-1 fire perimeters using software called Automatic Burned Area Mapping Software (ABAMS) (Bastarrika *et al.*, 2011), specifically developed for SAFER. ABAMS proved to be a flexible and adaptive software due to the possible modification of the algorithm in the in the user interface.

BSM-2: Fire severity

Fire severity product is generated by INSA following the methodology developed by De Santis et al. (2009), based on the inversion of a radiative transfer model and validated in several Mediterranean ecosystems (Portugal, Spain, Greece and California).

Geoportal

The GeoPortal is a website where the users will have access to geospatial information. The available data are focused to support the activities of the emergency decisions makers.

Currently available fire products are: Hot Spots; Cloud Mask; Burned Areas; Fire severity.

In order to ensure the interoperability of this tool, it is developed following the correspondent standards.

In the main view, the last hot spots per sensors and the last Seviri cloud mask are shown. Hot spots are classified according to their reliability and there is the possibility of downloading a KMZ Google Earth file which connects automatically with the database and present the last recorded CLM and hot spots data.

Figure 1. Example of the main view of the INSA GeoPortal

The "Search map" allows searching hot spots and burned area products from INSA repository using time and sensor type constraints. The search result can be downloaded directly from this view.

Finally, the "Product download" gives the possibility of downloading all the data stored in the INSA repository.

Conclusion

Forest fires are a major natural disaster with marked seasonality and wide geographical distribution. SAFER fire services, based on EO data, represent the only example, by the date, of a comprehensive and operational approach covering all phases of crisis management (preparedness/prevention, emergency response and recovery). Fire products were extensively validated and improved according to user needs and proved to be ready for their inclusion into the operational service portfolio.

References

Bastarrika, A., Chuvieco, E. and Martín, M. P. (2011). Mapping burned areas from Landsat TM/ETM+ data with a two-phase algorithm: Balancing omission and commission errors. Remote Sensing of Environment, Volume 115, Issue 4, Pages 1003-1012.

De Santis, A., Chuvieco, E., Vaughan, P.J. (2009). Short-term assessment of burn severity using the inversion of PROSPECT and GeoSail models. Remote Sensing of Environment,Volume 113, Issue 1, Pages 126-136.

ASSESSING THE AGREEMENT BETWEEN MODIS AND SEVIRI MAPS OF THE FIRE SEASON - A CASE STUDY IN THE CENTRAL AFRICAN REPUBLIC

P. H. Freeborn, M. J. Wooster

King's College London, Environmental Monitoring and Modelling Research Group, Department of Geography, London, WC2R 2LS, UK. patrick.p.freeborn@kcl.ac.uk, martin.wooster@kcl.ac.uk

Abstract

Maps of the fire season derived from satellite-based remote sensing products are used to define fire regimes, to explain differences in fire behaviour and effects, land use practices and emissions factors, and to evaluate large-scale models of fire occurrence. Since fire events are portrayed differently in different active fire (AF) products, this research compares maps of the fire season in the Central African Republic (CAR) as depicted by the Moderate Resolution Imaging Spectroradiometer (MODIS) and the Spinning Enhanced Visible and Infrared Imager (SEVIRI). One full year of MODIS and SEVIRI active fire pixels beginning on 20 July 2008 were spatially and temporally sorted into 30 combinations of 10 grid cell resolutions (ranging from 0.05° to 0.5°) and three compositing periods (either 8, 16 or 32 days). We define the start/end of the fire season as the first temporal compositing period in which the cumulative number of AF pixels equals or exceeds 10%/90% of the annual total. At 0.05° spatial resolution and 16-day temporal resolution, for example, MODIS and SEVIRI identify an identical start to the fire season in 52% of the grid cells and an identical end in 43% of the grid cells. In the remaining grid cells, MODIS claims an earlier start and a later end more often than SEVIRI. The overall agreement between MODIS and SEVIRI increases as either the spatial or temporal resolution of the compositing scheme is degraded such that at the coarsest spatiotemporal resolution (0.5° and 32-days), for example, MODIS and SEVIRI identify an identical start to the fire season in 83% of the grid cells. Regardless of the map scale, there is less of an agreement between MODIS and SEVIRI when characterizing the end or the duration of the fire season. Results here demonstrate that care should be taken when (i) deriving fire regime characteristics from different remote sensing products, and (ii) when using such characteristics to evaluate large-scale simulations of fire occurrence.

Keywords: fire season, satellite-based active fire products, map comparisons, shared information

Introduction

Satellite-based active fire (AF) products are imperfect representations of the landscape fires burning at the time of image acquisition. Satellite images only contain a sample of all fire events (Eva and Lambin 1998), and the portrayal of these events depends on the spectral, spatial, and temporal resolution of the observation as well as the sensitivity of the active fire detection algorithm. Differences between AF products are most apparent at the pixel level and on an instantaneous basis, yet most interpretations of fire activity are not performed at the native resolution of the remote sensing product. Instead AF pixels are typically accumulated and analyzed at coarser spatiotemporal scales.

While recognizing the differences between polar-orbiting and geostationary AF products, this work explores the information potentially shared between the two. In particular we examine the start, end, and duration of the fire season in the Central African Republic (CAR) as depicted by the polar-orbiting Moderate Resolution Imaging Spectroradiometer (MODIS) and the geostationary Meteosat Spinning Enhanced Visible and Infrared Imager (SEVIRI). In addition to contributing to the definition of a fire regime, the timing of fire activity has been used to explain seasonal differences in fire behaviour and effects, land use practices, and emission factors (e.g., Govender et al. 2006; Bucini and Lambin 2002; Hoffa et al. 1999). Furthermore, maps of the fire

season derived from satellite-based remote sensing products are increasingly being used to evaluate large-scale models of fire occurrence (e.g., Thonicke et al. 2010). In terms of characterizing the timing of fire activity at a particular location, we hypothesize that the agreement between MODIS and SEVIRI will improve if compared at coarser spatiotemporal scales.

Data and methods

The MOD14/MYD14 (MODIS Terra/Aqua) active fire products are generated over the CAR nominally four times per day at 1 km spatial resolution (Justice et al., 2002). The SEVIRI active fire product is generated 96 times per day at a nominal 3 km spatial resolution (Roberts and Wooster 2008). One full year of MODIS and SEVIRI active fire pixels beginning on 20 July 2008 were spatially and temporally sorted into 30 combinations of 10 grid cell resolutions (ranging from 0.05° to 0.5°) and three compositing periods (either 8, 16 or 32 days). In contrast to Giglio et al. (2006), MODIS fire pixel counts were not adjusted to compensate for the overpass geometry, and neither the MODIS nor SEVIRI fire pixel counts were adjusted to compensate for cloud cover. Rather than defining the fire season based on the absolute number of fire pixels detected in a compositing period (e.g. Giglio et al. 2006; Chuvieco et al. 2008), we define the fire season based on the relative number of fire pixels detecting in a compositing period calculated with respect to the annual total (e.g., Dwyer et al. 1999; Clerici et al. 2004). Cumulative distributions of the number of AF pixels detected in 8, 16, and 32-day intervals were constructed in each grid cell. For both sensors, the start/end of the fire season was identified as the first compositing period in which the cumulative number of AF pixels equalled or exceeded 10%/90% of the annual total. The duration of the fire season was determined as the difference between the starting and ending compositing periods. To reduce the complexity of the maps, the start, end, and duration of the fire season were each assigned a numeric classification. For instance, all compositing periods with a start date before 31 Nov 2008 were assigned to 'Start Class 1.' Start, end, and duration classes thereafter depended on the temporal resolution of the map and were composed of 20 classes at 8-day resolution, 11 classes at 16-day resolution, and 7 classes at 32-day resolution. The overall agreement between the MODIS- and SEVIRI-derived maps of the fire season was calculated as the percentage of grid cells in the CAR that were assigned an identical class.

Results

Maps of the start classes, end classes, and duration classes as determined from the MOD14/MYD14 active fire products are presented in Figure 1. At 0.05° spatial resolution, 6.8% and 5.3% of the grid cells in the CAR do not contain a MODIS or a SEVIRI active fire pixel, respectively. These statistics suggest that in the majority of the CAR, one is not further than ~8km from an area burned in 2008/09. Also at this scale, 3.5% of the grid cells contain a SEVIRI fire pixel, but not a MODIS fire pixel. Given the coarser spatial resolution of SEVIRI, such grid cells can be explained by (i) a MODIS error of omission, (ii) the ability of SEVIRI to detect fires between the MODIS overpasses, or (iii) a SEVIRI error of commission. Nevertheless, 91.2% of the 0.05° grid cells in the CAR contain both a MODIS and SEVIRI fire pixel. Hence polar-orbiting

and geostationary AF products seem to offer a reasonable level of agreement when characterizing fire return intervals in the CAR at this spatial resolution.

Figure 1 also illustrates (i) histograms of the start, end, and duration of the fire season in the CAR as determined by MODIS and SEVIRI, and (ii) the difference between the MODIS and SEVIRI maps of the fire season in the CAR. At 0.05° spatial resolution and 16-day temporal resolution, MODIS and SEVIRI identify an identical start class in 52% of the grid cells and an identical end class in 43% of the grid cells. The reduced agreement between MODIS and SEVIRI when identifying the end class is attributed, in part, to the seasonal profile of fire pixel counts. At the onset of the dry season there is an abrupt, discernable increase in fire activity which quickly drives the MODIS and SEVIRI cumulative distributions above the 10% threshold. At the end of the dry season, however, a longer tail in the temporal profile of fire pixel counts imparts a greater uncertainty in the compositing period that eventually breaches the 90% threshold. Uncertainties in the start and end classes combine such that there is only 31% agreement between MODIS and SEVIRI when characterizing the fire season duration at this spatiotemporal resolution.
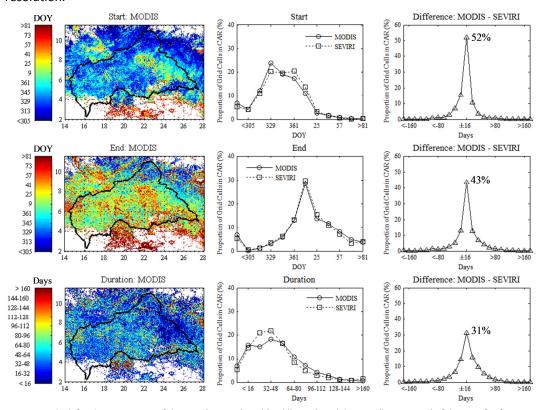

Figure 1. In the left column are maps of the start (top row), end (middle row), and duration (bottom row) of the 2008/09 fire season in the Central African Republic as determined from the MODIS active fire product. Fire pixels are sorted at 0.05° grid cell resolution (~5.57 km at the equator) and 16-day temporal resolution. The start and end classes are expressed in terms of the day of year (DOY), and the duration classes are expressed in days. In the centre column are the respective histograms of the start, end, and duration of the fire season as determined by MODIS and SEVIRI. In the right column are the respective differences (in days) between the MODIS and SEVIRI classifications.

From Figure 1, MODIS claims an earlier start to the fire season in 29% of the grid cells and a later start in 19% of the grid cells. In contrast, MODIS claims a later end to the fire season in 30% of the grid cells and an earlier end in 27% of the grid cells. At this spatiotemporal

resolution, obscuration by clouds and the presence of smaller and/or lower intensity fires at the beginning and end of the dry season are the most likely causes hindering the SEVIRI active fire detection algorithm and thus the ability of SEVIRI to more precisely recognize the start and end of the fire season. Consequently MODIS tends to claim a longer fire season than SEVIRI.
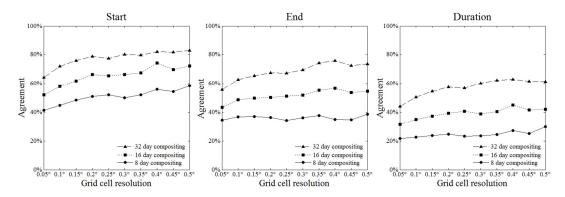

Figure 2. Overall agreement between the MODIS and SEVIRI maps of the fire season in the Central African Republic (CAR) as a function of spatiotemporal resolution. The agreement between MODIS and SEVIRI is calculated as the percentage of grid cells in the CAR that have an identical start (left), end (centre), and duration (right) of the fire season.

Figure 2 illustrates the agreement between MODIS and SEVIRI when characterizing the fire season at a variety of spatiotemporal resolutions. In general, the agreement between MODIS and SEVIRI improves as the grid cell resolution expands. Aside from assuaging the spatiotemporal nuances of the MODIS and SEVIRI sampling designs, an increase in the grid cell resolution provides a more synoptic view of fire activity. At 16-day temporal resolution, for example, the distribution of start classes in the CAR narrows as the size of the grid cells increase. That is, the proportion of extremely early start classes and extremely late start classes are reduced in favour of 'Start Class 4' (day of year = 329, 24 Nov 2008). Since both the MODIS and SEVIRI distributions become narrower at coarser grid cell resolutions, there is less opportunity for disagreement, and the overall agreement between the two sensors improves. Likewise, the agreement between MODIS and SEVIRI improves as the temporal compositing period expands. At the coarsest spatiotemporal resolution (0.5° and 32-days) MODIS and SEVIRI identify an identical start to the fire season in 83% of the grid cells. As with Figure 1, there is less agreement between MODIS and SEVIRI across all spatiotemporal scales when characterizing the end of the fire season, and even less when characterizing the duration.

Conclusions

MODIS and SEVRI offer reasonable, but not perfect, agreement when characterizing the start, end, and duration of the fire season in the Central African Republic. Results here demonstrate that care should be taken when (i) deriving fire regime characteristics from different remote sensing products, and (ii) when using such characteristics to evaluate large-scale simulations of fire occurrence. Although the fire season is characterized here based upon AF pixel counts, it is possible that further differences may arise if the fire season is alternatively characterized based on fire radiative power (FRP) or the number of days that a fire pixel is detected in particular grid cell.

References

Bucini, G., Lambin, E.F. 2002. Fire impacts on vegetation in Central Africa: a remote-sensing-based statistical analysis, Applied Geography, 22, 27-48.

Chuvieco, E., Giglio, L., Justice, C.O. 2008. Global characterization of fire activity: toward defining fire regimes from Earth observation data. Global Change Biology, 14(7), 1488-1502.

Clerici, N., Boschetti, L., Eva, H., Gregoire, J.-M. 2004. Assessing vegetation fires activity and its drivers in West - Central Africa using MODIS and TRMM data, International Geoscience and Remote Sensing Symposium (IGARSS), 3, 2087-2090.

Dwyer, E., Pereira, J.M.C., Grégoire, J.-M., and DaCamara, C.C. 1999. Characterization of the spatio-temporal patterns of global fire activity using satellite imagery for the period April 1992 to March 1993, Journal of Biogeography, 27, 57–69.

Eva, H. and Lambin, E.F. 1998. Remote sensing of biomass burning in tropical regions: sampling issues and multisensor approach, Remote Sens. Environ., 64, 292–315.

Giglio, L., Csiszar, I., and Justice C. O. 2006. Global distribution and seasonality of active fires as observed with the Terra and Aqua Moderate Resolution Imaging Spectroradiometer (MODIS) sensors, J. Geophys. Res., 111, G02016.

Govender, N., Trollope, W.S.W., and Van Wilgen, B.W. 2006. The effect of fire season, fire frequency, rainfall and management on fire intensity in savanna vegetation in South Africa, Journal of Applied Ecology, 43(4), 748–758.

Hoffa, E., Ward, D., Hao, W., Susott, R., and Wakimoto, R. 1999. Seasonality of carbon emissions from biomass burning in a Zambian savanna, J. Geophys. Res., 104(D11), 13841-1385.

Justice, C., Giglio, L., Korontzi, S., Owens, J., Morisette, J., Roy, D., Descloitres, J., Alleaume, S., Petitcolin, F., and Kaufman, Y. 2002. The MODIS fire products, Remote Sens. Environ., 83, 244–262.

Roberts, G., and Wooster, M. 2008. Fire detection and fire characterization over Africa using Meteosat SEVIRI. Ieee Transactions on Geoscience and Remote Sensing, 46(4), 1200– 1218.

Thonicke, K., Spessa, A., Prentice, I., Harrison, S., Dong, L., and Carmona-Moreno, C. 2010. The influence of vegetation, fire spread and fire behaviour on biomass burning and trace gas emissions: Results from a process-based model, Biogeosciences, 7, 697–743.

NATIONAL SCALE MAPPING OF BURNT AREAS AS A TOOL FOR THE EFFECTIVE DEVELOPMENT OF WILDFIRE MANAGEMENT STRATEGY. APPLICATION ON THE TWO DEVASTATING FIRE SEASONS OF 2007 AND 2009 IN GREECE

C. Kontoes[1], I. Keramitsoglou[1], I. Papoutsis[1], N. Sifakis[1], P. Xofis[2]

[1]Institute for Space Applications and Remote Sensing, National Observatory of Athens, Metaxa & Vassileos Pavlou Str, GR 152 36, Palea Pendeli, Athens, Greece. kontoes@noa.gr, ik@noa.gr, ipapoutsis@noa.gr, sifakis@noa.gr
[2]Forestry Directorate of Drama, Decentralized Administration of Macedonia and Thrace, Ag Konstantinou 1, Drama. pxofis@damt.gov.gr

Abstract

Wildfire forms, undoubtedly, one of the most significant driving forces in shaping the Mediterranean landscape with a history dating back to the first appearance of terrestrial vegetation of any kind. Despite the recent advances in both means and tactics in fire fighting, the extent, frequency and severity of wildfires is in-creasing dramatically and so do their detrimental effect. Most importantly, this situation is only going to deterio-rate, given the foreseen climate changes in the Mediterranean region and socio-economic changes occurring in the Mediterranean countryside. Thus, it is time to shift the focus from the current monothematic approach of fire suppression into an integrated fire management strategy. An integrated fire management has to consist of three distinctive but interrelated phases, namely: fire prevention, fire fighting and post-fire management.

The current study presents a semi-automatic methodology for large scale mapping of burnt areas at national level, based on a fixed thresholding method followed by photo-interpretation, known as BSM_NOA. The methodology was applied for the first time in 2006 and since then it is deployed operationally to map the massive forest fires over Greece including the major devastating events of 2007 and 2009 fire seasons. Ninety-nine satellite images of high (Landsat-5 TM, SPOT XS) and very high (FORMOSAT 2) spatial resolution, acquired shortly after the end of the two fire seasons were used for burnt area mapping. The results showed that in 2007 a total of 195,018 ha of burnt areas were mapped. The damages extended to an additional area of 32,175 ha because of the 2009 fires.

The generated Burn Scar and Damage Assessment products provide fire agencies and land managers with highly accurate and spatially consistent explicit data of wildfire dispersal over Greece for the two years which were the most devastating in the recent history of the country. The methodology presented here provides accurate spatial data on the affected areas which can be used for planning the pre and post fire management, both at national and local level, based on the historical ecology, current conditions and ecological peculiarities of a given area.

Keywords: Burn scar mapping; Wildfires; BSM_NOA; National scale

Introduction

Fire has had a significant impact on the current structure and composition of Mediterranean ecosystems, from the early stages of the establishment of Mediterranean climate (Naveh, 1975, 1999; Trabaud, 1987). For thousands of years fire constituted a natural factor with a regular periodic appearance and a positive role in ensuring the rejuvenation and productivity of Mediterranean ecosystems. However, the interaction between man and fire, altered the fire regime in many fire prone areas increasing dramatically fire frequency and turning, eventually, a natural ecological factor into a major disturbance factor and perhaps the most important threat for the conservation of Mediterranean Ecosystem's ecological integrity. As a result from the late 19th century a fire suppression policy has been adopted in many fire prone regions across the globe (Stephens & Ruth, 2005).

The fire suppression strategy, however, was developed under a rather narrow context, relying in most cases on improving fire fighting tactics and means alone. Despite the recent advances in fire fighting tactics and means and the increased amount of resources allocated in fire suppression (Bassi & Ketunnen, 2008), recent experience in Greece, Southern Europe and elsewhere demonstrates that the current policy of fire suppression is rather ineffective. Wildfires have became more catastrophic, affecting large areas and often with a significant cost in human lives.

Thus a careful reconsideration of the wildfire management strategy appears to be necessary in order to avoid the devastating impacts of wildfires in ecosystem's ecological integrity, society and economic activity. Such a strategy has to take seriously into account the historical and ecological role of fire as well as the contemporary patterns of wildfire distribution and behavior. Comprehensive, spatially consistent and highly accurate data on wildfire distribution and characteristics, at large national scales, are indispensable for the in depth understanding of wildfires phenomenon and subsequently the planning of an effective wildfire management strategy.

The current study presents a methodology for large scale burnt area mapping at national level which has been applied in two fire seasons, namely 2007 and 2009. The former is considered as the most devastating fire season ever recorded in Greece, where thousands of hectares of forested areas were affected and 69 civilians lost their lives. Such unusual events offer great opportunities for the study of wildfires patterns under extreme conditions and at the same time they demonstrate the huge limitations of the current wildfire policy. The 2009 fire season was not equally devastating but it mainly affected Attica, which is the most populated area of Greece with significant ecological, economic and social impacts.

Materials and methods

The BSM_NOA processing chain is a fixed thresholding approach. It relies on a combination of automatic processing of uni- and/or multi-temporal derived spectral indices (NBR, NDVI, multi date NDVI and ALBEDO) and a radiometric change vector analysis. The processing chain is divided into three main levels, namely BSM_NOA Pre-processing, BSM_NOA Core Processing, and BSM_NOA Post Processing. The full description of the methodology can be found in Kontoes *et al.* (2009).

In year 2007 (Figure 1, left), the BSM_NOA method was deployed over an area of 120,212 km^2 out of the 131,957 km^2 of Greece's territory, therefore covering the 91% of entire Greece. The remaining 9% of Greece was not affected at all by fires during the 2007 fire season. To cover the above mentioned large area, fifteen Landsat TM, two SPOT, and seventy-two FORMOSAT 2 images, from which 32 multispectral (8 m/pixel) and 32 panchromatic (2m/pixel) were acquired and used. The image data set required for the BSM_NOA service deployment over Greece was provided by ESA in the framework of the RISK-EOS/GSE project. Because of the severity of damages in the region of Peloponnese, it was decided to cover the entire damaged area with the FORMOSAT 2 very high spatial resolution images. Moreover the acquired Landsat TM and SPOT XS scenes covered the Administrative Regions at NUTS II level (Regions) of Peloponnese, Central Greece, Ionian Sea Islands, Epirus, Thessaly, Macedonia, and Thrace. The Regions of

Crete and Aegean Sea Islands were not processed as no significant wildfires occurred in this period.

In 2009 (Figure 1, right), the BSM_NOA service deployed in an area of 51,864 km^2 corresponding to the 39.3% of the entire Greece's territory. For this, a set of 10 full Landsat TM images has been used, covering the Administrative Regions at NUTS II level of Peloponnese, Central Greece, Ionia Sea Islands, Thessaly, Crete and Aegean Sea islands. The remaining areas in northern Greece remained unprocessed, as either no significant wildfires have occurred during the fire period of 2009 or no appropriate post fire satellite image could be retrieved.
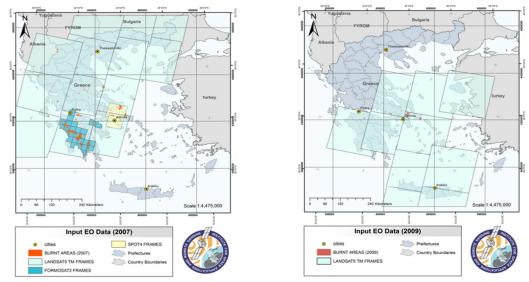

Figure 1. Satellite image distribution for mapping in 2007 (left), and 2009 (right)

Results

According to the results of the BSM_NOA service deployment, 256 wild fires were recorded in 2007 (fire size > 1 ha) and the total burnt area was 195,018 ha. In 2009 the total number of recorded fires was 144 and the corresponding total burnt area 32,175 ha. A classification of burnt area based on the Corine Land Cover maps shows that in 2007 44% of the burnt area was forests, 10% pastures, and 45% transitional woodland, shrub and other. In 2009 48% was forests, 10% pastures, 42% transitional woodland, shrub and other. In both seasons Southern Greece was affected much more than northern Greece as a result of the large fires in Peoloponnese in 2007 and the large fire of eastern Attica in 2009.

The fire size-frequency distribution is shown in Figure 2, and one can see that in 2007 approximately 90% of the fires had a size of less than 1000 ha while only 3.6% (nine fires) burnt more than 5000 ha each. In 2009 the situation is somewhat similar with 97.5% of fires having a size of less than 1000 ha and only 1.2 % (two fires) a size of more than 5000 ha. In fact the nine largest fires in 2007 burnt 142,716.5 ha or 73.2% of the total and in 2009 the two largest fires burnt 18,441.2 ha or 57.3 % of the total. If those extreme fires had been successfully suppressed then the total burned area would be approximately 52,302 ha in 2007 and 13,735 ha in 2009.
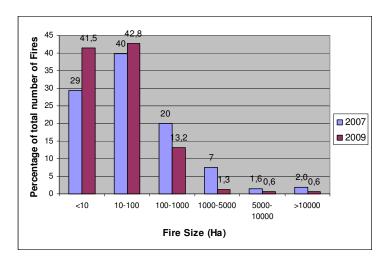
Figure 2. Fire size distribution for the two studied fire seasons

Discussion

The results presented above suggest that wildfires remain a significant threat for the environment and society despite the technological advances and the increased budget allocated to fire suppression. The southern and more arid parts of Greece are much more vulnerable to extreme fire events than the northern parts, threatening unique habitat types including the *Abies Cephalonia* forests of Attica and Peloponnese. The situation becomes even more critical given that those habitats have not developed mechanisms to undergo the detrimental effects of fire since their altitudinal distribution zone was, for thousands of years, above the fire prone zones of Mediterranean.

Of significant importance are the results regarding the fire size-frequency distribution. These results suggest that even for the devastating season of 2007 fire suppression was successful to the 90% of cases, restricting fires to a size of less than 1000 Ha, and only nine fire events turned a fire season from being usual to being the worst recorded ever. In 2009 fire suppression was successful to 97.5% of cases and two fire events alone, and especially the one in eastern Attica, was enough to characterize 2009 as a catastrophic fire season. In fact it is always the few large fires which determine the landscape patterns and cause detrimental effects to environment and society as suggested by Johnson *et al.* (2001).

These facts clearly demonstrate that the currently applied wildfire management strategy has reached its limits of effectiveness and can no longer be considered adequate for the protection of environment and society from wildfires. Although the summer of 2007 was characterized by the extreme weather conditions with three consecutive heat waves and wind patterns that favored the spread and intensity of fires there is no doubt that those weather patterns will occur again in the future and perhaps more extreme. The IPCC Forth Assessment Report (Christensen, *et al*., 2007) suggest that summer temperatures and precipitation are likely to increase and decrease, respectively, during the following decades leading to weather patterns that we have possibly never experienced or recorded before. Similar projections are given by other studies as well, including Mouillot *et al.*, 2002 and Carvalho *et al.*2011. Furthermore, fire

suppression, as it is currently applied, has been considered by many studies responsible for the transition from a fire regime with frequent small fires to a regime with less frequent large stand replacing fires (Minnich 1983, 2001), although this findings have been disputed by other authors (e.g. Keeley & Fotheringham 2001). Fuel build up in Greece and elsewhere in Mediterranean is thought to be also the result of countryside depopulation and the significant reduction of free grazing livestock in many mountainous areas, generating conditions that could favor large, high intensity stand-replacing fires.

The adoption of a contemporary and integrated fire management strategy appears inevitable if the phenomenon of wildfires is to be effectively controlled. The new strategy has to take seriously into account the historical role of fire in shaping the Mediterranean landscape as well as the contemporary setting in which wildfires occur. Fire should no longer be treated as the absolute evil which needs to be totally eliminated but it has to be treated as a "living organism" with a certain ecological behavior, distribution and dietary preferences. The aim of a contemporary wildfire management strategy has to be the conversion of a ravenous "organism" to an "organism" which is manageable and vulnerable to certain measures, but at the same time it will continue to play the highly significant historical and ecological role that has been playing for the last 3 million years in the Mediterranean region.

An integrated wildfire management strategy consists of three independent and interrelated phases, namely fire prevention, fire suppression and post fire management. The results presented in the current study can be used for the better planning of all three phases and offer a great tool to policy makers, land managers and agencies involved in wildfire management. It provides highly accurate data for the study and interpretation of wildfire distribution and behavior. Used in combination with highly accurate fuel maps it would provide extremely useful insights for the effective planning of fire prevention and allocation of resources for fire suppression. If additionally combined with highly accurate landcover and geomorphology maps the basis for the planning of post-fire treatments with focus on the most vulnerable areas where immediate intervention is required, is formed.

References

Carvalho, A. C.., Carvalho, A., Martins, H., Marques, C., Rocha, A., Borrego, C., Viegas, D. X., Miranda, A. I.. 2011. Fire weather risk assessment under climate change using a dynamical downscaling approach. Environmental Modelling & Software 26: 1123-1133.

Christensen, J.H., B. Hewitson, A. Busuioc, A. Chen, X. Gao, I. Held, R. Jones, R.K. Kolli, W.-T. Kwon, R. Laprise, V. Magaña Rueda, L. Mearns, C.G. Menéndez, J. Räisänen, A. Rinke, A. Sarr and P. Whetton, 2007: Regional Climate Projections. In: Solomon, S., D. Qin, M. Manning, Z. Chen, M. Marquis, K.B. Averyt, M. Tignor and H.L. Miller (eds.) Climate Change 2007: The Physical Science Basis. Contribution of Working Group I to the Fourth Assessment Report of the Intergovernmental Panel on Climate Change. Cambridge University Press, Cambridge, United Kingdom and New York, NY, USA.

Johnson, E.A., Miyanishi, K. & Bridge, S.R.J., (2001). Wildfire regime in the boreal forest and the idea of suppression and fuel build up. Conservation Biology 15: 1554-1557

Keeley, J. E. & Fotheringham, C. J. (2001) Historic fire regime in Southern California shrublands. Conservation Biology 15: 1536-1548

Kontoes, C.C., Poilvé, H., Florsch, G., Keramitsoglou, I., & Paralikidis, S. (2009). A Comparative Analysis of a Fixed Thresholding vs. a Classification Tree Approach for Operational Burn Scar Detection and Mapping, International Journal of Applied Earth Observation and Geoinformation, Vol. 11, Issue 5.

Minnich, R. A. (1983). Fire mosaics in Southern California and Northern Baja California. Science 219:1287-1294

Minnich, R. A. (2001) An integrated model of two fire regimes. Conservation Biology 15: 1549-1553

Mouillot, F., Rambal, S., Joffre, R., 2002. Simulating climate change impacts on fire frequency and vegetation dynamics in a Mediterranean-type ecosystem. Global Change Biology 8: 423–437.

Naveh, Z. (1975) The evolutionary significance of fire in the Mediterranean region. Vegetatio 29: 199-208.

Naveh, Z. (1999) The role of fire as an evolutionary and ecological factor on the landscapes and vegetation of Mt. Carmel. Journal of Mediterranean Ecology 1: 11-25.

Stephens S. L. & Ruth, L. W. (2005) Federal forest-fire policy in the United States. Ecological Applications 15: 532-542.

Trabaud, L. (1987). Fire and the survival traits of plants. In The role of fire in ecological systems (ed L. Trabaud), pp. 65-89. SPB Academic publishing, The Hague.

ASSESSMENT OF FIRE SELECTIVITY IN RELATION TO LAND COVER AT BROAD SCALE. A COMPARISON BETWEEN EUROPEAN COUNTRIES

S. Oliveira[1,2*], R. Boca[1], J. San-Miguel Ayanz[1], F. Moreira[3]

[1]*Institute for Environment and Sustainability, Joint Research Centre, European Commission;* [2]*Centre of Forestry Studies, Institute of Agronomy, Technical University of Lisbon. sandra.santos-de-oliveira@jrc.ec.europa.eu; sisoliveira@gmail.com;* [3]*Centre of Applied Ecology, Institute of Agronomy, Technical University of Lisbon*

Abstract

The behavior of a fire and its consequences are influenced, among other factors, by the underlying land cover. In this research, the relation between land cover types and fires was investigated at a broad spatial scale, by comparing the types of land cover most frequently affected by fires (fire selectivity) in several countries of Southern Europe. To assess fire selectivity, the selection ratio, defined as the ratio between the used and the available resources, was calculated; the used resources correspond to the proportion of each land cover type inside the fire perimeters, while the available resources correspond to the proportion of that same land cover type in a buffer created around each fire perimeter, representing the land cover existing before the fire occurred. The fire perimeters were obtained from the European Forest Fire Information System and land cover types were defined based on Corine Land Cover 2000 and 2006. The selection ratio was calculated for each land cover category for the entire study area and their significance assessed by estimating 95% confidence intervals.. The selection ratio was also calculated at country level and the results between countries were compared by means of the Kruskall-Wallis test. The selection ratio was also calculated for the topographic categories (4 classes of elevation, 7 classes of slope and 4 classes of aspect), to determine if land cover types within any of these categories were burned more than expected in the different countries.
Our results suggest a general tendency of fire selectivity in favor of grasslands and shrublands, while artificial surfaces, agricultural areas, transition natural-agriculture land and broadleaved forests burned less than expected. At country level, the results indicate different trends depending on the country, reflecting the dissimilar biogeographic characteristics, fire regimes, ignition patterns and the different management practices of the countries. Steeper slopes in southern exposures were more susceptible to burn in almost all the countries.
These findings contribute to understand the relation between fire and land cover distribution in different environmental and human conditions. The assessment of the most fire-prone land cover types in different countries can lead to the improvement of fire prevention strategies suitable to each country's situation.

Keywords: fire selectivity, land cover, burned areas, broad scale

Introduction

Land cover composition and the topographic conditions are two of the factors that influence fire patterns and their consequences in the landscape (Mermoz et al. 2005; Moreira et al. 2009; Viedma et al. 2009; Carmo et al. 2011). Understanding the relation between fires and the underlying land cover and topography is fundamental to define fire prevention and management strategies suitable to the area's characteristics. Previous studies at regional or national level investigated the relation between burned areas and land cover, focusing on the selectivity of fire towards specific land cover types. In Mediterranean areas, it was found that croplands, pastures and broadleaved forests were less affected by fire, while shrublands and coniferous forests were more susceptible to burn (Carmo et al. 2011; Moreira et al. 2001, 2009; Mouillot et al. 2003; Nunes et al. 2005). In Patagonia, shrubland and woodland were more susceptible to fire damage, while forest areas were less burned (Mermoz et al. 2005). In Canada, Black Spruce forests were more susceptible to fire as compared to deciduous forests

(Cumming, 2001). Carmo et al. (2011) also explored the selectivity of fire towards specific topographic conditions, having found that steeper slopes burned more than expected.

The main objective of this study was to analyze the relation between burned areas, land cover types and topographic conditions at a broad scale, with the purpose of:

- Assessing which land cover types are preferred or avoided by fire (fire selectivity) in Europe
- Analyzing the differences in fire selectivity between several European countries
- Exploring the potential influence of topographic conditions in fire selectivity

METHODS

Data collection

Burned areas were obtained from the European Forest Fire Information System (EFFIS), which maps the fire perimeters of approximately 40 ha or larger from MODIS satellite imagery at 250 m spatial resolution. In total, 8560 fires located in several countries were used for the analysis. Only the countries which had a minimum sample of 10 fires were selected (Figure 1).

Figure 1. Countries where fire perimeters were retrieved by EFFIS (n>10), between 2000 and 2008

The land cover data was obtained from the Corine Land Cover (CLC) map for the years 2000 and 2006 at a resolution of 100 m (EEA, 1994, 2002); this harmonized land cover database available at European level allows for comparisons between countries. The original 44 classes of CORINE were grouped into 8 larger categories of relative similarity with respect to fire, based on the potential influence of the land cover types in fire occurrence according to previous studies on this subject (Nunes et al. 2005; Moreira et al. 2009; Bajocco & Ricotta, 2008), namely broadleaved (brl), coniferous (cnf) and mixed forest (mix), shrubland (srb), grasslands and sparsely vegetated areas (grl), transition natural-agricultural areas (tna), agricultural areas (agr) and artificial surfaces (art). Topographic data was obtained from a Digital Elevation Model available for Europe, at 100 m resolution (Reuter et al. 2007; Jarvis et al. 2008). Elevation was divided in 4 classes (0-500 m; 500-1000 m; 1000-1500m and above 1500m); slope was divided in 7 classes (0-5%, 5-10%, 10-15%, 15-20%, 20-25%, 25-30% and above 30%) and aspect was divided in 4 main directions (N=315-45º, E=45-135º, S=135-225º and W=225-315º).

Data analysis

The methodology applied to assess fire selectivity is based on studies of resource selection in wildlife ecology (Manly et al. 1993) and in previous studies where similar methods were applied (Moreira et al. 2001, 2009; Bond & Keeley 2005; Nunes et al. 2005; Bajocco & Ricotta 2008; Carmo et al. 2011). The overall approach was to compare the land cover used (affected by the fires), represented by the burned areas, with the land cover available before the fire occurred, represented by a buffer of approximately the same shape and double the size of the burned area, created around each fire perimeter , including also the burned area. The selection ratio was calculated for each land cover category following the formula of Manly et al. (1993):

SR (n) = proportion of land cover type (n) used / proportion of land cover type (n) available

where SR is the selection ratio for each land cover type n; other factors are the proportions of land cover type used and available corresponding to the areas inside the fire perimeters and in the buffer, respectively, and n is each type of land cover considered. If the proportion of land cover burnt is higher than the proportion available within the buffer then SR > 1; this indicates that, the fire showed preference for that specific land cover type , i.e. burned more than expected by chance. On the contrary, if the proportion of land cover consumed by fire is lower than the proportion available then SR< 1, meaning that, this type of land cover was not preferred by the fire, i.e. burned less than expected based on its availability. SR for a given land cover type were averaged across the fires where it occurred.Confidence intervals (95%) were then estimated, in order to assess the significance of the values obtained. Using the same procedure applied to land cover, the relation between the topographic variables and fire selectivity was explored by calculating the selection ratio for each topographic category, in order to determine if specific topographic categories had burned more than expected in the different countries.

Results and discussion

The results of our study show that fires are selective regarding different land cover types in Europe. Grassland and shrubland were the land cover types generally preferred by fire, with a SR above 1 and significant at 95% level. Artificial surfaces, agricultural areas and transition natur_agric were the least preferred. Fig. 2 shows the number of countries in each SR condition per land cover category; coniferous and mixed forest showed the highest number of random situations (no significant SR), while transition natural-agriculture shows a significant low SR for all the countries. Shrubland and grassland present a significant SR >1 for more than half of the countries (n=7), while broadleaved forest has low SR for 9 countries.
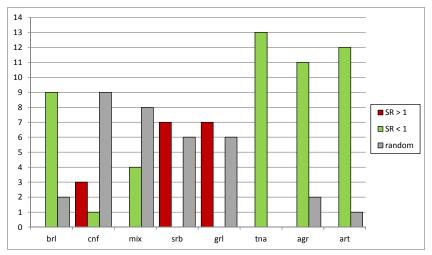
Figure 2. Number of countries (n=13) with significant SR >1, SR<1 or random, per land cover category. Cyprus was excluded for broadleaved (brl) and mixed forest (mix), due to lack of data.

At country level, it was found differences between countries for almost all the land cover categories (Fig. 3). Fires in Albania showed preference for grassland and shrubland, while in Bosnia & Herzegovina, Croatia and Turkey coniferous forest was the only land cover that significantly burned more than expected. In Bulgaria and France grassland was preferred to burn, while in Greece and FYROM shrubland was preferred instead. In Italy, Portugal, Serbia & Montenegro and Spain, both shrubland and grassland were preferred by fire.
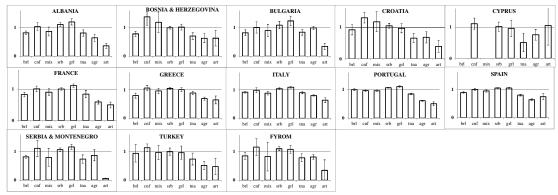

Figure 3. Selection Ratios per land cover category in each country and the corresponding confidence intervals at 95%

Previous authors found that shrubland and coniferous forests were more susceptible to burn in Portugal (Carmo et al. 2011; Moreira et al. 2001, 2009; Nunes et al. 2005, Silva et al. 2009) while agricultural areas were less burned, due to their low flammability. In Canada, conifers were also more susceptible to fire than deciduous forests (Cumming, 2001), while in the Great Lakes region in USA, Cardille and Ventura (2001) found instead that fires were more likely to occur in grassland and agricultural land, related to the accessibility of these areas to humans. In Patagonia shrubland and woodland were also more fire-prone than forests (Mermoz et al. 2005). This European wide preference of fire for grasslands and shrubland was to be expected, considering that these land cover types are easily ignited and highly flammable, independently of the place where they occur. The differences between countries could be explained by the

availability of the land cover types and the diverse biogeographic characteristics of each country, the management practices applied, the ignition patterns and the fire-fighting strategies (Silva et al. 2009; Moreira et al. 2009).

In relation to the topographic conditions, our results suggest that the selection ratio of topographic features is higher at higher altitudes, at higher slopes and in the southern aspect for most of the countries. However, general differences were found between the European Mediterranean region (EUMed) and the Balkans countries, with a higher proportion of fires occurring at higher altitudes in the Balkans in relation to the EUMed countries. This reflects the intrinsic differences in the biogeographic and human conditions of these two regions, which in turn affect the fire distribution patterns; besides, in the EUMed region, the majority of fires are human-caused (Leone et al. 2009; San-Miguel-Ayanz and Camia 2009) and population is mainly concentrated at lower altitudes (e.g. Catry et al. 2009), thus the abundance of ignition agents and the concentration of human activities at lower altitudes could explain the higher fire occurrence at elevations below 500m. The increasing fire proneness of higher slopes, particularly evident and significant in the EUMed countries, may be explained by the fact that the spread of fires is faster uphill (Rothermel 1983).

Conclusions

Understanding the relation between the underlying land cover, topography and fire behavior provides a valuable contribution for fire prevention strategies, by assessing the most and the least fire-prone areas. This study was a first attempt to characterize fire selectivity at a European broad scale. It revealed that shrubland and grassland are the most fire-prone land cover types in most countries due to its intrinsic vegetation characteristics, while agricultural areas are less fire-prone and could be used as fire breaks. The results obtained at country level suggest that the influence of the country's own environmental and human features in fire occurrence should be investigated more deeply in future studies.

References

Bajocco, S., Ricotta, C. 2008. Evidence of selective burning in Sardinia (Italy): which land-cover classes do wildfires prefer? Landscape Ecol. 23: 241–248.

Cardille J.A., Ventura S.J. 2001. Occurrence of wildfire in the northern Great Lakes Region: effects of land cover and land ownership assessed at multiple scales. Int J Wildland Fire 10:145–154

Carmo, M., Moreira, F., Casimiro, P., Vaz, P. 2011. Land use and topography influences on wildfire occurrence in northern Portugal. Landscape and Urban Planning 100: 169–176

Catry, F.X., Rego, F.C., Bação, F.L., Moreira, F. 2009. Modelling and mapping the occurrence of wildfire ignitions in Portugal. International Journal of Wildland Fire 18: 921–931.

Cumming, S.G. 2001. Forest type and wildfire in the Alberta boreal mixedwood: what do fires burn? Ecol. Appl. 11, 97–110.

EEA, European Environmental Agency, 1994. Corine Land Cover report. http://www.eea.europa.eu/publications/COR0-landcover

EEA-ETC/TE, JRC, 2002. CORINE Land Cover update: I&CLC2000 Project Technical Guidelines, August 2002

Jarvis A., Reuter, H.I., Nelson, A., Guevara, E. 2008. Hole-filled seamless SRTM data V4, International Centre for Tropical Agriculture (CIAT), available from http://srtm.csi.cgiar.org.

Leone, V., Lovreglio, R., Pilar Martín, M., Martínez, J., Vilar, L. 2009. Human Factors of Fire Occurrence in the Mediterranean. In Chuvieco, E. (Ed.), Earth Observation of Wildland Fires in Mediterranean Ecosystems, Springer, p.251

Manly, B., MacDonald LL, Thomas DL 1993. Resource Selection by animals: statistical design and analysis for field studies. Chapman and Hall, London.

Mermoz M, Kitzberger T, Veblen TT 2005. Landscape influences on occurrence and spread of wildfires in Patagonian forests and shrublands. Ecology 86:2705–2715

Moreira, F., Rego, F.C., Ferreira, P.G. 2001. Temporal (1958–1995) pattern of change in a cultural landscape of northwestern Portugal: implications for fire occurrence. Landscape Ecology 16: 557–567

Moreira, F., Vaz. P., Catry, F., Silva, J.S. 2009. Regional variations in wildfire susceptibility of land-cover types in Portugal: implications for landscape management to minimize fire hazard. International Journal of Wildland Fire 18: 563-574

Nunes, M.C.S., Vasconcelos, M.J., Pereira, J.M.C., Dasgupta, N., Alldredge, R.J., Rego, F.J. 2005. Land cover type and fire in Portugal: do fires burn land cover selectively? Landscape Ecology 20: 661-673

Rothermel, R. 1983. How to predict the spread and intensity of forest and range fires. USDA, Forest Service, Intermountain Forest and Range Experiment Station, General Technical Report INT-143.

San-Miguel-Ayanz, J. and A. Camia, 2009. Forest Fires at a Glance: Facts, Figures and Trends in the EU, in Birot Y. (Ed.) Living with wildfires: what science can tell us? A contribution to the Science-Policy dialogue, European Forest Institute, Finland, pp. 11-18.

Siegel, S., Castellan, N.J. 1988. Nonparametric Statistics for the Behavioral Sciences. McGraw-Hill, Inc., New York.

Silva, J.S., Moreira, F. Vaz, P., Catry, F., Godinho-Ferreira, P. 2009. Assessing the relative fire-proneness of different forest types in Portugal. Plant Biosystems 143 (3): 597-608

LAND USE CHANGE AND POST-FIRE IN SOUTHERN EUROPE

C.J. Kemper Pacheco[1,2], B. Duguy[3], D. Liberati[4]

[1]Department for innovation in biological, agro-food and forest systems (DIBAF), University of Tuscia, Via C. De Lellis, 01030, Viterbo, Italy; [2]Institute of agro-environmental and forest biology (IBAF), Area della Ricerca del C.N.R di Montelibretti. Via Salaria km 29.300, 00016, Monterotondo Scalo, Italy. claudia.kemper@mlib.imc.cnr.it.
[3]Dept. of Vegetal Biology, Faculty of Biology, University of Barcelona, Av. Diagonal 645 08028 Barcelona, Spain, bduguy@ub.edu; [4]Department for innovation in biological, agro-food and forest systems (DIBAF), University of Tuscia, Via C. De Lellis, 01030, Viterbo, Italy, dario.liberati@unitus.it

Abstract

The aim of this work was to assess the annual variations of land cover changes of forest areas affected by fires during the period (2000-2006) for European countries where data is available. Our study used a GIS-based methodology involving two CORINE Land Cover (CLC) maps, 2000 and 2006, and the EFFIS database available (since 2000 to 2006) at the JRC of Ispra. The studied countries were Portugal, Spain, France and Italy. We worked with the second CLC data level and when the results of the analysis indicated the occurrence of an important type of transition at a country level, the third CLC data level was used. The areas that were burned in each country for every year within the studied period were obtained from the annual fire maps of the EFFIS database. For each country, a set of seven masks (ArcGIS shape layers) was derived from these fire maps; i.e. one mask for each year from 2000 to 2006. Fires smaller than 50 ha were not included.

We Classified all the CLC transition classes into agradative, degradative or stable categories.We found clear differences between countries in the distribution of the total burned area respect to these three classification types.

The statistical data and map outputs represent a vast overview of changes in land use occurred in these four countries during the period 2000-2006. The most important land cover changes were in favour of "Transitional woodland-scrub" (classes 324) and were reported in all the years that were considered.

Our results suggest a slow post-fire vegetation dynamics in most of the countries studied.

The statistical characteristics of the EFFIS database in the period 2000-2006 along with the transformation of individual CLC classes during this period, and the percentage of their changes, have allowed us to make an accurate individualization of the studied classes to future changes in their land use.

Keywords: Land use change, Post-fire, GIS, EFFIS, CORINE Land Cover.

Introduction

The land use change is the main factor in causing biodiversity loss. The Mediterranean region has been affected by antropic disturbance for several years, and in this moment, it is one of the most significantly altered hotspots in the world (Falcucci et al., 2007). Unfortunately, wildfires in Southern Europe (Portugal, Spain, France, Italy and Greece) burn thousands of squared kilometres of forest, shrub lands, and grasslands every year. They cause extensive economical and ecological losses and, sometime human victims (C. Quintano et al., 2011). For this reason the study of the land cover change in burned areas and of the fire regime in Southern Europe has become fundamental.

The objective of our work was to assess the annual variations of land cover changes of forest areas affected by fires during the period (2000-2006) for European countries where data is available.

The countries studied were Portugal, Spain, France and Italy. Greece was excluded because the 2006 CLC map was not available for that country.

Methodology

Our study used a GIS-based methodology involving two CORINE Land Cover (CLC) maps, 2000 and 2006, and the European Fire Database (EFFIS) containing the annual forest fire information compiled by EU Member States and other European countries (http://effis.jrc.ec.europa.eu). The EFFIS database was used for the period 2000 - 2006.

We worked with the second CLC data level and when the results of the analysis indicated the occurrence of an important type of transition at a country level, the third CLC data level was used. The areas that were burned in each country each year throughout the studied time period were obtained from the annual fire maps of the EFFIS database. For each country, a set of seven masks (ArcGIS shape layers) was derived from these fire maps; i.e. one mask for each year from 2000 to 2006. Fires smaller than 50 ha were discarded from the mask (San-Miguel-Ayanz et al., in press).

Results

During the study period (2000-2006), the total burned area in the four considered countries was 1,395,119 ha. Half of this area (51%) consisted of CLC Level 2 class 32 ("Scrub and/or herbaceous associations"), followed by class 31 ("Forests") (34%). At CLC Level 3 fires affected mainly class 324 ("Transitional woodland-scrub"), corresponding to 23% of the total, class 312 ("Coniferous forest") (15%), followed by classes 311 ("Broad-leaved forest") (12%) and classes 313 ("Mixed forest"), 321 ("Natural grassland"), 322 ("Moors and heathland") and 323 ("Sclerophyllous vegetation"), representing each ca. 9% of the total burned area (San-Miguel-Ayanz et al., in press).

Overall, burned areas that suffered land cover changes became class main into 324 ("Transitional woodland scrub") mainly in Portugal and Spain and into 334 ("Burnt areas") in Spain, France and Italy respectively (Figure 1).

The statistical data and map outputs represent a vast overview of changes in land use occurred in this four countries during the period (2000-2006). The most important land cover changes were in favour of "Transitional woodland-scrub" (classes 324) and were reported in all analyzed years. In particular, land use change during the period 2000-2006, for each year, is reported in Figure 2.
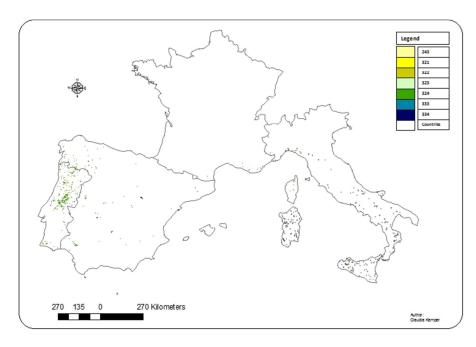
Figure 1. Burned areas where change in land use occurred. Code for land cover are: Land principally occupied by agriculture, with significant areas of natural vegetation (243); Natural grasslands (321); Moors and heathland (322); Sclerophyllous vegetation (323); Transitional woodland-scrub (324); Sparsely vegetated areas (333) and Burned areas (334).
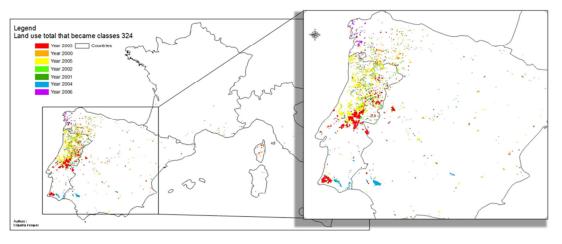

Figure 2. Land use total that became "Transitional woodland – scrub" (324) for year during the period 2000 – 2006 in Southern Europe.

The Classification of all the CLC transition classes into agradative, degradative or stable categories, shows clear differences among the considered countries in the distribution of the total burned area within these three classification types.

Conclusion

These results suggest a slow post-fire vegetation dynamics in most of the studied countries.
The statistical characteristics of the EFFIS database in the period 2000-2006 along with the transformation of individual CLC classes during this period, and the percentage of their changes,

have allowed us to make an accurate individualization of the studied classes respect to future further changes in their land use.

Acknowledgments

References

Falcucci A. and Maiorano L. 2007. Change in land-use/land cover patterns in Italy and their implications for biodiversity conservation. Landscape Ecol. 22:617 – 631.

Feranec J., Jaffrain G., Soukup T. and Hazeu G. 2010. Determining changes and flows in European landscapes 1990 – 2000 using CORINE land cover data. Applied Geography, 30, 19 – 35.

Quintano C., Fernandez-Manzo A., Stein A. and Bijker W. 2011. Estimation of area burned by forest fires in Mediterranean countries: A remote sensing data mining perspective. Forest Ecology and Management, 262, 1597-1607.

San-Miguel-Ayanz J., Camia A., Durrant T., Santos de Oliveira S., Boca R., Whitmore C., Giovando C. and Libertà G. 2010. Forest Fires in Europe 2009. Schmuck G., ISBN 978-92-79-16494-1.

San-Miguel-Ayanz J., Rodrigues M., Santos de Oliveira S., Kemper Pacheco C., Duguy B. and Moreira F., 2011. "Land cover change and fire regime in Southern Europe Forests", in Post-fire management and restoration of Southern Europe Forest Series Managing Forest Ecosystems, Springer, edited by Corona P., Moreira F. and Heras D., in press.

MONITORING TEN YEARS OF FIRE ACTIVITY IN WEST AND CENTRAL AFRICA

I. Palumbo, M. Clerici, J-F. Pekel, J-M. Gregoire

European Commission - Joint Research Centre, Institute for Environment and Sustainability, Via Fermi, TP 440, I-21027 Ispra (VA) ITALY. ilaria.palumbo@jrc.ec.europa.eu

Abstract

Fire has an important ecological role in many ecosystems worldwide, particularly in the African savannahs where the fire activity is regular and affects large areas every year. In the savannah fires contribute to maintain the balance between the herbaceous and the woody vegetation, and it can also stimulate grass regeneration with positive impacts on the animal community. Fire's effects can be positive or negative depending on the timing of burning, the rate of fire spread and the environmental conditions where fire occurs.

Besides its ecological role fire is also important for many land use practices like farming, agriculture and hunting. Understanding the temporal and spatial patterns of fire is therefore fundamental for an effective land manage-ment, civil protection and natural hazard control as well as for conservation purposes and the sustainable use of natural resources. As study area we chose Central and West Africa because this is a transitional region between the Sahara desert and the humid forests embracing different ecosystems. Our analysis provides information on the fire occurrence and its seasonality which can support fire management and decision makers. We used the MODIS active fire product from the year 2001 to 2011. For each year we considered the period from September to May to include the complete dry season. We arranged fire data in 10-day periods and applied a grid with 0.25 degree cell size. We determined, for each dry season, the number of decades when the first and third quartiles of the cumulative fire pixels were reached. Using this approach we also determined the length of the core fire season as the difference between the first and third quartiles (in decades). Results highlighted regional patterns in the temporal distribution and duration of fires, which were often associated to a change of ecoregion or the land cover type.

Keywords: MODIS, active fires, timing, fire management

Introduction

Fire is part of many ecosystems worldwide and it is used for different management practices as well. In Africa vegetation fires are particularly common in the savannah ecosystem and occur in large number every year across the continent. There are many positive effects associated with fires: they can improve vegetation structure limiting bush encroachment, they also stimulate vegetation renovation and can be used in conservation programs to maintain the habitat variability and therefore biodiversity (Mbow et al., 2000). In Africa fire is widely used by people in their daily activities (Hough, 1993); to mention a few fire is used to renovate the pasture for the cattle, prepare soil for new crops, gather firewood and improve visibility during the hunting activities.

Our analysis aimed at identifying fire patterns over time and space in Central and West Africa. In this region, from Senegal to Ethiopia, fires occur along a transition zone between the savannah and the forest domains. The objective of the study was to determine the fire distribution at regional and country level to support the design of effective fire plans and the environmental management.

Materials and methods

We analyzed ten years of MODIS fire data derived from the MODAPS (Davies et al., 2009) and MRR (Justice et al., 2002; Giglio et al., 2003) products to identify fire patterns and analyze their temporal trends. Both datasets are available at 1 km spatial resolution and provide daily information on the timing and location of the active fires. The MODAPS data cover the period from 2001 to 2010, whereas the MRR provides information for the year 2011 (not yet available on the MODAPS product).

We considered the region of West and Central Africa in the range of latitude between 20N and the equator. In this way we reached the desert limit at the northern boundary of the area of interest, beyond that limit fires are almost absent until the Mediterranean coasts of Morocco and Algeria, which we did not include in the study. In the northern hemisphere the dry season lasts from about October until May. Then, for the analysis we considered the period from the 1st of September until the end of May to cover a complete dry season in each year. The original satellite product has 1 km resolution, which is useful for applications at regional and local level, but can also produce noisy results when larger areas are considered. We therefore derived statistics and results at 0.25 degree resolution, which corresponds to an area of 25 by 25 kilometers, because this is a compromise for multiple scale analysis. We also used data at a different time step of the original daily observations. We cumulated the daily data over 10-day periods, per grid cell: this allowed to smooth out the effect of daily oscillation in the fire activity and facilitated the identification of temporal trends in the fire activity.

To study the temporal distribution of the active fires we computed the cumulative number of fire pixels for each year, at the end of the dry season. Then we derived the number of decades, from the beginning of the fire season, needed to reach the first and third quartile of the total fire pixels. We defined the core fire season as the difference, in decades, between the third and first quartile (Giglio, 2007; Roberts et al., 2009). We also determined the number of decades between the third quartile and the total fire counts. Each of these temporal steps is important to understand the dynamics of the fire activity, because the temporal distribution of fires during the dry season, informs about the type of burning and, consequently, on its effects on vegetation (Dwyer et al., 2000).

Results

1.1 *Fire occurrence*

The analysis of fire occurrence showed definite spatial patterns. We derived the maximum and minimum values of the fire counts during the ten years and show them in figure 1. In general we observed a latitudinal gradient with the highest values in the Sudanian and Guinea-Congolia/Sudania ecoregions.
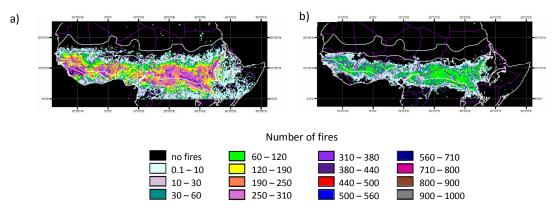
Figure 1. a) Maximum and b) minimum number of fire pixels. The ecoregions (White, 1983) and the country borders are indicated with a white line and a purple line, respectively.

The number of fires tends to increase in the inner part of the area, decreasing towards north, in the Sahel ecoregion, and south, in the Guineo-Congolian ecoregion. These patterns are largely related to the combination of the climatic conditions and fuel availability. Fire activity shows a sharp reduction on the eastern region along the limit between the Sudanian and Afromontane ecoregions, reflecting the strong eco-climatic difference of these regions. An exception to the general latitudinal gradient is found in Nigeria, where fires are less numerous (as minimum and maximum values) than in the surrounding areas. This difference is probably due to the high population density and the large proportion of agricultural land in this country. In summary, two regional bodies of fire activity are clearly evident: the West Africa one, from Senegal to Benin and the Central Africa one, from Cameroon to Sudan. The latter involving a larger area.

1.2   *Temporal analysis of the fire activity*

The results of the temporal analysis of the fire activity showed again clear geographic patterns related to the ecoregions and the land covers. Figure 2 shows the average number of decades, from the beginning of the dry season, to reach the first (figure 2a) and third (figure 2b) quartiles of the total fire counts. The longest durations were found in the Guineo-Congolian ecoregion with 12 to 21 decades to reach the first quartile and 15 to 24 for the third quartile. In the Sudanian ecoregion the first quartile showed a dominance of 6 to 9 decades duration, with the exception of Nigeria where the first quartile was usually reached later, after 9-12 decades. On the other hand, the third quartile had two dominant behaviours: a shorter duration (6 to 9 decades) in the western end (Senegal, Mali) and central-east (Sudan, Ethiopia); and a longer duration (12 to 15 decades or more) in the rest of the region. It is interesting to note that the areas where the first and third quartiles had short durations are dominated by deciduous woodlands, this vegetation type provides high levels of fuel availability and can explain the shorted time needed to reach 25% and 75% of the total fires. Another feature that can be observed in figure 2 is the inner delta of the Niger river in Mali: 15 to 18 decades are needed to reach the first quartile, while the surrounding region shows a much lower value, around 10 decades.

From the difference of durations between the first and third quartiles we also derived the length of the core fire season. As shown in figure 2 the time difference is usually very short (few decades), often less than 2 on average.
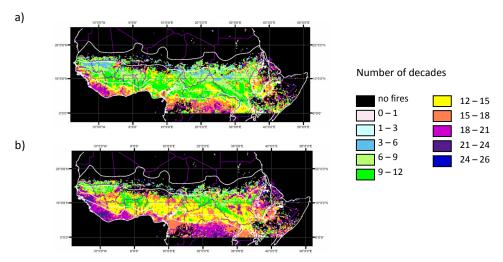
a)

b)

Figure 2. a) The average duration to reach 25% and b) 75% of the total fires. The ecoregions are indicated with a white line, the country borders are indicated with a purple line.

In order to characterize the end of the burning season (tail) we considered the number of decades needed to complete the last 25% of the fire counts (between the third quartile and 100% of the counts). In particular we considered the duration of the last 25% of fires where the third quartile was reached after more than 12 decades, in this way we isolated fires occurring in the mid or late dry season (figure 3).
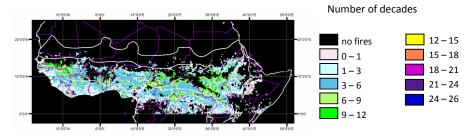

Figure 3. The average duration of the last 25% of the fires over grid cells where the third quartile was reached after more than 12 decades.

The duration of the tail follows a latitudinal gradient with most of the long-lasting tails in the Sudanian ecoregion. In this ecoregion we found tails lasting between 6-9 decades with few cases going up to 12 decades. The tail duration decreases moving southwards across the Guinea-Congolia/Sudania and the Guineo-Congolian ecoregions. We also found a decrease in the tail duration on the Eastern side at the border with the Afromontane ecoregion. On the Sudanian side the maximum tails reached the range 9-12 decades, whereas in the Afromontane ecoregion they were between 1 and 3 decades. In areas where the tail lasts longer than 6 decades we have late burnings, which are indicators of intense fires and have a strong impact on the vegetation cover. Therefore they are important to identify in any management plan.

Such late season fires are more difficult to control but might be extremely useful to limit bush encroachment and more generally to promote a proper variability of the natural habitats.

Conclusions

Our results showed definite spatial patterns in the distribution of the fire occurrence, in terms of fire counts and temporal trends. We observed a latitudinal gradient in the total number of fire counts with the highest values in the Sudanian and Guinea-Congolia/Sudania ecoregions. A strong reduction of the fire counts is visible towards the northern region of Sahel and the southern limit with the humid forest. The temporal analysis showed a general agreement in the patterns of the first and third quartile, especially in the area dominated by deciduous woodlands where both the first and third quartiles were shorter than the surrounding areas. At the same time, these quartiles had both longer durations in the Guineo-Congolian ecoregion. Additional information on the temporal trends was derived from the analysis of mid and late burnings. These were identified considering the regions with the third quartile duration greater than 12 decades. In these regions we considered the duration of the tail (last 25% of fire counts) to distinguish areas where late burnings were occurring. These types of fires tend to be more destructive and can be used, for example, to limit bush encroachment. Areas with late burnings were found in the Sudanian ecoregion, in Senegal and Mali, and in South-Sudan and Ethiopia.

This study provides new insights about the fire activity in terms of fire seasonality and occurrence of burning. These findings can support land managers and policy makers in their environmental management plans. Fire plans and prescribed burnings are crucial to improve biodiversity as well as the sustainable use of natural resources, which can only be designed with deep understanding of the fire patterns in time and space.

References

Davies, D.K., Ilavajhala, S., Wong, M.M., and Justice, C.O. 2009. Fire Information for Resource Management Sys-tem: Archiving and Distributing MODIS Active Fire Data. IEEE Transactions on Geoscience and Remote Sens-ing 47 (1):72-79.

Dwyer, E.; Pereira, J.M.C.; Grégoire, J.-M.; Dacamara, C.C. 2000. Characterization of the spatio-temporal patterns of global fire activity using satellite imagery for the period April 1992 to March 1993. J. Biogeogr. 27, 57-69.

Giglio, L., J. Descloitres, et al. 2003. An Enhanced Contextual Fire Detection Algorithm for MODIS. Remote Sens-ing of Environment 87 (2-3): 273-282.

Giglio, L. 2007. Characterization of the tropical diurnal fire cycle using VIRS and MODIS observa-tions. Remote Sens. Environ. 108, 407-421.

Hough, J.L., 1993. Why burn the bush? Social approaches to bush-fire management in west African national parks. Biological Conservation, 65(1993), 23-28.

Justice, C.O., Giglio, L., Korontzi, S., Owens, J., Morisette, J.T., Roy, D., Descloitres, J., Alleaume, S., Petitcolin, F., and Kaufman, Y. 2002. The MODIS fire products. Remote Sensing of Environment 83, 244-262.

Mbow, C.; Nielsen, T.T.; Rasmussen, K. 2000. Savanna fires in east central Senegal: distribution patterns, resource management and perceptions. Hum. Ecol. 28, 561-583.

Roberts,G., Wooster, M.J., and Lagoudakis, 2009. E. Annual and diurnal african biomass burning temporal dynamics. Biogeosciences, 6, 849–866,.

White F. 1983. Vegetation map of Africa. (UNESCO: Paris).

OPERATIONAL USE OF REMOTE SENSING ON FOREST FIRES IN EUROPE: REAL-TIME PROCESSING AND POST DISASTER INFORMATION MANAGEMENT.

E. Stein, E-M. Bernhard, C. Strobl, G. Strunz

DLR, German Aerospace Center, German Remote Sensing Data Center, Dpt. Civil Crisis Information and Geo-Risks, 82234 Oberpfaffenhofen, Germany. Enrico.Stein@dlr.de

Abstract

Every year forest fires occur across Europe. In the Mediterranean Region (Italy, Portugal, Greece and Spain) the number of fires has increased over the past decades. In 2009 more than 320.000 hectares of land were lost due to forest fires. Forest fires require immediate action and reaction in order to prevent damages to life, private property and ecosystems. Furthermore, forest fires affect global warming due to rising CO_2-emissions. Knowledge about past fire events and the damage they caused will greatly enhance the knowledge base that will allow for a better understanding of the risks, and increase the forecasting quality of fire scenarios.

In this context the Center for Satellite Crisis Information (ZKI) covers several activities of the disaster manage-ment cycle. The ZKI is a service of the DFD (German Remote Sensing Data Center) of DLR (German Aerospace Center). It provides a 24/7 service of rapid provision, processing and analysis of satellite imagery during natural and environmental disasters, for humanitarian relief activities and civil security issues worldwide.

To provide information about forest fires a burnt-area mapping tool was developed. This semi-automatic, ob-ject-based, multi-sensor rapid mapping algorithm is based on very high resolution (VHR) optical (like Spot) as well as radar (TerraSAR-X) remote sensing data. The algorithm includes a decision-tree classifier, which relies on spectral indices, e. g. MSAVI (Modified Soil-adjusted Vegetation Index) and BAI (Burnt Area Index).

To reduce the limitations in optical data due to the cloud cover and/or haze, the algorithm was improved with a change detection technique based on image differencing, rationing and the NCI (Normalized Change Index) of TerraSAR-X data.

Next to these rapid mapping activities the ZKI offers an automatic operational service on active fire detection from space. Based on MODIS (Moderate Resolution Imaging Spectroradiometer) data from Terra-1 and Aqua-1 satellites a Web Processing Service (WPS) generates fire hot spots. Two X-band antennas which are operated by the DFD enable near real-time receiving and processing of MODIS data. The MODIS based fire service is acces-sible for everybody through the ZKI Internet Portal.

Keywords: forest fires, disaster management, burnt area mapping, hot spot detection

Introduction

Wildfires are one of the main causes of forest destruction in the countries of the Mediterranean Basin. About 50000 fires sweep through 700000 ha of forest and agricultural land each year, causing enormous economic and ecological damage as well as loss of human life. Globally, and particularly in European countries located in the Mediterranean Basin, the frequency of wildland fires has significantly increased in the recent years. The increase of forest fire occurrences in the Mediterranean basin is due to the land-use changes (rural depopulation increases land abandonment and consequently, fuel accumulation) and climatic change (which is reducing fuel humidity and increasing fire risk and fire spread) (Chuvieco 2009). Natural wildland fires are caused by lightning, sparks from falling rocks, volcanic activity, natural heat waves and many other causes which can act as natural fire ignition source. But the primary cause of wildland fires is human activities. According to a study conducted by the European Commission over 80% of the forest fires in the Mediterranean Basin are caused by human

activities. While the vast majority of wildfires are anthropogenic, the risk of such fires is expected to increase in forthcoming years under the impact of climate change. The vegetation becomes more inflammable (due to thermal stress and drought) and fire services are faced with difficulties when trying to suppress a fire due to increased inflammability and water shortage.

Civil Protection Services, Forest Fire Services and Environmental Services were faced with the management of multiple fires, the evolution of simultaneous extensive fire fronts and the monitoring of heavy smoke emitted during wildland fires. Timely and reliable detection of new outbreaks is particularly crucial for effective wildfire management, particularly in largely inaccessible mountainous areas.

Near real time tracking and monitoring of active hot spots is also very important during crisis management concerning the optimal distribution of ground and aerial forces (Sifakis et al. 2011). The role of satellite observations in the resolving of the previous issues has considerably increased during the last twenty years as the spatial, spectral and temporal characteristics of the sensors have been constantly improving, and new methods for the exploitation of satellite data have been developed (Gitas et al. 2009; Justice et al. 2001; Lentile et al. 2006).

According to the management disaster cycle, which represents the different stages before and after a disaster, the following points should be taken into a consideration of any type, but especially for wildland fires: prevention/preparedness (e.g. fire risk), emergency response (e.g. fire locations, burn scars, affected infrastructure) and recovery (e.g. monitoring of the fire effects).

The main objective of the presented paper is emergency response activations. Next to the rapid mapping services (see chapter 2) the DLR/ZKI offers an operational service on active fire detection from space (ZKI-Fireservice, 2011) (see chapter 3).

Burnt area mapping

After the occurrence of a natural or man-made disaster the necessity of fast and reliable spatial information is important not only for crisis control centers but also for relief organisations and rescue teams. Civil protection authorities have to meet the demand for adequate crisis information in order to ensure an appropriate decision process and an effective crisis management. Therefore all possibilities obtaining spatial crisis information have to be taken into account, particularly earth observation data proved to provide significant information input. In order to cover these user requests in crisis situations, DLR set up a rapid mapping service to ensure fast access to available, reliable and affordable crisis information worldwide. After the mandatory decision process whether satellite analysis is appropriate for the respective crisis, the area of interest has to be defined and cross checked to avoid false geo location. Following this iterative process, it has to be assured that all applicable satellites are programmed for data acquisition. This can either be coordinated within the International Charter "Space and Major Disaster" or a GMES initiative like the project SAFER (supported by the Seventh European Frame Work Programme) by the responsible project manager, or through commercial satellite tasking. According to the requirements of the user, the information products are delivered in the form of maps, GIS-ready geodata or dossiers which are then used to support disaster management operations, humanitarian relief activities or civil

security issues. The rising number of natural disasters, humanitarian emergency situations and threats to the civil society increases the demand for timely and precise information on many different types of scenarios and situations. ZKI uses all kinds of satellite imagery for the extraction of relevant crisis information like flood extent, damaged infrastructure, burnt areas or evacuation areas. Besides response and assessment activities, ZKI derives geo-information products for the use in medium term rehabilitation, reconstruction and crisis prevention activities. It operates in national and international context, closely networking with German public authorities at national and state level, non-governmental organisations, satellite operators and space agencies. Since 2003 the ZKI prepared about 35 maps in 11 activations in the context of wildfires (http://www.zki.dlr.de/).

In this chapter an operational object-based algorithm for burnt area mapping will be presented using the example of wildland fires that occurred in Greece and La Palma during July and August 2009. The algorithm is based on SPOT5 (data pair before and after the fires in La Palma and one post-disaster scene in Greece) and TerraSAR-X StripMap (two data pairs before and after the fires in Greece and one data pair in La Palma) images. The applied pre-processing for the optical images includes orthorectification, topographic normalization, co-registration to the other satellite data and atmospheric correction. The radar images were multi-looked to a resolution of 3x3 meters per pixel, filtered (Gamma-DE-Map), radiometrically calibrated, geocoded, orthorectified, topographically corrected and converted to the radar backscatter coefficient sigma nought. Due to a lack of ground truth data, the accuracy of the algorithm was assessed by using the fire perimeter that resulted after visual interpretation of the SPOT5 images and digitalization of the image and additional data from the European Forest Fire Information System (EFFIS).

A backscatter and reflectance analysis of burnt and unburnt objects was applied to the pre-processed SPOT5 and TerraSAR-X scenes. The single- as well as the multi-temporal analysis of the SPOT5 data showed highly different values over burnt areas compared to the unburnt parts. The separability between affected and unaffected areas was highest in the NIR and MIR infrared bands. Therefore, the indices MSAVI, BAI and NDSWIR were applied for classification to avoid misclassifications between burnt areas, cloud shadows, coastal areas and open space. The single-temporal analysis of the TerraSAR-X data showed only slightly higher backscatter values over burnt areas compared to the unburned parts, which turned out as insufficient for burnt area detection. However, the multi-temporal backscatter analysis showed a clear increase over the burnt areas compared to the pre-disaster image. The VV-polarization difference values were higher (3.4 dB) than the HH difference values (1.6 dB). These higher backscatter difference values can be explained by the fact that vertical polarization is more sensitive to vertically oriented objects than horizontal polarization. Vertical polarization interacts stronger with remaining stems, also strengthened through the double bounce effect arising between stems and the ground. This leads us to the assumption that burnt area mapping might profit from the use of VV polarized data instead of HH polarized data.

All pre-processed satellite images were analyzed in the eCognition Developer software, and the algorithm has been developed in cognition network language (CNL). The object-based segmentation and classification was separately applied to both data types. In the case of optical

images the burnt area detection was possible with post-disaster images only as well as with pre- and post-disaster images. Whereas with radar images, forest fire detection was just possible with a comparison of pre- and post-disaster images. Both data types were integrated into one algorithm. In order to simplify and accelerate image classification, a user friendly graphical user interface (GUI) in eCognition Architect - with which all parameters used can be modified interactively - was generated.

Burnt areas do not show any uniform texture or shape characteristics. In order to receive a useful segmentation, a two-dimensional segmentation approach was applied. For the optical images, the spectral information of the near and middle infrared bands was of the highest interest, whereas for the radar images, the change information between before and after the fires was significant. Therefore, three different change detection techniques (image differencing, image rationing and the Normalized Change Index) were calculated and used for segmentation. The second step was the classification of the burnt areas. In case of the optical images the classification was based on the indices MSAVI, NDSWIR and BAI. To avoid misclassifications, most unburned parts of the image were excluded by a fuzzy classification using the indices MSAVI and NDSWIR. Subsequently, cloud shadows were extracted with the help of the normalized middle infrared. Finally, the burnt area was classified by means of a fuzzy classification approach containing the MSAVI, BAI and NDSWIR. The applied classification steps are threshold based, whereas the threshold values were determined by literature review and visually by an iterative approach. In order to take multi-temporal data sets into account, a change detection algorithm was developed as well. Therefore, a fuzzy approach based on the reflectance differences between pre- and post-disaster objects was used. For this purpose, the temporal difference of the previously listed spectral indices was used (dBAI, dMSAVI, dNDSWIR). The optical burnt area classification showed an overall accuracy of 91% for the single-temporal approach and an overall accuracy of 95% for the multi-temporal approach.

The radar classification procedure was based on the change information between pre- and post-disaster images. In a first step areas covered by water were extracted in order to avoid misclassifications. Subsequently, the information given by the previously calculated difference, ratio and normalized change index layer was used for burnt area detection. The classification result of the radar algorithm achieved an overall accuracy of 78%.

The goal of the work was to exploit the advantages of both optical and radar data. Radar data are generally less intuitive in interpretation (for untrained image analysts) than optical images, but offer high acquisition rates due to their ability to penetrate clouds and haze, and their independence of sun illumination (Attema et al., 1998). Thus, the burnt area algorithm first detects burnt areas in the optical satellite image. If cloud or cloud shadows preclude the burnt area, the radar classification is considered. Is an object classified as cloud or cloud shadow in the optical image, but as burnt in the radar image, than it gets finally classified as burnt. Thus, the whole image, also containing regions covered by clouds and cloud shadows, can be analyzed and the burnt area can be detected (figure 1). With regard to the high accuracy of the classification it should be noted that transferring the algorithm to other regions in the Mediterranean Basin normally leads to modifications of the thresholds (Polychronaki & Gitas, 2010). This depends on the following reasons:

- differences in the atmospheric conditions of the optical images,
- differences in the degree of burn severity,
- differences in topography and land cover,
- differences in the time period between the fire incident and the acquisition of the satellite images and the existence of old fire scars and recently burnt areas in the same image.

The transferability of the algorithm was assessed by applying it to other wildland fires sites in Sardinia and Greece, where devastating fires occurred in 2009, respectively 2007.
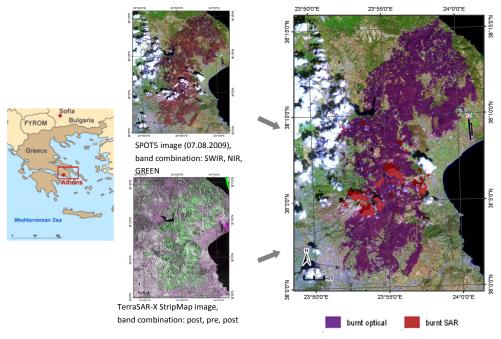

SPOT5 image (07.08.2009), band combination: SWIR, NIR, GREEN

TerraSAR-X StripMap image, band combination: post, pre, post

Figure 1. Fires in Greece 2009. Mapping of the burnt areas with SPOT5 and TerraSAR-X data.

MODIS - Active Fire Detection

Based on data of the NASA owned MODIS sensors on board of the Terra-1 and Aqua-1 satellites, wild and forest fires can be detected. Users can view, download and automatically receive information on current fires in Europe. The MOD14 algorithm used for fire detection was developed at the University of Maryland and is an internationally acknowledged standard. In Europe, the German Remote Sensing Data Center (DFD) is the only institution operating two X-band antennas enabling it to receive and process observation data from both satellites simultaneously and allowing for up to eight daily observations. DFD is offering its capability to the European community and its people providing daily hot spot detection free of charge. The software has been developed in close cooperation between Mexico's National Commission on Biodiversity Research (Conabio) and DFD. The MOD14-based processing chain is now running in a WPS frame work which enables the easy implementation of further processes like the calculation of cloud cover or land surface temperature. This could be also the technical pre-condition for the creation of higher level products like the determination of the daily fire risk, which is actually under development.

Conclusion

In the presented paper a short overview over the activities of the DLR-ZKI is given. The example shows, that earth observation can successfully provide a beneficial support for an operational burnt area mapping. The multisensoral, fast but at the same time precise algorithm is a highly useful tool for the detection of wildland fires and the resulting burnt areas in the European Mediterranean. The integration of the burnt area mapping algorithm (ruleset) into a user friendly graphical user interface (GUI) in eCognition Architect supports the operational efficiency during a disaster event. Because of the large spatial extent and high spatial and temporal variability of wildfires, robust near real time post-fire monitoring tools are needed on the one hand to inform humanitarian relief activities and civil security issues and on the hand to an improved adaptive management and advance the understanding of post-fire vegetation response rates and ecosystem health. In combination with additional geographic data (e.g. land cover), possible threats to properties, infrastructures and to human life can be predicted and ideally, mitigated. Low-cost, rapidly available, and accurate assessment of landscapes following the disaster will lead to improved predictive capabilities and more informed management decisions (van Leeuwen et al., 2010).

References

Attema, E., Duchossois, G., Kohlhammer, G. 1998. ERS-1/2 SAR land applications: Overview and main results. IEEE – geoscience and remote sensing symposium, IGARRS: 1796-1798.

Chuvieco, E., 2009. Global impacts of fire. In: Chuvieco, E. (Ed.): Earth observation of wildland fires in Mediterranean ecosystems. Heidelberg, Springer-Verlag GmbH: 1-11.

Gitas, I., De Santis, A., Mitri, G., 2009. Remote sensing of burn severity. In: Chuvieco, E. (Ed.): Earth observation of wildland fires in mediterranean ecosystems. Heidelberg, Springer-Verlag GmbH: 129 - 149.

Lentile, L. B.; Holden, Z. A.; Smith, A. M. S.; Falkowski, M. J.; Hudak, A. T.; Morgan, P.; Lewis, S. A.; Gessler, P. E., Benson, N. C., 2006. Remote sensing techniques to assess active fire characteristics and post-fire effects. International Journal of Wildland Fire 15: 319-345.

Pausas, J. G., Llovet, J., Rodrigo, A., Vallejo, R., 2008. Are wildfires a disaster in the Mediterranean basin? - A review. International Journal of Wildland Fire 17: 713 - 723.

Polychronaki, A., Gitas, I. Z., 2010. The development of an operational procedure for burned-area mapping using object-based classification and ASTER imagery. International Journal of Remote Sensing 31(4):. 1113 - 1120.

Justice, C., O., Koronzti, S., 2001. A review of the status of satellite fire monitoring and the requirements for global environmental change research. In: Ahern, F. (Ed.): Global and regional vegetation fire monitoring from space: planning a coordinated international effort, SPB Academic Publishing BV, Amsterdam,. 1 - 19.

Sifakis, N. I., Iossifidis, C.; Kontoes, C., Keramitsoglou, I., 2011. Wildfire Detection and Tracking over Greece Using MSG-SEVIRI Satellite Data. Remote Sensing 3: 524-538.

van Leeuwen, J.D.W., Casady, M. G.; Neary G. D.; Bautista, S.; Alloza, A. J.; Carmel, Y.; Wittenberg, L.; Malkinson, D. Orr, J. B, 2010. Monitoring post-wildfire vegetation response with remotely sensed time-series data in Spain, USA and Israel. International Journal of Wildland Fire 19: 75-93.

ZKI-Fireservice, 2011. ZKI-Fireservice, Map. http://www.zki.dlr.de/fireservice/map (accessed 10 Aug. 2011).

POSITIVE AND NEGATIVE EVIDENCE OF BURN FROM SPECTRAL INDICES FOR BURNED AREA MAPPING IN MEDITERRANEAN REGIONS

D. Stroppiana[1], G. Bordogna[2], M. Boschetti[1], P. Carrara[1], L. Boschetti[3], P.A. Brivio[1]

[1]IREA-CNR, Via Bassini 15, 20133 Milano, Italy. stroppiana.d@irea.cnr.it; boschetti.m@irea.cnr.it; carrara.p@irea.cnr.it; brivio.pa@irea.cnr.it
[2]IDPA-CNR, via Pasubio 5, 24044 Dalmine (BG), Italy. gloria.bordogna@idpa.cnr.it
[3]Department of Geography, Univ. of Maryland, College Park, MD, USA 20740. luigi@hermes.geog.umd.edu

Abstract

We propose a method to map burned areas from single date Remotely Sensed imagery by integrating partial positive evidence of burn provided by multiple Spectral Indices (SIs). The method exploits a region growing algorithm where seeds and maximum growing boundaries are revised with negative evidence of burn brought by the indices. Six Landsat TM images were acquired for the year 2003 over Portugal, Spain, Greece, southern France and Croatia and a set of eight SIs were computed from the surface reflectance measured in the TM bands (NBR, NBR2, NDVI, CSI, SAVI, MIRBI, EVI, EVI2). Training pixels were collected over burned areas, topographic and cloud shadows, water and vegetation and used to define the membership functions of positive and negative evidence of burn. The membership degrees of partial evidence were integrated with soft computing techniques to derive layers for seed selection and region growing. The negative evidence is used for revising the positive evidence of burn brought by the indices to reduce the commission errors. We assessed the accuracy of the proposed method for a TM scene acquired over Portugal (path/row 203/034) and found that the use of negative evidence of burn reduces the commission error from 59% to 1% and increases the overall accuracy from 41% to 91%.

Keywords: fire, Landsat TM, multi-criteria approach, fuzzy membership functions

Introduction

Vegetation fires play a key role in biogeochemical cycles at the local, regional and global scales (Crutzen and Andreae 1990) and they are the major disturbance factor of forested ecosystems (Thonicke et al. 2001). Despite the fact that fire is the most important damaging agent in southern Europe, most of the Mediterranean countries lack systematic monitoring of fire perimeters. Remote sensing techniques are now recognized as the only cost-effective source of information for mapping burned areas at regional/national scale. However, algorithm development is still an open issue when dealing with high/very high resolution data for which systematic fire products have not been developed yet. The Landsat TM/ETM+ sensors were proven suitable for the Mediterranean environment and Spectral Indices (SIs) have been often used for mapping fire perimeters (Bastarrika et al. 2011). We propose a method for mapping burned areas in Mediterranean regions from single date Landsat TM images. It relies on the convergence of positive evidence of burn brought by SIs and on the use of negative evidence for reducing the commission error due to spectral confusion between burns and low albedo surfaces. In particular, it consists of a region growing algorithm where the seed and growing layers are derived from the integration of the SIs performed with soft computing techniques. The approach described here is the result of the continuous improvement of previous work (Carrara et al. 2009; Stroppiana et al. 2009; Boschetti et al. 2010) aiming at building a robust method applicable at regional scale.

The proposed method and the data

The flowchart of the proposed method is shown in Fig. 1. First, a set of SIs are computed from the TM bands and converted to layers of partial positive and negative evidence of burn through soft constraints (μ_{SI}). Second, the layers of the membership degrees of the positive evidence are integrated into the layer for candidate seed selection (PE_{seed}) and candidate region growing boundary (PE_{grow}) by applying two distinct partially compensative integration operators: a strict convergence of evidence for candidate seeds and a looser convergence for region growing maximum boundary. The membership degrees of negative evidence are integrated into the overall layer of negative evidence (NE) with a completely compensative integration operator of the t-co-norm family (the max). The layer NE is used to revise the integrated layers used for seed selection ($rPE_{seed}=PE_{seed}-NE$) and for growing ($rPE_{grow}=PE_{grow}-NE$). A set of seed burn pixels is selected from rPE_{seed} to be grown over the layer rPE_{grow} to derive the final burned area map.
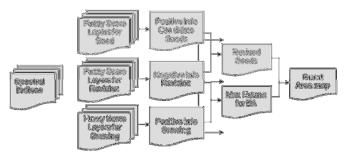

Figure 1. The flowchart of the proposed method for mapping burned areas from spectral indices.

1.1 *The experimental dataset*

Landsat TM images were acquired in 2003 over Portugal (Path/Row 203/034 and 204/032, dates: 24/10 and 12/08), Spain (202/032, 15/09), France (195/030, 14/09), Croatia (189/029, 04/09) and Greece (184/034, 2003/10) and processed to derive surface spectral reflectance (ρ_i) in the TM bands (i=1,..,7) (Masek et al., 2006). Eight SIs were computed: NDVI ($\rho_4-\rho_3/\rho_4+\rho_3$) (Rouse et al., 1973),   NBR ($\rho_4-\rho_7/\rho_4+\rho_7$) and NBR2 ($\rho_5-\rho_7/\rho_5+\rho_7$) (Key and Benson, 1999), MIRBI ($10\rho_7-9.5\rho_5+2$) (Trigg and Flasse, 2001),   CSI (ρ_4/ρ_5) (Smith et al., 2005),   SAVI ($\rho_4-\rho_3$)(1+L)/($\rho_4+\rho_3+L$) (Huete 1998), EVI ($G*(\rho_4-\rho_3)/(\rho_4+C1\rho_3-C2\rho_1)$) (Huete et al., 2002), EVI2 ($G*(\rho_4-\rho_3)/(\rho_4+C3\rho_3+1)$) (Jiang et al., 2008), where L=0.5, G=2.5, C1=6, C2=7.5 and C3=2.4. The NDVI enhances the signal of green vegetation and, although several authors pointed out that it is not the best index for burned area mapping (e.g. Pereira et al., 1999), it is still widely used. The Soil Adjusted Vegetation Index (SAVI) is derived from the NDVI to correct for its sensitivity to soil colour and moisture whereas the Enhanced Vegetation Index (EVI) was specifically developed for the Terra and Aqua Moderate Resolution Imaging Spectroradiometers (MODIS) to improve sensitivity in high biomass regions while minimizing the influence of soil and atmosphere. The two-band EVI was developed to maintain the characteristics of EVI while not relying on the blue band thus being applicable to satellite sensors which do not carry a band in the blue wavelengths.

Among the indices developed for enhancing the signal of burned surfaces, the Normalized Burn Index (NBR) is widely used for mapping burn severity and the Char Soil Index (CSI) was found to perform well for burned area mapping with Landsat TM images by Smith et al. (2007). Finally, the Mid-Infrared Burn Index (MIRBI) was proposed as a robust index with respect to intrinsic perturbing factors (e.g. pre-fire vegetation conditions) as well as to scattering by even optically thick smoke plumes.

1.2   The membership functions

Fig. 2 shows the histograms of probability density derived from the training set for NBR and MIRBI. The membership functions of the soft constraints identifying positive and negative evidence of burn were defined as linear interpolation between maximum and minimum values of the class histograms (i.e. burns in the case of positive evidence). For example, the NBR's membership function for positive evidence (black continuous line in Fig. 2) is defined as $\mu_{i,b}=1$ if NBR<-0.325, $\mu_{i,b}=0.66-1.06*$NBR if $0.325<$NBR≤0.620, $\mu_{i,b}=0$ if NBR>0.620. The partial positive evidence of burn was computed for the other indices by applying membership functions similar to NBR's. An analysis of separability pointed out NBR and MIRBI as the best indices for deriving the negative evidence. Hence, the membership functions of negative evidence were defined to fit the frequency distribution of shadows and vegetation for NBR and MIRBI, respectively, as shown in Figure 2.
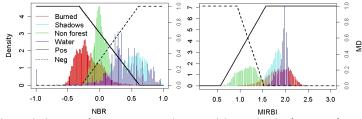

Figure 2. Histograms over burns, shadows, non forest vegetation and water and the membership functions of positive (continuous line) and negative (dashed line) evidence of burn for NBR and MIRBI.

1.3   The integration functions

Soft integration functions, i.e. Ordered Weighted Averaging (OWA) operators (Yager, 1988), were used for integrating the partial positive evidence scores into the overall positive evidence for all of the eight SIs. We chose two distinct functions for identifying seeds (PE$_{seed}$) and the wider possible boundaries for region growing (PE$_{grow}$): a very strict operator (OWA$_{most90}$) that identifies a seed when 90% of the partial evidence scores are high and a looser integration operator (OWA$_{most50}$, i.e., half of the partial evidence scores are integrated) for the growing layer. For the integration of membership degrees of negative evidence we used the maximum operator.

Results

Figure 3 shows some burned area maps (bottom row) derived over TM image 203/034 (Portugal, 24/10/2003) (top row). The accuracy of the map was evaluated by comparison with burned area perimeters (red polygons) provided by J.M.C. Pereira of the Technical University of Lisbon. The figure shows an example of correctly classified burns (panels b and f) although

unburned small patches inside the major perimeter produce omission errors. In figure 3a an extensive area of agricultural lands in the Beja district, Portugal, is erroneously classified as burned where the reference dataset registered only one polygon (figure 3e). As shown by the RGB (543), this area represents a challenge for the algorithm since agricultural fields at the end the season (soils) can be spectrally confused with burns. In some cases, the omission error could be inflated by inaccuracy of the reference dataset (figure 3c), which is also affected by errors since the ground truth cannot be reproduced with a 100% accuracy. Finally, omission errors can be due to fires occurred a long time before satellite acquisition in which case the post-fire processes could significantly change the spectral signal. The land cover characteristics and fire severity are two major factors influential on the persistence of the burn spectral signal.
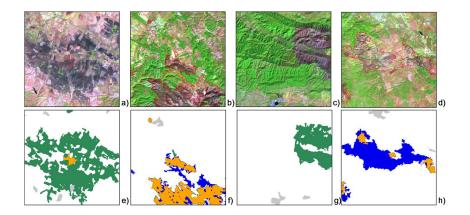

Figure 3. Example maps extracted from the TM images 203/034 (top row: RGB 543).Bottom: correctly classified burns are orange, omission in blue and commission in green, correctly classified unburned areas are white. Grey regions have been masked out. Red perimeter are the reference dataset.

Global figures provided by the validation are very encouraging since the commission error is less than 2%, omission is 21% and overall accuracy is slightly less than 92%. The same approach described above and applied without the revision of the seed and growing layers, based on the negative evidence, provided a burned area map with a commission error of 59% and an overall accuracy of 42%.

Conclusions

We propose a method for mapping burned areas in Mediterranean regions from Landsat TM/ETM+ images based on the integration of spectral indices and performed with soft computing techniques. Preliminary results are very encouraging since validation shows that commission and omission errors are 1.3% and 21.1%, respectively, and overall accuracy is less than 92%.

References

Bastarrika, A., Chuvieco, E., Pilar Martín, M., 2011. Mapping burned areas from Landsat TM/ETM+ data with a two-phase algorithm: balancing omission and commission errors. Remote Sensing of the Environment 115: 1003-1012.

Boschetti, M., Stroppiana, D., Brivio, P.A., 2010. Mapping burned areas in a Mediterranean environment using soft integration of Spectral Indices from high-resolution satellite images, Earth Interactions, 14: 1- 20.

Carrara, P., Bordogna, G., Boschetti, M., Brivio, P. A., Nelson, A., Stroppiana, D., 2008. A flexible multi-source spatial-data fusion system for environmental status assessment at continental scale. International Journal of Geographical Information Science 22: 781–799.

Crutzen, P.J., Andreae, M.O. 1990. Biomass burning in the tropics: impact on atmospheric chemistry and biogeochemical cycles, Science 250: 1669-1678.

Huete, A.R., 1998. A soil-adjusted vegetation index (SAVI). Remote Sensing of the Environment 25: 295–309.

Huete, A., Didan, K., Miura, T., Rodriguez, E.P., Gao, X., Ferreira, L.G., 2002. Overview of the radiometric and biophysical performance of the MODIS vegetation indices. Remote Sensing of the Environment 83: 195-213.

Jiang, Z., Huete, A.R., Didan, K., Miura, T., 2008. Development of a two-band enhanced vegetation index without a blue band. Remote Sensing of the Environment 112: 3833-3845, DOI: 10.1016/j.rse.2008.06.006.

Key, C.H., Benson, N.C., 1999. Measuring and remote sensing of burn severity. In: Proc. Joint Fire Science Conference and Workshop, L.F. Neuenschwander & K.C. Ryan (Eds.), vol. II, Moscow, ID: Univ. of Idaho and Int. Ass. of Wildland Fire, 1999, p. 284.

Masek, J. G., Vermote, E.F., Saleous, N., Wolfe, R., Hall, E.F., Huemmrich, F. et al., 2006, A Landsat surface reflectance dataset for North America, 1990–2000, IEEE Geoscience and Remote Sensing Letters 3: 68–72.

Pereira J.M.C., Sá, A.C.L., Sousa, A.M.O., Silva, J.M.N., Santos, T.N., Carreiras, J.M.B., 1999. Spectral characterisation and discrimination of burnt areas. In: Remote Sensing of Large Wildfires in the European Mediterranean Basin, E. Chuvieco, Ed. Berlin, Germany: Springer-Verlag, pp. 123–138.

Rouse, J.W., Haas, R.H., Schell, J.A., Deering, D.W., 1973. Monitoring vegetation systems in the Great Plains with ERTS. Third ERTS Symposium, NASA SP-351 1: 309-317.

Smith, A.M.S., Wooster, M.J., Drake, N.A., Dipotso, F.M., Falkowski, M.J., Hudak, A.T., 2005. Testing the potential of multi-spectral remote sensing for retrospectively estimating fire severity in African Savannahs. Remote Sensing of the Environment 97: 92–115, DOI: 10.1016/j.rse.2005.04.014.

Stroppiana, D., Boschetti, M., Zaffaroni, P., Brivio, P. A., 2009. Analysis and interpretation of spectral indices for soft multi-criteria burned area mapping in Mediterranean regions. IEEE Geoscience and Remote Sensing Letters 6: 499–503.

Thonicke, K., Venevsky, S., Sitch, S., Cramer, W. 2001. The role of fire disturbance for global vegetation dynamics: Coupling fire into a Dynamic Global Vegetation Model, Global Ecology and Biogeography 10: 661–677.

Trigg, S., Flasse, S., 2001. An evaluation of different bi-spectral spaces for discriminating burned shrub-savanna. International Journal of Remote Sensing 22: 2641-2647, DOI: 10.1080/01431160110053185.

Vafeidis, A.T., Drake, N.A., 2005. A two-step method for estimating the extent of burnt areas with the use of coarse-resolution data. International Journal of Remote Sensing 26: 2441-2459.

Yager, R.R., 1988. On ordered weighted averaging aggregation operators in multicriteria decisionmaking. IEEE Trans. Syst. Man Cybern. 18: 183–190, DOI: 10.1109/21.87068.

European Commission

Abstract
This report contains the proceedings of the 8th International Workshop of the European Association of Remote Sensing Laboratories (EARSeL) Special Interest Group on Forest Fires, that took place in Stresa, (Italy) on 20-21 October 2011. The main subject of the workshop was the operational use of remote sensing in forest fire management and different spatial scales were addressed, from local to regional and from national to global. Topics of the workshops were also grouped according to the fire management stage considered for the application of remote sensing techniques, addressing pre fire, during fire or post fire conditions.

How to obtain EU publications

Our priced publications are available from EU Bookshop (http://bookshop.europa.eu), where you can place an order with the sales agent of your choice.

The Publications Office has a worldwide network of sales agents. You can obtain their contact details by sending a fax to (352) 29 29-42758.

The mission of the JRC is to provide customer-driven scientific and technical support for the conception, development, implementation and monitoring of EU policies. As a service of the European Commission, the JRC functions as a reference centre of science and technology for the Union. Close to the policy-making process, it serves the common interest of the Member States, while being independent of special interests, whether private or national.

JRC
EUROPEAN COMMISSION

Publications Office